PROCESSING AND CHARACTERIZATION OF FUNCTIONALLY GRADED METAL AND POLYMER COMPOSITES

Thesis submitted to

Cochin University of Science and Technology

for the degree of

Doctor of Philosophy

in

Faculty of Technology

by

JAYAKUMAR E.

(Reg. No. 4158)

under the supervision of

Dr. T.P.D. RAJAN

Material Science and Technology Division

CSIR-National Institute for Interdisciplinary Science and Technology (CSIR-NIIST)

Thiruvananthapuram-695019

December 2016

Processing and Characterization of Functionally Graded Metal and Polymer Composites

Ph. D. Thesis

December 2016

Author:

Jayakumar E.
Material Science and Technology Division
CSIR-National Institute for Interdisciplinary Science and Technology (CSIR-NIIST)
Thiruvananthapuram-695019
Email: ejkumar@yahoo.com
Tel: 9495070799 (Mob)

Supervising guide:

Dr. T.P.D. Rajan
Senior Scientist
Material Science and Technology Division
CSIR-National Institute for Interdisciplinary Science and Technology (CSIR-NIIST)
Thiruvananthapuram-695019
Email: tpdrajan@niist.res.in
Tel: 0471 2515327 (Off)

Dedicated to

my family …

DECLARATION

I, **Jayakumar E.**, hereby declare that, the thesis entitled "***Processing and Characterization of Functionally Graded Metal and Polymer Composites***" is a bonafide record of the research work done by me under the supervision and guidance of Dr. T.P.D. Rajan, Senior Scientist, CSIR-National Institute for Interdisciplinary Science and Technology, Thiruvananthapuram and no part of this dissertation has been submitted previously for the award of any degree in any other University.

In keeping with the general practice of reporting scientific observations, due acknowledgement has been made wherever the work described is based on findings of other investigators.

Jayakumar E.

Thiruvananthapuram
16 December, 2016

Council of Scientific and Industrial Research
CSIR - NATIONAL INSTITUTE FOR INTERDISCIPLINARY SCIENCE AND TECHNOLOGY (CSIR-NIIST)
Industrial Estate P.O., Thruvananthapuram - 695 019, India

Dr. T.P.D. Rajan
Senior Scientist
Materials Science and Technology Division

Tel: 91-471-2515327
Fax: +91-471-2491712
E-mail: tpdrajan@niist.res.in

December 16, 2016

CERTIFICATE

This is to certify that the thesis entitled **"Processing and Characterization of Functionally Graded Metal and Polymer Composites"** is a bonafide record of the research work carried out by **Mr. Jayakumar E**, under my supervision in partial fulfillment of the requirement for the degree of Doctor of Philosophy of the Cochin University of Science and Technology and further that no part of this thesis has been presented previously for the award of any other degree. All the relevant corrections, modification and recommendations suggested by the audience and the doctoral committee members during the pre-synopsis seminar of Mr. Jayakumar E have been incorporated in the thesis.

Dr. T.P.D. Rajan
(Thesis Supervisor)

Acknowledgements

It is indeed very much overwhelming feeling when a sailor in a deep sea senses the end of a tiring journey. He forgets all the obstacles that he has come across during the course of his journey. He would like to express his sincere gratitude and thanks to all the crews who have been his source of inspiration and gives enough strength and perseverance since the beginning. While doing this, he is bit wordless.

First and foremost, I praise the Almighty for bestowing upon me with abundant love, inspiration, wisdom, determination and good health during the period and for showering his blessings throughout my life.

I would like to express my deep sense of gratitude to my supervising guide, Dr. T.P.D. Rajan, Senior Scientist, MMS/MSTD, for his timely suggestions and support during the course of my research work. I could benefit a lot from his excellent ideas and invaluable academic experience, which would certainly help me in future.

I am also very grateful to Dr. A. Ajayaghosh, Director, CSIR- NIIST, former Directors Dr. Suresh Das and Dr. B. C. Pai for providing all the necessary facilities to carry out this work and their encouragement and constant support. I am very much grateful to Dr. P. P. Thomas, Former Chief Scientist, CSIR NIIST and Prof. K.E. George, Former Professor and Head, Dept. of Polymer Science and Rubber Technology, CUSAT, Kochi for their timely support, constant encouragement and advices.

I take this chance to sincerely thank My Chairman, Honourable Minister of Transport, Govt of Kerala, the Principal, Sree Chitra Thirunal College of Engineering, Dr.R. Ajith , the Head, Department of Mechanical Engineering and Dr. S. H. Anilkumar (Former Head) SCT college of Engineering.

My sincere thanks to Dr. P. Prabhakar Rao, Head MSTD and former heads Dr. K.G.K. Warrier, Dr. M.T. Sebastian and Dr. M.L.P.Reddy for their support. I am also grateful to section heads Dr. K. Harikrishna Bhat and Mr. M.C. Shaji.

I also extend my heartfelt thanks to Dr. U.T.S. Pillai, Dr. M. Ravi, Dr. A. Srinivasan, Dr. S.S. Sreejakumari, Dr. Manoj Rama Varma, Dr. S. Ananthakumar, Mr. M. Brahma Kumar, Mr. K.K. Ravikumar and Dr. J. D. Sudha.

I take this chance to sincerely thank Mr. V. Antony, NIIST for the help received from him throughout the research work for his valuable help to carry out the castings

and optical micrographs. It is worth to mention that the thesis would not have come to the final shape without his help.

I take this chance to sincerely thank the members of mechanical workshop for specimen preparations and other help to carry out the smooth casting process.

I express my sincere thanks to Dr. Arun Boby and Mr. Abhilash Viswanath, Mr. Athul, Mr. Akhil. S. Karun, Mr. Sree Manu K.M, Mrs. Lekshmi V, Mrs. Resmi, Dr. J.P. Deepa, and Dr. K.K. Ajithkumar, NIIST for the technical discussions and the help given to me during the course of this research work.

A special mention is worth to Mr. N. Anand, Mr. Jasim Akber Hyder, Mr. P. Manikandan, Mr. Prince Joseph, Mr. S. Prasanth and Mr. S. Rajesh, NIIST, Trivandrum for their help throughout this work. I also thank all members of Light Metals, Alloys and Composite Group, and workshop, NIIST, Trivandrum for the help throughout my work.

Heartfelt thanks to my parents, father in-law, mother in-law, brother in-law, sister in- law and Dr. E. Sreekumar, my brother, who always have concern about my progress, for their encouragement and untiring support.

Special thanks to my wife Deepa devi. V and my son Anand. J for their encouragement, constant support and patience.

Preface

Engineering components and structures with location specific property requirements and performance under service conditions are of great demand for a variety of modern technological applications. A gradual transition in the composition or microstructure motivates the changes in the functions of a specified location for meeting the needs. These tailored materials are functionally graded materials (FGM). The mechanical and thermal responses of materials with spatial gradients in composition and microstructure have considerable usage in the areas like high temperature technology, biomechanics, processing of cutting tools, aerospace applications, thermal coatings, manufacturing processes and automobile industries. The graded transition in density, porosity, grain size or dispersed particles in the matrix of two materials, across an interface can easily reduce thermal stresses, stress concentration and the crack tip stress intensity at the crack tip.

Among the various techniques, centrifugal casting is one of the simplest and economically viable methods for the production of FGMs. In the centrifugal casting process the components having axial symmetry, generally cylindrical shapes are processed under centrifugal force. When the composite or melt containing different phases in the slurry is subjected to centrifugal force, different regions are formed in the melt with difference in concentration of phases; i.e. generally one end enriched and another end depleted with a transition in between. Functionally Graded Metal Matrix Composites (FGMMC) of aluminium alloys with dispersoids like alumina, zirconia and SiC are formed; initially making a composite melt by liquid metal stir casting followed by pouring it into a rotating mould at specific temperature and allows for solidification. Functionally Graded Polymer Matrix Composites (FGPMC) with epoxy matrix and SiC reinforcement particles are also processed similarly. A mixture of epoxy resin with proportionate hardener and fixed volume SiC particles are externally prepared and then transferred to the spinning moulds.

The objective of the present study is to process FGMMC and FGPMCs by centrifugal casting technique and characterize the gradation in microstructure, composition and correlate it with properties. The functionally gradient materials are evaluated for their hardness, tensile and compressive strength properties, thermal

expansion coefficient and wear resistance. FGMMC finds interesting applications to the present growing demands of automobile industries in disc brakes, cylinder liners and IC engine pistons.

The present thesis is divided into 8 chapters. The first chapter gives a very brief introduction to composites, their classification, properties and comparisons. Followed by the introduction of FGM concept and the various FGM preparation methods are discussed. The chapter concludes with detailed explanation of the centrifugal casting of the FGMs and the advantages of the process.

The second chapter on literature survey gives an extensive and an exclusive study of the field of FGM preparation by centrifugal casting method and the different applications. Starting with the FGM concept used by Japanese for thermal barriers in their space application programme to the recent developments in automobile engine piston developments is summarised. The literatures related to aluminium FGMMC and Epoxy FGPMC are described in details.

The third chapter, materials and experimental methods enlightens the composition and properties of different aluminium alloy matrices such as A319, A390 and A6061 which are used for preparing of MMC followed by FGMMC. For FGPMC preparation epoxy matrix reinforced with SiC particles are used. The various properties of epoxy were also given in this chapter. The composition and the properties of the SiC reinforcement particles are described along with the details of MMC melt preparation, centrifugal casting conditions and processing parameters. The details of specimen preparation, characterizations methods, testing parameters and instrument specifications are described in the experimental method section of the chapter.

The fourth chapter titled “processing and characterisation of A319–SiC functionally graded metal matrix composites” begins with the preparation of MMC melt with SiC ceramic reinforcement particles of 23 μm average particle size for different compositions of 10, 15 and 20 wt percentages followed by the casting of respective FGM discs of size 300mm diameter and 30mm thickness. A319 is a hypo eutectic silicon alloy of aluminium with 5-7 % of Si and is a precipitation hardenable and heat treatable cast alloy. With the denser SiCp ex-situ particle addition and the centrifugal force of the casting process produces different regions of particle concentration and microstructure leading to a graded structure.

While, in fifth chapter “processing and characterisation of A390 functionally

graded metal matrix composites", A390 aluminium hyper eutectic silicon alloy with 16-18 % Si is selected for the MMC and FGM preparation. Here in addition to ex-situ addition of denser SiC reinforcement particles, reinforcements of lighter Mg_2Si phases were also produced by in-situ chemical reactions and effectively used the primary Si in the alloy phase. The Magnesium addition to the alloy melt is carried out in two different methods, one by direct pure Magnesium addition to the melt and the other by Magnesium Master Alloy addition. These two ways of in-situ preparations show remarkable variations in properties. As a practical industrial application, a twin pistons metal mould suitable for the centrifugal casting of A390 alloy is designed and fabricated. FGM pistons of A390 alloy with 0.5 % Mg suitable for automobile IC engine are produced and detailed characterizations are also done as a part of the study.

The sixth chapter "processing and characterisation of A6061–SiC functionally graded metal matrix composites" discusses the processing and characterisation of wrought A6061 aluminium FGM with ex-situ SiCp with 10 and 20 wt% additions. Study of tribological characteristics is done to found out the influence of hard SiC particles on dry wear conditions. Here A6061 is a wrought alloy with very less alloying elements and will have the properties almost comparable as that of pure aluminium.

In the seventh chapter "processing and characterisation of epoxy– SiC functionally graded polymer matrix composites" starts with processing parameter optimization of epoxy and hardener ratio for gravity casting. And then the ratio is extended to centrifugal casting. It is found that a ratio of hardener to epoxy 1:10 is well suited. The effects of SiC reinforcement particle loading on curing and glass transition temperature is also carried out by DSC and Rheology tests to ensure proper polymerisation and good casting. The mould rotation is also optimized to lower level of 500 rpm in order to ensure a successful FGM casting with in a considerable less processing time of curing of 45-50 minutes rather than 24 hours (commonly used in industrial applications). The mechanical testing along with dry wear tests are also conducted for characterisation of the functionally graded polymer composite with epoxy and 5 wt % SiC particles.

The results are summarized in chapter eight and discussed the scope for further extension of the work towards frontier areas of materials science and technology.

Contents

List of Figures

List of Tables

Chapter 1

Introduction

1.1 INTRODUCTION

The human quest for finding new material to perform under specified environmental conditions is never ending. This has prompted researchers to enhance their research work for addressing to the materials need of the ever expanding and ever challenging human world. It is well known in the materials world that one can create new materials with unique properties, which can be tailor-made and are different from their basic constituent ingredients. This very concept is responsible for creating composite materials of various types with a matrix that is strengthened by the reinforcement it contains.

1.2 COMPOSITES

A composite material is a heterogeneous material composing of two or more materials on a macroscopic scale with distinct interface between constituent materials. Generally it is composed of reinforcements in the form of fibers, particles, flakes or fillers embedded in a matrix [1-2]. The matrix holds the reinforcement to form the desired shape while the reinforcement improves the overall mechanical properties of the matrix. When designed and fabricated properly, the new combined material exhibits better properties than that of each individual material. Unlike conventional materials the properties of the composite material can be designed considering the structural aspects. The design of a structural component using composites involves both material and structural design. Composite properties can be varied continuously over a broad range of values under the control of the designer. Careful selection of reinforcement type enables finished product characteristics to be tailored to any specific engineering requirement.

The composites can be processed to achieve any of the following purposes.

- To increase stiffness, strength and dimensional stability.
- To increase toughness and impact strength.
- To increase heat deflection temperature.

- To increase mechanical damping.
- To reduce permeability to gases and liquids.
- To modify electrical properties.
- To reduce cost.
- To decrease thermal expansion.
- To increase chemical, wear and corrosion resistance.
- To reduce weight.
- To maintain strength/stiffness at high temperatures while under strain conditions in a corrosive environment.
- To increase secondary uses and recyclability and
- To reduce negative impact on the environment.

1.3 TYPES OF COMPOSITES

Composite materials are classified on the basis of type of matrix materials and on the type of reinforcements used for the preparation and processing. The classifications of composites based on matrix materials are namely; polymer matrix composites (PMC), ceramic (CMC) and metal matrix composites (MMC).

1.3.1. *Polymer Matrix Composites (PMC)*

Two types of polymers are used as matrix materials for fabrication polymer composites: Thermosets (epoxies resins, phenolics) and Thermoplastics (Low Density Polyethylene (LDPE), High Density Polyethylene (HDPE), polypropylene, nylon, and acrylics). Polyester and vinyl esters are the most widely used and least expensive polymer resins. These matrix materials are generally used for fiber glass reinforced composites. Even with high specific mechanical strength compared with their mass, the main disadvantages of PMCs are their low density, low maximum working temperature, high coefficient of thermal expansion and sensitivity to atmospheric influences like radiation and moisture, resistance to aggressive environments, electric and thermal properties. Compared with metals and ceramics, the strength and stuffiness are lower for PMCs. Polymer Matrix Composites (PMC) are used for manufacturing: secondary load-bearing aerospace structures, boat bodies, canoes, kayaks, automotive parts, radio controlled vehicles, sport goods (golf clubs, skis, tennis racquets, fishing rods), bullet-proof vests and other armour parts, brake and clutch linings[3-6].

1.3.2 *Ceramic Matrix Composites (CMC)*

One of the main objectives in producing CMCs is to increase the toughness. Ceramic materials are resistant to oxidation and deterioration at elevated temperatures. Some of these materials would be ideal candidates for use in high temperature applications, specifically for components in automotive and aircraft gas turbine engines. The developments of CMCs has lagged behind mostly for the reason that most processing routes involve higher temperature and only employed with high temperature reinforcements [7-11]. Matrix material for long-fiber (continuous fiber) composite may be silicon carbide ceramic, alumina (alumina-silica) ceramic or carbon. CMCs are fabricated by chemical vapour infiltration, liquid phase infiltration, sol-gel, direct metal oxidation and chemical bonding methods. Silicon carbide matrix composites are used for manufacturing combustion liners of gas turbine engines, hot gas re-circulating fans, heat exchangers, rocket propulsion components, filters for hot liquids, gas-fired burner parts, furnace pipe hangers, immersion burner tubes. Alumina and alumina-silica (mullite) matrix composites are used for manufacturing heat exchangers, filters for hot liquids, thermo-photovoltaic burners, burner stabilizers, combustion liners of gas turbine engines. Carbon-Carbon Composites are used for manufacturing high performance braking systems, refractory components, hot-pressed dies, heating elements, turbojet engine components.

1.3.3 *Metal Matrix Composites (MMC)*

Metal matrix composites (MMC) are considered as materials with broad technological and commercial significance in recent applications [12-21]. MMCs due to their superior properties are considered as an alternative to monolithic metals and commercial alloys in specialised applications. In MMCs a metal, Aluminium, magnesium, iron, cobalt, copper etc or its alloy forms the matrix and binds an inter-metallic compound, an oxide, carbide, nitride or even secondary phases formed in the alloy, which will function as the reinforcements.

The reinforcements used for composite preparations may be in the form of particulates, fibers, whiskers and secondary phases. The reinforcements are generally stiffer, stronger and/or harder than the matrix. Classification of composites based on the reinforcement materials used are namely; particle reinforced composites and fiber reinforced composites.

1.3.4 *Particle Reinforced Composites*

Particulates are the most common and cheapest reinforcement materials. These produce the isotropic property of composites, which shows a promising application in structural fields. Initial attempts were to process MMCs of Aluminium alloys with lower volume fractions graphite powders. The higher volume fractions of reinforcements have been achieved even with particles like oxide, carbide, and nitride of Silicon, Boron and Titanium. The SiC-particulate-reinforced Aluminium matrix composites have a good potential for use as wear resistant materials. Like carbon black particles in a matrix of polyisobutylene rubber for automobile tyres and, fine and coarse aggregates (sand and basalt rocks) in concrete cement matrix. Particulates lead to a favourable effect on properties such as hardness, wear resistance and compressive strength.

1.3.5 *Fibre Reinforced Composites*

The fibre reinforcements can be of either continuous or short in aligned or misaligned conditions. The continuous fibres reinforcements in composites include boron, graphite, alumina and silicon carbide. The fibre is unique for unidirectional load when it is oriented in the same direction as that of loading, but it has low strength in the direction perpendicular to the fibre orientation. Since continuous aligned fibres are highly expensive than discontinuous fibres, they are used only for specific purposes applications. Fibre-reinforced composite materials have gained popularity (despite their generally high cost) in high-performance products that need to be lightweight, yet strong enough to take harsh loading conditions such as aerospace components (tails, wings, fuselages, propellers), boat and scull hulls, bicycle frames and racing car bodies.

The short fibres and whiskers show high strength in composites, considering aligned fibres. Nevertheless, disoriented short fibres have been used with some success as Aluminium Matrix Composite (AMC) reinforcement. Short fibres are still used mainly for refractory insulation purposes due to their low strength compared with others, but they are cheaper than continuous fibres and whiskers. Whiskers are characterized by their fibrous, single crystal structures, which have no crystalline defect. Numerous materials, including metals, oxides, carbides, halides and organic compounds have been prepared under controlled conditions in the form of whiskers. Generally the whiskers are free from any type of crystal defects. The relative freedom from dislocation means that the yield strength of a whisker is close to the theoretical strength of the material.

1.4 ADVANTAGES AND APPLICATIONS OF METAL MATRIX COMPOSITES

MMCs have become one of the most important advanced materials used for aerospace, automotive, defence and general engineering applications. MMCs with ceramic reinforcements are processed and used widely due to their superior properties compared to other reinforcement types. Ceramic reinforcements may be silicon carbide, boron, alumina, boron carbide, alumina etc. In particular, aluminium matrix composites (AMC) have higher wear resistance and lower friction coefficient with increasing volume fraction of reinforcement particles, compared to aluminium alloys without reinforcements. MMCs have superior electrical and thermal conductivities, excellent resistance to moisture, flame and radiation. Automobile manufacturers have recently begun to use MMCs in their products. Engine components consisting of an Aluminium-alloy matrix reinforced with Aluminium oxide and carbon fibers. They are light in weight and resists wear and thermal distortion. Drive shafts (that have higher rotational speed and reduced vibration noise levels), extruded stabilizer bars, and forged suspension and transmission components. The aerospace industry also uses MMCs intensively. Structural applications include advanced Aluminium alloy metal matrix composites with boron fiber reinforcement are used for the Space Shuttle Orbiter, and continuous graphite fibers for the Hubble Telescope. MMC structures are used mainly because of the following characteristics:

- They have higher application temperature ranges,
- They have higher transverse stiffness's and strengths,
- In general, they have high toughness values,
- When present in metal matrices, the moisture effects and the danger of flammability are absolutely absent and they have high radiation resistances,
- They have high electric and thermal conductivities,
- MMC have higher strength-to-density, stiffness-to-density ratios, as well as better fatigue resistances, lower coefficients of thermal expansion (CTE) and better wear resistances as compared with monolithic metals, and
- They can be fabricated with conventional metal processing methods.

MMCs can also be tailored to have superior properties such as high specific strength, stiffness, high temperature performance, better thermal and mechanical properties, wear resistance, fatigue and creep resistance than those of monolithic alloys. Properties of MMCs can be varied by proper selection of the matrix and reinforcements,

for example thermal and electrical properties can be varied by appropriate adjustment of reinforcement volume fraction, morphology and distribution [22-34].

1.5 FUNCTIONALLY GRADED MATERIALS (FGM)

According to Gasik "A functionally graded material (FGM) is a material with engineered gradients of composition, structure and/or specific properties with dissimilar constituents aiming to become superior over homogeneous material"[35]. The first concept of FGMs was proposed in 1984 by Niino and co-workers [36] at the National Aerospace Laboratory of Japan, as a preparation method for thermal barrier materials. The final target of the proposed concept was to produce a material which could endure both the maximum temperature of 2000 K and the temperature difference of 1000 K primarily for the space plane application. The original idea of FGMs has been later expanded for a variety of applications (cuttings tools, coatings, packages, semiconductors, optical and biomaterials). Theoretical prediction of the usefulness of functional composites with a graded structure came already in 1972 from the work of Bever and Shen [37]. However, their work had only limited impact, probably due to the lack of suitable production methods. During the last decades, FGMs have been developed from single specimens to industry oriented applications. In fact, several national R&D programs (Japan, China, and Germany) have started in this field very recently. The overview of the production routes, properties and applications of FGMs are described in several monographs and review articles [38-39].

1.6 DESIGN AND PROCESSING OF FGM

The processing of FGMs can be divided in two steps: building of a structure with a gradient and later transformation of the designed structure into bulk material. The gradation process is usually classified in three main groups: constitutive, homogenizing, and segregating processes. Stepwise build up of a graded material from precursor materials is the basic constitutive process. In homogenizing processes a sharp interface between two materials is converted into a gradient by material transport i.e. diffusion. Segregating processes start with a macroscopically homogeneous material which is converted into graded material by material transport caused by an external field (gravitational or electric field). The primary advantages of the homogenizing and segregating processes is a possibility to produce a continuous gradient. Afterwards, usually drying and sintering (or solidification) follows the gradation step. This

consolidation step needs to be adapted for a particular material selection and attention has to be paid also to non uniform shrinkage rate during the sintering of FGMs. Very extensive review of the processing techniques has been given by Kieback et al. [37]. It is emphasized that "conventional" powder metallurgy (PM) remains the most useful method for mass production of FGMs.

(a) Continuously graded **(b) Discretely layered**

Figure 1.1: Gradient architecture of FGMs

FGM holds continuous changes of the microstructure, the composition and the properties in some specific directions, i.e., inhomogeneous on both macroscopic and microscopic scales. On the other hand, particle-, fiber- or platelet-dispersed composites are regarded as macroscopically homogeneous and microscopically inhomogeneous. FGM's are having two types of gradient architecture structures (a) continuous and (b) discrete/stepwise (Figure1.1). In the first type, the change in composition and/or microstructure occurs continuously with position while in the second one the microstructure feature changes in a stepwise manner, giving rise to a multilayered structure with interfaces existing between discrete layers. The fabrication processes of continuous FGM are broadly classified into Constructive processes (Figure 1.2) and Transport based processes (Figure 1.3).

In the constructive processes the FGMs are constructed layer by layer, in a manner that starts with an appropriate distribution of constituents of the FGM, the gradients are literally constructed in space. Powder densification, lamination and coatings are some of the constructive manufacturing methods using for FGM processing.

Powder densification is the conventional powder metallurgy route through which powder components are compacted and sintered to get the desired product. Porosity gradients and pore-size gradients can be created in the structure. The former can be achieved by the deposition of powder mixtures with different particle shape or by varying the deposition parameters and the latter by the variation of particle size. The deposition of powders with a continuous change in the composition of the mixture during sintering will lead to a single phase material with a smooth change in the

distribution of elements. If a liquid phase is used for activated sintering the resulting microstructure consists of two or more phases with gradients in volume content or in grain size which were predetermined during the deposition of the powders.

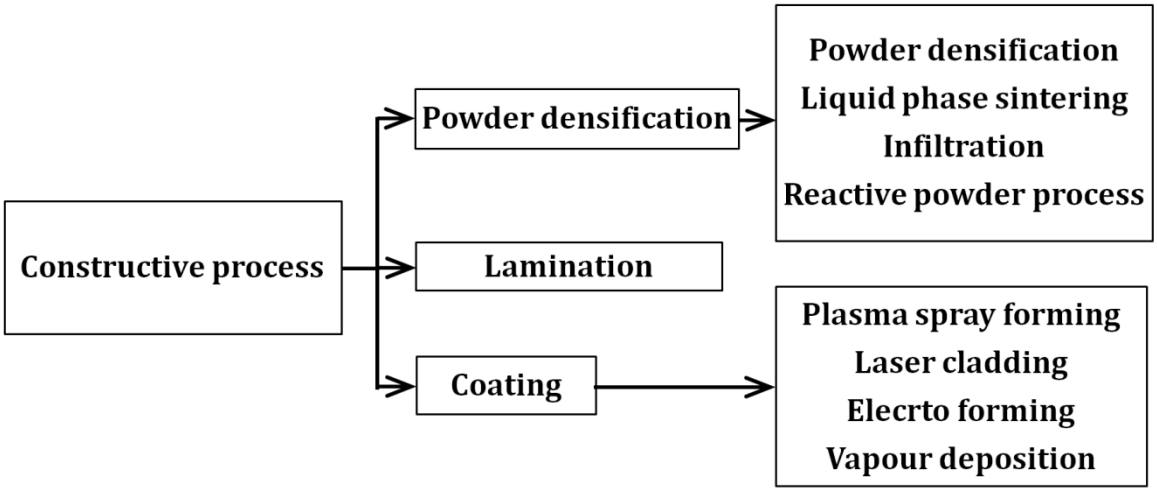

Figure 1.2: Continuous FGM by constructive processes

The combinations of varying phases can include metal–metal, metal–ceramic and ceramic–ceramic systems. Microstructural gradients can also be produced by controlling the phase equilibrium during liquid-phase sintering with gradients of the components. In the lamination methods, thin sheets with different compositions can be produced and joined to form a stepped gradient. The process involved the stacking of a large number of foils, followed by diffusion bonding and cold rolling. By varying the relative thicknesses of foils used across the structure, variations in phase volume fractions and layer widths, and hence in local properties, were produced across the rolled material. The coating can be done either by wet powder spraying or by slurry dipping. Suitable powder suspensions are developed to deposit thin powder layers on a substrate by an air brush system. By including a mixing system and controlled feeding, of two or more suspensions, graded powder layers can be deposited on a flat, curved or rotating substrate. Simultaneous drying allows building up parts reaching millimetre thickness with only small variations from layer to layer. The minimum thickness of the layers is controlled by the size of the sprayed droplets and may be less than 50μm. If a porous body is sequentially dipped into slurries with varying powder characteristics, the liquid drag into pores by capillary forces leaves surface layers with a stepped gradient behind. The functionally graded layers can serve as an optimal transition between a bulk component and an outer coating that will protects the component from

harsh conditions of temperature, corrosion, or erosion in an external service environment. The currently employed processes are plasma spraying, laser cladding, electroforming and vapour deposition.

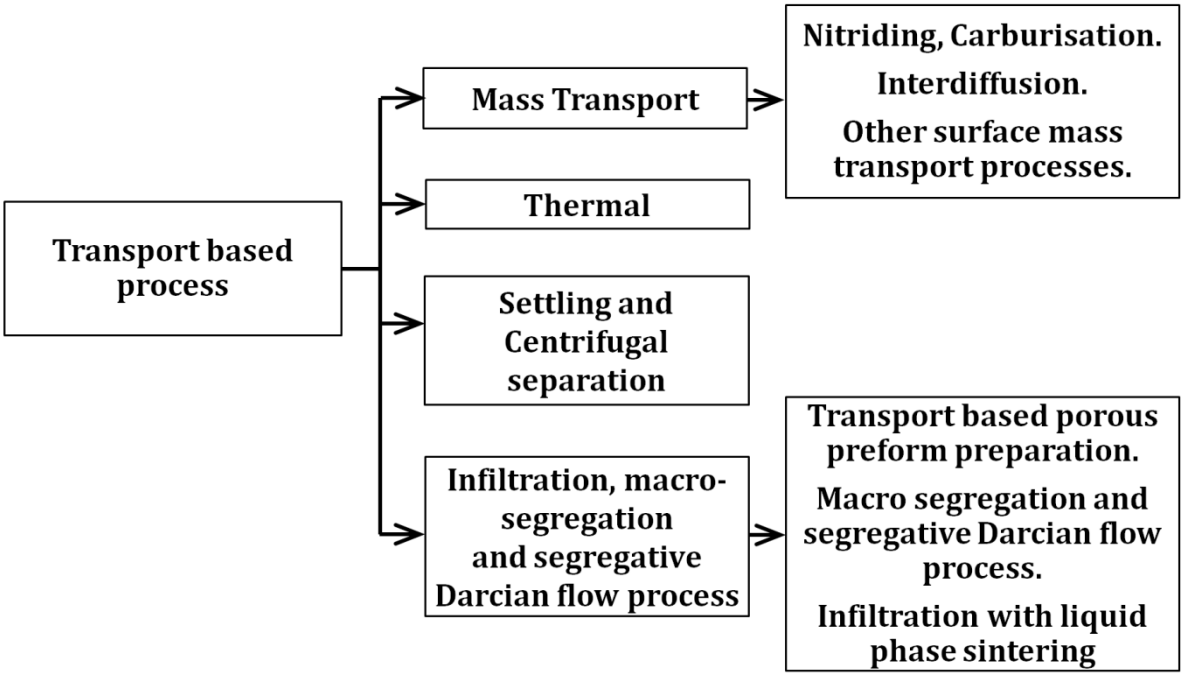

Figure 1.3: Continuous FGM by Transport based processes

The transport based processes rely on the natural transport phenomena (like the flow of fluid, the diffusion of atomic species and the conduction of heat to create gradients in local microstructures/compositions) to create gradients within a component. The various processes used are namely mass transport, thermal, settling, infiltration and centrifuging. Steel carburizing and nitriding use the diffusion transport of carbon and nitrogen atoms at the outer surface of a component to create a hard outer 'case', with a gradual transition to a tougher and softer core. Thermal processes create gradients in material properties by heat diffusion, the variations in thermal diffusion cause changes in microstructure and local properties. Hardenable steel (i.e. steel that can be quenched to form martensite) provides the prime example of thermally processed FGMs because of the strong dependence of its properties on thermal history. Flame hardening, induction hardening and laser hardening are the techniques used for thermal processes. The settling and centrifuging type of FGM processes consists of the production of a suspension of different phases, followed by separation of phases by holding the mixture in gravity, or using applied centrifugal force.

Based on the nature and state of processing of functionally graded materials can be classified as solid state processes, liquid state processes and deposition processes. The various FGM fabrication techniques are listed in Table 1.1.

Table 1.1: The various techniques for fabricating the FGM

Solid State processes	Liquid State Processes	Vapour State Processes
Powder Metallurgy	Infiltration	Chemical Vapour Deposition
Sintering	Settling	Chemical Vapour Infiltration
Powder Stacking	Centrifugal Casting	Physical Vapour Deposition
Powder Infiltration	Directional Solidification	Spray Deposition
Slurry Technique	Sol-Gel Method	Laser Deposition
Plasma Activated Sintering	Electro Deposition	
Diffusion Bonding	Electro Less Plating	

1.7 CENTRIFUGAL CASTING OF FGM

The centrifugal casting is a pressure casting method in which the force of gravity when pouring the molten metal into the mould is increased by rotating or spinning the mould assembly. Centrifugal casting consists of producing castings by causing molten metal to solidify in rotating moulds. The speed of rotation and melt pouring rate vary with the alloy and size and shape being cast. The idea of employing centrifugal force to make castings had been known for a long time, it was A. G. Echardt's original patent of 1809 which revealed the understanding of basic principles involved [40]. Centrifugal casting has greater reliability than static castings. They are relatively free from gas and shrinkage porosity. The operation involves the rotation of the mould at a specific speed while the molten metal is poured at a constant rate. A solidification rate is established which is determined by the degree of superheat of the molten metal, mold preheating temperature, speed of rotation and pouring rate. Along with this, fluid flow during pouring and solidification also determines the soundness and quality of the casting produced.

There are essentially two basic types of centrifugal casting machines: the horizontal type which rotates about a horizontal axis and the vertical type which rotates about a vertical axis. Horizontal centrifugal casting machines are generally used to make

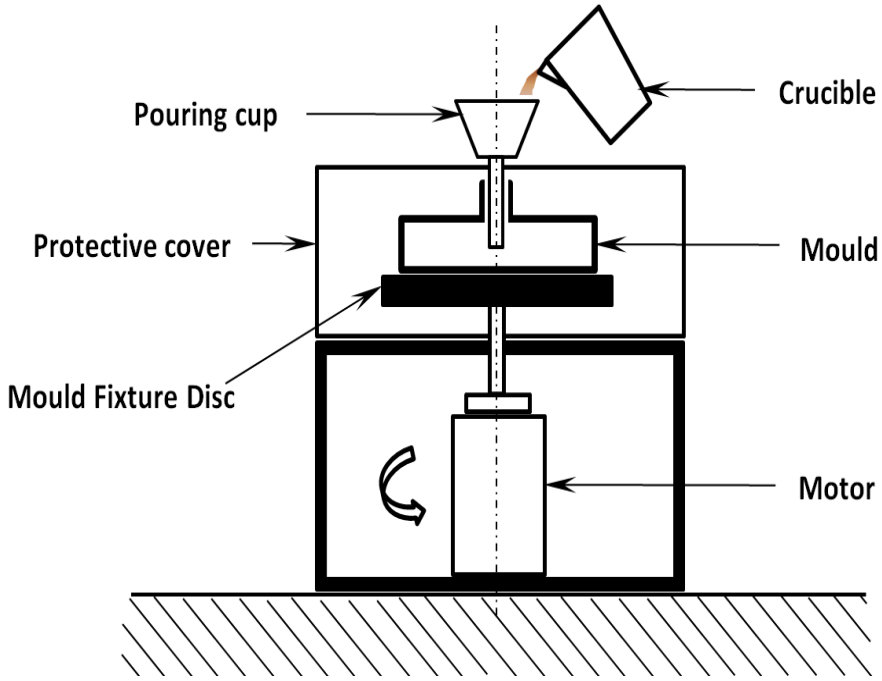

Figure 1.4: The schematic diagram of vertical centrifugal casting

pipe, tubes, bushings, cylinder sleeves (liners), and cylindrical or tubular castings that are simple in shape. Figure 1.4 shows the schematic diagram of a vertical centrifugal casting machine. The advantages of this type is it has relatively superior metallurgical structure, 100% yield, no requirements of cores, uniform wall thickness, less machining allowances and excellent casting finish. The range of application of vertical centrifugal casting machines is considerably wider. Castings that are not cylindrical, or even symmetrical, can be made using vertical centrifugal casting. This type of casting has advantages such as very short parts can be cast, easier to handle, odd configurations and products not suitable for static casting can be cast.

1.7.1 *Process Parameters for Centrifugal Casting*

Similar to metals and alloys, the properties of the cast metal matrix composites are largely dependent on the solidification behaviour. This is prescribed by the thermal and physical properties of the melt, the mould and the interfacial heat resistance between the mould and the metal. Likewise, in centrifugal casting, heat is removed from the solidifying melt through the mould wall. Solidification starts at the outer periphery of the casting, which is in direct contact with the melt, and continues towards the inner diameter of the casting. Parameters that influence the solidification are mainly the mould material, mould wall thickness, initial mould temperature, thickness and thermal

conductivity of the mould coatings used, the degree of superheat of the melt, pouring rate of the melt and the speed of rotation of the mould. From the above said parameters, the degree of superheat of the melt and the mould wall thickness are the most crucial ones, since they directly affect the local solidification conditions and hence modify the structure of the casting.

Pouring temperature exerts a major influence on the mode of solidification and needs to be determined in relation to the type of solidification and the type of structure required. Lower pouring temperatures are favourable for maximum grain refinement with equiaxed structures. But at the same time it should be ensure that there is satisfactory metal flow and freedom from cold laps and cold shuts. Change in the temperature results in change in viscosity, in solidification thereby change in formed phases and the phase distribution in the radial direction of the casting. The mould temperature is of secondary importance in relation to structure and grain refinement. Its importance lies with the mould expansion while preheating: expansion diminishes the risk of tearing in centrifugal castings. Generally found that, a minimum temperature of 300^{o}C is good to avoid the surface defects in the casting.

Slow pouring speed offers a number of advantages in the directional solidification and the feeding are promoted. And also at the same time, the slow development of full centrifugal pressure on the outer solidified skin reduces the risk of tearing. The pouring rate depends on the size of the casting to be produced and the alloy or metal being poured. Slow pouring rates can introduce porosities whereas faster pouring rates can slow down the solidification and if excessive, it can induce longitudinal cracking. Too high rate of pouring can cause excessive turbulence and rejection of externally added reinforcements from the melt. The quality of the casting is affected by the type of process used for the processing of the melt. As the processing method always determines the porosity content, the homogeneity of the melt, inclusions and the oxide layer formations in the melt; a proper selection of melt processing method is also essential for getting a satisfactory casting.

The speed of rotation of the mould is the governing factor in true centrifugal casting as it retains the bore shape against gravity whilst avoiding longitudinal tearing through excessive hoop stress. In the case of semi centrifugal and pressure castings the main criterion is the feeding pressure. The calculation of speed is mainly depends on the axis of rotation, properties of melt and the diameter of the casting. The speed of rotation

is measured by the 'G' factor. It is the ratio of the centrifugal force (Fc) to the gravitational force (Fg). The centrifugal acceleration can be up to 100 times the gravitational force. Higher rotational speed increases the grain refinement, but at the same time it may leads to turbulence and high tensile stresses are induced in the outer periphery resulting in longitudinal cracks of the casting. High rotational speeds can also produce vibration inducing circumferential segregation. At the same time low rotational speeds can result in poor cylinder formation and surface finish. Hence it is always advisable to use consistently optimal higher speeds in order to avoid tearing. In horizontal axis casting, the metal entering the mould must rapidly acquire sufficient velocity to prevent instability and raining (raining is the falling of melt in the form of droplets, under the influence of gravity, as it passes over the top half of the mould during its movement along with the rotating mould). The theoretical minimum value of this velocity is slightly above 1G, but in actual practice, 3G to 4 G is used for getting the full advantage of the process.

In vertical centrifugal casting the minimum speed is established by the tendency to form a parabolic bore owing to the gravitational component of the force acting on the metal. The effect is defined by the expression,

$$\omega^2 = \frac{2gL}{r_t - r_b}$$

where L = axial length (m)
r_t = top radius of bore (m)
r_b = bottom radius of bore (m)

$$\text{Hence, } N = \frac{30(2g)^{1/2}}{\pi} \cdot \left(\frac{L}{r_t - r_b}\right)^{1/2}$$

$$= 42.3\left(\frac{L}{r_t - r_b^2}\right)^{1/2}$$

Konstantinov has developed a formula for finding out the required speed that provides good mechanical properties, adequate pressure tightness and other characteristics to the casting [40]. FGMs are metallurgically designed materials for a particular gradient thickness and volume fraction and are fabricated with minimum two different materials having different densities, states (liquid metal and solid particles), size and shape of particles. So the G value applied for the homogenous mixture doesn't work. It should be determined by the above calculated factors. Lesser the G value means lesser speed and centrifugal force which leads in less volume fraction within more

radial gradient thickness. Higher G value means higher centrifugal force for denser particles and higher volume fractions in outer zones of castings with steeper gradient.

From various alloys, if the centrifugal force acting on the melt reaches the value at which its effective density becomes equal to 340g/cm^3. According to him, the rotational speed (N) may be calculated with the formula,

$$N = \left(\frac{5520}{\sqrt{\rho r}}\right)$$

where, 5520 = The value of coefficient, taken to be constant for all alloys
ρ = The density of a casting
r = The internal radius of the casting

In casting of shaped parts, the filling of metal in contours will be an important matter. As from experiments it is found that for best results the rotational speed of a mould is so chosen that the peripheral speed of a casting point most distant from the axis of rotation is equal to 3 - 5m/s. The peripheral speed (v) of any point of a rotating body may be calculated by the formula.

$$v = \pi dN / 60$$
$$N = 60\ v / \pi d \qquad \text{d = diameter (2r)}$$
$$= 30\ v / \pi r$$

where, N = The speed of rotation (rpm)
r = The radial distance from the point to the axis of rotation (m)

1.7.2 *Advantages of Centrifugal Casting*

The main advantages of centrifugal castings can be summarised to the following points.

- As a production process centrifugal castings can be made to have rapid production rate.
- They can be used for both ferrous and non-ferrous metals and alloys.
- Large cylindrical parts can be produced by the centrifugal casting process.
- Generally patterns and cores are not required and hence the process is less expensive and economical.
- The inner periphery containing slag and impurities can be machined off easily.
- The centrifugally cast parts have good surface finish.
- Castings made from the centrifugal process have better life than sand castings.
- Centrifugal castings can be manufactured with a wide range of microstructures suited to meet the demands of the specific application.

- The process can produce good soundness, structure, texture and mechanical properties in the end product.
- Centrifugal castings have dense and even microstructure. They have radial and uniform grain flow.
- Castings are found to have better tensile strength and hardness.
- Overall centrifugally cast parts have high degree of metallurgical cleanliness and homogeneous microstructures.
- Centrifugally cast parts do not exhibit the anisotropy of mechanical property like rolled, welded and forged parts.

The main disadvantages of centrifugal castings are,

- Increased segregation of alloy components during pouring under the forces of rotation, for which reason not all the alloys can be cast by centrifugal method.
- Finishing allowances should be given for machining of the internal surfaces.
- Control of gradation in case of FGM is difficult due to a number of reasons.

1.7.3 *Applications of Centrifugal Casting*

Centrifugal casting is used to produce axi-symmetric components such as pipes, bushings, cylinders and other shapes like gear blanks, pulley sheaves, wheels, impellers, and electric motor rotors. This can also be used to produce valve bodies and bonnets, plugs, yokes, brackets, and a wide variety of various industrial castings. Centrifuging refers to forcing of metal from centre into the individual mould cavities. Here several identical moulds are located in radial positions and metal is fed into the cavities through a number of radial gates. The whole mould is rotated with the central sprue has the widest field of application. In this method, the casting cavities are arranged about the centre axis of rotation like the spokes of a wheel, thus permitting the production of multiple castings. Horizontal centrifugal casting machines are generally used to make pipe, tubes, bushings, cylinder sleeves (liners), and cylindrical or tubular castings that are simple in shape. Engineering applications like, Al-SiC FGM fishing boat cable pulleys and clutch drums composed of hard TiC particles embedded in Aluminium bronze matrix for naval applications are fabricated successfully by centrifugal casting method.

Chapter 2

Literature Review

2.1 INTRODUCTION

FGMs are advanced class of composite materials having discrete or continuously varying compositions and microstructural properties over a definable geometrical length. Since the volume fraction of reinforcement varies from one point to another in a given direction, there is transition in both mechanical and tribological properties of the material. For these reasons, FGMs are one of the most potential and prominent systems for the design and fabrication of components and structures with gradient properties with wide applications in the aerospace and automotive sectors.

Centrifugal casting is a pressure die casting technique for shaping and feeding according to the variation of the process employed. The principle of the process was established long back. A. G. Echardt in 1809 got a patent for the first time in the history of centrifugal casting technology [40]. The first industrial use of the process was started, since in 1848, in Baltimore when the centrifugal casting was used to produce CI pipes. In the 1890s the principles, already known and proved for liquid in rotation about an axis, were extended to liquid metal and in the early 1920s, the mathematical theory of centrifugal casting was developed. After these, in 1920 a process has established for making cast iron pipes for large scale. Now the process has been using for wider range of alloys and different shapes. The major events in the field of centrifugal castings and FGMs are summarised in the Table 2.1.

Table 2.1: The major events occurred in the field of Centrifugal Castings and FGMs

Year	Milestones
1809	First patent on centrifugal casting process obtained in England by A.G. Echardt.[40]
1848	First industrial use of the process in Baltimore to produce cast iron pipes.
1920s	Large-scale manufacturing of cast iron pipes and development of mathematical theory for centrifugal casting.
1972	Theoretical papers on usefulness of FGM by M.B. Bever, P.F. Duwez , & N.Shen [37]

1980s	Fabrication of metal matrix composites by centrifugal casting
1987	Research on the basic technology for the development of functionally gradient material for relaxation of thermal stress, commenced in Japan.
1987	First proposal of a graded interlayer concept in metal/ceramic bonding by Kawasaki and Watanabe
1987	FGMs concept applied to create a fuselage surface and engine parts for a space plane by M.Niino, T.Hirai and R.Watanabe [37].
1990	Processing of functionally graded materials by centrifugal casting by Yasuyoshi Fukui [41]
1990	Proc. 1st int. Symposium. On 'functionally gradient materials', Sendai, Japan, 1990, functionally graded materials forum And the society of non-traditional technology by M. Yamanouchi, M. Koizumi, T. Hirai, And I. Shiota (Eds):
1994	A solidification analysis on centrifugal casting of metal matrix composites containing graphite particles
1994	First time FGM was manufactured by S.A.Venkshinskii [40]
1997	Polymer composites with a gradient of reinforcements by centrifuging by N. J.Lee, J.Jang, M.Park, C.R.Choe [101]
1996-98	Monbusho project, physics and chemistry of functionally graded materials(1996-1998) by Toshio Hirai and Watanabe
2000s	Functionally grade aluminium composites by centrifugal in-situ casting
2000	Modelling the solidification of functionally graded materials by centrifugal casting by J.W. Gao, C.Y. Wang [48]
2006	Mathematical modelling of particle segregation during centrifugal casting of metal matrix composites by Emila Panda et al. [99]
2007	Numerical modelling of centrifugal casting of functionally-graded aluminium matrix composites by Gustavo Gutierreza, O. Marcelo Suárezb, and Mauricio A. Giordano [99]
2007	Methods of preparing polymeric gradient composites by J.Stabik, A.Dybowska [124]

2.2 GROWTH OF FGM

In1991, Fukui had conducted a fundamental investigation of FGM manufacturing system using centrifugal force for a suitable centrifugal casting technique for ceramic-metal FGM [41]. A mixture of plaster and corundum was cast into rings with four different volume fraction of corundum at three different G factors (speeds). The corundum profiles along the radial direction were measured and a mathematical model with cubic order polynomial was developed for correlation of the volume fractions at various positions. Since the plaster ($CaSO4.2H_2O$, white in colour) has a density 1.7 and corundum (Al_2O_3 black in colour) has a density 3.1g/cm^3, during casting the denser corundum will diffuse towards the outer diameter of the ring giving a white to dark

gradation in colour which is directly proportional to the volume fraction of the reinforcements at different locations. Fukui was able to successfully analyse, develop the model and explain the usefulness of the centrifugal casting method for the production of functionally graded materials (FGMs).

Determination of temperature distribution during centrifugal casting process, and solidification time of centrifugal castings by experimental techniques is very difficult, as the mould rotates at a high speed during solidification. In view of this, accurate data on solidification time were not available. Therefore, it was necessary to estimate and their influence on other processing parameters through indirect means. An one dimensional heat transfer analysis during centrifugal casting of Al-Si alloy composite containing graphite particles has been studied by C G Kang and P K Rohatgi [42]. An explicit finite difference scheme was adopted and the results indicated that the thickness of the graphite segregated region due to centrifugal force was strongly influenced by speed of rotation of the mould. This layer thickness near the inner periphery decreases with increase in speed and thereby increasing the volume fraction of dispersion. The solidification time of the casting was also dependent upon the speed of rotation, and it decreased with increase in speed. Meanwhile, the presence of particles increased the solidification time of the casting.

In 1995, A. Mortensen and S. Suresh tried to categorise and bring together the multiplicity of processing methods in the field of FGM. They classified the FGM processes into broad families, and discuss the fundamental issues significant to each process class [43]. Attention also been devoted to discuss thermal and mechanical analysis of FGM structures, with a particular emphasis on thermal stresses, plasticity and failure, which were highly relevant to FGM structures containing metals. Since graded composites contain a large number of microscopic and macroscopic interfaces, the micro-mechanisms of fundamental and practical interest can extend over a broad range of size scales. While atomic level modelling is necessary for a complete understanding of microscopic interfaces, the interface separation laws gives the knowledge of the force-displacement relations in an atomic level and the conditions for macroscopic failures.

An in-situ Al-Fe FGM composite pipe with $Al_{13}Fe_4$ phase as reinforcements were processed by Wang Qudong and Jin Junze [44]. The denser reinforcements, during solidification, moved towards outer regimes forming different layers, as reported. The

microstructure, hardness and wear properties obtained were proportionate with the volume of primary $Al_{13}Fe_4$ present in the location, from which the samples are prepared. Akira Kawasaki and Ryuzo Watanabe, in their article, discussed briefly about the various processing method existed and a detail discussion of the production of FGM by powder metallurgy route [45]. The processing of two types of FGMs has been explained: Thermal stress relief type of PSZ/SS304 and Thermal barrier type of SiC/AIN/Mo. The design, fabrication and evaluation of microstructure characteristics and control of composition property of these FGMs were also explained in detail.

A numerical model for Al-SiC FGM was developed by Y. Watanabe, Noboru Yamanaka and Y. Fukui and the simulation results were compared with plaster-corundum FGMs with varying volume fraction of corundum [46]. They were able to establish that the results of computer simulation did not contradict the experiment using the mixture of plaster and corundum. Moreover, it was shown that the composition gradation can be controlled more precisely by simultaneously using mixed particles of different mesh sizes. And the computer simulation was also useful to predict the graded composition of the products manufactured by the centrifugal method.

The formation of the copper alloy /graphite FGM containing 7 and 13vol.% graphite particles, cast at 800 and 1900 rpm, was studied as a function of the rotational speed of the mould and the volume fraction of graphite particles by J. K. Kim and P. K. Rohatgi [47]. The thickness of graphite-rich zone was observed to increase with increasing volume fraction of graphite particles and with decreasing rotational speed of the mould. A fixed grid, finite volume method, fully implicit one dimensional solidification model of FGMs processed by centrifugal casting were developed by J.W. Gao and C.Y. Wang in 2000[48]. By taking particle transport into account, the numerical model was able to focus the interplay between the freezing front propagation and particle migration during the solidification. As per the simulation, the factors responsible for creation of the particle concentration gradient were: the geometrical nature of particle flow in the cylindrical mould, the angular velocity, and the solidification rate. Y. Watanabe, Akihiro Kawamoto and Koichi Matsuda tried to study the particle size distributions in FGMs by a model of plaster-corundum [49]. The particle size distributions were directly determined by the extraction of the particles from the plaster matrix. The results revealed that the larger particles were located in

the outer part of the tube. It was also found that the particle distribution was affected by the G number as well as the mean volume fraction of particles.

As there are more than 83 metals found in the periodic table, the field of metal matrix composite is too much to handle. Even with light metals and alloy system a detailed survey is unimaginable. A specific review on the literature with a very limited parameters, basically only aluminium matrix phase systems and the processing method should have the concept /similar to that of centrifugal casting/centrifuging will give a clear insight of the present status of area of research and can substantiate the selection of present material and the processes for the present research.

2.3 CENTRIFUGAL CASTING OF ALUMINIUM METAL MATRIX COMPOSITES

The study on the literature of centrifugal casting of aluminium metal matrix composites by centrifugal casting method is classified into several groups in terms of microstructural characteristics, gradient distribution of reinforcements, effect of gradation on mechanical properties, wear characterisations, use of new characterisation technologies, new fundamental techniques/methods developed and the computer modelling of FGMs etc.

2.3.1 *Microstructural Characteristics*

The fundamental properties of materials are governed by its basic microstructure, so in-turn; it is possible to evaluate the properties by a proper microstructural characterisation.

In this review article by Y. Watanabe and Y. Fukui, the Al-base intermetallic compound-dispersed functionally graded materials (FGMs) fabricated by a centrifugal method were reviewed on focusing the microscopic features observed by several analytical techniques [50]. FGMs were divided into three categories depending on the initial state of dispersed second phase at the processing temperature. Those were Al/Al_3Ti FGM fabricated by the centrifugal solid-particle method, Al/Al_3Ni and Al/Al_2Cu FGMs fabricated by the centrifugal *in-situ* method and Al/(Al_3Ti+Al_3Ni) hybrid FGM made by the simultaneous combination of both solid-particle and *in-situ* methods. The relation between microstructure and graded composition was also described. Moreover, Al-Ti supersaturated solid solution induced by wear of Al/Al_3Ti FGM was also shown.

They have suggested a mechanism which was applicable not only for the eutectic alloy but also for hypo-eutectic and hyper-eutectic alloys. The mechanism to form a

composition gradient in the *A-B* alloy system, which makes *A* matrix and an *AmB* intermetallic compound, by the centrifugal *in-situ* method was summarized as follows; Due to the density difference, partial separation of *A* and *B* metals in the liquid state will occur. A chemical composition gradient will be formed before the crystallization of the primary crystal. The primary crystal migrates according to density difference, and a further compositional gradient was formed.

A detailed study of microstructures was conducted by Y. Watanabe and Shin Oike in the Al–Al_2Cu FGMs fabricated by the centrifugal in situ method [51]. The particle sizes of the Al_2Cu and Al primary crystals were dependent upon their locations in the ring thickness. The graded structure appearing in the eutectic specimen was caused by the difference in the densities between Al and Cu in liquid state.

The microstructure and tribological performance of functionally graded Al–Mg/AlB_2 metal–matrix composites (MMCs) produced by centrifugal casting were investigated by Z. Humberto Melgarejo et.al [52]. Al–B master alloy was mixed with Al–Mg alloys to obtain different Al–2wt. % Mg alloys containing 1, 2, 3, and 4 wt.% boron. Thus the boron content of the alloy was made the primary variable to be investigated, while other process parameters important to centrifugal casting such as temperature, rotational velocity, and Al-diboride particle size were kept constant for all the samples. The rotation speed was set at 20 G and the pouring temperature of the alloy was 850°C. The 16 mm diameter and 25 mm long cylindrical castings were cut at 0 at inner, 5, 10, 15 and 20mm at the outer, along the radial direction.

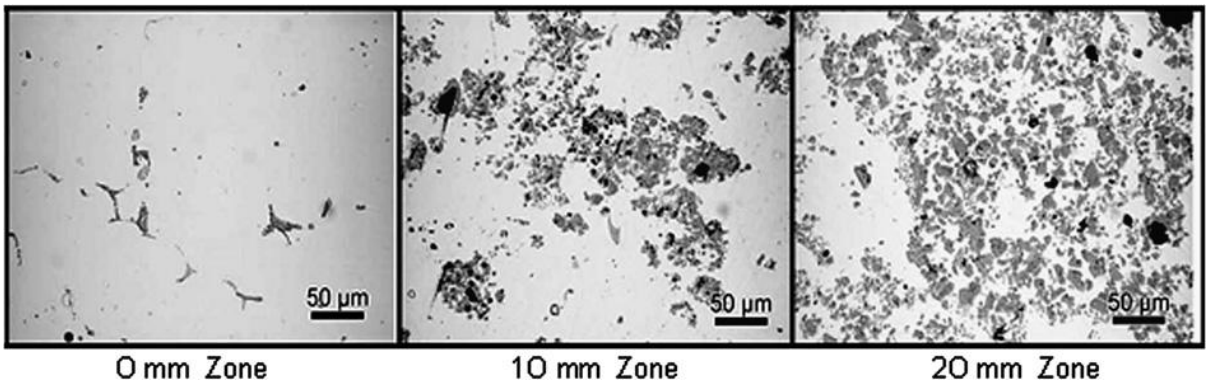

Figure 2.1: Micrographs of Al-2Mg-2B composite in various test sections [52]

Microstructural characterization of the centrifugally cast composites was performed along the radial direction of the casting and compared with that of homogeneous gravity cast composites. The microstructural characterization shows a significant enrichment of aluminium diboride particles at the outer regions (Figure 2.1).

Appreciable increments in hardness were observed even at lower radial distances for higher the boron contents. Low load Vickers microhardness tests were performed exclusively in the matrix of the composites also showed an increase with increasing boron content, an effect attributed to the higher dislocation density due to the higher volume fraction of AlB_2 particles. Consistent with trends in hardness, a corresponding increase in wear resistance were also observed in the outer regions of the FGM casting. Topographical and morphological analysis of worn surface by AFM and SEM/EDS analyses revealed abrasive and oxidative wear modes, the extent of which was dependent upon the boron content of the composite and the radial distance at which the tests were performed.

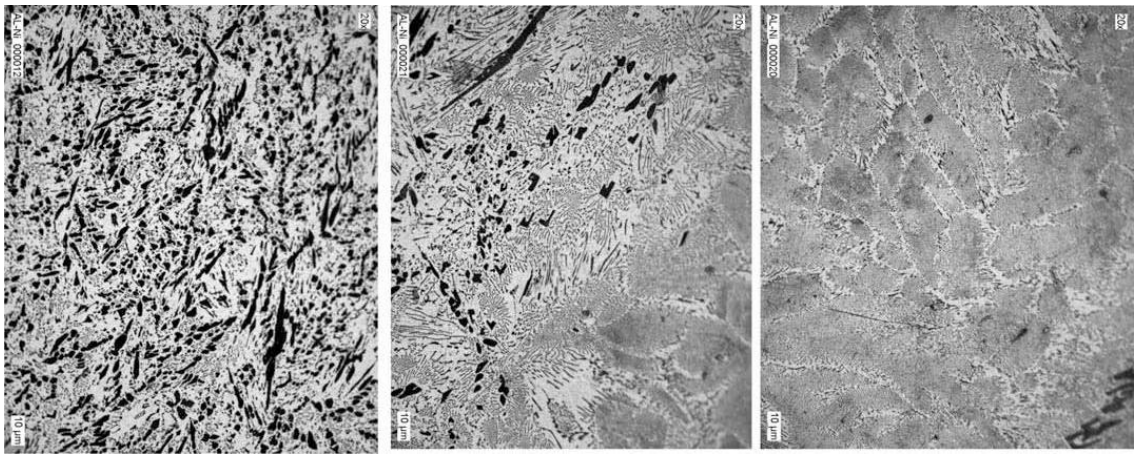

Figure 2.2: Optical micrographs of Al-Al_3Ni FGM formed using Al-20% Ni from outer to inner periphery of the casting [53]

Rajan and Pai correlated the gradient microstructures and the processing parameters of a wide range of Al alloy FGMs [53-54]. The systems processed were (a) Al-SiC FGM by A356(Al-7Si-0.35Mg) alloy reinforced with green variety SiCp particles of 23μm average particle size; (b) Al- B_4C FGM by A6061 (Al-1Mg-0.6Si) alloy with B_4C of 20 μm average particle size; (c) Al-Si FGM using A390 (Al-17Si-4Cu-Mg) hypereutectic, where the in situ primary Si particles act as reinforcements;(d) Al-Al_3Ni FGM formed from Al-20%Ni alloy(Figure 2.2) ; (e) Al-SiC-Graphite hybrid FGM using A356 reinforced with 23μm SiC and 60μm graphite particles; (f) Al-Si-Graphite hybrid FGM using A390 with ex-situ 60μm graphite particles and (g) Al-Si-Mg_2Si hybrid FGM using A390 with 5% Mg forming Mg_2Si. The densities and size of the reinforcements play a major role in the formation of graded microstructures, the high density particles/phases, both SiCp and Al_3Ni, form gradation towards the outer periphery with maximum volume fraction at outer regions and low density particles like graphite, primary silicon and Mg_2Si form

gradation towards inner periphery with maximum concentration at inner regions. The B_4C particle having closer density to Al alloy has given more scattered distribution compared to other systems.

2.3.2 *Reinforcement/Particle Distributions*

The location specific functional properties of FGM composites are mainly determined by the volume of reinforcement phases or particles present in that region. So it is very important to study the distribution of reinforcement particles or phases in the FGM in spatial directions.

In 1999, Thomas C Chamlee obtained a US patent for particulate field distribution in centrifugally cast composites of polymer resin and Al-Si alloy [55]. The SiC particles of 3-30μm sizes were used for A356 and A359 alloys. Particle size of 15 μm was used with low viscosity epoxy resin (CER-112-1). The particle distribution related to the speed of rotations 700, 1500 and 2200 rpm was given at different radial distances from inner towards outer diameter of the castings.

The effects of those parameters on graded distributions of the volume fraction and orientation of platelets were investigated by P. D. Sequeira et.al by fabricated FGM rings using Al alloys with different Al_3Ti platelet volume fractions and platelet sizes by the centrifugal solid-particle method [56]. Al-platelet/plaster FGMs were used as a model system. It was found that an increase in initial volume fraction and particle size leads to steeper gradients of volume fraction and orientation distributions within the Al-Al_3Ti FGMs. The results of the experimental studies are compared to those of the model material. With some limitations, the proposed model system and 3D orientation observation system would be useful in the study of the formation mechanisms of the graded distributions in the FGMs.

Functionally graded Al-Al_3Ni in situ intermetallic composites using commercially pure aluminium and Al-75wt. % Ni master alloy were processed by Rajan et.al [57]. To the aluminium melt, the required amount of master alloy was added at 800°C and poured into a mould, rotating at 1500 rpm, fixed in the vertical centrifugal casting machine. Different alloy systems, Al-*x*Ni (*x*= 0, 20, 30 and 40 wt. %) were studied. Higher pouring temperatures were maintained for having sufficient fluidity and time for Al_3Ni phase formation and its diffusion towards the outer periphery before the solidification of the mix. The holding and pouring temperatures used for different

aluminium-nickel alloys were 800 °C for Al-10Ni and 900°C for Al-20, 30 and 40Ni systems. The microstructural characteristics and hardness profile of these FGMs have been evaluated. The gradation in microstructural features were reflected in hardness values too. The FGM composite formed from Al-20 Ni showed a high volume fraction of Al_3Ni primary phases near the outer periphery and a depleted region near the inner periphery. The region near outer periphery had a hypereutectic microstructure and that nearer the inner periphery was hypoeutectic. The FGM composite formed from Al-10Ni showed almost a hypoeutectic microstructural features everywhere except near the outer periphery region, which containing a few Al_3Ni phase. However there were variations in volume fraction of eutectic phase, higher near the outer periphery and lower near the inner periphery for each system. The FGM formed from Al-30Ni and Al-40Ni showed only a hypereutectic microstructural features throughout. Amongst the four alloy systems studied, Al–20Ni gives the best graded microstructure.

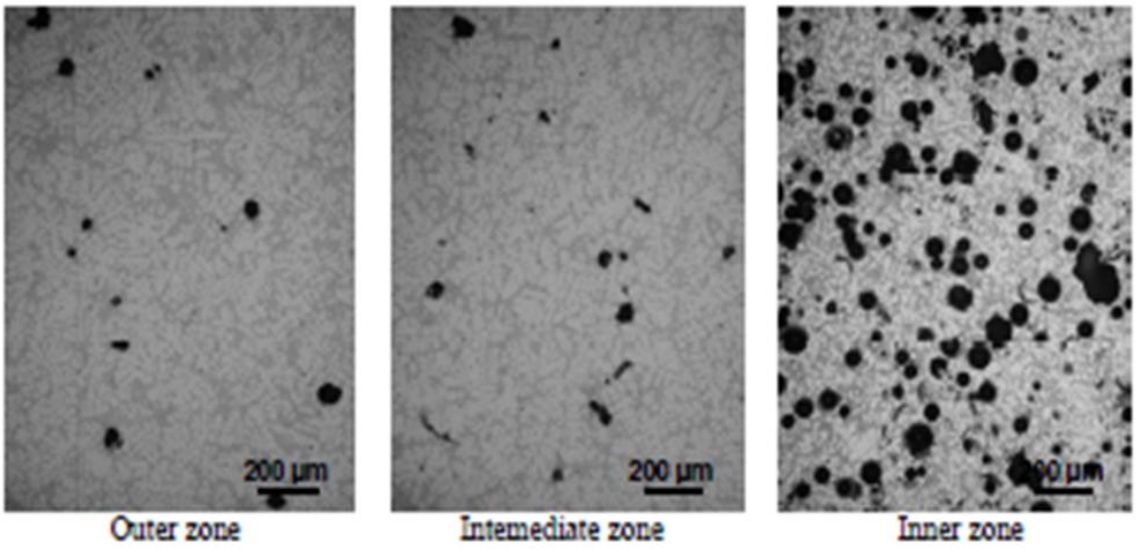

Figure 2.3: Microstructure of Al/10vol.% SiO_2-Al_2O_3 SFGMMC from outer towards Inner zones [58]

Particle gradients in the centrifugally cast composites were investigated by quantitative image analysis of optical micrographs for a syntactic functionally graded metal matrix composite (SFGMMC) with hollow ceramic microspheres (microballoons) by S.C. Ferreira et.al [58]. Aluminium based SFGMMC rings were fabricated by radial centrifugal casting. The density of the SiO_2-Al_2O_3 microballoons is lower than that of molten aluminium; the particles show a tendency to remain closer to the inner periphery of the ring. Thus the microballoon volume fraction increases along the radial direction of the ring from the outer to the inner periphery. The commercial SiO_2-Al_2O_3

microballoons (particle size: 50 μm; particle volume fraction: 5 and 10 %) with Al-7Si-0.3Mg (A356) alloy composite was melt under an Argon atmosphere at 850°C and directly poured into a rotating mould rotating at 750 rpm for 1 minute, in order to obtain a ring-like SFGMMC. A steep reinforcement distribution gradient was observed between the intermediate and the inner zones, the microballoons tending to remain confined to the latter (Figure 2.3). Also, the presence of reinforcement particles seems to induce a higher matrix porosity level in the inner zone, as compared to the microballoon-depleted zones.

Hypereutectic Al-xSi-yMg functionally gradient composites reinforced with primary Si and Mg_2Si particles by centrifugal casting were made. The influence of Si and Mg contents on microstructures of the Al-xSi-yMg FGM composites was investigated by Xuedong Lin et.al [59]. Commercial Aluminium alloy of Al-18Si-1.2Mg, pure Si and Mg metals were mixed to get the required alloy compositions. The seven types of hypereutectic Al-Si-Mg alloys were studied and they were divided into two groups. In the first group, three kinds of Al-Si-Mg alloys were prepared with different Mg levels 2, 4, and 6%, with Si content kept constant at 20%. In the second group, four kinds of Al–Si–Mg alloys were prepared with different Si levels 17, 19, 21, and 23%, with Mg content kept constant at 4%. The raw materials were melted with an electronic resistance furnace. After modification at 740°C, seven kinds of alloy melts were poured at temperature of 720°C into a hot mould of 200°C in a horizontal centrifugal machine.

The microstructural observation found that, the tubes consist of an inner layer, the middle layer, and the outer layer measured in the radial direction. The inner layer segregates blocky primary Si and Mg_2Si particles, the middle layer contains no primary Si and Mg_2Si particles, and the outer layer contains few primary Si and Mg_2Si particles. During the solidification, both Mg_2Si and primary Si will move towards the inner wall of the tube together (Figure 2.4). It was found that the blocky primary Mg_2Si particles have greater centripetal velocity than that of primary Si particles due to it's lower density. The primary Si particles were pushed by blocky primary Mg_2Si particles. Calculating the volume fractions of primary Si and Mg_2Si particles in the segregation region of the inner layer, it was found that, with the content of 20% Si unchanged, the mean volume fraction of primary Mg_2Si particles showed an ascending tendency, and that of primary Si particles showed a descending trend as the Mg content gradually increased. With the

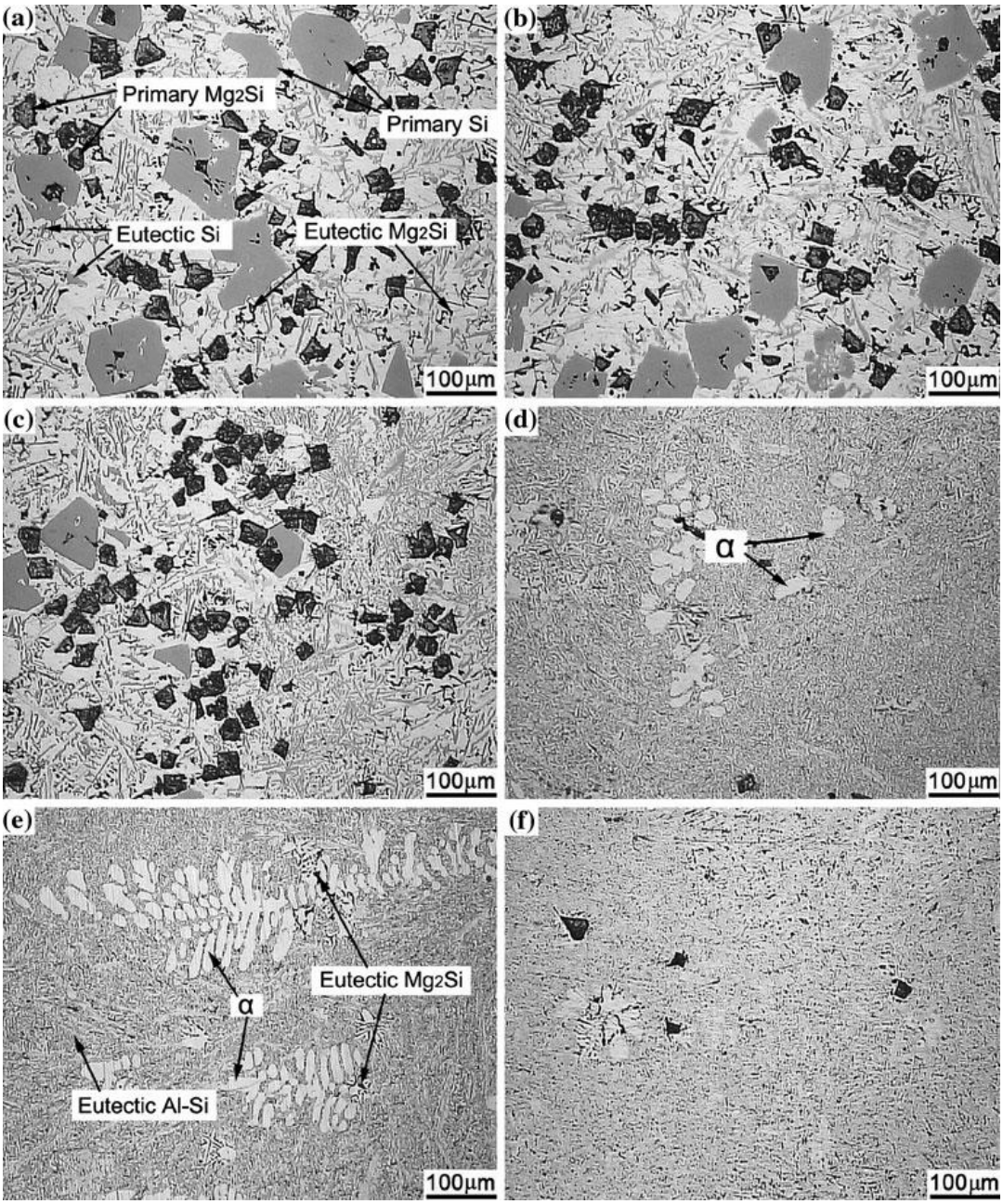

Figure 2.4: Microstructures in different regions at a 1.5 mm, b 3.0 mm, c 4.5 mm, d 7.0 mm, e 9.5 mm, and f 12.0 mm in the cross section of Al–20Si–4Mg tube [59]

content of 4% Mg held constant, the average volume fraction of primary Si particles first decreased, and then increased. Average volume fraction of primary Mg_2Si particles rose at first, and then remained in a relatively stable state as the Si content increased gradually. Calculating the sizes of primary Si and Mg_2Si particles in the segregation region of the inner layer of the five alloy tubes, it was concluded that, the average size of primary Si particles was mainly determined by two factors. One was the content of Si, the more the content of Si the larger the Si particles in the final casting. The second

factor was the pushing effect of primary Mg_2Si particles to primary Si particles. As the volume fraction of Mg_2Si particles increases the pushing effect also increases and the larger will be the size of the primary Si particles. The average size of primary Mg_2Si particles had a slight increase as the content of Mg increases.

2.3.3 *Effects of the Speed of Rotation of the Mould*

In centrifugal casting, one of the critical parameters which determines the gradation of chemical composition, microstructure and reinforcement particles (phases) is the G factor (the ratio of centrifugal force to the gravitational force). The G factor is directly related to the speed of rotation of the mould during the casting process.

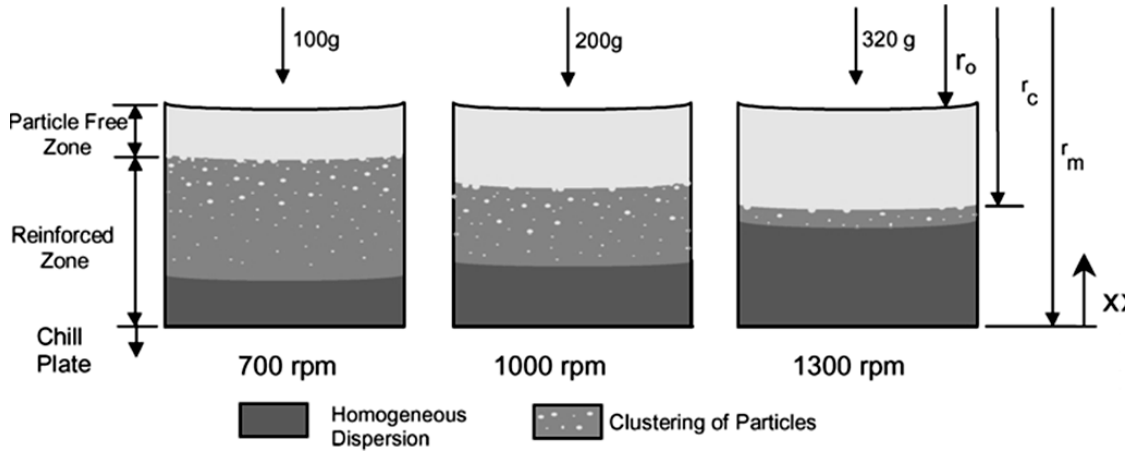

Figure 2 5: Schematic cross sections of the three castings [60]

The characterisation results at different speeds rotation of the mould were discussed on SiC particles distribution, particles solidification front interactions, matrix micro-structure, and porosity distribution in the castings as a function of the centrifugal forces applied. Rodriguez-Castro and Kelestemur used the centrifugal casting method for the processing A359-20 vol % SiC particles FGM composite [60]. The reinforcement particles were essentially single crystal alpha-SiC, with a median particle size of 12.8±4.2 μm. It was reported that the concentration of particles was very homogeneous for the 1300-rpm casting, whereas some clustering of particles was detected in the 700-rpm and 1000-rpm castings (Figure 2.5). The volume fraction profiles varied as the centrifugal force was applied, and concentrations as high as 44 vol % were obtained at the outer circumference for the maximum angular speed. The casting conditions used in the 1300-rpm casting resulted in a homogeneous progressive concentration of particles due to the engulfment promoted by the high relative velocity between the solidification front and the particles, and also due to the elevated cooling rates. The matrix structure

was modified in the reinforced region as a consequence of rapid solidification and also due to breaking of dendrites by the combined loading action of accelerated particles and loaded dendrites. Quench modification of the eutectic structure was observed in the casting from inner towards outer in radial direction. They had detected microporosity in the castings at 1300 rpm case, in contrary to expectations and concluded that it may be due to the higher concentrations of particles, which decreases the ability of inter-dendritic fluid flow to feed solidification shrinkage.

The speed of rotation of the mould the centrifugal casting process in order to optimise the reinforcement distributions in the inner regions of the aluminium cylinder liners were analysed by Bonollo et.al [61]. A357-15% SiC particles (average size: 10 microns) composite, centrifugally cast in a cylindrical mould rotating at 500-1000-1500 rpm was fabricated and tested. They found a combination of the main processing parameters of casting temperature 750 °C, mould temperature 350 °C and the initial reinforcement vol % of 15 were found to be an optimal one, with an ideal reinforcement distribution, for the cylinder liner fabrication.

Xie Yong et.al processed in-situ FGM cylinders at different speeds and mould temperatures with equivalent of Al-19Si-5Mg alloy [62]. 3% of phosphorus salt modifier for the primary silicon modification and 0.2% of rare earth alloy for compound modification were added to the melt at 780°C. The metal mould was pre-heated to 220,250° and 360°C and the pouring temperature of the melt was 706 and 786°C. The melt was poured into a mould rotating in a vertical centrifuge machine at different speeds of 450, 600 and 800 rpm. *In-situ* FGM cylinders of outer diameter of 130mm and wall thickness 15 mm were obtained. Across thickness of the casting, microstructure characteristics showed that accumulation of Mg_2Si particles and a portion of primary silicon particles in the inner layer and in the outer layer with a little Mg_2Si and primary silicon particles (Figure 2.6). While in the middle region, no Mg_2Si or primary silicon particles were observed. As the centrifugal speed was increased, the amount of Mg_2Si and primary silicon increased in the inner layer and when the temperature of the preheated mould was increased, more Mg_2Si and primary silicon grains gathered in the inner layer and a more obvious graded distribution of the phases was formed in the component owing to a longer solidification period of the molten metal in the mould. A higher pouring temperature facilitates the formation of a stronger graded distribution of the phases were observed. The results indicated that the rotation rate of centrifugal

casting, mould temperature, and melt pouring temperature have evidently affected the accumulation of the secondary phase particles. Also, the higher the centrifugal rotation rate, mould temperature, and melt pouring temperature, the more degree of accumulation of Mg_2Si and primary silicon particles in the inner layer were evident.

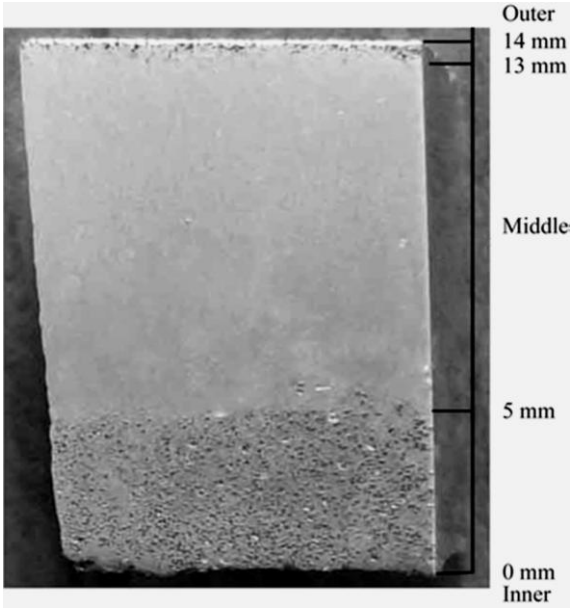

Figure 2.6: Macrostructure of the test section showing the three-tier distribution of particles [62]

The influence of the flow of molten metal during the horizontal centrifugal casting of hyper eutectic Al-2Si alloys at various rotational speeds were studied by Mukunda et.al [63]. The speed was varied from 200 rpm to 2000 rpm. At an optimum speed of 800 rpm, a uniform cylinder was formed. For the rotational speeds below and above these speeds, irregular shaped castings were formed, which was mainly due to the influence of melt. It was found that at the optimized speed, the mechanical properties of the casting improved.

As a function of rotational speed and pouring temperature of the melt, the redistribution of AlB_2 and AlB_{12} reinforcing particles in functionally graded Al-B-Mg composites was investigated by Tunde Kingsley Adelakin and Oscar Marcelo Suárez [64]. Al-2B-6Mg composite was prepared with pellets of pure aluminium (>99.999%), commercial Al–B and Al–Mg master alloys with 7.2% boron and 10% magnesium, respectively. The required composition was melted in a graphite crucible at 850°C, homogenized and poured at (690°C and 800°C) to the cylindrical graphite mould at 500°C rotating at (300rpm and 400 rpm) in a centrifugal casting machine. The resulting dimensions of the specimens were 60mm long with 12mm in diameter. The density of

the aluminium borides are higher (3,190 kg/m^3 for AlB_2, and 2,600 kg/m^3 for AlB_{12}) than liquid Al, estimated at 2,400 kg/m^3 for normal casting temperatures, i.e., 700°C and at higher temperatures the density of molten aluminium decreases even further. The microstructure was characterized both qualitatively and quantitatively on four different sections along the centrifugal direction of the casting (Figure 2.7).

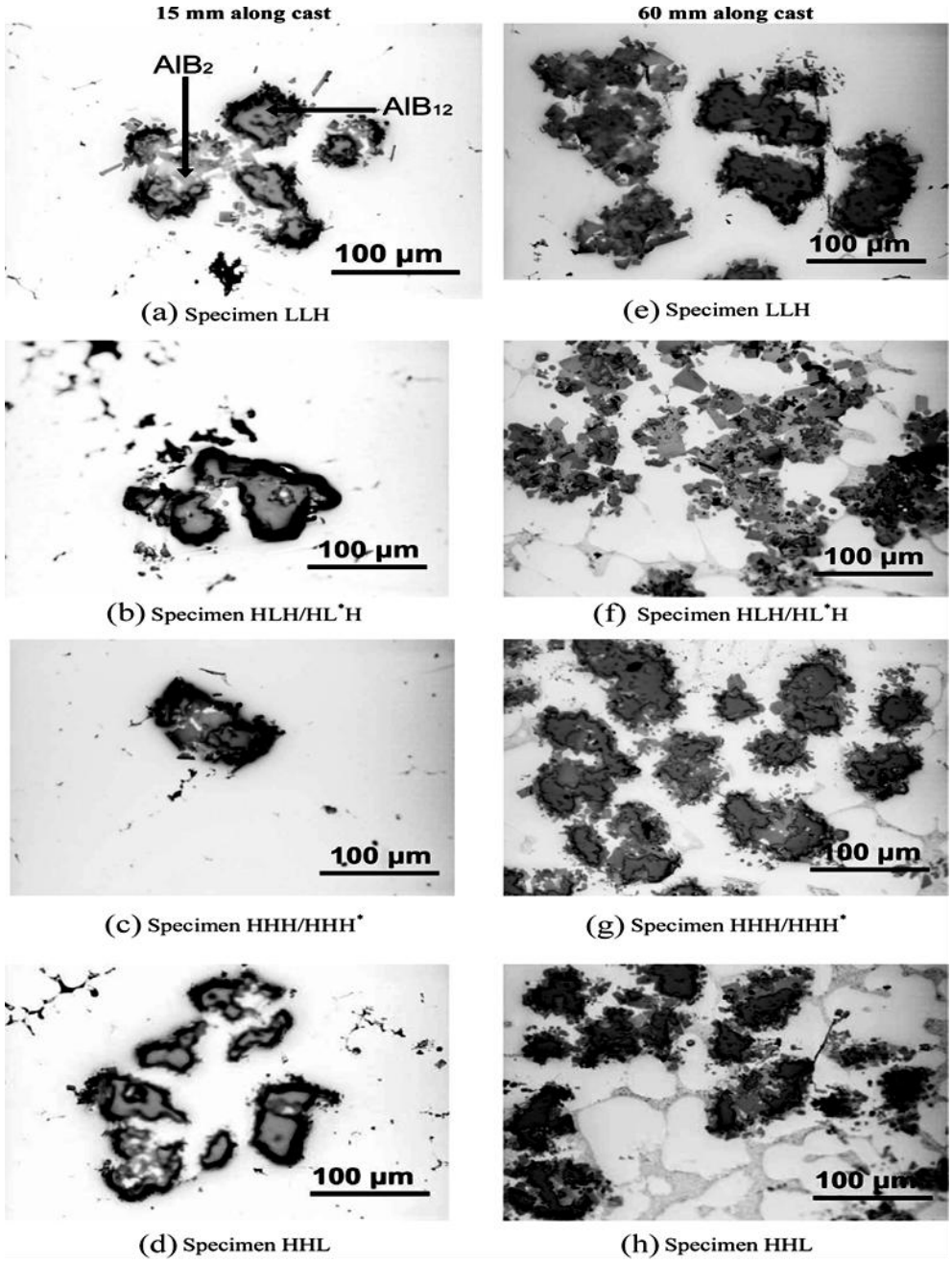

Figure 2.7: Optical micrographs of as-cast microstructures of Al–B–Mg along the main axis of the cylindrical castings at different parameter combinations [64]

The resulting FGM composite showed an evident gradient of particles concentration, with more particles at the external zone than at the internal zone of the

casting. Processing temperature was found critical for its direct effect on the viscosity of the liquid, which regulates the segregation of the reinforcements. As expected, the higher concentration of particles on the external regions of the castings raised the measured superficial Rockwell hardness and Vickers microhardness of the composite. The energy dispersive spectroscopic analysis (EDS) indicated that Mg was dissolved in the AlB_2 dispersoids but not in the AlB_{12} particles. The addition of magnesium favours the transformation of AlB_{12} into smaller $Al_xMg_{1-x}B_2$ particles. SEM analysis revealed the difference in morphology between AlB_{12} and AlB_2 particles in terms of shapes and contrast. The rotational speed for this composite was the less significant processing parameter in promoting a compositional gradient and its influence was probably masked by the pouring temperature and the casting time.

2.3.4 *Effect of gradation on Mechanical properties*

The practical application of FGM components basically lie with the effective gain in the changes achieved in specified properties which are very essential for the proper functioning of the system. The mechanical properties are the fundamental requirements for any component for the structural rigidity of the components used for automobile and aerospace applications.

The effect of the composition gradient on the Young's modulus and internal friction of Al-Al_3Ni FGM from the transverse free-free vibrations of rectangular beam specimens have been measured and analysed by Y. Fukui, K. Takashima and C. B. Ponton [65]. The thickness of the rectangular beam specimens was varied to change the composition gradient of each specimen. The effect was determined by the measurement of flexural resonant frequencies using a forced-resonance technique on four rectangular bar specimens of differing thickness and hence composition. The average volume fraction of the granular Al_3Ni second phase in an Al-Al_3Ni, FGM manufactured by a centrifugal casting method was found to be 33.5, 36.4, 38.5 and 40.3 vol % for the nominal 6, 5, 4 and 3 mm thickness specimens, respectively. The Young's modulus of the Al_3Ni second phase was determined from the measured resonant frequencies as 140.6, 140.4, 139.2 and 139.1GPa for the nominal 6, 5, 4 and 3 mm thickness specimens, respectively, by applying a rule of mixtures. The average Young's modulus of the Al_3Ni second phase is found to be 140GPa. The Young's modulus variation within the 6 mm thick bar specimen ranged from a maximum of 100.8GPa to a minimum of 81.5GPa,

corresponding to an Al_3Ni content of 43.2 and 15.2 vol %, respectively. The internal friction of the FGM increases with increasing mean volume fraction of Al_3Ni and appears to depend mainly on the resultant increase in the interface density.

A comparison of mechanical properties of specimens obtained by both centrifugal casting technique and gravity casting technique were made in hypoeutectic, eutectic, and hypereutectic Al-Si alloy by G. Chirita et.al [66]. It was observed that the centrifugal effect produced an increase in rupture strength in approx. 50%, and in rupture strain in about 300% as compared to the gravity casting. The young modulus also increased about 20%. The higher the distance in relation to the rotation centre (higher centrifugal force) the bigger the increase in mechanical properties. The graded effect on mechanical properties seems to be material dependent. The main features of centrifugal effect on castings were divided into three: centrifugal pressure; intrinsic vibration of the process; and fluid dynamics. The centrifugal casting process was effective even for materials with similar phase densities or metal densities in the same alloy. It was possible to obtain much better mechanical properties along the whole casting, as compared to the gravity casting process. The process could be explained based on at least two variables: centrifugal pressure + vibration or centrifugal pressure + fluid dynamics. The silicon content plays a very important in the effectiveness of the previous variables on Al-Si alloys.

Mechanical and metallurgical properties of a hypereutectic Al–18Si alloy were investigated to found out the influence of the vertical centrifugal casting technique by Chirita et.al [67]. Due to the inherent vibration of the centrifugal casting technique, and in order to study and understand the individual effects of the equipment vibration and the centrifugal force (pressure or fluid dynamics) and the combined effect of both, separate tests were carried out for gravity, gravity with vibration and for the centrifugal casting. The centrifugal pressure did not to substantially influence the casting properties. The inherent vibration of the centrifugal casting had a significant influence on casting mechanical properties, by promoting a quicker solidification rate (Figure 2.8). The fluid dynamics effect of the centrifugal casting was the main factor promoting higher mechanical properties by dispersing the mould temperature transfer through the whole mould thereby increasing the solidification rate. The properties of the centrifugal casting process were found depend on the combined effect of the centrifugal pressure and/or fluid dynamics and on the inherent vibration.

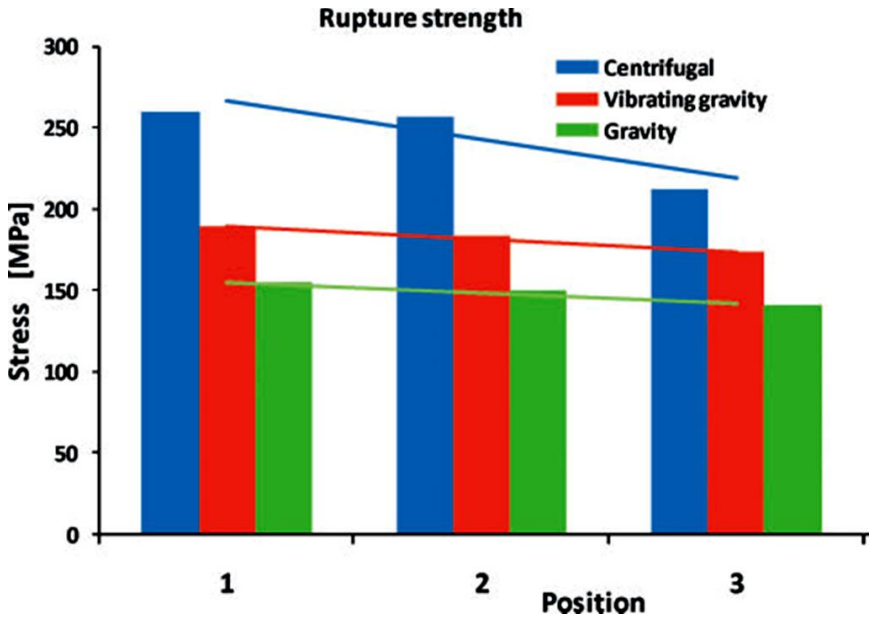

Figure 2.8: Rupture strength for three casting techniques: gravity; gravity with vibration (8 Hz); centrifugal casting [67]

The advantages in mechanical properties of using the vertical centrifugal casting technique over the traditional gravity casting for the production of structural components were compared by Chirita et al. [68]. The material used for castings was an aluminium alloy AS12UN with a composition: Fe-0.75, Si-(11.50–13.00) Zn-0.20, Mg-(0.75–1.30), Ni-(0.80–1.30), Pb-0.10, Sn-0.05, Ti-0.20 in percentages with balance Al. The material was melted at 670°C and poured into the permanent mould which was preheated at 130°C. It was observed that the centrifugal casting increased the rupture strength by 35%, and rupture strain by 160% over the gravity casting technique. The Young modulus also increased 18%. The fatigue life experienced an increase of about 1.5times and the fatigue limit increased by 45%. The centrifugal casting process was found to be much more effective in terms of obtained mechanical and fatigue properties as compared to gravity casting. The previous effects vary within the FGM casting, the higher the distance in relation to the rotation centre (higher centrifugal force) the bigger the increase in mechanical properties.

2.3.5 *Wear Characterisations*

Another important functional parameter which is very essential for the design and selection of material for the components of machines and mechanisms with a relative motion between them so that there exists either a sliding or a rolling contact surface is the wear characteristics.

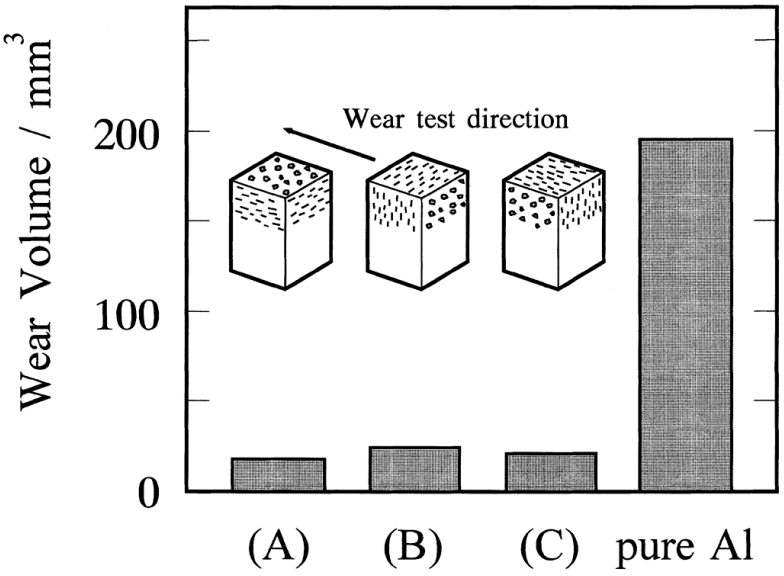

Figure 2.9: The wear volumes of the composites tested under an applied stress of 0.5 MPa at 2 km sliding distance [69]

A thick-walled tube of Al-Al_3Ti FGM, by the centrifugal method from a commercial ingot of Al-5Ti master alloy, was processed by Watanabe, Noboru Yamanaka and Fukui [69]. The alloy was heated to a temperature where solid Al_3Ti particles resided in a liquid Al matrix, and then the centrifugal method was carried out. The Al_3Ti particles were arranged with their platelet planes nearly normal to the radial direction as a result of the applied centrifugal force. The wear resistance of the Al-Al_3Ti composite was significantly higher than that of pure Al. Wear-resistance anisotropy and dissolution of the Al_3Ti into the Al matrix at the near-surface region, around 100mm in depth, were also observed (Figure 2.9). The volume fraction of the Al_3Ti platelets was enriched at the tube's outer region, where Al_3Ti platelets were arranged with their platelet planes nearly perpendicular to the radial direction, *i.e.*, in the centrifugal force direction. A wear-induced supersaturated solid solution layer (supersaturated layer) was formed near the worn surface region, roughly 100 mm in depth. The formation of the supersaturated layer was considered to be a result of the large subsurface strains and plastic deformation rather than from rapid quenching.

The wear mechanisms, in Al FGM Composite by reciprocating pin-on-plate sliding wear tests were investigated Gomes et.al [70]. The experiments were performed without lubrication and in the presence of an aqueous solution of 3% NaCl to simulate a corrosive environment. A comparative analysis was established between nonlubricated and lubricated tests for the tribocorrosion behaviour of AMCs. For sliding under no

lubricated condition, the friction coefficient was not significantly affected by SiC content on the FGM composite (f =0.42). A lower friction and wear values were obtained for the FGM composite with higher amount of reinforcing particles (33.4%) due to their ability to anchor iron-rich protective tribolayers and load-supporting effect given by SiC particles. The presence of an aqueous sodium chloride solution was neither promoted any significant lubricious effect and nor affected in the wear rate of the composites. Together with the corrosion phenomena, removal of material by wear from the Al-based matrix and pull-out of SiC particles due to the dissolution of the particle/matrix interface became dominant factors, which determines the weight loss of the material.

The wear tests, and wear track analysis were conducted for Al–B–Mg FGM composites. Humberto Melgarejo et.al manufactured aluminium FGMs reinforced with in-situ AlB_2 by centrifugal casting [71-72]. A commercial Al–5wt. %B alloy and an experimental Al–4wt.%B with 2 wt.% Mg alloys were used. The casting was carried out with a rotational speed of 200 rpm and the pouring temperature was set at 750°C. As a result of the inertial forces created during the centrifugal casting process, the AlB_2 reinforcement particles (with higher bulk density, 3.19 g/cm^3, than liquid aluminium, 2.4 g/cm^3) segregate towards the surface regions. It was observed that the wear rate and the hardness values were consistent with the observed microstructural gradient. The higher volume density of AlB_2 particles in the outer regions of the FGM sample imparts a higher hardness and higher overall wear resistance on those regions. While, the internal regions were fairly depleted of boride reinforcement particles and were subject to higher wear rates. As expected, the gravity-cast composite displayed an intermediate behaviour as the volume fraction of diborides is evenly distributed throughout the composite. Al–B composites did not fully display the gradient behaviour resulting lower superficial hardness and microhardness than Al–Mg–B composite.

The sliding wear behaviour was studied using a ball-on-ring configuration (sliding wear parameters: 3N, 0.5m/s, 1800m, room temperature) with a high-carbon chromium steel ball (AISI 52100) as counter body. Vieira et.al processed Al alloy/SiCp FGMMC with a non-commercial Al alloy (Al–10Si–4.5Cu–2Mg) and SiCp of average grain size of 37.8μm by centrifugal casting at two different mould rotating speeds (1500 and 2000 rpm)[73]. The homogeneous composites were melted at 850°C, under an Argon atmosphere (3bar) and poured into a radial rotating mould. A good correlation was evidenced between the dry sliding behaviour of FGM composites and the distribution of

SiC reinforcing particles. FGM cast at low centrifugal speed (1500 rpm) presented a smooth gradient on SiCp distribution, while FGM cast at higher centrifugal speed (2000 rpm) revealed a sharper gradient distribution. A relation between the wear coefficient and the relative area fraction of SiC particles was found: the increase of SiC content up to~5% resulted in a fast decrease of the FGM composite wear coefficient, followed by an additional, but much slow, decrease of the wear coefficient values with the incorporation of SiC particles above 5%. Also, a relation was found between the amount of SiC reinforcing particles and the type of wear regime: for SiC contents lower than~2% the severe wear regime was dominant, followed by a continuous transition to a mild wear regime when the highest content of SiCp was attained (~36%). For the aluminium-based FGM composites considered two-body abrasion wear, oxidative wear, adhesion and delamination were the main wear mechanisms identified. Formation of a mechanically mixed layer was also reported, mainly constituted by iron, aluminium oxide, iron oxide and intermetallic compounds of Al-Fe and Al-Fe-O.

The worn surface morphology and the sub-worn surface layer of Al-5Zr FGMs by the centrifugal solid-particle method under applied centrifugal force of 30, 60 and 120G were investigated by Shimaa El-Hadad et.al [74]. The processing temperature was fixed to be 925°C and the molten Al-Zr alloy was poured into a spinning cylindrical mould preheated up to 650°C. Microstructural observation along the centrifugal force direction showed that Al_3Zr platelet particles were almost oriented normal to the applied centrifugal force direction. Volume fraction of Al_3Zr particles increases close to the ring surface. Moreover, this distribution range of Al_3Zr particles becomes broader with decreasing the applied centrifugal force. The wear anisotropy of the fabricated Al/Al_3Zr FGMs was strongly influenced by the platelet particles orientation at the test position (Figure 2.10). The plastic deformation induced wear was the dominant mechanism during the wear process of Al/Al_3Zr FGMs samples. Therefore, some of the tested samples were severely deformed and an Al_3Zr particles-free layer containing Al-Zr supersaturated solid solution was observed very near to the worn surface during the wear test. A subsurface layer contains Al-Zr supersaturated solid solution without the presence of Al_3Zr phase was formed very near to the worn surface during block-on-disc wear test of the fabricated FGMs. This layer was more identified when the tests were performed perpendicular to the Al_3Zr platelet particles alignment. The abrasive wear was coexisted as sub-wear regime during the wear testing of FGMs samples.

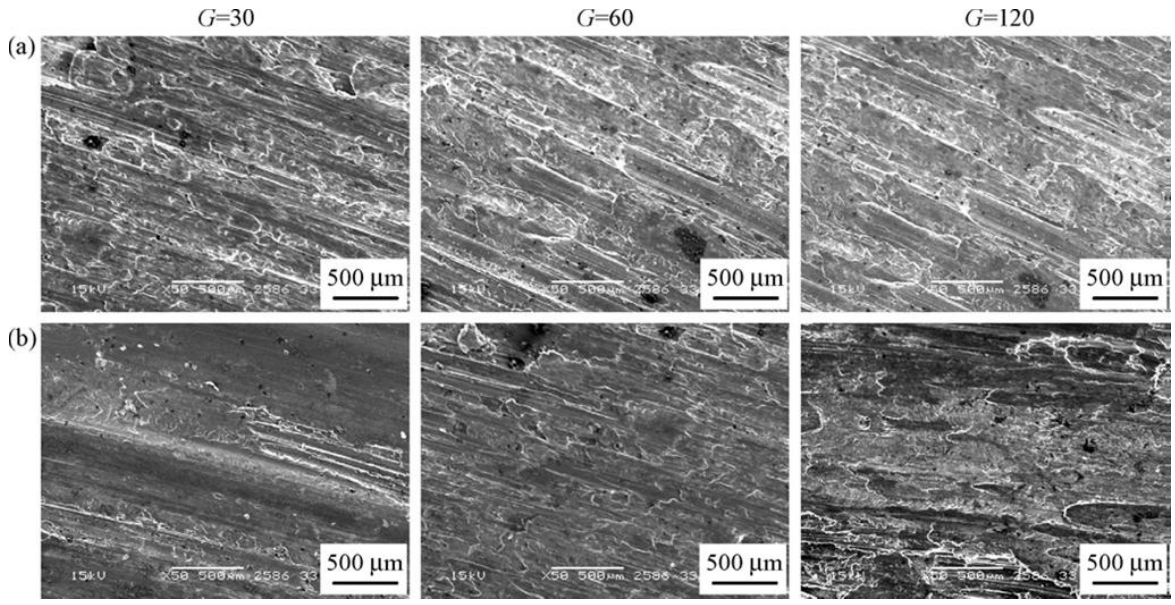

Figure 2.10: The Worn surface morphology of FGMs samples tested in: (a) in the wear plane direction and (b) normal to wear plane directions [74]

2.3.6 *Effect of gradation on Corrosion properties*

The corrosion resistance is one of the important functional properties of any components of automobile, aerospace and of industrial applications as it works on varying surrounding and environmental conditions. The lack of proper corrosion resistance reduces drastically the useful operating life of the components and systems.

The corrosion behaviour of the Al/Al_3Ti and Al/Al_3Zr FGMs in a 0.6 M NaCl in the outer region of the centrifugally cast FGMs rings were studied Ferreira et.al [75]. The open-circuit potential, potentio-dynamic polarisation and electrochemical impedance spectroscopy (EIS) tests were conducted. The EIS spectra were modelled and analysed with an equivalent circuit that reflected the evolution of corrosion behaviour during 1, 3, 6 and 10 days of immersion. The electrochemical behaviour of FGMs samples showed that galvanic effects between the intermetallic particles and the metal matrix affect the overall corrosion resistance of FGMs. In case of Al/Al_3Ti FGMs group, the samples obtained with 60 *G* had the better corrosion resistance. In case of Al/Al_3Zr FGMs group, sample obtained with 30 *G* exhibited better behaviour when compared with the obtained with 60 *G* and 120 *G.*

By using potentiodynamic polarization test in a composite containing Al–5B in a solution of 3.5% NaCl, Nairobi B Duque et.al studied the corrosion behaviour of Al-AlB_2 FGMs produced by centrifugal casting [76]. The centrifugal casting process was carried

out with a rotation speed of 400 rpm while the pouring temperature of the material was 750°C. Centrifugally cast composites of Al–5B, Al–7.2B and Al–4B–2Mg were processed and the volume fraction distribution of reinforcements and Rockwell hardness were measured. The materials containing Al–5B and Al–4B–2Mg showed particles segregation towards the outer region on the cast piece and higher hardness level than the ones containing Al–7.2B in the external zone. The centrifugally cast composites exhibited in their external zones a greater volume fraction of reinforcement particles and higher Rockwell hardness than the internal zones. The corrosion tests revealed that corrosion rate (CR) values were minimum for the centrifugally cast samples than that of the as-received Al–5B composite. They concluded that the process of centrifugal casting is beneficial as it will reduce notably the corrosion rate in the external zone of the FGM in the Al–5 B composite while it enhances the composite hardness on the external casting zones.

2.3.7 Different systems with *Basic Characterisations*

Various alloy systems which are not so common in practice like A132 alloys which were also used for the FGM preparations. Such systems are listed here along with the general ones which gives rather importance to any one property but to the feasibility of the processing of an FGM by the selected systems.

Qin et.al processed A132 aluminium-alloy matrix FGC tube reinforced by SiC particles [77]. The particle-rich zone could also be at inner layer and both in inner and outer layers of the casting by controlling stirring condition and temperature. The average size of SiC particles in sample1 was 10μm and 3.5μm in sample 2. SiC particles were preheated up to about 873 K for about 30 min in argon atmosphere, before being added in molten aluminium-alloy. The microstructures of particle-rich and particle-poor zones along radial direction were different. The aluminium silicon eutectic in particle-rich zone is finer than that in particle-poor zone due to SiC particles in particle-rich zone providing more nucleation sites during solidification.

The functionally graded Al matrix composite discs based on Al-SiC ex-situ with A356 (Al-7Si-0.35Mg) alloy and 20 vol. % SiC particles of 23 μm average particle size along with in-situ Al-Si , FGM cylinder, in A390(Al-17Si-4Cu-Mg) alloy composites were processed and characterised by Rajan et.al [78]. In the case of ex-situ Al-SiC FGM disc, the particles were segregated in a gradient towards the outer periphery of the casting

exhibiting high strength and hardness at the outer periphery. While the Al-Si in situ A390 FGM cylinder shows the dispersion of primary Si particles towards the inner periphery of the casting providing higher hardness and wear resistance at the inner region (Figure2.11). The FGM cylinder fabricated by the in situ method could provide a better hardness, wear resistance and durability compared to those fabricated by a homogenous gravity casting with A390 alloys. The improved properties in the braking area of the disc (outer diameters) enhance its braking efficiency and made A356-20SiC FGM a potential candidate for automobile brake disc applications. While the in situ formed by primary Si reinforced A390 FGM hollow cylinder with improved inner diameter properties could be used for automobile engine cylinder liners applications.

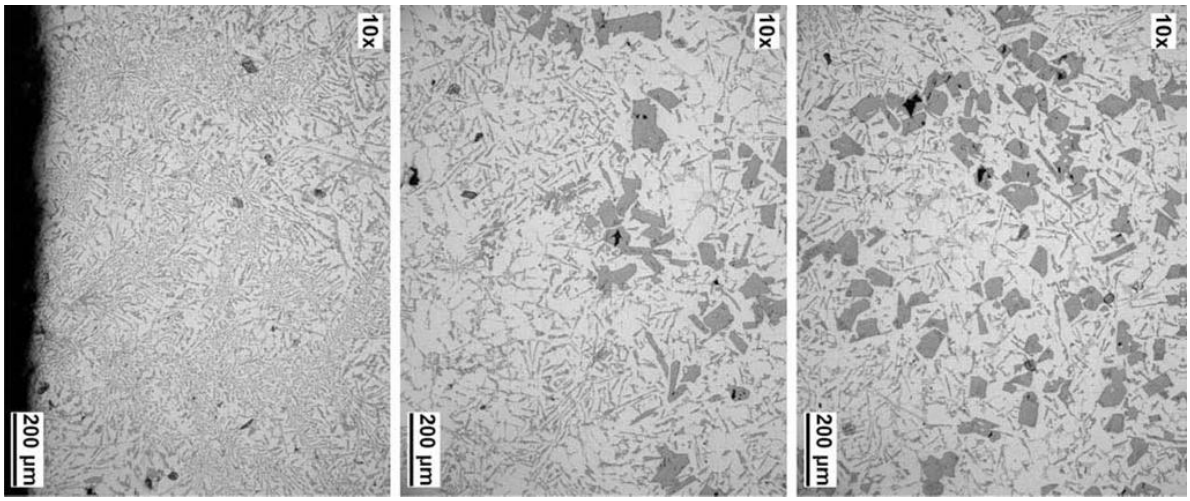

Figure 2.11: Optical micrographs at different locations from outer to inner periphery of in-situ reinforced functionally graded aluminium matrix composite hollow cylinder fabricated using A390 alloy [78]

In a review article by Watanabe et al., reported the studies on the microstructures and composition gradients in Al/SiC, Al/Shirasu, Al/Al_3Ti, Al/Al_3Ni and Al/Al_2Cu FGMs [79]. The Al/SiC, Al/Shirasu and Al/Al_3Ti FGMs are fabricated by the centrifugal solid particle method where SiC, Shirasu and Al_3Ti are the ex-situ reinforcements in the melts. While in Al/Al_3Ni and Al/Al_2Cu FGMs were, with in-situ Al_3Ni and Al_2Cu reinforcements, by the centrifugal method and have lower liquidus temperatures than the processing temperatures. The feature of Al/(Al_3Ti+Al_3Ni) hybrid FGM, which was fabricated by a method combining both the centrifugal solid-particle and in-situ methods. The microstructures of Al-based FGMs with particle distribution in normalised radial thickness were described in detail along with the effect of particle sizes in the distribution was also studied.

Z1104 aluminium alloy reinforced with 20 vol.% silicon carbide particle composites, an FGM cylinder were produced by centrifugal casting. The microstructural characteristics and Brinell hardness of FGM were investigated by Wang Kai et.al [80]. The mould was pre-heated to 500°C, and the pouring temperature of melt was 750°C. The centrifugal casting was performed at 800 rpm (or 54*g).* Macrostructure and XRD analysis showed that most of SiC particles dispersed by centrifugal force segregated to the external circumference of the cylinder, the remaining agglomerated SiC particles and most of alumina oxides were maintained in the inner circumference of the cylinder, and a free particle zone was left in the middle circumference of the cylinder. The SiC particles in aluminium melt can promote the refinement of primary α(Al) during solidification and this in turn promote the uniform distribution of SiC particles. Brinell hardness of composites was connected with not only the volume fraction of SiC particles, but also the distribution of SiC particles in matrix alloy. The phase diffusions created by the centrifugal force prevented the growth of dendritic primary α(Al) and flaked eutectic silicon, so the thin granular eutectic Si phase and some coarse non-dendritic primary α(Al) phases were also visible in free particle zone.

Two FGMMCs using A356 (Al-7.5Si-0.35Mg) cast and A2124 (Al-4.5Cu-1.6 Mg-0.25Zn-0.2Si) wrought alloys were prepared by Rajan et al. [81]. Green variety SiC particles of 23μm average particle size were used as reinforcements. A356-15SiC and A2124-15SiC composite melts were processed by liquid metal stir casting method and poured to the cylinder mould rotating at 1100rpm in a horizontal centrifugal casting machine. The pouring temperature of melt was 750°C and the metal mould was preheated to 250°C. The microstructural features of the A356-15SiC varied from outer to inner periphery. The size of the primary aluminium phase in particle enriched zone was very fine (25μm average size), which became coarser towards the interior (120μm average size). This variation in microstructure was caused by different phenomena taking place during solidification under centrifugal force.

The presence of high volume fraction of SiC particles inhibits growth of primary aluminium and the shear caused by movement of ceramic particles diffusion could break the arms of dendrites to form fine structure. The measurement of volume fraction of the SiCp by image analysis measured a maximum of 45 and 40% SiC particles at the outer periphery of the A356-SiC and A2124-SiC FGMMC casting respectively. Comparison of the distribution pattern of SiCp in the FGMs showed that there was a

sharp transition between the SiCp enriched and depleted zones in FGM of A356, whereas a gradual or smooth transition was observed in A2124 FGM. This was obviously due to the presence of varying amount of eutectic liquid, i.e. A356 alloy contains more eutectic liquid compared to A2124 alloy, due to the difference in freezing range (longer freezing range of A2124 alloy is 637-490 °C than A356 alloy is 615-564°C) Hence, the freezing range of the matrix alloy dictated the nature of transition from particle enriched to depleted zone. The hardness variations in both FGMs closely follow the microstructure variations. The maximum hardness obtained at the outer periphery after heat treatment for A356-SiC and A2124-SiC FGMMC was 155 BHN and 145 BHN.

Al-Si composite pistons locally reinforced with in situ primary Si and primary Mg_2Si particles using centrifugal casting by Hao Xuhong et.al [82]. Commercial ZL104, Al-29 Si, Al-Sr, Al-Ti and AZ91 alloys were used to prepare the Al-20Si-4Mg alloy. This was melted at 770℃ and poured into the mould which was preheated at 400 ℃. The pistons were produced in a vertical centrifugal casting apparatus at 800rpm. The general characterisation results shown that primary Si and Mg_2Si particles mix up with each other in melt and segregate at the regions of piston top and piston ring grooves under the effect of centrifugal force. Particulate reinforced regions had a higher hardness and better wear resistance compared with the unreinforced regions and this performance increases after heat treatment.

In composite solidification process, primary Si particles precipitated foremost and grew up faster than primary Mg_2Si particles. As moving forward, primary Si particles collided with each other and integrated, which could be the cause the larger size of primary Si than that of primary Mg_2Si particles. Finally, the Si and Mg_2Si particles moved at approximately the same velocity and obtained the effect of mixed strengthening. It was found that the velocity difference of primary Si and primary Mg_2Si particles caused by the difference of their densities was compromised by the growth of primary Si due to the self collision and fusion. Test results showed that mixed primary Si and primary Mg_2Si particles had obviously improved the hardness and wear resistance of the composite piston. The degree of the hardness and wear resistance improved was proportional to the volume fraction of particles. After solution and aging heat treatment, the hardness and wear resistance were improved further.

2.3.8 *New Characterisation techniques.*

Introduction of new characterisation techniques enlarge the scope of scientific explanations to various critical phenomena or observations, which are unsolved or not even possible by the normal characterisation techniques in practise until that time. So for the steady scientific growth of any field it is very essential to apply new ways of approaches or characterisation techniques/tools for understanding the various systems and controlling parameters for the effective applications of science to society.

Zhang et.al was used electron microprobe with a scanning diameter of 0.2 mm for the measurement of the radial segregations [83]. To reveal the effects of casting parameters, they focused on the solidification of Al- 33.4 wt. % Cu in a DC magnetic field intensity of 0.23 tesla, while the mould was rotated at 1200 and 2000 rpm. The radial segregations were measured *via* electron microprobe with a scanning diameter of 0.2 mm. it was observed that the electromagnetic stirring (EMS) effectively influences the structure and segregation of the binary Al-$CuAl_2$ system solidified in centrifugal casting. The macrostructure was refined by forming equiaxed grains in the inner regions and columnar structure in the outer zones. The stirring promotes the structural transition of eutectic from lamellae to rods and then to blocks as the magnetic field was intensified. Meanwhile, the stirring enhanced macro segregation to a certain extent in the eutectic alloy.

Although conventional techniques based on 2-D metallographic image analysis are quite capable of estimating important parameters, namely particle size distribution and particle volume fraction some 3-D stereological parameters, namely inter-particle connectivity are beyond its reach. Such parameters can only be accessed directly by techniques where the three-dimensional nature is an intrinsic characteristic, as is the case with tomography. Moreover, the features under evaluation, by their scale, demand spatial resolutions in the order of 10μm or less, thus leading to the use of X-ray microtomography with synchrotron radiation.

In the work, Velhinho et al. applied the X-ray tomography to an Al/SiCp functionally graded composite, in order to investigate the distribution of the reinforcements and how they interact with the porosity present in the material [84]. It was observed that as a consequence of centrifugal casting SiC particles were partially clustered, with some pores gathered with them, this being associated to imperfect wetting of ceramic particles by the molten aluminium alloy. Also, small spherical pores,

associated to trapped gas bubbles, were observed dispersed in the matrix. In addition, it was possible to quantify the particle volume fraction profile along the centrifugally cast FGM composite. The results showed a relatively smooth gradient of ceramic particles along the sample, which increased the mechanical properties of the material.

The holotomographic analysis was used by Francisco Braz Fernandes et.al to study the SiC reinforcement distribution in an Al matrix functionally graded composite fabricated by centrifugal casting [85]. Precursor composites were prepared from an Al 10Si2Mg alloy and SiC particles (with two different sizes, 12 μm in one case and 37 μm in the other) by rheocasting. The cylindrical samples of size 1 mm in diameter were machined by EDM. The microtomographic measurements were performed with beam energy of 20 keV, and a multilayer was used as monochromator. For each sample, several sample-detector distances were used (100, 200 and 400 mm). Proper superposition of the images from different distances was done in order to enhance contrast between SiC particles and aluminium matrix. Particle clustering has been evaluated in number and volume, showed that a lower mean particle size was related to more clustering. The results also explain that the dispersion of smaller SiC particles was harder to achieve because of poor wettability of molten aluminium with SiCp.

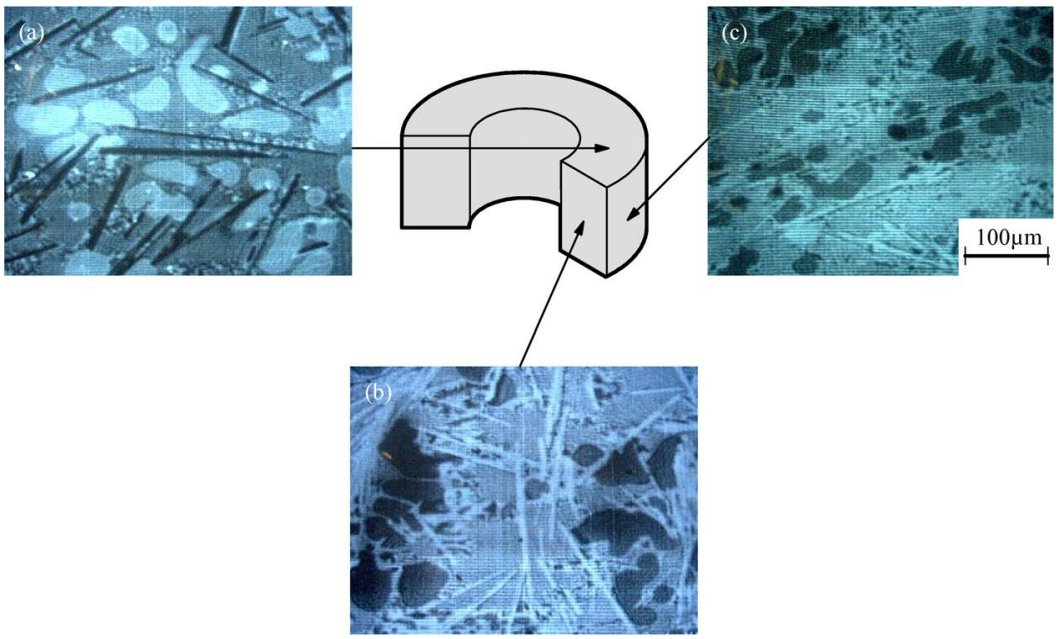

Figure 2.12: SAM photographs of Specimen C surface observed at 400 MHz on three orthogonal planes, i.e.,(a) perpendicular to the rotation axis, (b) perpendicular to the rotation direction, (c) and perpendicular to the centrifugal force direction [86]

Scanning acoustic microscope (SAM) can provide subsurface images and 3D shape of reinforcements, which is difficult to achieve by other methods. Watanabe et al. prepared the ternary Al–13.8Cu–1.6Fe alloy from Al–Cu and Al–Fe alloys at 1000°C by a centrifugal in situ method and studied by using SAM [86]. In the FGM rings processed four different phases were observed, namely, Al, Al_2Cu, Al_7Cu_2Fe (ω) and $Al_{13}Fe_4$ phases. The shape of ω phase was found to be fibre (needle) by the scanning acoustic microscope (SAM) (Figure 2.12). The position dependence of the microstructure was examined on the fabricated FGM rings, and the volume fraction of ω phase was found to increase toward the outer region of the ring. Moreover, the orientation and aspect ratio of the ω phase varied in the rings in a gradually graded manner. 3D fibre orientation distribution in composite materials had a significant effect on the mechanical and physical properties of the materials.

X-ray diffraction and differential scanning calorimetry (DSC) were used for the systematic study of the structure changes of the liquid Al-16 Si alloy with temperature on the solidification during the vertical centrifugal casting of Al-Si alloys. Weimin Wang et.al observed pre-peaks on the diffraction-intensity and $S(Q)$ curves of the alloy at high temperatures (≥850 °C) [87]. The pre-peak also exists in the intensity and $S(Q)$ curves at 670 °C when the alloy was overheated at high temperatures (≥850 °C), but disappeared after the solidification. The rapid solidification and centrifugal casting experimental results also showed that after overheating at high temperatures, the primary silicon phase was easy to coarsen and segregate under the additive force, which was confirmed by the microsegregation of Si atoms in the melt at high temperatures. The DSC measurements indicated that the temperature and latent heat for primary solidification increase with the overheating temperature, which means that the nucleation of primary silicon becomes easier by the segregation of Si atoms, and the primary solidification developed more sufficiently after overheating at high temperatures.

2.3.9 New *methods*

It is a known fact that with a single method it is impossible to process all materials successfully. From the conventional ways of centrifugal casting methods the scientists and researchers tried out a lot of practical, more easy and economical ways of casting new materials for specific applications.

In 1998, a more practical way to fabricate an FGM with Mg_2Si reinforcements was tried out by Jian Zhang et.al [88]. A novel process of producing an FGM tube with high inside wear-resistance was achieved. In-situ Mg_2Si reinforcements were present in both the inside and the outside wall of the tube specimen obtained by centrifugal casting.. The cluster of primary Mg_2Si particles reduced the ductility contribution of the Al matrix during deformation and resulted in a poor UTS and elongation, although they enhanced the material's hardness. A significant increase in both strength and ductility in the middle area of the as-cast specimen provides insurance of reliable strength for the gradient material. In short, a new in-situ particle reinforced metal matrix composite (PMMC) system that can produce concentrations of reinforcements in both the inside and outside wall of the tube, especially in the inside area with high volume fraction of Mg_2Si, through centrifugal casting was introduced.

A near-net-shape products having a graded distribution of intermetallics were manufactured successfully by backward extruding at a molten metal and solid intermetallic coexisting temperature by Y. Fukui et.al in 2000[89]. The machinability of the metal-intermetallics system was excellent and the ability of the Al-Al_3Ni FGM as a structural and component material was enhanced. The volume fraction of intermetallics at the cup bottom was more than 60 vol.% in normal setting and then decreased toward the wall region. However, in the case of reverse setting, a residual aluminium zone was formed and the Al_3Ni volume fraction of the cup bottom was 54vol.% of Al_3Ni. The optimum operation temperature was found to be 660°C, for Al-Al_3Ni FGM, because the fine grain structure.

In 2004, Watanabe et.al[90] developed a new fabrication method named “reactive centrifugal casting method (RCCM).” based on the self-propagating high-temperature synthesis reaction (SHS) and centrifugal casting method for the fabrication of an aluminide/steel clad pipe having an excellent resistance to corrosion and oxidation as well as a considerable level of toughness. Reactive casting is one in which involves an exothermic reaction between elemental liquids, and enables one to produce the liquid of a high melting point intermetallic compound without the need for external heating. They have produced a liquid of NiAl of 2480 K by simply mixing aluminium liquid of 1023 K and nickel powder. An increment in temperature over 1000 K was achieved by heat generation from an exothermic reaction between Ni and Al to produce NiAl. The base liquid is poured onto a base material such as steel, the surface of the base

material is melted due to heat generation, and the produced NiAl is strongly bonded to the base material. When aluminium liquid is poured onto nickel powder placed on the inner surface of a rotating steel pipe, the liquid and powder exothermically react and produce a composite layer on the inner surface of the steel pipe. The heat generated by the reaction melts the inner surface of the steel pipe and bonds the composite layer to the steel. The reaction was remarkably promoted by increasing the pouring temperature of aluminium, the preheating temperature of the nickel and the centrifugal force. The amounts of initial aluminium and nickel play an important role in the control of the microstructure.

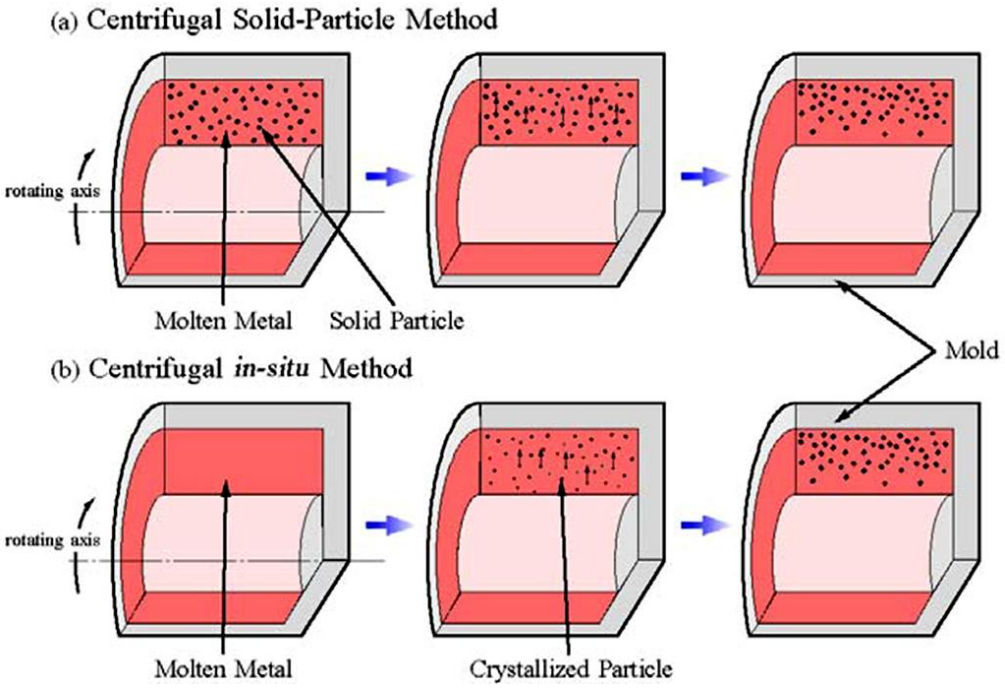

Figure 2.13: Schematic diagrams for (a) Centrifugal solid particle method and (b) Centrifugal in-situ method [91]

It is difficult to introduce the selected orientation of the Al_3Ti platelet particles into Al–Al_3Ti FGM products. The centrifugal solid-particle method was used by Sequeira et.al, in 2005 [91] to study the volume fraction gradient and anisotropic orientation of Al3Ti platelets in a backward extruded Al–Al_3Ti functionally graded material (Figure 2.13). To overcoming the inherent brittleness of the intermetallic compound in Al-base FGMs, the semi-solid extrusion method was used. Al_3Ti particles will drift on the molten flow during semi-solid process and form a near-net shape product with a unique distribution having superior orientation arrangement of Al_3Ti particles. The initial master-alloy ingot was a commercial Al alloy with 5 mass% Ti, which contains Al_3Ti

platelets in the matrix. It was heated to 900 °C resulting in solid Al_3Ti platelets in a liquid Al. The melt was directly poured into the rotating mould through the pre-heated inlet and was solidified under the application of a centrifugal force set at 50G. Semi-solid backward extruded Al–Al_3Ti FGM cups were produced from billets cut from Al–Al_3Ti FGM ring. The variation of Al_3Ti volume fraction and the orientation of platelets both before and after extruding were observed and discussed with respect to properties and processing. An Al_3Ti platelet volume fraction gradient was observed in the FGM cups, with a decrease from the centre of the cup-bottom to the cup-wall region. Higher extrusion processing temperature lowered viscosity and led to a more moderate volume fraction gradient.

A novel FGM fabrication of centrifugal mixed-powder method for processing FGMs containing nano-particles, along with a brief description of the centrifugal solid-particle method, in 2009, was explained by Watanabe et.al [92]. The Cu/SiC FGMs containing nano SiC particles and Al/TiO_2 FGMs containing TiO_2 nano-particles were also fabricated by this new method (Figure 2.14). Cu-30SiC and Cu-44SiC powder mixtures were fabricated using pure Cu and SiC powder. In order to investigate the effects of the SiC particle size, three kinds of SiC powders with 150μm, 50μm and 500 nm in diameter were used. The applied centrifugal force was G = 100, and the spinning mould containing the powder mixture was heated up to 800 °C.

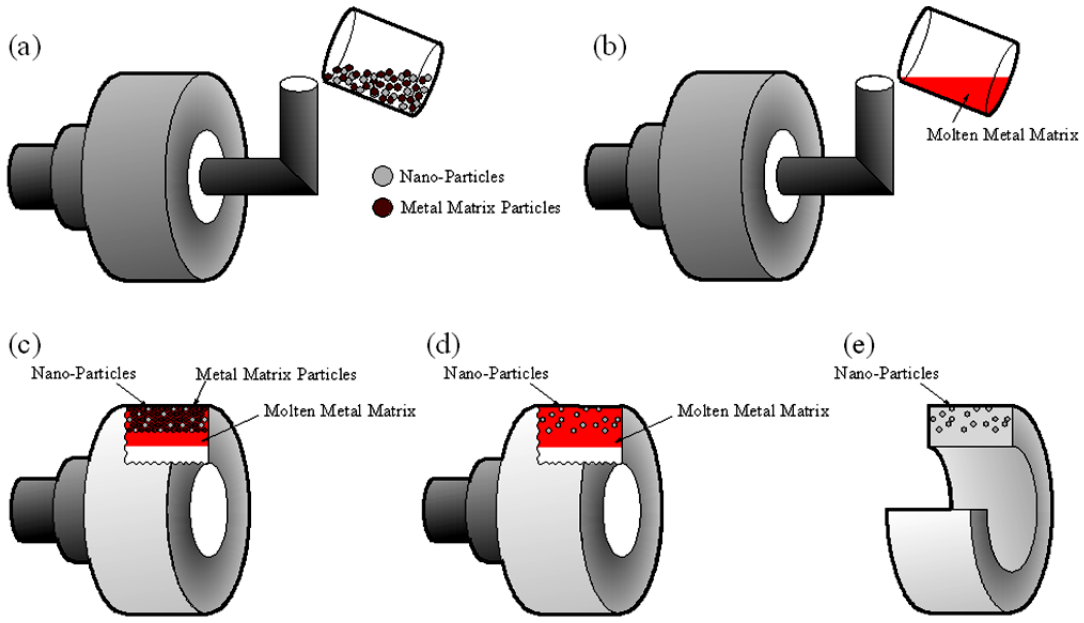

Figure 2.14: The schematic illustration showing the process of the centrifugal mixed-powder method [92]

A pure Cu ingot with purity of 99.9% was melted in a crucible with an induction furnace, and the molten Cu was poured into the spinning mould in a vertical casting machine. In the case of, Al/TiO_2 FGM of Al-10TiO_2 and Al-30TiO_2 were prepared. The primary particle-diameters of the Al and the TiO_2 powders were 93μm and ~500 nm mixed. Al/TiO_2 FGMs were fabricated by the centrifugal mixed-powder method using these powder mixtures in a horizontal-type centrifugal casting machine with an applied centrifugal force was G= 80. The fabricated FGM cylinder has the outer diameter of 90mm, the length of 30mm and thickness of about 20mm. Disperse nano-particles were found only on the surface of FGMs and moreover the distribution of nano-particles in the FGM has no dependence on density difference between matrix and particle. At the same time, hardness on the surface of FGM was improved by dispersion of nano-particles. Finally, it was concluded that the centrifugal mixed powder method was an effective method for fabrication of FGMs containing nano-particles on the surfaces.

A flux assisted reaction synthesis followed by centrifugal casting A6061-B_4C FGM was developed in an economical way by Rao et.al in 2010 [93]. The boron carbide was mixed with calculated amount of K_2TiF_6 flux such that Ti/B_4C:0.1 was employed, and the former was taken equal to half the weight percentage of B_4C. The charge composition was prepared to achieve an Al-10% B_4C composite. This mixture was added to A6061 melt at 900°C in the crucible and held for 2-3 minutes for completing the flux metal reaction. The composite was poured into the rotating mould, which was preheated at 250°C coated with zircon wash. The density of boron carbide (2.52 g/ cm^3) and molten Al alloy (2.385 g/cm^3) are very close; therefore, in order to study the segregation of boron carbide due to centrifugal force, the FGM composites were prepared at two different speeds (600 and 1100rpm). Optical and analytical microscopy examination of FGM reveals the gradient of boron carbide particulate in aluminium matrix. The microhardness of FGMs exhibits a gradual change of hardness from 55Hv in aluminium to 150Hv in B_4C rich outer region. The desired B_4C gradient was achieved through centrifugal force, despite close density values of molten aluminium and B_4C particles. Reaction synthesis method using K_2TiF_6 flux was most attractive route for the synthesis of Aluminium B_4C particle reinforced composites. The titanium rich thin interfacial reaction layer was responsible for the incorporation of B_4C in aluminium matrix which prevents the formation of unwanted reaction products like Al_3BC and AlB_2. An increase

in volume fraction of particulates led to progressive increase in the microhardness level with an increase of centrifugal force by changing the speed from 600 rpm to 1100 rpm.

As a development of centrifugal mixed-powder method (CMPM), reaction centrifugal mixed-powder method (RCMPM) has been presented by Shimaa El-Hadad [94]. Using RCMPM, Al-Al_3Ti/Ti_3Al FGMs, with good surface properties and temperature controlled compositional gradient, were processed and the effect of processing temperature on the reinforcement particles morphology, size and distribution were studied. RCMPM showed a slower particles distribution at higher casting temperatures. At relatively lower temperatures (1150-1250 °C) fine granular Al_3Ti intermetallics particles, Ti_3Al intermetallics compound and un-reacted Ti phase were observed. While, at a processing temperature of 1350°C only coarse Al_3Ti platelet particles were seen. Casting at a still higher temperature, 1450°C, resulted in coarsening of the Al_3Ti platelets. The hardness distribution in the fabricated FGMs showed a clear dependency on the particles type, their size, and their distribution at the processing temperature.

By mixed salt reaction route, Kumar et.al, were synthesized the in-situ reinforcement particles TiB_2 and TiC and functionally graded aluminium alloy matrix in-situ composites (FGAMCs) were fabricated using the horizontal centrifugal casting [95]. A commercial A356 and an Al-4Cu alloy were used as matrices. K_2TiF_6 and KBF_4 were added in the proper ratio to the liquid alloy at 800°C and stirred to get 5 wt. % of TiB_2 particles. K_2TiF_6 and graphite are added in the defined ratio at the temperature of 1200°C to get 5 wt. % of TiC particles. The in-situ composites prepared were A356-5 TiB_2, Al-4Cu-5 TiB_2, and A356-5TiC. The melt was poured (with and without stirring) into the centrifugal mould at 900°C. The mould was preheated to different temperatures (300°C, 600°C, and 900°C). The centrifugal force was controlled by varying the rotational speed of the mould from 1000 to 2000 rpm. It was found that the segregated in-situ formed TiB_2 and TiC particles change the morphology of primary silicon particle during the solidification of Al-Si alloy. A maximum of 20 vol % of reinforcement at the surface was achieved in the Al-4Cu-TiB_2 system by this process. The stirring of the melt before pouring caused the reinforcement particles to segregate at the periphery of the casting, while in the absence of stirring; the particles are segregated at the interior of the casting.

The application of a centrifugal casting procedure was investigated by Sánchez et.al for manufacture carbon fibre reinforced aluminium matrix composites [96]. The

centrifugal force was used to infiltrate a preform to manufacture a metal-matrix composite (Figure 2.15). Preform was located inside the mould towards the outer diameter, at the end of a rotational axis. Composites with volume fraction of reinforcements above 7 vol.% and porosity values lower than 0.5 vol.% were coated with nickel. Preforms, made of short carbon fibres either uncoated or with electroless nickel-coated, were pre-heated to temperatures above 600°C to allow the penetration of molten aluminium. The hardness of the composites increased with the volume fraction of reinforcement and the nickel coating, caused an additional hardening effect due to the formation of nickel intermetallics.

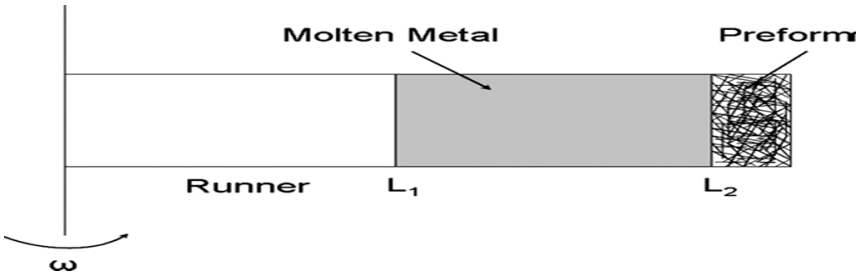

Figure 2.15: Scheme of a centrifugal infiltration process [96]

2.3.10 *Numerical modelling*

In modern science, after the growth of parallel processing and clustering of computers, the numerical modelling and simulations of possible and impossible experimental methods is an essential part of any research. A true numerical model will give the researcher to vary the influencing parameters of a study to its extremities and can analyse what next?

In 2003, Hiroshi Okada et.al has made an attempt, as a continuation, to the work of Fukui et.al (2000), to numerical analyses on the flow/deformation characteristics of Al–Al_3Ni FGM during semi-solid forming process [97]. Finite element method (FEM) for incompressible flow was applied with a spatial variation in the effective viscosity of melt. Since the processes of backward forming were relatively slow, the assumption of Stokes flow was adopted and terms associated with time derivatives were neglected. Similar to that of experiments, the trend, of Al_3Ni particles move much farther in the cup-wall region in the case of reverse setting than that of normal setting, was found in the results of numerical analysis. Certain limitations were accepted by the authors that the simulation were unable to predict correctly the Al rich layer forming in the top of the cup and the Al_3Ni rich bottom regions formed during the experiments.

A 2-D dynamics simulations having the effect of the solidification front along the other effects to predict the distribution pattern obtained during centrifugal casting were created by Prem E. J. Babu et.al [98]. The molten metal was regarded as a viscous liquid and the motion of ceramic particles in the viscous liquid under a centrifugal force, the composition gradient formation was simulated. Mixtures consisting of aluminium matrix and SiC particles were chosen for the experiments and rings having various graded compositions were manufactured. The gradient pattern of SiC particles in aluminium matrix were analyzed at various time steps, using the simulation and were compared with the results obtained from centrifugal casting experiments to validate the efficiency of the theory.

A numerical model for a centrifugal casting process for diboride particles in an aluminium matrix were developed and studied by Gustavo Gutierrez et.al [99]. Particles with a spatial uniform random distribution and a Gaussian diameter size distribution were assumed as initial condition of the casting process. The boride particles were modelled as spherical particles subject to a drag force in a Stoke flow in the liquid aluminium matrix. The effect of temperature on the viscosity was also considered by solving the energy equation. From parametric studies in the numerical model, the viscosity dependence of the temperature has a strong effect and could not be assumed constant. They found that variable viscosity tends to generate a more uniform particle distribution as compared with the constant viscosity case. The effect of the average particle diameter was also important as the bigger the diameter of the particles as faster their motion. The two important control parameters of the casting were the rotation speed and the time of centrifugation that could be estimated by numerical analysis and could able to maintain an appropriate particle concentration inside the sample.

Zhang Wei-Qiang and Lou Chang-Sheng presented **a**nother two-phase numerical model coupled with heat transfer to describe the radial distribution of SiC particles on centrifugally-cast metal matrix composite [100]. The concept, of a transverse static magnetic field was concurrently imposed to induce electromagnetic stirring of the melt as it revolved with the mould, were also incorporated in the model. The time-dependent particle distribution was obtained by integrating the trajectories of all particles present instead of solving mass and momentum conservation equations for the particle phase (Figure 2.16). Experimental validations were also carried out to examine the radial distribution of SiC particles in pure aluminium. The computational results show that the

particles tend to be congregated by the centrifugal force, and both increasing the imposed magnetic field and decreasing the particle size tend to result in even distribution of the particles. With the magnetic field varying from 0 to 1 T (tesla) and the particle size from 550 to 180 μm, a uniform distribution of the particles in the aluminium matrix could be obtained among the computational results. Experimental observation also shows similar tendency, however, the chilling effect from the mould wall results in an outer particle-free zone, which was not involved in the numerical model.

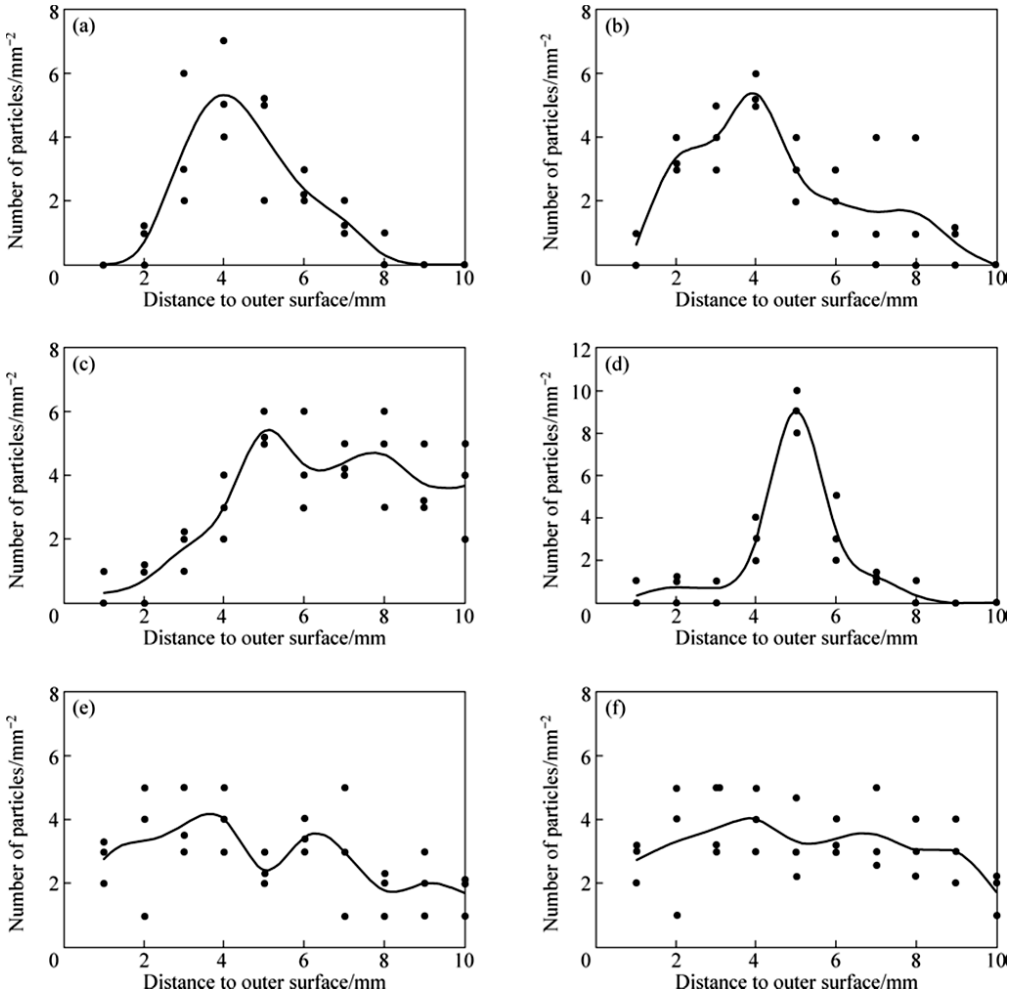

Figure 2.16: Quantitative results of particle distribution in Al matrix: (a) B=0 T, d_p=550μm; (b) B=0.10 T, d_p=550μm; (c) B=0.15 T, d_p=550μm; (d) B=0 T, d_p=180μm; (e) B=0.10 T, d_p=180μm; (f) B=0.15 T, d_p=180μm [100]

2.4 CENTRIFUGAL CASTING OF POLYMER MATRIX COMPOSITES

The progress in the field of polymer composite castings by applying the concept of centrifugal force is systematically reviewed and described for the last 15 years. From the space plane thermal barrier coating concept of FGM developed in Japan by the mid of

1980's onwards, there was a leap in the field of FGMs processing and applications. As the centrifugal casting is one among the economic ways of production, a lot of attention has gone into the various aspects of casting parameters and the properties of obtained products, even in the sector of polymer FGM.

2.4.1 *Epoxy with Carbon fibre systems*

In polymer matrix composites, the major applications orient towards fibre reinforced composites either with glass or carbon. There is no wonder that a lot of research were also gone into the area of epoxy /carbon fibre systems processed by centrifugal casting methods.

The centrifugal force was employed by Lee et.al, in order to induce a spatial gradient of fibre distribution in the epoxy/carbon fibre system [101]. The gradient structure of the epoxy/carbon fibre composite was controlled by varying the rotation time and the material parameters, such as fibre length, fibre content and matrix viscosity. The spatial gradient distribution of carbon fibres in an epoxy matrix was achieved by the combined mechanism of packing and settling. The mechanical properties of the functionally gradient epoxy/carbon fibre composite were also investigated. The Carbon Fibres were aligned perpendicular to the direction of centrifugal force at the bottom of the specimen while in the upper region; they were aligned parallel to the direction of centrifugal force. The flexural strength of the functionally gradient epoxy/CF composite was higher than that of the isotropic one, due to its unique internal structure.

The effects of centrifugal force on fibre dispersion in Nickel with coated short carbon fibres system were examined by Mashiro Funabashi [102]. Gradient composite samples were made of an epoxy resin filled with the coated carbon fibres under a centrifugal force field and analysed. The conductivity and aspect ratio of these fibres are higher than those of the uncoated carbon fibres. The fibre dispersion and fibre orientation distribution in the matrix resin were also investigated by measuring the distribution of both the volume fraction of fibres and the electrical conductivity in the direction of centrifugal force. The fibre content gradient was observed to be affected by the magnitude of the centrifugal force. A constant electrical conductivity was measured in the direction of the centrifugal force and it was independent of both the rotation speed and position. But, the conductivity measured perpendicular to the centrifugal

force direction increases with increasing rotation speed or decreasing distance from the bottom of the samples. Conductive materials with smaller amount of fibres were derived by applying the carbon fibre coated with nickel having an aspect ratio higher than 100. They suggested that the distribution of fibre orientation can be estimated by the electrical conductivity measurement.

Klingshirn et.al created functionally gradient materials with an epoxy resin matrix filled with short carbon fibre (SCF) by controlling the parameters centrifugation speed, centrifugation time and viscosity of the mixture [103]. A major point was controlling the viscosity, which depends upon the temperature, the local filler volume fraction, general filler type and the progress of the curing of the resin. The fretting wear rate decreased dramatically with a growing SCF content.

2.4.2 *Effect of Gradation on Physical and Mechanical Properties*

Compared with MMCs, PMCs have less mechanical and physical properties regarding strength, melting point, hardness etc. For any practical application, it is very essential to know about these parameters of the functionally graded polymer cast components.

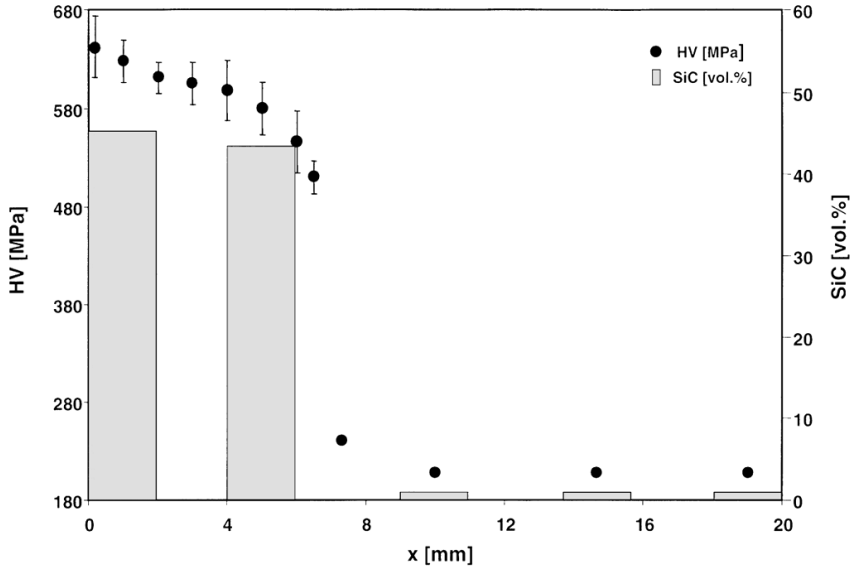

Figure 2.17: Variation of Vickers hardness and the SiC volume content along the centrifugal direction for a specimen prepared at 5000rpm [104]

The gradient of mechanical properties was mapped, by Krumova et.al, along the centrifugal force axis by micro hardness measurements [104]. In this research FGMs with controlled hardness and wear resistance over the cross section of the samples was achieved. A continuous increase of the hardness from 210 upto 640 MPa was measured

over the length of the sample. It was proved that micro hardness test is one of the most approximate techniques for studying the mechanical properties of gradient materials. Additivity law in composite materials was checked by plotting Vickers hardness versus the volume content of SiC particles (Figure 2.17). Filler fraction was calculated and dynamic mechanical thermal analysis was also performed. The viscoelastic behaviour was tested on thin slices of about 2 mm thickness cut perpendicular to the centrifugal force direction. The complex modulus and loss tangent were determined at a frequency of 10 Hz over a temperature range of 20 to 300°C. SEM images were also taken from a polished sample cut parallel to the centrifugal force direction.

Compression tests were conducted by Tsotra et al. on the functionally graded rings of an epoxy matrix with SiC fillers [105]. In order to have accurate information about the material properties, tension and compression tests were performed on isotropic specimens having various SiC volume fractions. The finite element simulations (FEM) of the compressed rings verified the experimental data, as the stress/strain components in the representing locations were able to predict the failure. They got a 2D quarter model with a layered structure approximates properly the behaviour of ring specimens under compression loading. The behaviours of resin and the composites were different under tensile and compression loading and they have much larger strength under compression than under tension. The graded SiC distribution along the cross-section of the FGM ring was indirectly evaluated by a set of micro hardness measurements. During compression loading for rings with homogeneous distribution breakage occurs in the upper or lower tensile zone whereas in the case of graded distribution in the tensile zones of the horizontal plane.

Goncharov et al. fabricated **t**he rotary units of antifriction polymeric multi–component compounds of hub type by centrifugal formation to carry out the detailed investigations of compositions polymerization process [106]. The thermodynamic conditions influence on to quality factors, the composition and structure of the elementary layers forming the bush along with the tribological properties of the component were determined. The surface layer of antifriction material in the shaft–bush pair undergoes wear on account of the stress due to the external loads and the presence of abrasive particles in the lubricant. The internal structure of the material was determined by the composition of the polymer composite and the thermodynamic conditions of centrifugal casting. They found that to reinforce polymer composites with

fibre additives were useful. Various composites were investigated: the matrix used was ED-20 epoxy resin with F-4 fluoroplastic and the different reinforcements were GS-1 graphite, molybdenum disulfide MoS_2, or metallic powder (iron and bronze), shredded glass fibre or carbon fibre; glass fabric and cotton fabric. The composite bushes were characterised the density, hardness, surface roughness, the dimensional precision, the tensile and compressive strength. The frictional coefficient and wear rate also found out. The results were used for the correction of the control to maintain optimal thermodynamic conditions. The developed antifriction composites of epoxy fibre with different combinations of fillers can be used to produce slip bearings and parts for high quality hydraulic-cylinder sealing systems.

The influence of graphite filler on electrical properties of cast composites due to the sedimentation of graphite during gravitational casting produced composites with different filler content throughout the thickness of specimens were evaluated by Szczepanik et al. [107]. Addition of 3-6vol.%. of graphite to epoxy resin caused limited, almost linear, decrease of surface resistivity in depth direction of specimens. Higher content of filler (9-12vol.%) in polymeric composite caused rapid, non-linear with layer depth, decrease of surface and volume resistivity. Addition of lesser amount of graphite filler (3-6%vol) does not have large influence on volume resistance and resistivity. Applied gravitational casting method was found suitable for producing functionally graded polymers with very low surface resistivity on one plate side and very high surface resistivity on the other side.

Siddhartha et al. processed functionally graded epoxy composites, with Titania (TiO_2) reinforced, by vertical centrifugal casting technique [108]. Investigations on mechanical and wear characteristics of TiO_2 reinforced homogeneous epoxy composites and its functionally graded composite materials developed for tribological applications were done. Series of test were conducted on a pin-on-disc machine with three sliding velocities of 105, 209 and 314 cm/s under three different normal loading of 20 N, 30 N and 40 N. Out of all samples 20 wt.% epoxy–TiO_2 epoxy graded composites exhibited lowest specific wear rate (Figure 2.18). TiO_2 particle additions on epoxy graded composites have a dramatic effect on the flexural strength, tensile modulus and impact strength in comparison to homogeneous composites. The tensile modulus increased over a range of 4% for 10 wt.% filler content and an increase 6% for 20 wt.% filler content .

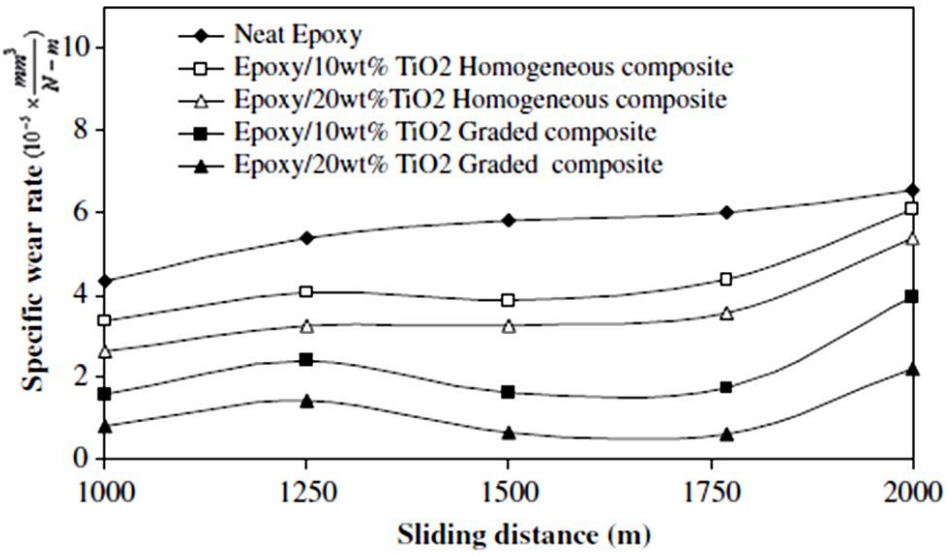

Figure 2.18: Variation of specific wear rate with sliding distance for the TiO_2/epoxy composite at load 30 N and sliding velocity 209 cm/s [108]

2.4.3 *Effect of Gradation on Particle/Reinforcements Distribution*

Hashmi et.al developed a graded graphite–epoxy material by use of a centrifugation technique and the profile of graded dispersion was evaluated using morphological, electrical, and wear properties [109]. It is reported that by controlling the centrifugation time, the graded distribution of graphite in epoxy resin and a quick estimation of the concentration gradient of graded materials by the abrasive wear tests were possible.

As a part of recycling and green environment, Hashmi et al. processed graded composites using short glass fibre bundles separated from cutting waste of printed circuit board, and considered the change of viscosity of dispersion medium with time and irregular shape of fibre bundles [110-111]. They have estimated the concentration profiles of fibre bundles moving in a polymerising matrix during the centrifugal casting of FGMs.

In an attempt to further improve the tribological properties of cotton–polyester composites, graphite was incorporated as a friction modifier in cotton–polyester composite and characterized for friction and sliding wear performance of composite. The experimental study on unsaturated polyester resin with the graphite particles of 38 to 45μm concludes that the coefficient of friction and wear depend on concentration of graphite powder, sliding time and applied load. Addition of graphite reduces coefficient of friction, and wear rate by formation of a transfer lubricating graphite film at the

contact interface. The incorporation of cotton fibres in the unsaturated polyester resin improved the structural integrity of material under sliding wear condition. The addition of graphite in the cotton–polyester composites further enhanced the capability of material to withstand against sliding wear test. The specific wear rate of polyester resin decreased with the cotton fibre reinforcement. The composites exhibited further reductions in specific wear rate against the normal load in the specimens those containing graphite. The coefficient of friction increased with the addition of cotton fibre in the polyester resin and decreased on increasing graphite content in the composite. The graphite in the composite provided the lubricating effect under the dry sliding conditions against the steel disc. Significant reduction in the contact-surface-temperature was observed on addition of graphite in cotton–polyester composites

PFGMs with epoxy resins having different amount and sort of fillers (copper powder (A-53SS), anisotropic ferrite powder (AMM), ferrites ($BaFe_{12}O_{19}$, $SrFe_{12}O_{19}$, graphite powders (PV60/65, SV94, GK3), anthracite coal and hard coal were processed by Stabik et al. [112]. Properties such as electrical surface resistivity, magnetic induction, coefficient of friction were tested and analyzed. Additionally distribution of filler particles in polymeric matrix was investigated along with the magnetic properties. They have come to a conclusion that; it was possible to prepare compositions that contain up to 50 vol.%. of filler powders depending on the manufacturing method and higher amount of fillers increased viscosity, which did not allowed to cast and prepare acceptable samples. It was also reported that to control gradient of particles concentration and in this way gradient of properties by proper selection of matrix properties, particles properties and technological parameters of casting was also possible. The wear, electrical and magnetic properties are dependent on initial and final filler particles concentration.

Further studies in polymeric composites with fillers of strong magnetic properties were conducted by Stabik et al. [113]. They were reportedly complicated because of interactions between particles and matrix along with an existing gradient. The epoxy resin (Epidian 6) and curing agent (triethylenetetramine) were used as a matrix. The ferrite powders, barium ferrite ($BaFe_{12}O_{19}$) and strontium ferrite ($SrFe_{12}O_{19}$) were used as fillers. By using centrifugal casting, they were able to prepare compositions that contain up to 30 vol. % of ferrite powders. Near the exterior surface of the sample, of 10 vol.%, a magnetic induction of 1.4mT for barium ferrite and 1.6mT for

strontium ferrite were obtained. For 30 vol. %, the maximum of magnetic induction were 11.3mT and 10.4mT respectively.

Stabik and Chomiak studied **t**he dependence of the surface resistivity on the filler content in the composite and the angular velocity in centrifugal casting of FGMs processed by epoxy resin as matrix, the same anthracite coal and hard coal of earlier studies as fillers [114]. The hard coal fillers had a favourable surface resistivity change on outer layers to a level that will avoid static electricity accumulation. Anthracite coal yields lower values of surface resistivity and the lowest resistivity values obtained was about 11%. (Figure 2.19)

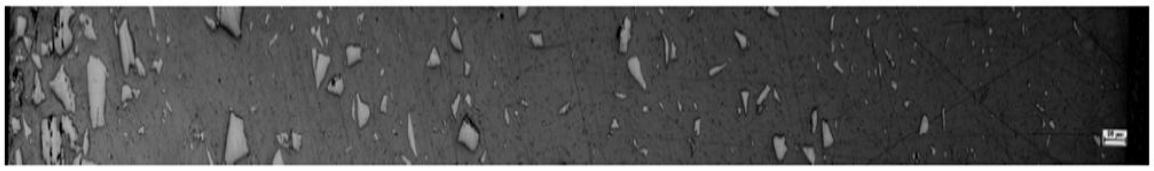

Figure 2.19: Panorama Photograph of structure of a specimen containing 12% Anthracite coal manufactured by centrifugal casting at 577 rpm [114]

Magnetic composite materials reinforced with different amount of ferrite powders were processed by Stabik et al. and afterwards investigated their magnetic properties [115]. The purpose of this study was to investigate the magnetic properties and the influence of the volume fraction of magnetic powder on magnetic properties of manufactured composite materials.

2.4.4 *Numerical Modelling*

Chul Rim Choe et al. developed a simulation technique and used the previous experimental results of epoxy/short carbon fibre systems for validation [116]. Since carbon fibres do not have a definite diameter, modification on the controlling equation for the computer simulation was done in order to apply the equation for describing the motion of fillers in a viscous medium under centrifugal force. They suggested that more intensive studies should be carried out for fibre systems with different aspect ratios to produce a systematic and physically meaningful value for the modification form factor *K*.

Tsotra and Friedrich made a correlation between the microstructure and the electrical conductivity of carbon-reinforced epoxy resin composites by using different centrifugation parameters, initial volume fraction and type of carbon fibres, composites with different gradient of electrical conductivity subjected to a centrifugal force [117-

118]. Blends of epoxy resin with three different kinds of carbon fibres were studied with respect to their electrical and mechanical properties. The fibre length influences greatly the formation of electrically conductive paths and thus the electrical conductivity. The percolation threshold can be reached for the long fibres at lower volume fractions in comparison to that of short fibres. The flexural properties of the composites are significantly influenced by the graded structure and longer fibre specimens have higher flexural strength compared to that of isotropic or shorter ones. The fibre orientation and dimensions were applied in the modelling, and the calculated values were in good agreement with the experimental percolation threshold and the electrical conductivity of the carbon-fibre composites. In the other study they have used the epoxy resin/polyaniline with short carbon fibres for their conductive blends and their influence on the electrical and mechanical properties was studied for graded distributions of the fillers. The electrical and mechanical properties showed graded profiles across the samples thickness and it related to the local fibre concentrations, and, it can be hence tailored by cautious selection of the centrifugation parameters.

Taguchi method of experimental design, an optimization technique, were used by Cavus Falamaki and Jamileh Veysizadeh for the processing of a system to perform experiments for all the influencing factors and their pertaining effective levels of membrane preparation by the centrifugal casting method by considering the complex process of sample preparation and characterization [119]. The second outcome was that the product of surface porosity x (1/surface average pore diameter) was a major membrane support characteristic and should be used effectively in evaluating the experimental results of statistical design of experiments.

A simulation was developed by Hashmi to observe the nature of the concentration profile that resulted from variation in time of centrifugation /sedimentation, volume fraction of particles and size distribution of particles in functionally graded polymer based composites [120]. It revealed that there exists the possibility of two graded profiles, namely low and high concentration profiles, in one sample of graded material made either by centrifugation or sedimentation. The size of the particle significantly affects the low concentration profile, as compared to high concentration profile.

A predictive model for the velocity of particle moving in a matrix which is getting polymerized with time and the evaluation of concentration changes of particles during

centrifugal casting of FGM at different cross-sections was developed by Hashmi and Dwivedi [121-123]. That evaluates the changes in velocity and concentration of particle dispersed under centrifugal force and explaining the progress of different zones formed; like clear, sediment and graded concentration zone. That can be extended to multi particle systems, to study the various parametric trends and to compare with experimental data. They have also tested the model by using a combination of $CaCO_3$ with polysulphide modified epoxy resin and the experiments are validated the predictions. Further as an extension of this work they have developed a series of FGMs using SiC in polysulphide epoxy resin under influence of gravity and centrifugal force. The previous predictive Model was employed to evaluate and compare the concentration variation in FGMs.

2.4.5 *Reviews*

The growth of any field of science is systematic; review articles will give the summarised information of a specific area of research until those period and available new trends.

J. Stabik and A. Dybowska made one of the first few reviews in 2007 where the basic methods of preparing polymeric gradient materials were discussed [124]. The aim was to brief the various conventional methods, products and differentiate with the FGM methods and products. The possibilities, in the centrifugal casting to influence the gradient of many properties by controlling the gradient of filler particles and the side effects of higher volume fraction filler contents with high viscosity were researched. The influence of concentration, type of filler and casting parameters, on the mechanical properties (strength, stiffness, hardness, wear resistance and other), electrical properties (surface and cross resistivity and permeability, thermal properties and optical properties were also discussed.

Again in 2012, Stabik et.al had published a review by combining and streamlining the processing of polymeric graded materials (FGPMs) [125]. There are three main means enabling properties gradation shaping: by composition selection, by processing parameters control and by post manufacture parts treatment. The paper presents only those technologies that were used by the authors. Others, worth mentioning are multi-injection, integral foam injection, deposition of multilayer coatings of different technologies, or rotational moulding of multi-walled tanks.

2.5 SUMMARY AND SCOPE OF THE INVESTIGATION

FGMs are advanced class of composite materials having discrete or continuously varying compositions and/or microstructure and properties over a definable geometrical length. Since the volume fraction of reinforcement varies from one point to another in a given direction, there is a smooth transition in both mechanical and tribological properties in the material. For these reasons, FGMs are one of the most potential and prominent system for the design and fabrication of components and structures with gradient properties with wide applications in the aerospace and automotive sectors. Various techniques are being developed for the fabrication of FGM components.

Studies have shown that centrifugal casting is one of the potential and economic techniques for the fabrication of functionally graded materials. Even though various investigations are carried out on processing FGMs, there is a lot of scope for design and tailoring the functionally graded microstructures and properties within a component using new systems of matrix-reinforcement combination suiting to specific engineering applications.

Functionally graded metal matrix composites (FGMMC) are FGMs with metal matrix and ceramic or metallic reinforcements. The advantages in properties obtained by using the FGMMCs are adjusted thermal mismatching, reduced interfacial stresses, increased adhesion at metal–ceramic interface, high temperature surface wear resistance, surface friction and better thermal properties, minimized thermal stresses, increased fracture toughness and crack retardation. Among numerous processing methods of FGMs existing today centrifugal casting has been proposed as one of the most economical and effective methods for the fabrication of FGMs. The conventional centrifugal casting method involves synthesis of MMC by stir casting method followed by centrifugal casting to form the gradient in microstructure due to centrifugal force. When particle-containing slurry is subjected to centrifugal force, distinct regions of varying particle/matrix densities are formed. Depending on the density, the lighter particles segregate towards the axis of rotation, while the denser ones move away from axis of rotation. Centrifugal forces cause heavier ceramic particles in the liquid metal to be displaced towards the outer surface of the casting. In this casting method the centrifugal force provides the required pressure needed for good mould filling

combined with good microstructure control, resulting in excellent mechanical properties in the cast composite. The compositional gradient in the composite is determined mainly by the pouring temperature of the melt, the rotational speed of the mold, the density and size of the reinforcement particles, the material cooling rate, casting time, and melt viscosity. Properties of centrifugally cast component also depend upon centrifugal pressure, vibration of the mould and fluid dynamics of the melt. Centrifugal casting of aluminum FGMs has been processed previously by ex-situ or in-situ methods and have obtained higher reinforcement (SiC, alumina and zircon) volume fraction towards the outer periphery due to their higher density than that of melt leading to better surface properties of the material. The lighter constituents (graphite and mica) and the porosities are collected at the inner periphery of the component.

Functionally graded polymer matrix composites (FGPMC) with ceramic or metallic reinforcements have good abrasion, impact, corrosion resistance along with high fracture resistance and specific stiffness. Rheological properties of thermoplastic materials depend upon shear history, temperature, and flow geometry whereas for thermosetting material, reaction kinetics and elapsed cure time are very important. The cure kinetics of thermosetting polymer depend upon the concentration of reacting reagents, reaction temperature, extent of cure that can be correlated with time elapsed. Centrifugal forces cause denser ceramic particles in the polymer to be displaced towards the outer surface of the casting. The centrifugal force provides the required pressure needed for good mould filling combined with good microstructure control, resulting in excellent mechanical properties. The compositional gradient in the composite is determined mainly by the rotational speed of the mould, the density and size of the reinforcement particles, the material cooling rate, casting time, and viscosity of the polymer. Centrifugal pressure, vibration of the mould and curing temperature of the polymer also affects the properties of the cast.

Epoxy resins a class of thermosetting materials used extensively in structural and specialty composite applications because of their unique combination of properties unattainable with other thermosetting resins is appropriately chosen to form the matrix phase. cold-castability, low toxicity, low shrinkage and excellent adhesion of epoxy are some of the main reasons for picking it to form the matrix phase. Silicon Carbide (SiC) is the candidate chosen as the reinforcement material due to its properties such as low thermal expansion, high strength, thermal conductivity, hardness, excellent thermal

shock resistance, superior chemical inertness and higher density in comparison with that of the matrix.

2.6 OBJECTIVE OF THE INVESTIGATION

The present research aims for a systematic study on the tailoring of functionally graded microstructures and the properties in metal and polymer matrix composites by vertical centrifugal casting. SiC particles of 99.999% purity and with an average particle size of 23μm are chosen as the external reinforcement particles for tailoring the properties. The processed FGMs are characterized for its graded microstructures, mechanical and tribological properties.

The functionally graded metal and polymer composite systems investigated are

- A319 – an Al-Si hypoeutectic cast alloy with 5-7 % Si
- A390 – an Al-Si hypereutectic cast alloy with 18 % Si.
    - Role of Mg addition (pure and master alloy) on the structure and properties using different percentages of 1,2,3,4 and 5% Mg.
    - Design, fabrication and evaluation of prototype FGM IC engine piston.
- A6061- a wrought aluminum alloy
- Epoxy resin matrix reinforced with SiC at optimized hardener ratio.

Chapter 3

Materials and Experimental Methods

3.1 INTRODUCTION

In the present study the processing of Aluminium Metal matrix composites (AMCs) with different aluminium alloys are used as the matrices and in the processing of polymer matrix composites (PMC) the epoxy resin is used as the matrix. SiC particle of average particle size of 23 μm is used as the reinforcements in common. In the in-situ preparations of composite with hypereutectic aluminium alloys, magnesium (Mg) is used as the modifying agent. The addition of Magnesium into the alloys can be achieved by two methods. This can be done by adding pure magnesium to the alloy melt directly in a safe manner with extra magnesium for the compensation for oxidation and other possible losses during the addition. It is found that in general 2-3% of the mass calculated of pure Mg will be added as extra. Which will reacts with excess primary silicon phase to produce hard Mg_2Si phase in addition Mg will assist to refine the residual primary silicon present in the hypereutectic system. In the case of Master alloy addition method, a proper Al-Mg master alloy will be selected and according to its composition, the effective Mg gain will be calculated and will be added to the alloy melt while processing. In this case magnesium loss is to the minimum levels and found that the more correct compositions can be repeatedly processed with minimum difficulty. In the master alloy addition, the Mg will react with the excess primary silicon available in the melt. But at the same time, the dilution of overall composition occurs due to the aluminium contribution by the Al-Mg master alloy. This added aluminium in the matrix will also react with the primary silicon available forming Al-Si eutectics. Out of these two reactions it is found that at lower percentages of magnesium addition the eutectic reactions are more favourites in master alloy additions. Modifier and Grain refiners are to be added to the molten Al-Si alloys to get combined grain refinement and modification effects. Many have reported the grain refinement and modification by addition of gain refiner and modifier simultaneously. However, it is a difficult task to

control the addition levels of individual grain refiner and modifier in actual industrial practice.

The different matrix alloys used for the composite preparations are A6061, A319 and A390 aluminium alloys and araldite epoxy resin is used in the case of polymer matrix. In the following sections the matrix materials are discussed with their characteristics and properties. And later the common particle reinforcement SiC is being described. In this section the preparation and processing of composite melt along with the vertical centrifugal casting is explained. In the characterisation part each techniques of sample preparation and the various parameters of testing conditions along with the details of instruments are given.

3.2 MATERIALS

3.2.1 *A319 (cast aluminium hypoeutectic silicon alloy)*

Hypoeutectic, A319, Al-Si alloy was used for the preparation of the composite. The chemical composition of the alloy used for MMC processing is analysed by SPECTRO MAXX optical emission spectrometer and is shown in Table 3.1 along with standard specifications. The chemical composition is 88.83% of Aluminium with 6.35 % of Si and 3.87% of Cu as major alloying elements and less than 0.2 % minor alloying elements. Based on the aluminium–silicon (Al–Si) system, the main alloying elements are copper (Cu) and magnesium (Mg). Iron (Fe) considers the principal impurity and detrimental alloying element for alloy 319. Enhancement in strength depends on amount of Cu and Mg, which leads to form strengthening precipitates / secondary phases such as Al_2Cu and Mg_2Si. The $Al_{15}(FeMg)_3Si_2$ Fe intermetallic phase have less harmful effect than normal needle like Fe intermetallic (β-$FeSiAl_5$) due to its compact morphology (Chinese script-like in appearance). The intermetallics adopt various morphologies and form at various times, prior to, during or after the Al–Si eutectic formation period and can significantly affect the mechanical properties in the alloy. A319 alloy have good ductility, hardness, moderate strength, machinability, good toughness, weldability, corrosion resistance and good casting qualities (Table 3.2). Typical applications of castings of A319 include internal combustion engine cases; gasoline and oil tanks; and oil pans. It is used in numerous commercial casting applications and has been extensively used in recent years for automotive engine crankcases, intake manifolds and cylinder heads. It is also used to cast oil pans for autos and trucks. The solidification

modes and moderate level of silicon contents have already made the alloy very attractive choice for semi solid processing. A319 alloy is a precipitation hardening alloy. The standard T6 condition heat treatment procedure followed is as described: solution heat treatment for 8 hours at 778K (505°C) followed by quenching at 353K (80°C) hot water then precipitation or age hardened at 428K (155°C) for 5 hours[126-127].

Table 3.1: Chemical composition of A319, A390 and A6061 alloys

Details of Alloy	Alloying Elements in %								Al in %
	Si	Cu	Mg	Fe	Mn	Zn	Ni,Cr	Ti	Al (balance)
A319 as per standards	5.5- 6.5	3 - 4.0	0.10	1.00	0.50	1.00	0.35	0.25	86.3-91.5
A319 ingot	**6.35**	**3.87**	**0.072**	0.205	0.34	0.148	0.046	0.14	88.83
A390 Standards	16 - 18	4.0 - 5.0	0.45 to 0.65	1.3	0.10	0.1	0.10	0.1	78 - 80
A390 Ingot	**18.1**	**4.0**	**0.31**	0.4	0.06	0.05	0.1	0.01	77.07
A6061 Standards	0.40-0.80	0.15-0.40	0.80 to 1.20	Max. 0.70	Max. 0.15	Max. 0.25	0.05	Max. 0.15	96 - 98
A6061 Ingot	**0.82**	**0.259**	**0.646**	0.154	0.098	0.040	0.151	0.022	97.81

3.2.2 *A390 (cast aluminium hypereutectic silicon alloy)*

Another aluminium alloy used for synthesizing FGMMC is A390 which is also a cast aluminium alloy. The composition and properties of the alloy are given in the Table 3.1 and Table 3.2 respectively. It is well known that a coarse primary silicon phase and long need-like eutectic silicon exist in the microstructure of unmodified hypereutectic. The properties results from the presence of primary silicon phase in a eutectic matrix encourage the application of the alloys in the heavy duty engines and some aeronautic components. The hypereutectic 3XX alloys (390, B390, 393) are used primarily in wear applications (engine blocks, compressors, pistons, pumps, pulleys, brake systems, etc.) but they are also popular for very thin parts, since they have exceptional fluidity. These alloys, because of the low ductility associated with the presence of primary silicon crystals, are not candidates for high integrity die casting, even though they are heat treatable and capable of high strength and hardness. Their commercial interest is because of the excellent properties such as low thermal expansion coefficient, good

casting performance, good weldability, high wear resistance, and high temperature strength. Pistons for automobiles are also cast from the 3XX alloys. Alloy A332 is the traditional car engine piston material; but A339 and B390 alloys, which are better able to withstand the stresses of modern high specific output engines, are increasingly replacing A332. The standard T6 heat treatment procedures, solution treatment at 495 °C for 8 hours, quenching in warm water and artificially aging at 175 °C for 8 hours, are used for A390 specimens.

Table 3.2: Standard properties of the A 319, A390, A6061 alloys

Property	A319	A390	A6061
Density (gm/cm^3)	2.79	2.72	2.7
Melting Point (^{0}C)	516-604	507-649	582 - 652
Tensile Strength(T6)(MPa)	230-250	320	310
Tensile Strength, Yield (MPa) @ strain 0.2%	138	260	276
Percent Elongation (%)	1.5	1	12
Modulus of Elasticity (GPa)	74	81.3	69
Poisson ratio	0.33	0.33	0.33
Thermal Conductivity (W/mK)	109	134	167
Coefficient of Thermal Expansion (μm/m ^{0}C)	23.1	22.5	25.2
Hardness (T6)(BHN)	65-95	120	95

3.2.3 *A6061 (wrought aluminium alloy)*

A6061 aluminium alloy used for producing the metal matrix composite is a wrought alloy. It is a precipitation hardening aluminium alloy, containing magnesium and silicon as its major alloying elements. It has higher mechanical properties with minimum alloying elements in the base aluminium. The composition and standard properties are given in Table 3.2 and Table 3.3 respectively. A6061 alloy is highly corrosion resistant, exhibits moderate strength and are easily extrudable. It is widely used in numerous engineering applications including automotive, marine and construction where superior mechanical properties such as tensile strength and

hardness are essentially required. These alloys show good aptitude for hot transformation by rolling, extrusion and forging. These alloys posses a high level of mechanical properties which can be further improved by adding silicon and a good aptitude to arc welding and brazing. They are good in cold formability (bending of profiles, deep drawing of sheets) in the Fully Annealed, Soft temper (O) condition and, to a lesser extent, the T4 temper, and have attractive surface appearance after brightening or anodising. All these properties account for the extensive use of this alloy series, especially in the field of metallic fittings. It is frequently used for extruded products (bars, profiles, tubes), cold-drawn, as well as rolled and forged products. It is used for structures requiring both average mechanical strength and good resistance to corrosion, in diverse fields of technology: transport (railcars, commercial vehicles), tubing (pipelines), welded boiler work, mechanics applications, and tubular furniture The standard T6 heat treatment procedures, solution treatment at 535 °C for 4 h, quenching in warm water and artificially aging at 175 °C for 8 h, is used for A6061 test specimens.

3.2.4 *Silicon Carbide Particle (SiC)*

Figure 3.1: Photograph of SiC particles of average particle size of 23 µm

In all ex-situ, particle additions have done with common particle reinforcement, i.e. green SiC particles (SiCp) (Figure 3.1). The SiC particles of density 3.2g/cm^3 with an average particle size of 23µm are used as reinforcements. Ultrasonic cleaning is done by using distilled water followed by acetone and finally they are dried before storing. The particles are preheated at 600°C for 2 hours before powder addition process. The standard properties of SiC particles are given in Table 3.3. Silicon carbide is composed of tetrahedra of carbon and silicon atoms with strong bonds in the crystal lattice. This produces a very hard and strong material. Silicon carbide is not attacked by any acids or

alkalis or molten salts up to 800°C. In air, SiC forms a protective silicon oxide coating at 1200°C and is able to be used up to 1600°C. The high thermal conductivity coupled with low thermal expansion and high strength gives this material exceptional thermal shock resistant qualities. Silicon carbide ceramics with little or no grain boundary impurities maintain their strength to very high temperatures, approaching 1600°C with no strength loss. Chemical purity, resistance to chemical attack at temperature, and strength retention at high temperatures has made this material very popular as wafer tray supports and paddles in semiconductor furnaces. The electrical conduction of the material has lead to its use in resistance heating elements for electric furnaces, and as a key component in thermistors (temperature variable resistors) and in varistors (voltage variable resistors). SiC particles are denser than aluminium alloys with a high melting point. They are thermally stable and have a percentage of thermal elongation less than one. By the addition of SiC particles the effective hardness, thermal properties and wear resistance properties of soft aluminium alloys can be improved.

Table 3.3: Standard properties of the SiC particle

Property	SiC Particles
Density g/cm^3	3.21
Melting Point °C	2730
Elastic Modulus GPa	410
Compressive Strength, MPa	3900
Poisson's Ratio	0.14
Percent Elongation %	Less than 1
Coefficient of Thermal Expansion (µm/m ^{0}C)	4.0
Thermal Conductivity (W/mK)	360
Hardness, kg/mm^2	2800

3.2.5 *Epoxy Resin*

The most common matrix used for advanced polymer composites and for a variety of demanding applications is epoxy. The operating temperature for epoxy resin can be up to 140^{o}C. Here the epoxy resin being used is Shell Epon 828 (XY 100) which is a low temperature cure resin (up to 80^{o}C). The present epoxy resin is having a curing temperature of 90^{o}C. The hardener (curing agent) being used is Aradur HY 951 IN from Petro Araldite Pvt. Ltd. It has low viscosity at room temperature and appears in liquid

form at room temperature. Epon 828 Epoxy resin is a liquid mixture containing difunctional bisphenol A and epichlorohydrin. This resin is cross-linked (hardened) with Araldite HY951 (a low viscous aliphatic amine). The proportion of mixing was 10:1 and the araldite curing offers very good mechanical strength and improved chemical resistance against atmospheric degradation. The properties of EPON™ Resin 828 Epoxy resin are given in Table 3.4. The epoxy resins can be used for the production of

- Fibre reinforced pipes, tanks and composites
- Tooling, casting and moulding compounds
- Construction, electrical and aerospace adhesives
- High solids/low VOC maintenance and marine coatings
- Electrical encapsulations and laminates
- Chemical resistant tank linings, flooring and grouts
- Base resin for epoxy fusion technology

Table 3.4: Properties of the EPON 828 Epoxy resin

Property	Values
Density g/ml	1.16
Physical form	Clear liquid
Kinematic Viscosity Pa-Sec	11-15
Elastic Modulus MPa	2750
Tensile strength MPa	69
Percent Elongation %	300
Shear strength MPa	41

3.3 METHODOLOGY FOR METAL MATRIX FGM ANALYSIS

In the present research the various processing steps and experimental investigations are done in a scientific manner so as to keep a control over the effective optimization of casting, machining, and other processing parameters. The Figure 3.2 shows the flow chart represents a schematic flow of various steps taken in sequence for the experimental procedures for the preparation of metal matrix composites and the corresponding FGM and their characterisation techniques used.

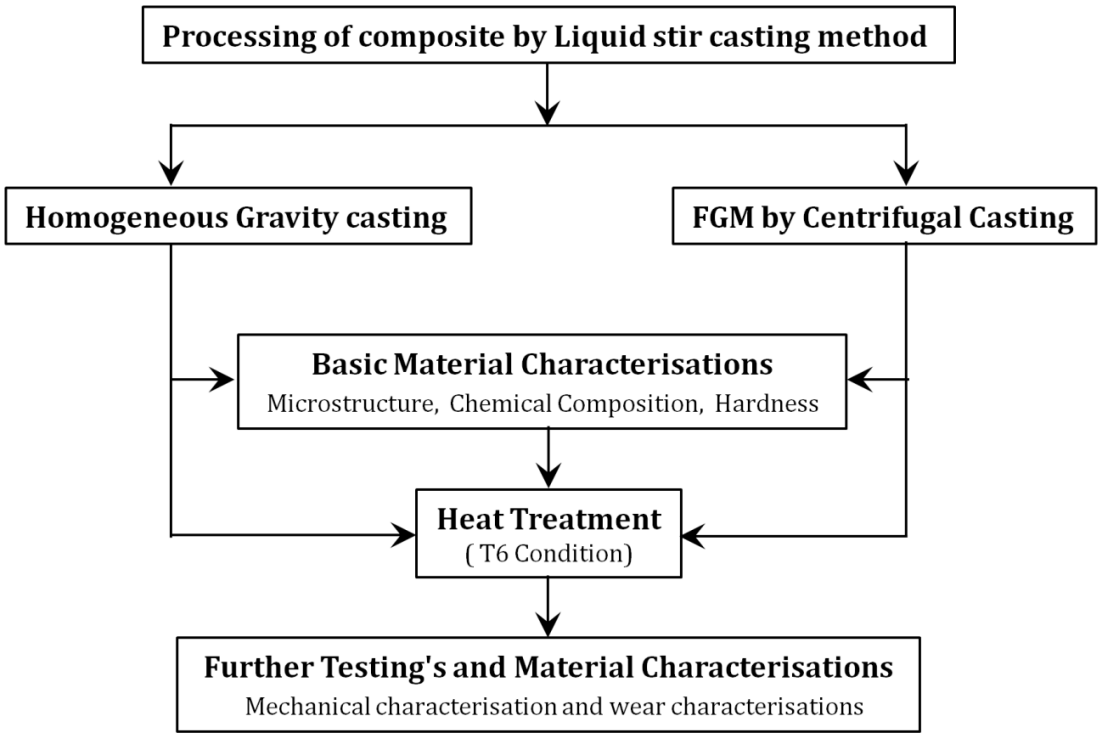

Figure 3.2: Flow chart for MMC preparation and experimental procedures

3.4 METHODOLOGY FOR POLYMER MATRIX FGM ANALYSIS

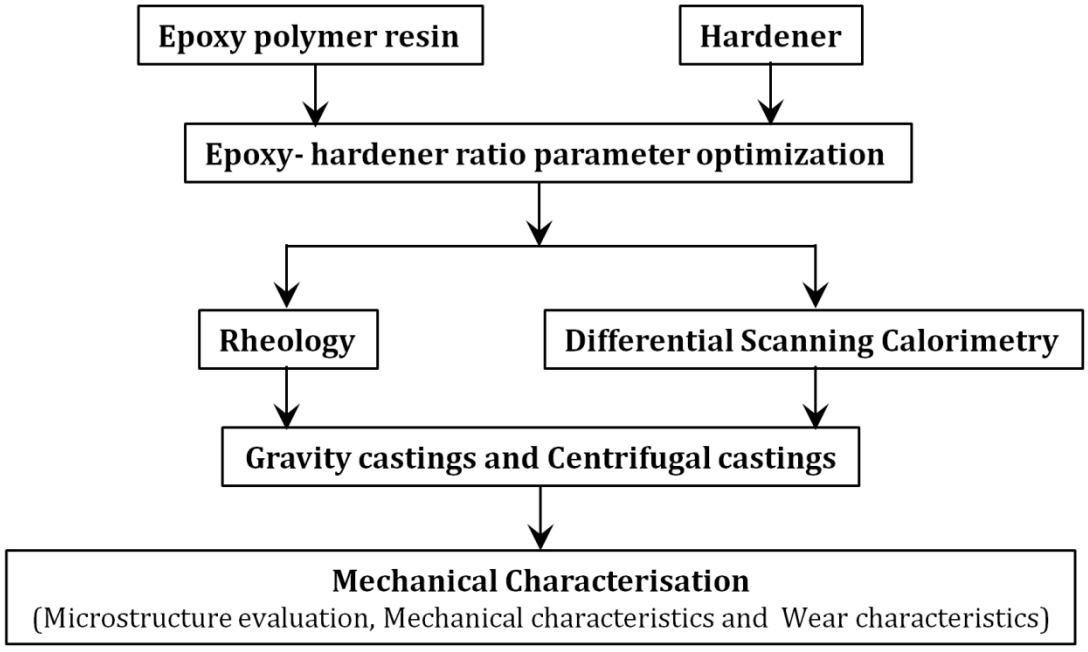

Figure 3.3: Flow chart of the methodology of polymer FGM experimental work

The flow chart (Figure 3.3) depicts the various experimental procedures carried out during the processing and characterization of polymer epoxy-SiC composites using gravity and centrifugal castings of epoxy alone, epoxy-5% SiCp gravity and FGM castings with optimised process parameters.

3.5 METAL MATRIX COMPOSITE MELT PREPARATION

3.5.1 *Liquid Metal Stir Casting for the Homogeneous Composite Melt Preparation*

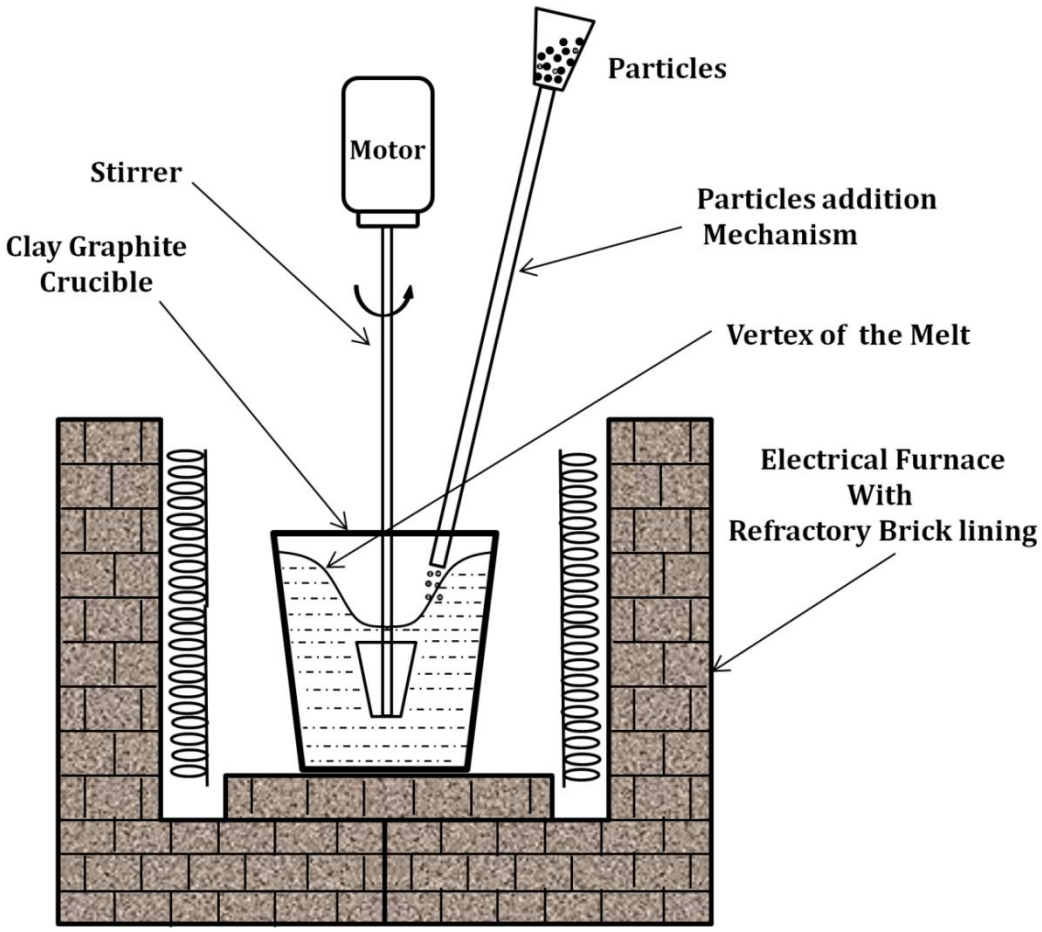

Figure 3.4: Schematic diagram of Liquid Stir Casting process

Liquid Metal Stir Casting involves the fabrication composite materials wherein the reinforcements are incorporated into the molten metal by mechanical stirring. The liquid composite material is then cast by the conventional casting methods and may also be processed by conventional metal forming technologies. Since most of the reinforcement systems exhibit poor wetting, mechanical force is required to combine the phases, generally through stirring. This method is currently the most inexpensive manner by which we can produce metal matrix composites (MMCs), and lends itself to production of large quantities of material, which can be further processed via casting or extrusion. The simplest dispersion process in current use is the vortex addition method, which consists of a steady vortex is maintained by a controlled speed stirring of the liquid metal and the pretreated (cleaned, dried, preheated and coated/uncoated) particle reinforcements are added to the vortex slanting surface in a very controlled

constant feed rate about 20g/min in 10 Kg melt batch. Throughout the addition process the melt will be kept at desired temperature levels of 720-740°C. The schematic diagram of stir casting process is shown in Figure 3.4. The various parameters which control the success of a stir casting are stirrer speed, powder preheating temperature, pretreatment of reinforcements, melt temperature during the powder addition and the size of reinforcements.

The composite melt synthesis was carried out in a 10kg capacity annealed clay graphite crucible in an electrical resistance furnace. Selection of various wt % SiCp are chosen to obtain the best dispersion in order to get a consistent MMC melt and good gradations in the properties of casted FGMMCs. The steady vortex was maintained by a hydro-drive dynamometer with a graphite coated mild steel stirrer rotating at a speed of around 350-400 rpm [128]. The calculated weight of cleaned and dried SiC particles are preheated to 600^{o}C, for 2-3 hours, before adding to the melt. To improve the wettability 1% Mg is also added while stir casting before the SiC addition [129-131**]**. The melt temperature was maintained in the range of 1003-1013K (730-740°C). After the completion of powder addition, the stirring is continued for 20 minutes and stopped. A baffle is introduced into the melt for consistency and uniform mixing of the composite and then stirring was restarted, continued for another 15 more minutes at1033K (760°C). The crucible was taken out of the furnace; in order to remove any slag or dirt particles, a thin layer from the top of the melt was skimmed off. Hand stirred and a portion of the melt was poured at 993K (720°C) to the preheated (523K (250°C)) gravity die casting moulds for homogeneous composite cast specimens for reference. From the balance of MMC melt, calculated quantity is taken in appropriate preheated crucibles for the FGM preparations. Since it is difficult to measure quantity of melt exactly in the melt condition, for getting similar quantity melt for every casting, pre-marked proper sized crucible are annealed and prepared early itself. In order to minimize Fe going into the melt, all utensils used during the casting which comes in direct contact with the melt are cleaned, coated with graphite, thoroughly preheated at 100^{o}C and dried (in order to avoid aluminium come in contact with water droplets).

3.5.2 *Vertical Centrifugal Casting for FGMMC Processing*

The FGM composites were made by two steps: Preparation of homogeneous composite melt of desired composition by liquid metal stir casting technique. Followed

by, FGMMC are processed in a vertical centrifugal casting machine for well established parameters. A circular disc shape mould of dimension 300 mm diameter and a thickness of 28 mm were used for FGMMC cast preparations. The mould was preheated for 2 hours at a temperature of 523K (250°C). Just before pouring, the mould was transferred from the preheating furnace, fixed on the shaft of the vertical centrifugal casting machine and kept in rotation with a speed of 1300 rpm (Figure 3.5). At a melt temperature of 1013K (740°C), with the help of a pouring cup, MMC melt was uniformly and steadily poured into the rotating mould to obtain FGMMC castings. After cooling, the castings are removed from the moulds and cleaned (Figure 3.6). The standard specimens are prepared from the desired locations of the casting for detailed characterization.

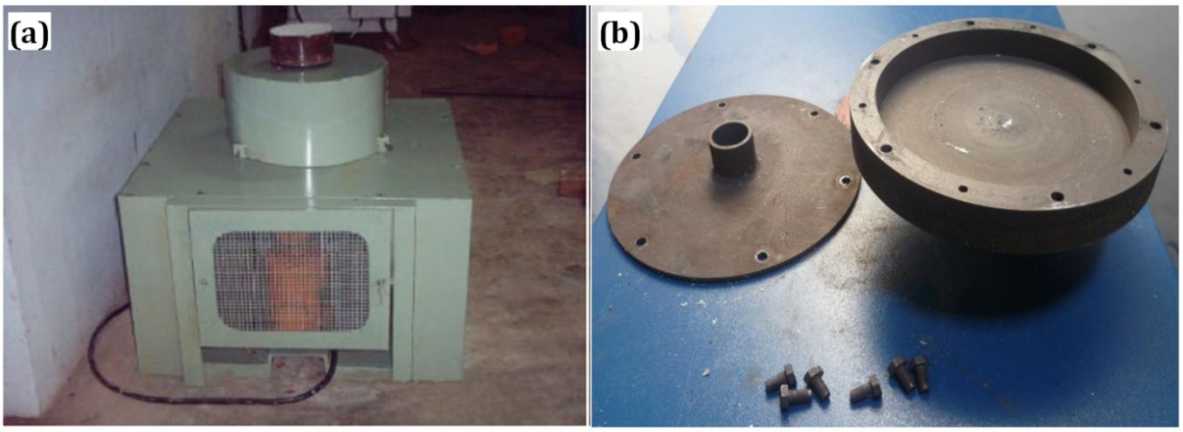

Figure 3.5: (a) Vertical centrifugal casting machine and (b) Mould for FGM rings

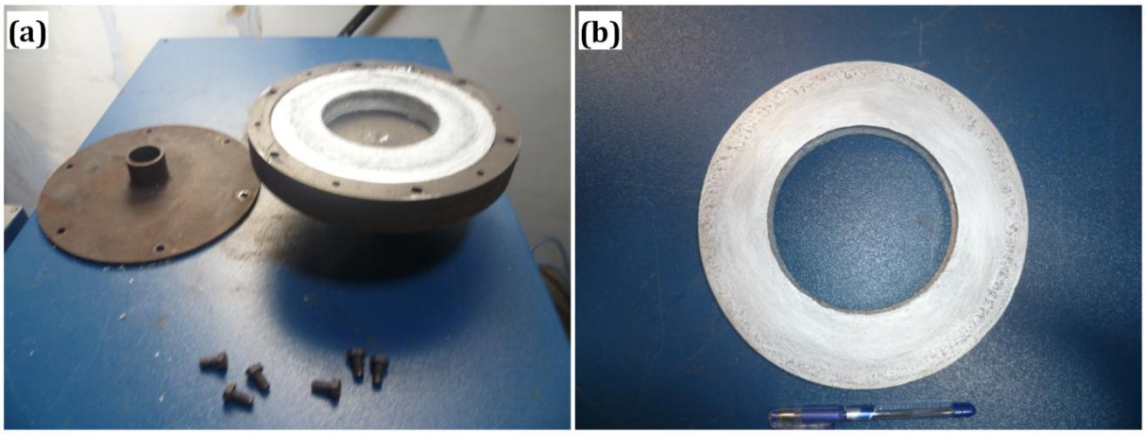

Figure 3.6: FGM castings are removed from the moulds and cleaned

Melt temperature during particle addition and the preprocessing of SiC particles/ reinforcements during the melt preparation are the controlling parameter to

yield a consistent MMC melt. The success of a FGMMC preparation mainly depends on speed of rotation of mould in the casting machine, the pouring temperature and pouring speed of the melt through the pouring cup into the rotating mould, the mould coatings and mould temperatures. The control of mould speed is very important for successful production of a FGM casting since it influences the structure, centrifugal force generated (effective pressure head) and the diffusion rate of different density phases in the melt. Speed of rotation is generally measured by the 'G' factor. It is the ratio of the centrifugal force (Fc) to the gravitational force (Fg). The centrifugal acceleration can be up to 100 times the gravitational force. It is important to determine the optimum speed of rotation. At higher speeds of rotation high tensile stresses are produced in the outer periphery of the casting resulting in longitudinal cracks. High rotational speeds can produce vibration inducing circumferential segregation. At the same time low rotational speeds can result in poor cylinder formation and surface finish. Hence the determination of critical speed is of prime importance in centrifugal casting. The most common effects of increase in speed are grain refinement and densification due to absence of gas porosity.

Pouring temperature exerts a major role on the mode of solidification and needs to determine partly in relation to the type of structure required. Low temperature is associated with maximum grain refinement and equiaxed structures while higher temperature promotes columnar growth in many alloys. However practical consideration limits the range. The pouring temperature must be sufficiently high to ensure satisfactory metal flow and freedom from cold laps, at the same time, avoiding coarse structures. The pouring speed is governed primarily by the need to finish casting before the metal become sluggish; although too high a rate can cause excessive turbulence and rejection. In practice slow pouring offers a number of advantages. The directional solidification and feeding are promoted even as the slow development of full centrifugal pressure on the other solidification skin reduces and risk of tearing. Excessive slow pouring rate and low pouring temperature would lead to form surface lap. The main significance of mould temperature lies in the degree of expansion of the die with preheating. Expansion diminishes the risk of tearing in casting. In nonferrous castings, the mould temperature should neither be too low nor too high. The mould walls should be sufficiently thick (at least 25mm), with the thickness increasing with size and weight of casting, in order to prevent damages in die geometry and bending

during the thermal expansions. Various types of mould coating materials are used to reduce the heat transfer to the mould. The defects like shrinkage and cracking that are likely to occur in metal moulds can be eliminated; thereby the die life can be increased. In addition to this the mould coating acts as a parting material between the mould surface and the outer surface of the casting which enable us for the easy release and removal of the cast from the mould. For aluminium alloys, the coating is a mixture of silicate and graphite in water.

3.5.3 *Vertical Centrifugal casting for Epoxy Polymer FGM Processing*

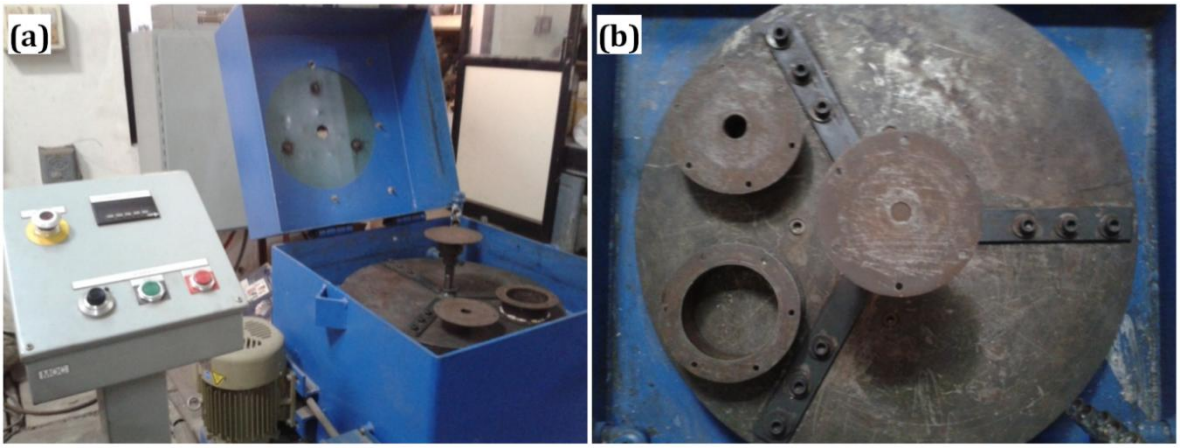

Figure 3.7: (a) Vertical centrifugal casting machine with (b) Mould used for fabricating Polymer FGM components

The centrifugal casting is a pressure casting method in which the centrifugal pressure force, when pouring the epoxy–hardener with SiC into the mould, is increased by rotating or spinning the mould assembly and causing the mix to cure and solidify in rotating moulds. The speed of rotation and mix pouring rate vary with the polymer, size and shape of the product to be moulded. Centrifugal casting has greater reliability than static castings since; the castings are relatively free from gas and shrinkage porosity. Figure 3.7 shows the vertical centrifugal casting machine Model JA/WC from Centrifugal Casting Machine Company Inc, USA and the mould used for doing the casting.

3.6 TESTING AND CHARACTERISATION METHODS

3.6.1 *Microstructural Evaluation*

The samples for characterization are prepared using standard metallographic techniques. The samples for taking microstructure are cut along the axial direction from

the castings. Specimen sectional surfaces are polished for microstructural examination (Figure 3.8 a). First the polishing is done on SiC papers of grit size 100, 220, 400, 600 and 1000 by the hand. The machine disc polishing (Figure 3.8 b) is carried out in a rotating wheel fixed with sylvet cloth with a gentle applied pressure and using diamond paste of varying size ranging from 6, 3, and 0.25 μm to get final mirror polish finish. Either distilled water or kerosene is used as the lubricating coolant medium. The micro structural features are observed using Leica optical microscope (Figure 3.9).

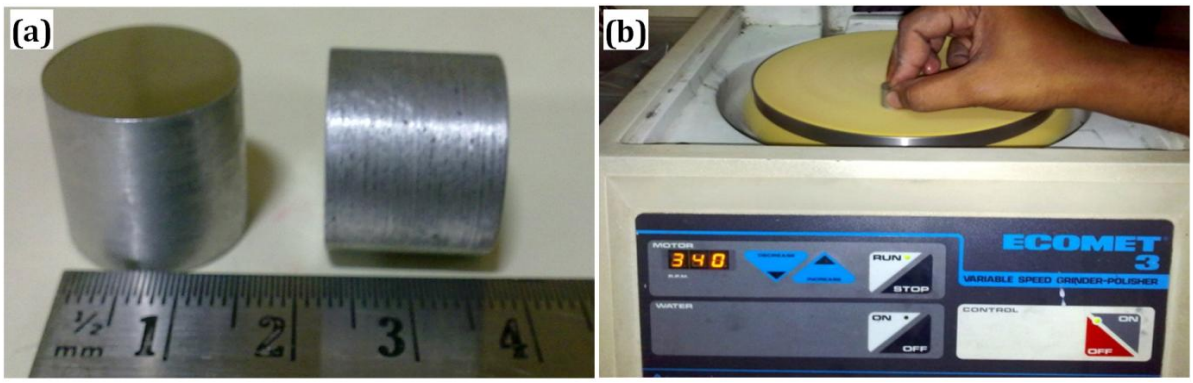

Figure 3.8: Photograph of (a) polished sample used for micro structural evaluation. (b) ECOMET, Disc polisher used for final polishing

Figure 3.9: Photograph of Leica Optical Microscope

The Light optical microscope remains the most important tool for the study of microstructure despite the evolution of other sophisticated metallographic instruments. All examinations of microstructure on Leica optical microscope had begun with the use of light microscope, starting at low magnification such as 5X followed by progressively higher magnifications for efficient assessment of the basic characteristics of the microstructure

3.6.2 *Hardness Evaluation*

The samples similar to that of microstructure study are polished by using silicon carbide abrasive papers of grades 80, 100, 220, 400, 600 and 1000. In Brinell hardness testing, a steel ball indenter of diameter of 2.5 mm, by applying a load of 62.5 kg using for 15 seconds, indentation marks are made. Hardness measurement for alloy and composite were determined on both as-cast as well as heat treated specimens. The micro hardness of a substance is an important parameter to define the strength of materials. Physically speaking, hardness is the resistance offered by the crystal for the movement of dislocations and practically it is the resistance offered by the crystal for localized plastic deformation. Hardness testing provides useful information about the mechanical properties like elastic constants, yield strength etc. of the material.

Brinell Hardness Number (BHN) was calculated using the formula

$$\text{Hardness (BHN)} = \frac{\text{Load on the ball}}{\text{Area of Indentation}}$$

$$\text{BHN} = \frac{2P}{\pi D\left(D-\sqrt{D^2-d^2}\right)}$$

where,
P = applied load (kgf)
D = diameter of the ball indenter (mm)
d = diameter of the indentation (mm)

Figure 3.10: The INDENTEC Hardness Testing Machine

In the study of epoxy polymer composites, INDENTEC Hardness Testing Machine (Figure 3.10) with a Vickers diamond pyramidal indenter having a square base and pyramidal angle of 136^0 is applied to evaluate the micro hardness enhancement. The specimens are subjected to a load of 3 kg with a dwell time duration of 20 s. Average values of five readings are taken and reported as the micro hardness of the samples. The average hardness of five readings was taken using average diagonal length of the residual indentation mark on the composite sample.

Vickers hardness number (HV) can be calculated by using the formula

$$HV = 1.8544(F/d^2)$$

where, F - load (kg) and

d - The average diagonal length (mm).

3.6.3 *Optical Emission Spectroscopy for Chemical Composition*

Figure 3.11: Optical emission spectrometer

The chemical composition analysis of the alloy samples were done in Amtek SPECTROMAXx optical emission spectrometer (Figure 3.11) using arc spark excitations. In optical emission spectrometry, electrical energy in the form of spark is generated between a pointed electrode and the specified surface of the metal sample, thereby vaporizing the surface and subsurface atoms to a high energy state within a so-called "discharge plasma". These excited atoms and ions in the discharge plasma will create characteristic emission spectral lines specific to each element. The discharge light is the collection of the spectral lines generated by the elements in the sample. This light is split by a diffraction grating to extract the emission spectrum for the target elements. The intensity of each emission spectrum depends on the concentration of the element in the sample. The Charged Coupled Device (CCD) detectors measure the presence or absence of an element from the extracted characteristic spectral lines. The intensity of the spectral lines gives a quantitative analysis of the elements. The alloying elements including traces of minor elements can be determined using this analyzer, Pre-defined calibration modules are available for the relevant elements such as Si, Fe, Al, Cu, Ni, Co, Ti, Cr and Mg. Tests are repeated at different locations of the specimen and an average value is generated for the alloying elements present in the material.

3.6.4 *Tensile and Compressive properties*

The tensile test which is the most common test carried out to evaluate the mechanical properties was done using INSTRON 1195 – 5500R series electromechanical

materials tester (Figure 3.12). The tensile samples of MMCs and FGMMCs were prepared from the cast according to the ASTM standards B557M (Figure 3.13). The samples are heat treated before being tested according to the ASTM standards E-8.

Figure 3.12: INSTRON 1195 – 5500R series electromechanical materials tester

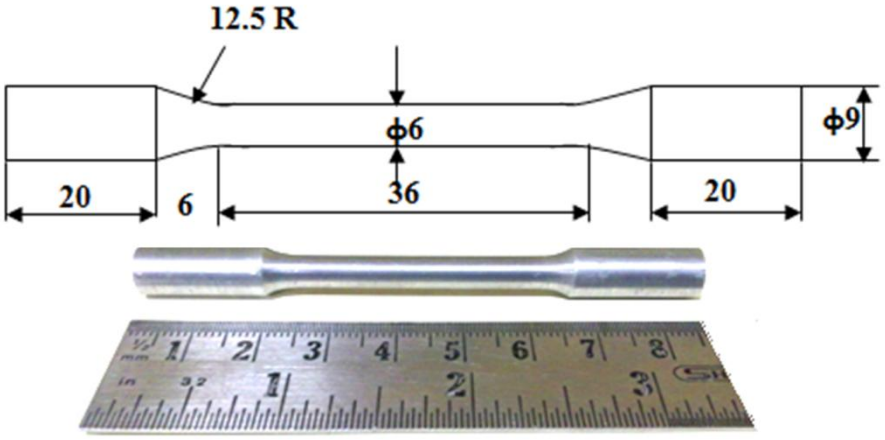

Figure 3.13: Tensile specimen for MMCs and FGMMCs (All dimensions are in mm**)**

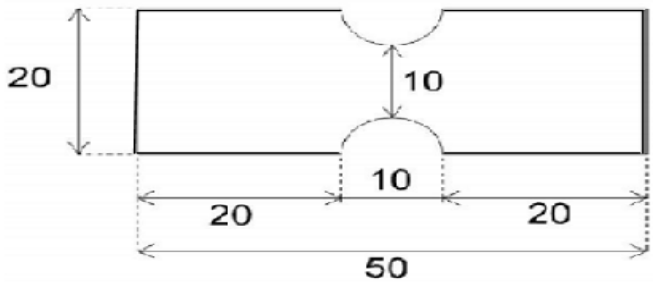

Figure 3.14: Specimen of polymer epoxy composites and FGMs for Tensile Testing

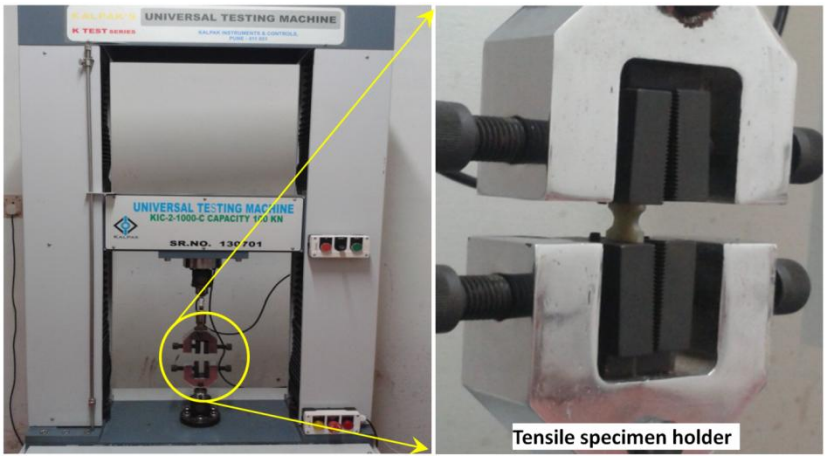

Figure 3.15: Photograph of Universal Testing Machine

The tension tests are conducted for evaluating mechanical properties of the polymer epoxy gravity and FGM castings. The test were conducted on the specimens prepared to the size as shown in the Figure 3.14 with a uniform thickness of 2 mm .The tensile specimens are taken from different locations of the centrifugal castings basically inner, transition and outer regions in the axial direction of the castings and tested in Kalpak's K Test Series (KIC 2-1000- C) Universal Testing Machine (Figure 3.15).

3.6.5 *Wear Analysis*

Figure 3.16: DUCOM (TR-20 LE) pin on disc tribometer with the computer interface

Dry linear wear test of MMCs are carried out in a DUCOM pin-on-disc tribometer with EN 31 steel disc and heat treated pins taken from different zones of the castings (Figure 3.16). The pin can have any shape to simulate a specific contact, but spherical tips are often used to simplify the contact geometry (Figure 3.17). The dimensions of the pin are 6 mm in diameter and 30 mm in length. The dry wear tests are conducted: for 15 minutes duration at four different loading conditions (1, 2, 3 and 4 Kg), for a

sliding distance of 1800 m with a relative velocity of 2 m/s. The weight loss method is used to find out the wear rate behaviour of the pins. A pin on disc tribometer consists of a stationary "pin" under an applied load in contact with a rotating disc. Coefficient of friction is the ratio of the frictional force to the loading force on the pin.

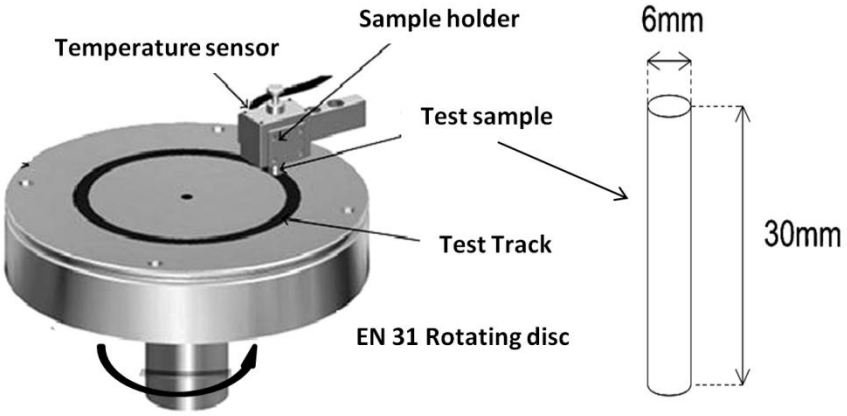

Figure 3.17: Standard Wear Test Specimen (All dimensions in mm**)**

The test conditions employed to carry out the wear test are as follows

- Use of steel disc without any lubrication so as to carry out dry sliding test.
- Track radius is 70 mm
- The speed of rotation of the disc is 272 rpm (Approx.)
- The Relative velocity is 2 m/s
- The sliding distance 1800 m
- Duration of each experiment is about 15 minutes (Approx.).

The understanding of the wear, friction and lubrication behaviour of materials, lubricants and coatings in a variety of test conditions has become increasingly important in the recent years. The tribology studies of the polymer epoxy composites are conducted at varying conditions to analyze the wear properties of these gravity cast and centrifugally cast composites developed. The test conditions followed in the epoxy composite are as follows. Since wear properties of epoxy is different from that of metals systems, the relative velocity and the sliding distances are modified as per the previous literatures.

- Test is dry sliding test and steel disc is used without any lubrication.
- Sliding relative velocity of 3 m/s is fixed.
- Sliding distance of 3000 m.
- Track radius is fixed to be 70 mm.

- Speed of rotation of disc is 410 rpm (Approx.).
- Duration of testing is 17 minutes (Approx.).

For in-situ FGM preparations by Al-Mg master alloy addition in addition to pin on disc unidirectional wear, bidirectional reciprocating wear is also conducted in similar testing conditions. The testing conditions for both wear tests are; with a sliding velocity of 0.6m/s for a total sliding distance of 500 m at loads 1, 2, 3 and4 Kg in a dry testing condition. For the reciprocating wear the stroke length was 10cm. And for pin on disc the radius was 70 mm and speed was100 rpm (Approx.). The time of experiment was approximately 13minutes.

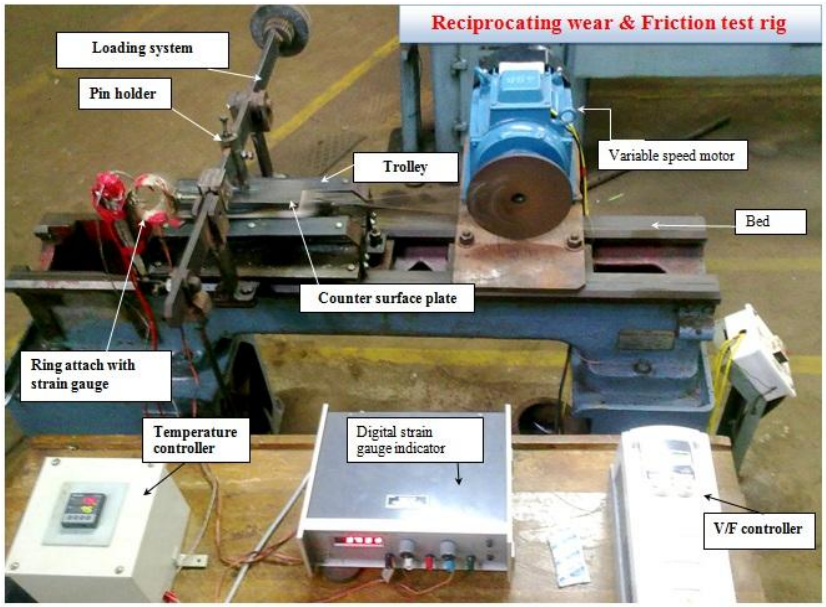

Figure 3.18 Reciprocating wear test rig

The main features of the reciprocating wear test rig are shown in Figure 3.18. The slider crank mechanism is connected to a crankshaft assembly which is attached to electric motor. This will give a reciprocating motion to the reciprocating trolley on which the tribo-element counter surface is attached. Provisions are made to ensure constant loading, varying the stroke length and the frequency of reciprocating motion. Loading, pin holding and a temperature control mechanisms along with dry/wet lubrication systems are also provided. The pin holding was designed to perform several functions such as accurate positioning of wear test pin in relation to the counter surface, holding the pin in such a way that there is no relative motion between the pin and the pin holder and easy loading/unloading of work piece. The pin holder was attached to the lever arm of the setup. For studying the high temperature wear and friction behaviour of composite, the counter surface was heated with a heat source. The heating

system consisted of an electrical heating element, and temperature controller (thermostat) capable of controlling temperature of counter surface up to 1000^0C with an accuracy of ±1°C. A Teflon sheet was clamped with the heating element to ensure that only counter surface heated.

3.6.6 *Wear Surface Stereo Micrograph Analysis*

Figure 3.19: Photograph of Prog Res C5 stereo microscope

Figure 3.19 shows the Zeiss stereo microscope used to take stereo images of the wear surfaces. For a better understanding of the involved wear mechanisms, the surface morphology microstructures of the worn out pin surfaces are taken. All the micrographs are taken at a constant magnification of 10x for the easy size measurements and physical observations of worn out surfaces.

3.6.7 *SEM Analysis*

Figure 3.20: Zeiss EVO 18 Scanning Electron Microscope

The scanning electron microscope (SEM) uses electrons probe instead optical light. From the spot illuminated by the electron beam, various signals, such as

secondary electrons, backscattered electrons, characteristic X-rays, and cathodoluminescence, are emitted depending on the form of the specimen, the density of the substance and the elements contained inside. The Scanning Electron Microscope (SEM) normally detects secondary electrons to form an image for observation. As the intensity of the generated secondary electrons varies depending on the angle of the incident electrons onto the specimen surface, subtle variations in the roughness of the surface can be expressed according to the signal intensity.

The signals carry information about the surface topography, morphology, composition and crystallographic information. The topography will give the surface features of and its texture: which can be utilised for fractographic and tribology studies. The morphology provides information about the basic constituents leading to direct relation between these structures and material properties. The elemental information gives relationship between composition and materials properties. The crystallographic information directs to specimen material properties. In the most common or standard detection mode, secondary electron imaging, the SEM can produce very high-resolution images of a sample surface, revealing details about less than 1 to 5 nm in size. Back-scattered electrons (BSE) are beam electrons, which are reflected from the sample by elastic scattering, are often used in analytical SEM along with the spectra made from the characteristic X-rays.

In the present study SEM imaging is primarily used to study the surface conditions and distribution of the reinforcement materials in the fabricated composites. Investigation of the wear surface is to study the material removal happening at the interface and to suggest a suitable material removal mechanism occurring in the developed systems. Jeol scanning electron microscope and Zeiss EVO 18 scanning electron microscopes (Figure 3.20) with an accelerating voltage of 20-30 kV are used in the study.

3.6.8 *CTE Analysis*

When MMCs are cooled, misfit strains might set in if large differences exist between the thermal expansion coefficients of the matrix and the reinforcement [132]. This strain induces thermal stresses that may create dislocations and lead to an increase in the dislocation density. Practically, both the CTE and the Poisson's ratio of the ceramic particle reinforcement are much lower than that of any metal matrix. The

matrix tries to shrink more than that of the reinforcement during cooling, which is actually hindered by the reinforcement, which induces volumetric strain in the matrix as well as the reinforcement. Therefore an understanding of the CTE of the FGM's are required with samples taken from different locations and tests are done on a SII TMA SS/7300 CTE analyser (Figure 3.21).

Figure 3.21: Photograph of SII TMA/ SS7300 CTE analyser

3.6.9 *Physical Property (Density) Measurements*

Figure 3.22 Balance with Density measurement kit

The density of the gravity cast composites and FGM's at similar locations are different. The theoretical density of the gravity cast composites are compared with experimental values. The densities of the FGM's at different locations are measured. For calculating the density, the specimens are weighed in air and water with the balance

(Figure 3.22). Using the dry weight and immersed weight the density of the specimen can be calculated as follows.

$$Density = \frac{Dry\ weight * Density\ of\ water}{Dry\ weight - Immersed\ weight}$$

3.6.10 *DSC Analysis*

Figure 3.23: Photograph of Differential Scanning Calorimeter

The differential scanning calorimetry (DSC) is a thermo-analytical technique in which the difference in the amount of heat required to increase the temperature of a sample and reference is measured as a function of temperature. Using this technique it is possible to observe fusion and crystallization events as well as glass transition temperatures T_g. DSC is used widely for examining polymeric materials to determine their thermal transitions. The Pyris-TM 6 Series instrument is used to do DSC test (Figure 3.23). The system utilizes a precision-machined disc of hardened nickel chromium to form a strong thermal link between the sample and the low-mass furnace. Typical applications include: glass transition point, crystallization temperature, rates and times, degree of cure and percent of crystallinity.

3.6.11 *Rheology Analysis*

The visco-elastic behaviour of the composite system is studied using parallel plate rheometer. Anton Par Physical Modulated Compact Rheometer 150 with disposable parallel stainless steel plates of 50 mm diameter are used for the purpose (Figure 3.24). A rheometer is a device used to measure the way in which a material responds to applied force. Rheometers are classified according to the sensor being used and are rotational-cylinder, cone-plate and plate-plate type. In rotational cylinder type

rheometer, one cylinder is rotated in the annulus of the other, and is mainly used to measure the shear rate inside the cylinder. Parallel plate rheometers are widely used to measure the visco-elastic properties.

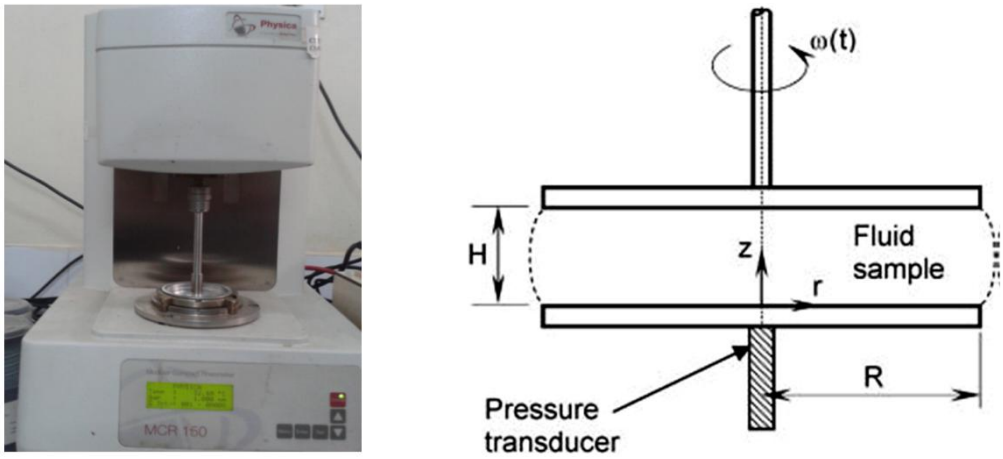

Figure 3.24 Photograph of Compact Rheometer

The various visco-elastic properties measured by the rheometer includes storage modulus, loss modulus, complex viscosity, torque and damping factor. The temperature, strain amplitude, frequency are set according to our need by the software. The experiments were done in the oscillatory shear mode. A small amount of the sample was placed between two parallel plates and a gap width between the plates was maintained at 1 mm. oscillating strain amplitude of 1 % and a angular frequency of 10/s was given as input. The experiment is conducted at room temperature.

Chapter 4

Processing and Characterisation of A319–SiC Functionally Graded Metal Matrix Composites

4.1 INTRODUCTION

Aluminium-silicon based alloys, due to their high strength to weight ratio, have received a considerable attention in the various mechanical manufacturing sectors. The weight reduction in the components of aerospace and automobiles leads to a significant impact on the fuel economy. A319, A356 and A390 alloys are well suited for wear-resistant and weight critical applications such as brake drums, cylinder liners, pistons, cylinder blocks, connecting rods and clutch housing in automobiles. Silicon based aluminium alloys are used in helicopter structural parts applications such as parts of the body, support for rotor plates and drive shafts. They are also suitable for producing rotor vanes in compressors and aero-engines [133-135]. Functionally graded materials (FGM) are a class of advanced composite materials consisting of two or more phases, with variation in composition and /or microstructure in spatial direction. FGMs can be processed to obtain higher superficial hardness with adequate internal toughness properties that are not attainable by a monolithic or a homogeneous material [136-138]. The gradation reduces the local stress concentration, thermal and residual stresses, which are commonly experienced in traditional composites. Gradation can also modify the location specific mechanical and thermal properties, with a proper combination of different matrices and reinforcements with suitable properties, size and/or shape. A metal matrix FGM with ceramic reinforcements can provide a single material with good thermal protection and load carrying capability thereby eliminating the possibility of cracking and spalling of tiles that are experienced in the Space Shuttle outer surfaces. Even though FGMs developments started as thermal barrier materials for aerospace structural applications and fusion reactors, now they are strongly considered as a potential structural material for the design of high speed aerospace vehicles and for components in the high temperature environments. Light weight composite airframes can also increase the payload capacity, speed, range, and

endurance. The properties of composites are greatly influenced by the type of reinforcement particles, size of particles and its volume fraction. The industrial interest in FGMs is mainly related with the opportunity of controlling the gradation of the physical and /or chemical properties, through microstructural manipulation. By centrifugal casting method, the volume of reinforcement addition and its radial distribution can be controlled to produce components with better thermal dimensional stability and more wear resistance properties. The A319 exhibits good casting qualities including pressure tightness, moderate strength, good weldability and corrosion resistance. In the automobiles components like the brake discs, liners and pistons, only the rubbing surfaces or the contact regions require more wear resistance property and the other portions can be less populated or even reinforcement free [139]. The FGM formation with SiCp reinforcements with location specific wear-resistant properties leads to increased component service life due to the minimum wear and tear. In the case of automobile pistons and cylinder liners, in addition to the external reinforcement additions, better thermal and mechanical properties can also be achieved by the second phase gradations like the gradation of in-situ primary silicon [140-141].

The reinforcements can be introduced into the MMC melt by ex-situ and in-situ methods of preparations. In the in-situ composite preparations, the reinforcements like, TiB2, TiC and AlB2 are formed by reactions that are occurring during the processing [142]. By suitably setting the process parameters, the sizes of the reinforcements and their homogeneity in distribution can be well controlled. The clean interfaces of fresh reinforcements increase their wettability with the matrix [143]. FGMMC with graded properties can also be prepared by the ex-situ additions with Al_2O_3, TiB_2, TiO_2, SiC, TiC, B_4C, graphite and SiC particles. The lower wettability problems arises in ex-situ additions due to the presence of oxide films on the surface of molten metal and the adsorbed contaminant on the reinforcements can be well controlled either by metallic coatings or heat treatment of reinforcement particles and by the addition of smaller percentages of reactive elements, like magnesium, calcium or titanium, to the molten metal during processing [144-145].

Centrifugal casting is one of the simple pressure die casting method by which FGMs can be manufactured economically. An increased centrifugal force is applied to the melt containing reinforcement particles or phases by pouring the melt into the rotating moulds and thereby forming different zones of reinforcement concentrations

during solidification. The extent of particle concentration, relative locations and the zone sizes within the casting are mainly controlled by the melt temperature, melt viscosity, cooling rate, the densities of the particles and the matrix. The particle size, the initial volume of addition during the melt preparation and magnitude of centrifugal acceleration determines the magnitude and the position of maximum concentration point [146-151].

4.2 MATERIALS AND EXPERIMENTAL METHODS

The processing of A319 Aluminium functionally graded metal matrix composites reinforced with 10 and 15 wt. % SiCp, of average particle size of 23 μm, has been done then extended to 20wt %. The different concentrations of reinforcements are selected in such a way that the variations are clearly visible during the characterisations. Addition of less percentages of particles will not yield a significant improvement in properties while, on the other hand, very high percentage additions of SiCp leads to difficulty in getting a good MMC melt with neat dispersion due to the high viscosity and increased particle agglomeration tendency. Liquid metal stir casting method is adopted for the composite preparation and FGMMC castings are produced by vertical centrifugal casting technique. Mechanical and tribological characterisations have been carried out.

4.3 STUDIES ON A319-10 Wt. % AND 15Wt. % SIC FGMMC

4.3.1 *Microstructural Evaluation*

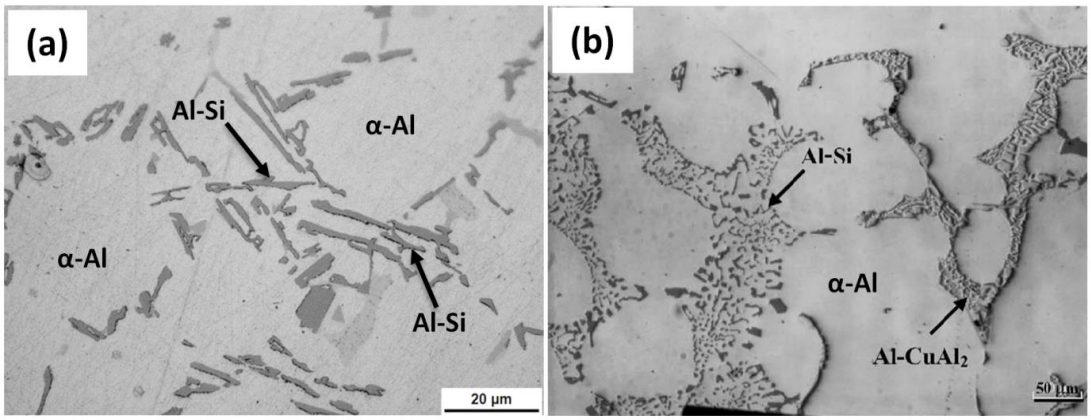

Figure 4.1: Microstructures of A319 alloy with Al-Si Eutectics and Al-$CuAl_2$ phases

Figure 4.1 shows the optical micrographs of the gravity cast A319 aluminium alloy. The dark needle like eutectic silicon phases, the grey $CuAl_2$ phase and white α-Al matrix phases are observed. In Figure 4.2 (a) evenly spaced secondary dendritic arms of

A319 are visible in the microstructure. Figure 4.2 (b), (c) and (d) show the optical micrograph of 10,15 and 20 wt % SiCp gravity castings in the as cast condition.

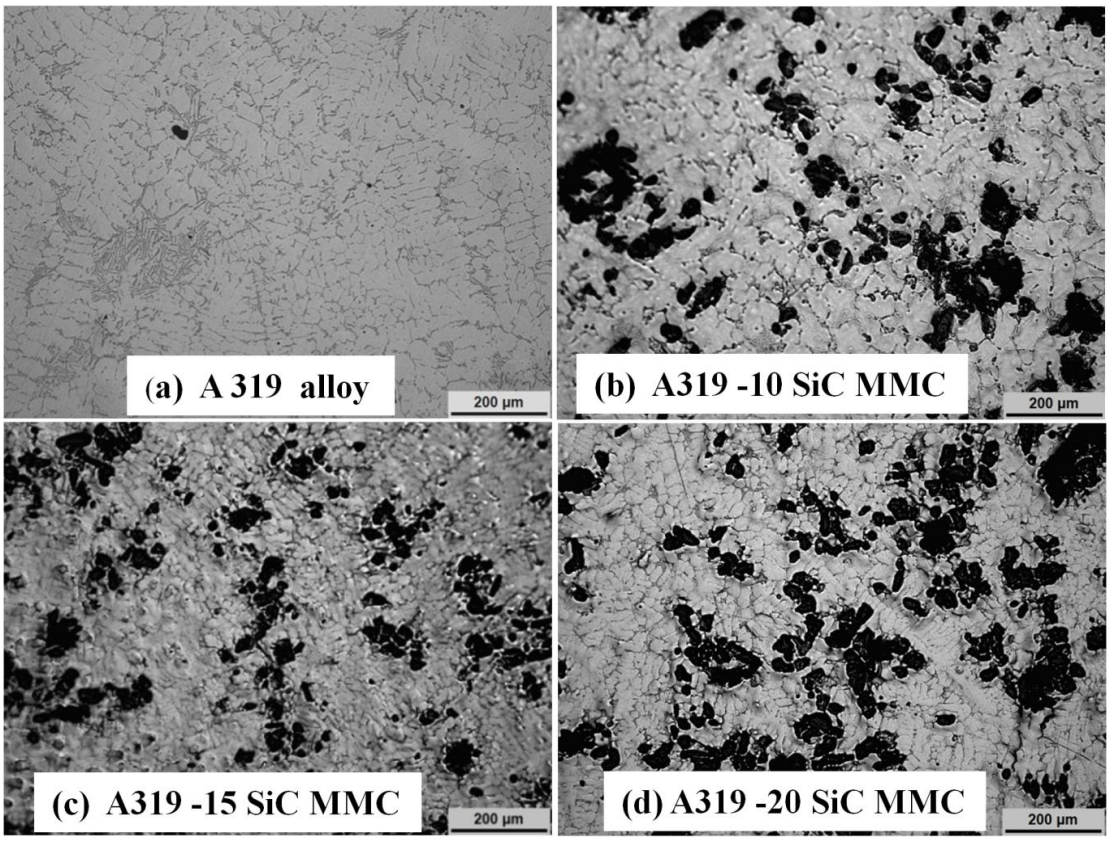

Figure 4.2: Microstructures of gravity cast (a) A319 alloy, (b) A319-10%SiC MMC (c) A319-15% SiC MMC and (d) A319-20% SiC MMC

The micrograph of composite depicts uniform distribution of silicon carbide particles (dark) in Aluminium alloy matrix. Figure 4.3 shows the schematic diagram of a centrifugally cast FGMMC disc with observed zones and locations, from where test specimens are prepared for microstructure, hardness, density, tensile, compression and wear analysis. Figure 4.4, Figure 4.5 and Figure 4.6 show the optical micrographs of centrifugally cast A319-10 wt % SiCp FGMMC (10-FGM) ,15wt % SiCp FGMMC (15-FGM)and 20wt % SiCp FGMMC disc (20-FGM) taken from inner towards outer in the radially outward direction respectively. In all, four microstructure regions are observed and namely they are; the matrix rich zone (the inner region which are free from the reinforcement particles), the transition, particle rich and the chilled zone (the outer most periphery of the disc). For the completion solidification a cast disc of diameter 300mm and thickness 28mm will takes about 2-3 minutes. The solidification process (solidification front) in a centrifugal casting is a directional one and is from outer most

periphery of the mould towards the inner diameter of the casting, i.e. radially inward direction. While the denser silicon carbide reinforcement particles and the secondary phases will diffuse from the inner diameter towards the outer diameter due to the centrifugal force, i.e. diffusion front is in radially outward direction. The position of the particle rich zone, size and the maximum value of particle concentration depend on the solidification time and the centrifugal force (G effect). Even though there is the chilled zone, of size 2-3 mm radial, oppositely moving solidification front and the particle diffusion fronts will meet outside the chilled zone and this radial position will determine the exact location and magnitude of maximum particle concentration. The specific heat capacity of SiCp (1300 $Jkg^{-1}K^{-1}$) is higher that of the aluminium matrix alloy (963 $Jkg^{-1}K^{-1}$ in liquid state and 1084 $Jkg^{-1}K^{-1}$ solid state). Hence the composite with higher volume fraction SiCp have more heat content to release leading to longer solidification time enabling more particle diffusion towards outer periphery. The maximum particle concentration position was observed near at 55 mm for 10-FGM with 18.5 wt % of SiCp and near at 75mm for 15-FGM with 28 wt% of SiCp from inner diameter of the casting towards the outer diameter in the radial direction.

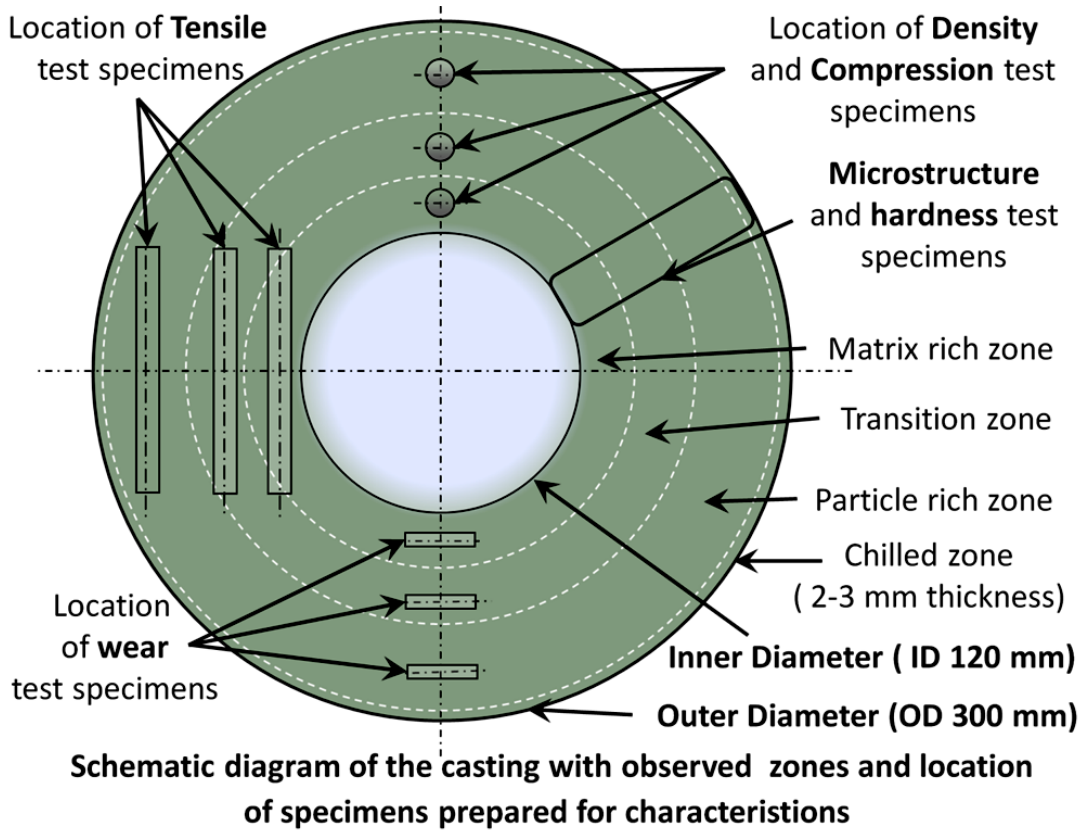

Figure 4.3: Schematic diagram of the casting with observed zones and location of specimens prepared for characterisations

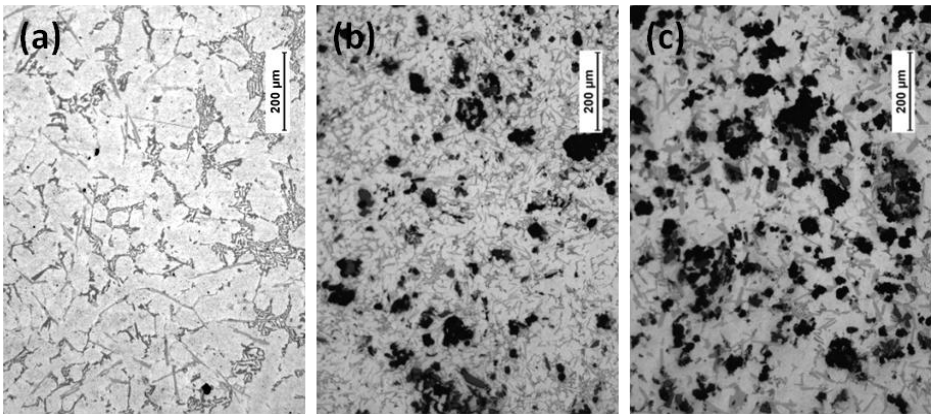

Figure 4.4: Microstructures of 10-FGM from inner to the outer periphery of the casting (a) Inner matrix rich zone / powder depleted region (average zone size 15 - 20mm radial thickness), (b) Transition zone (average zone size 10 - 20 mm radial thickness), (c) Particle rich zone (average zone size 15 - 25 mm radial thickness)

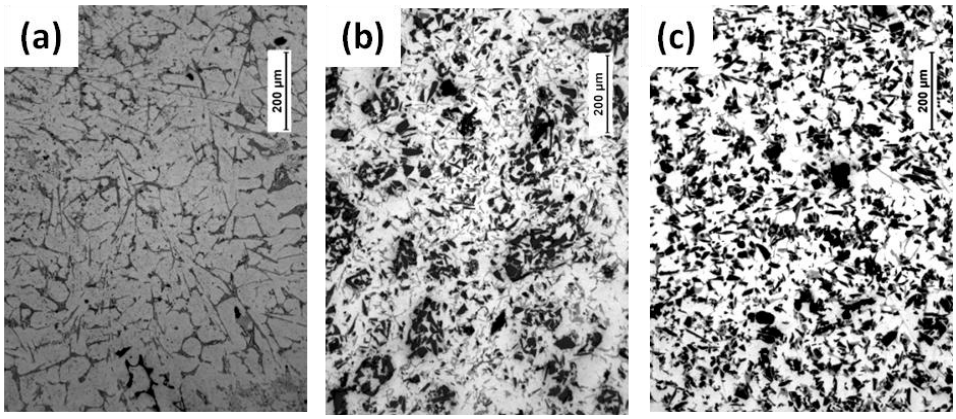

Figure 4.5: Microstructures of 15- FGM from the inner to outer periphery of the casting (a) Inner matrix rich zone / powder depleted region (average zone size 15 - 25mm radial thickness), (b) Transition zone (10 - 20 mm), (c) Particle rich zone (15 -25 mm)

Figures 4.4 (a) and 4.5(a) show the inner matrix rich zone / powder depleted region of average zone size 25 - 30mm radial thickness. In both microstructures only α-Al and eutectic Al-Si phases are visible. Very few particles are being observed in the near vicinity of transition zones. Towards the inner most diameters the microstructures shows gas porosity and particle agglomerations (not shown). In the case of a real application, those inner most regions can be properly machined off during the finishing operations. Figure 4.4 (b) and 4.5(b) show the transition zone of average zone size 20 mm radial thicknesses. Clear variations in particle concentrations are observed in the

transition zone microstructures. Figure4.4 (c) and Figure 4.5(c) show the particle rich zone (average zone size 25-40 mm radial thickness). The outer most periphery/ chilled zone has an average zone size of 2-3 mm radial thickness with less concentration of particles compared to the adjacent region. This is due to the immediate solidification of the liquid composite melt which comes in contact with the mould surface. The region near outer with higher concentration of particles, near inner with a depletion of particles and the connecting transition region in the middle with a less and varying concentration of reinforcement particles clearly constitute a graded microstructure. Figure 4.6 (a-c) shows the microstructures of A319 base centrifugal casting taken from similar radial positions that of FGMMC castings. Since A319 is a hypoeutectic alloy (Al 6Si 3.5Cu), gradation in primary silicon particles are not observed in the microstructure. Due to the higher solidification rate, the grain size of the primary aluminium (α-Al) and eutectic silicon phases are finer towards the outer periphery. Both the inward solidification and the outward centrifugal forces sweep the light weight agglomerated reinforcements and segregated gas porosities towards the inner periphery of the casting and produces a clean dense porous free regions of microstructures throughout the castings.

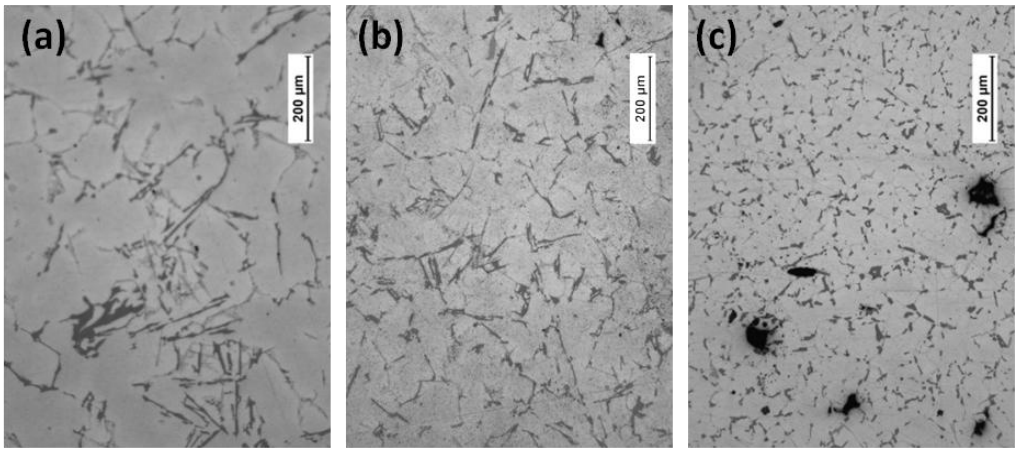

Figure 4.6: Microstructures of A319 base centrifugal casting from the inner to outer periphery. Microstructures (a), (b) and (c) are taken from similar radial positions that of FGM castings.

4.3.2 *Density Calculations*

Figure 4.7 shows the Densities of the homogeneous gravity cast composites and that of FGMMC specimens taken from different zones located at distances of 30, 55 and 75mm from inner towards outer. The density value of homogeneous gravity cast A319-

10 SiCp is 2.756 g/cm^3 and that of A319-15 SiCp is 2.789 g/cm^3. Both the composites show similar behaviours in density variations. In the case of matrix rich region specimens (from 30mm) clearly show lesser density value of 2.754 g/cm^3 and 2.742 g/cm^3 respectively and are due to the absence of denser SiC particles. The density of both FGMMC specimens taken from the particle rich regions are high as expected due to the presence of maximum percentages of particles and the respective values of 10-FGM and 15-FGM are 2.83 g/cm^3 (at 55mm) and 2.87 g/cm^3 (at 75mm).

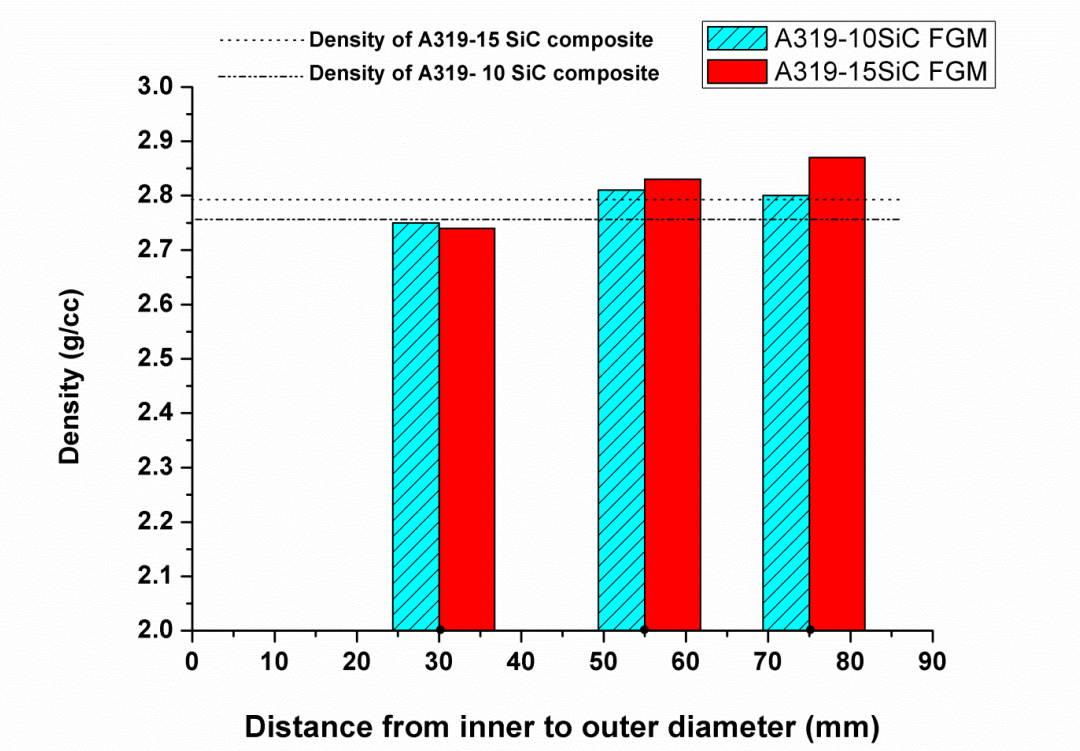

Figure 4.7: Density of both 10-FGM and 15-FGM castings at a distance of 30, 55 and 75 mm from inner towards outer diameter of the casting

4.3.3 *Image Analysis*

Figure 4.8 shows the volume percentage distribution of SiCp in radial direction is calculated by image analysis from inner to outer diameter of the casting. For 10-FGM the maximum concentration is observed at a distance of near 55 mm from the inner towards the outer diameter and the maximum point, for 15-FGM, is obtained at near 75mm from the inner diameter. There is an outward shift in position of maxima in the case of 15-FGM. The calculations closely follow the experimental values of density and support the hardness values obtained from the similar locations of the FGM specimens.

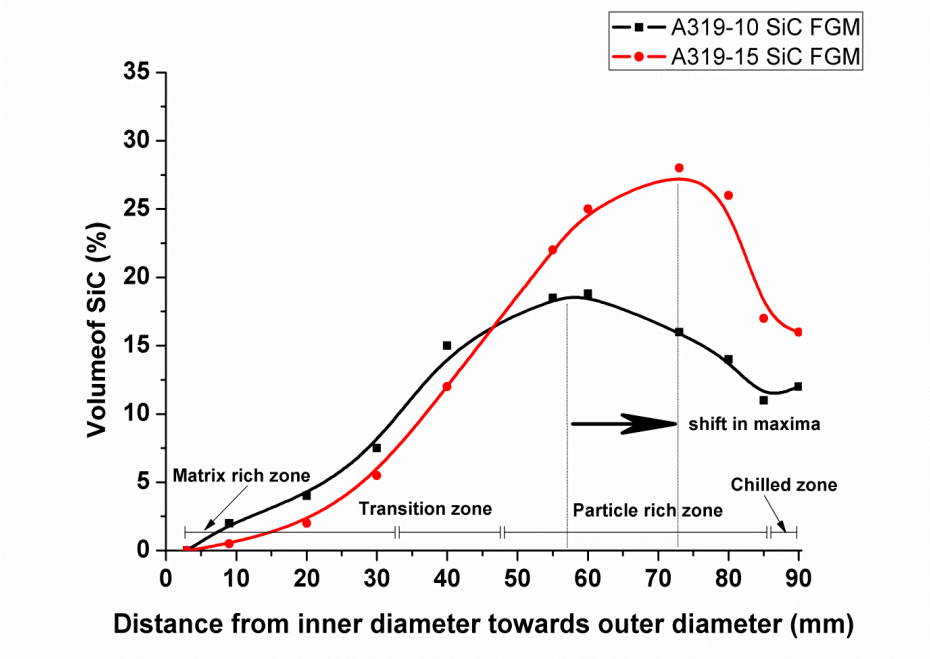

Figure 4.8: Volume percentage distribution of SiC reinforcements in radial direction of both 10-FGM and 15-FGM castings from inner towards outer diameter of the casting.

4.3.4 *Hardness Behaviour*

Table 4.1: Hardness of A319 Al alloy, A319-10 SiC and A319-15 SiC homogeneous gravity die casting under as cast and T6 heat treated conditions (in HRB)

Material specification	Gravity Castings In Rockwell Hardness (B-Scale) **HRB**	
	As Cast conditions	Heat Treated T6 conditions
A319	50	70
A319-10SiC	55	72
A319-15SiC	70	80

Table 4.1 shows the Rockwell hardness (HRB) of gravity casted alloy and the composites before and after heat treatments. Hardness variations along the radial direction of as cast as well as the heat treated samples of 10-FGM is shown in Figure 4.9 (a) and that of 15-FGM is shown in Figure 4.9(b). It is observed that the location wise changes in density values at different zones of FGMMC's closely follows the variations in hardness value suggesting the influence of SiCp concentrations. Heat treatment improves the hardness as well as other mechanical properties due to the redistribution

of $CuAl_2$ phases [152 -156]. It is observed that in all the centrifugal cast FGMMC, the hardness value increases from very low values in the inner periphery, due to porosity, to a maximum in the particle rich zones and then decreases to a normal values towards the chilled zone of the casting. The hardness values of the heat treated samples are higher than that of as-cast samples.

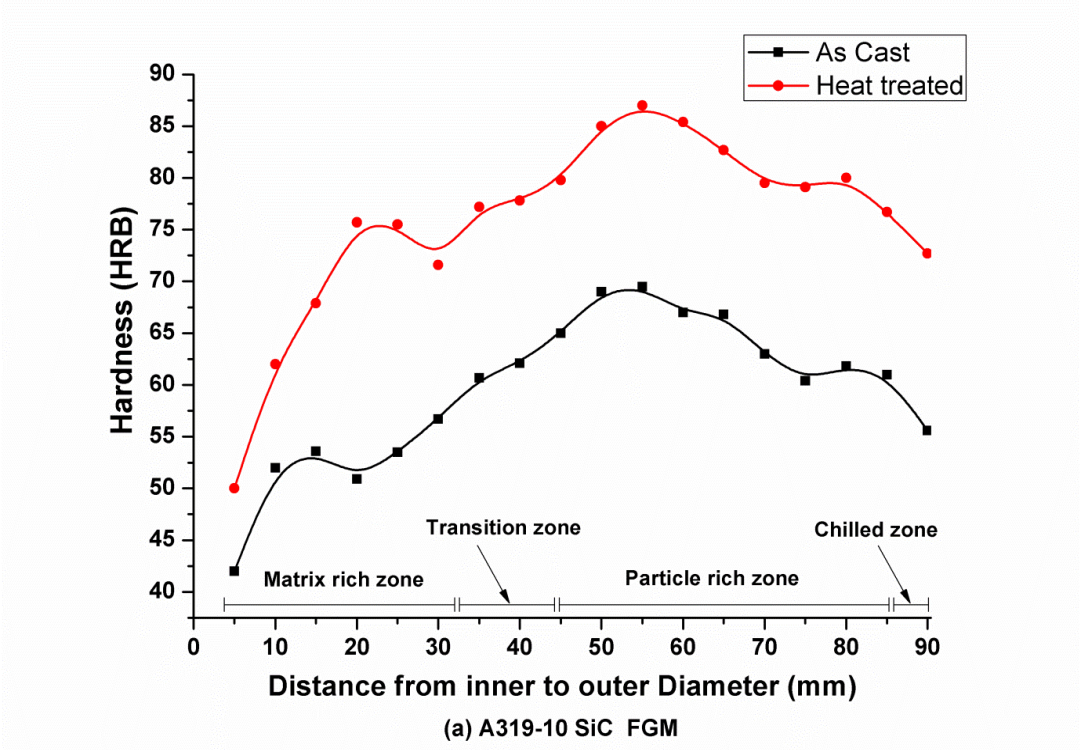

Figure 4.9: (a) Hardness variation from the inner diameter of the ring towards the outer diameter regions of FGMMC rings in both as Cast and after T6 Heat treatment conditions of 10- FGM

In Figure 4.9 (a) the maximum hardness of, 87 HRB, is observed between 45-55mm and in Figure 4.9(b) a value of, 94.4 HRB, at 65-75 mm. This shows that the SiCp impart strength and hardness to the zones in which they are present. The hardness values at the point where iron intermetallic are seen have combined effects of concentration of SiCp and Al_5FeSi [157-159]. Al_5FeSi is found in the transition zone towards inner region and they are formed due to the iron diffusion from the mild steel stirrers used during the melt preparation process.

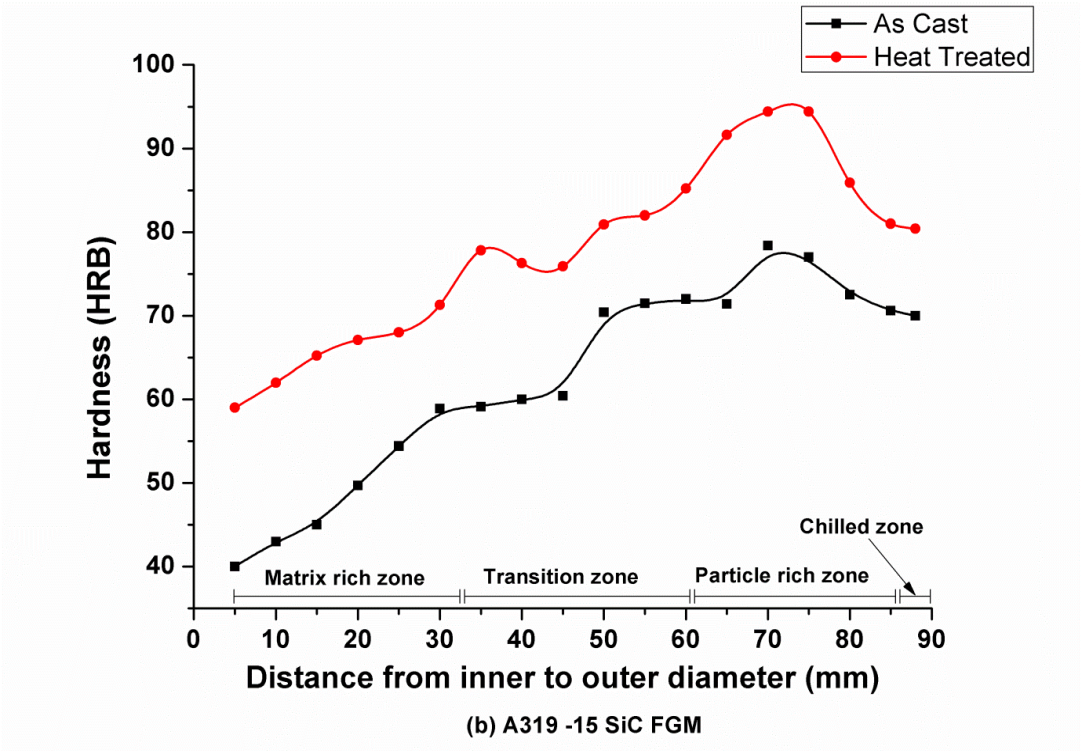

Figure 4.9: (b) Hardness variation from the inner diameter of the ring towards the outer diameter regions of FGMMC rings in both as Cast and after T6 Heat treatment conditions of 15- FGM

4.3.5 *Thermal Expansion Behaviour*

Figure 4.10 shows the CTE value taken on both FGMMCs at different zones and it is clearly seen that the increase in the amount of SiCp has a major role in the CTE value of the composites. As MMC melt cools to solidify, misfit strains set in due to the large difference between the coefficients of thermal expansion (CTE) of the matrix and the reinforcements. The thermal stresses induced by the misfit strains increase the dislocation density by creating new dislocations. The rule of mixtures holds well only when the CTE and the elastic properties of the matrix and the reinforcement are the same or comparable. Therefore an understanding of the CTE of the FGMs is very essential for practical applications. The CTE values of A319 alloy, SiCp and the MMC in gravity cast conditions are given in Table 4.2. The high concentration of SiCp reinforcements in the particle rich zone yields low value of CTE and good thermal stability to that region. The grain refinement effects also lowers the CTE value of the outer region of 10-FGM to 20.62 µm/mK The lowest CTE value of 20.1 µm /mK has been obtained for the 15-FGM specimen at 75 mm.

Table 4.2: Coefficient of Thermal Expansion (CTE) value of homogenous gravity castings and SiC particle for the temperature range 303 – 573K (30 -300^0 C)

CTE µm/mK Range 303 – 573K (30-300^{0}C)	A319 alloy	SiC_p	A319-10SiC composite	A319-15SiC composite
	22.9	2.77	22.6	20.7

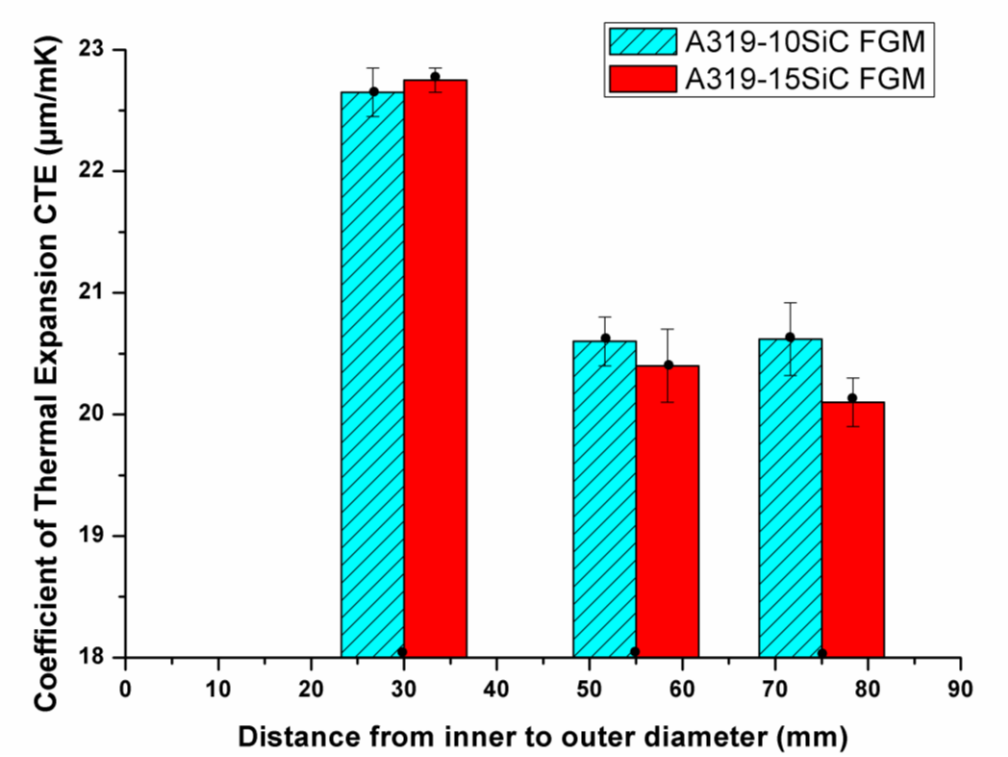

Figure 4.10: CTE of 10-FGM and 15- FGM castings measured at three regions (namely matrix rich, transition and particle rich outer regions at a distance of 30, 55 and 75 mm respectively from inner towards outer diameter of the casting.)

4.3.6 *Tensile and Compressive Properties*

The ultimate tensile strength (UTS) of the A319 base alloy is 230 MPa and that of the gravity casting of the composites with 10% and 15% SiCp are 257 and 262 MPa respectively. The presence of SiCp on the aluminium matrix decreases elongation resulting reduced ductility and hence during testing the brittle failure mode occurs. Figure 4.11 shows the UTS values of specimens taken from the FGMMC rings at distances of 30, 55 and 75 mm in the radial outer direction. For 15- FGM; the UTS value was minimum 220 MPa at 30 mm which is lesser than that of A319 base alloy itself. Then the UTS value increases to 267 MPa at 55mm due to more SiCp concentration

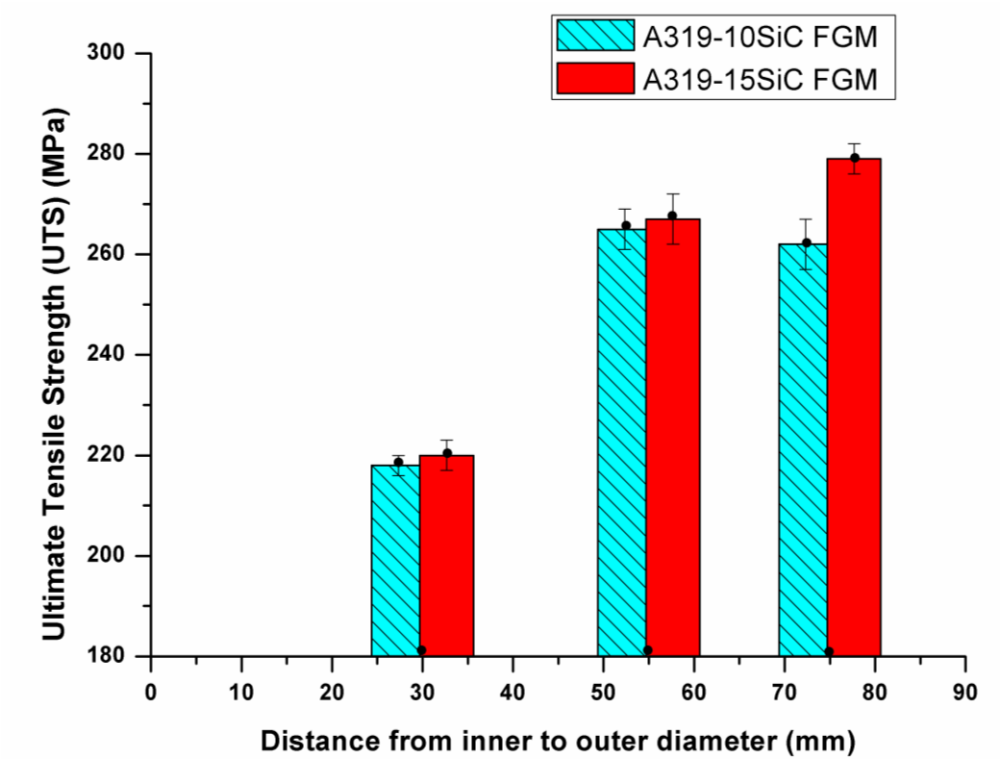

Figure 4.11: Ultimate Tensile Strength (UTS) of 10-FGM and 15-FGM castings measured at a distance of 30, 55 and 75 mm respectively from inner towards outer diameter of the casting

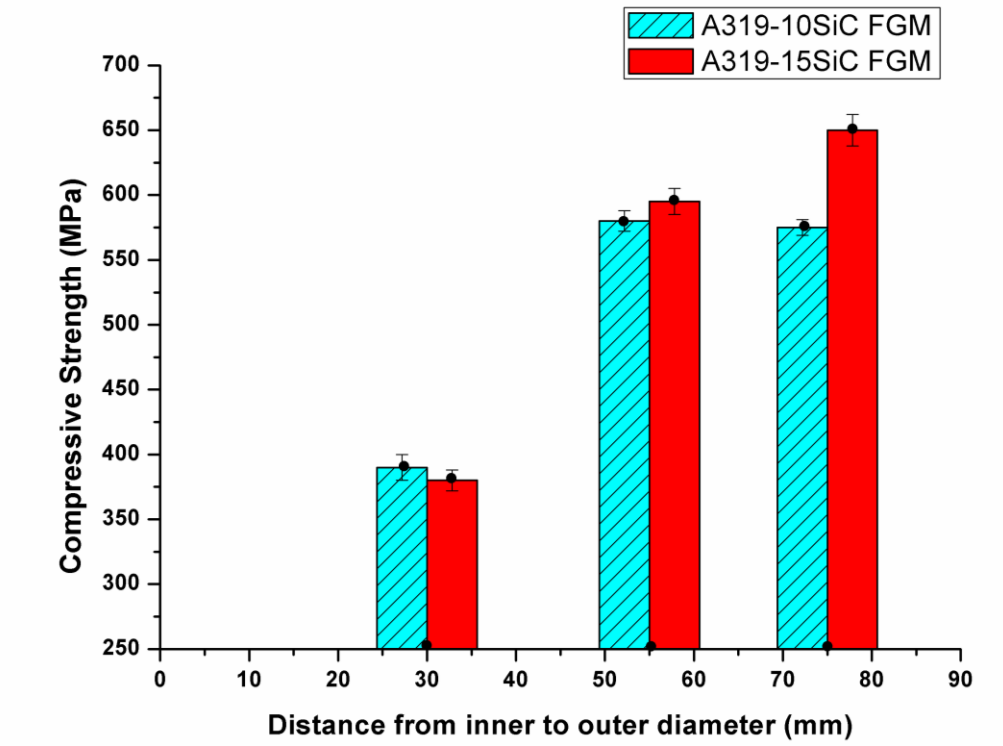

Figure 4.12: Compressive strength of 10-FGM and 15-FGMs measured at a distance of 30, 55 and 75 mm respectively from inner towards outer diameter of the casting

(approx. 22%) and the maximum value of 279 MPa was obtained at the particle rich zone (at 75mm with 28 % SiCp concentration). In the case of 10-FGM UTS values are 218MPa, 265MPa and 262MPa at 30, 55 and 75 mm respectively. At 75 mm, the grain refinement effect enhances the UTS values of 10-FGM is closer to the maximum value. Figure 4.12 shows the compressive strength values obtained for specimens taken from same locations. They also follow the similar trend of UTS values, indicating that the properties are high at particle rich zone and are very much sensitive with concentrations of SiCp.

4.3.7 *Wear Characteristics*

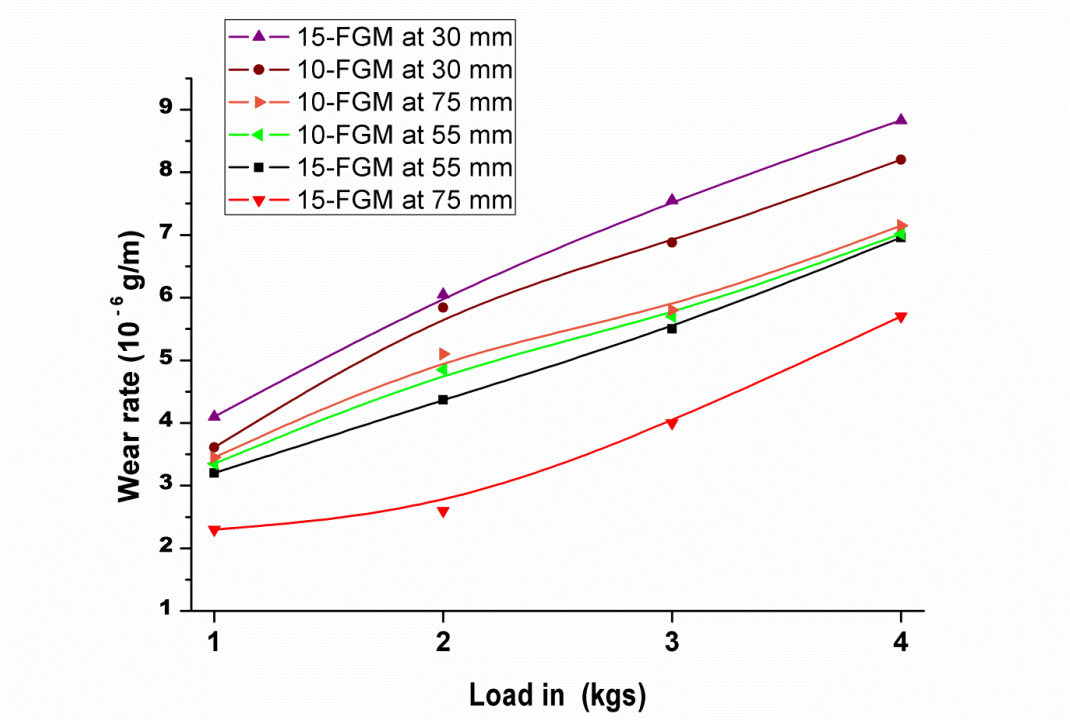

Figure 4.13: Wear rate of 10-FGM and 15-FGM heat treated pins taken from three regions of 30, 55 and 75 mm respectively from inner towards outer diameter

Dry wear tests are conducted using pin on disc tribometer with heat treated FGMMC pins taken from the same radial locations FGMMC rings (i.e. at 30, 55 and 75 mm). The test is repeated for four different loads (1, 2, 3 and 4kg). The wear rates are calculated in terms of weight loss and plotted in Figure 4.13. At lower loads 15-FGM outer pin at 75mm shows minimum wear loss and as loading increases the slope of wear curve changes rapidly and loss increases. For 10-FGM pins at 55 mm show lesser wear rate is observed (but higher than that of 15-FGM pin from particle rich zone at 75mm) without any sharp transition regions. The pin of 15-FGM at 55mm shows lesser

wear rate than particle rich pin at 55 mm of 10-FGM due to more SiCp concentration and grain refinement. The outer pin at 75mm of 10-FGM very closely follows the above two curves at higher loads. For the pins from inner zones have high wear rate due to the direct contact of base alloy with disc and the rate is proportional to the applied loads.

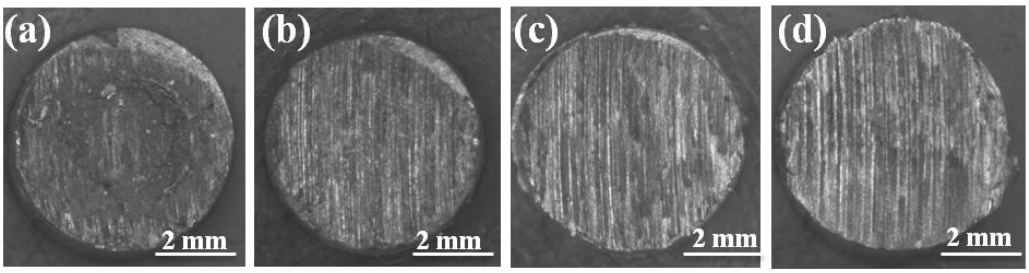

Figure 4.14: Stereo micrographs of wear pins (of size 6mm diameter) worn out surface of 10-FGM and 15- FGM from different regions at the maximum 4 Kg load condition. Wear pins are made from regions namely from a) 10- FGM ring inner zone at 30mm b) 10- FGM ring particle rich zone at 55 mm c) 15- FGM ring inner zone at 30 mm d) 15-FGM ring outer zone at 75 mm

The worn out surfaces morphology stereo micrographs of FGMMC pins from inner and outer particle rich zones at different loads are shown in Figure 4.14. Even at the maximum load only abrasion grooves are visible indicating mild abrasive wear as the prominent one. For further understanding, the SEM images of worn out surfaces of inner and outer FGMMC pins at 1kg and 4kg loading conditions are taken at different magnifications (Figure 4.15(a-c)). SEM analysis of pins shows the characteristic abrasion grooves, cracks, craters, debris and oxide layers caused by abrasion wear mechanism [160-161]. The SEM micrograph of the worn surface reveals anchoring of tribolayers at protruding SiCp particles as well as the tribolayer delamination.

The presences of protruding reinforcing particles at the worn-out surface indicate the existence of a strong reinforcement / matrix interface. SiCp act as load-bearing elements in Al/SiCp p composites, promoting the formation of a thick stabile adherent tribolayers and improve the wear resistance. The formation of adherent tribolayer and its rate of formation will protect the aluminium matrix from wearing out. The SEM images show only a few delaminated particles, confirming the mild abrasive wear, even at high load. SEM micrographs of wear tracks surfaces revealed that in mild abrasive wear conditions, the oxidized surface characteristics and scoring are the major causes responsible for the material loss. Fine debris generated during the dry sliding have two contradictory roles. They may get locked between the sliding contact surfaces

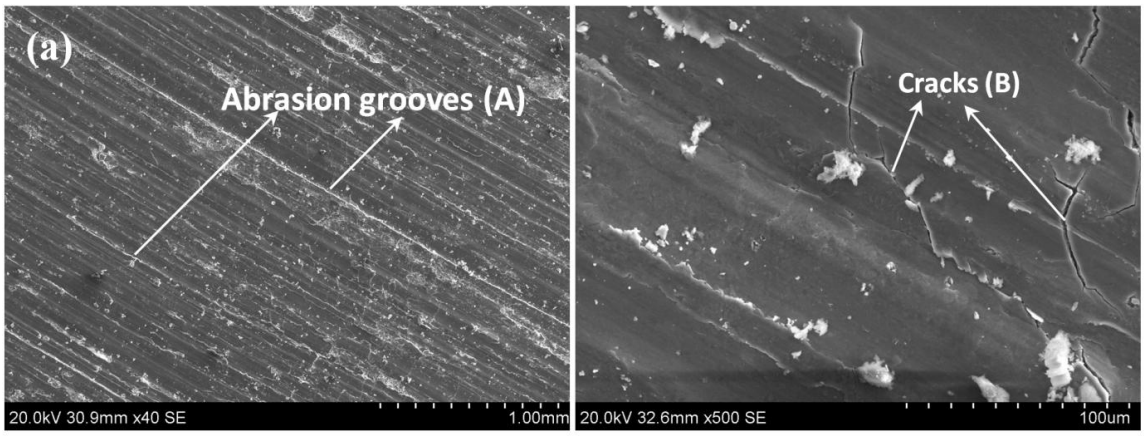

(a) SEM images of the worn out surface of 10 - FGM pin (at 30mm) at 4 kg loading condition (40 x and 500 x).

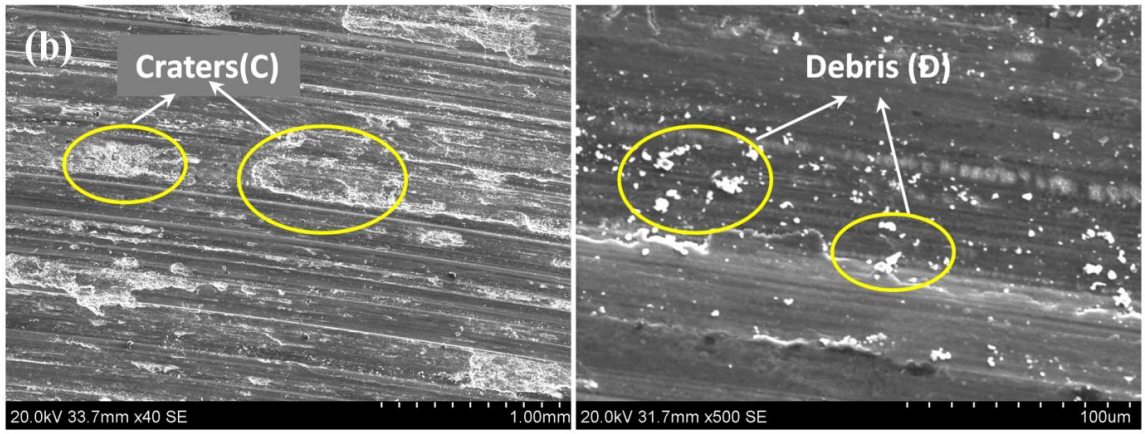

(b) SEM images of the worn out surface of 15 - FGM pin (at 75mm) at 4 kg loading condition (40 x and 500 x).

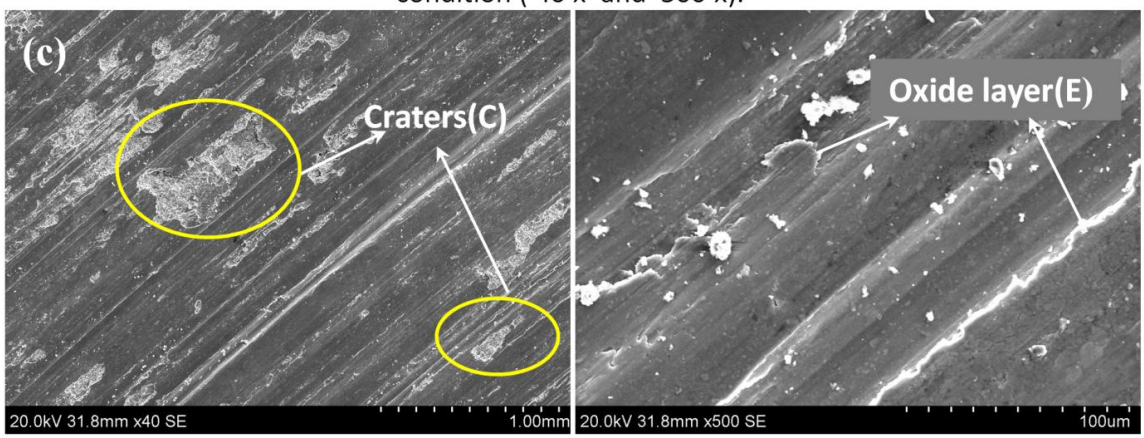

(c) SEM images of the worn out surface of 15 - FGM pin (at 30 mm) at 4 kg loading condition .(40 x and 500 x)

[A- Abrasion grooves , B - Cracks, C - Craters , D - Fine wear debris and E - Oxide layers]

Figure 4.15: SEM Micrographs of wear pins worn out surfaces of 10-FGM inner region pin (a) at 30 mm, (b) 15 - FGM outer pin at 75 mm and (c) 15 - FGM inner pin at 30 mm, at 4 kg load condition.

and promote the three body wear, which should enhance the volume loss in wear. In contrary, these oxide particles in the debris may locked between the sliding surfaces and get compacted to form a protective hard transfer layer, so hard that there are no further scoring possible and in turn, reduces the wear rate. Transfer layers can either adhere to the rubbing surfaces or flakes off from the surfaces, due to the micro-cutting and abrasion, during the dry sliding wear conditions [162-163].

Since the processing and characterisation of both FGMMC 10 and 15 wt% are successful, the study is extended to A319-20 wt % SiC FGMMC and the properties are compared with that of A319 and A319-10 wt% SiC FGMMC. The extended study was conducted with another permanent metal mould having a different cavity dimensions capable of producing a casted ring of outer diameter 250 mm and thickness 25 mm in order to observe the variation in mould dimensions on the nature of hardness variation, the microstructure and the wear behaviour.

4.4 STUDIES ON A319-20 Wt. % SIC FGMMC

4.4.1 *Microstructural Evaluation*

Figure 4.16(A-C) shows the optical micrographs taken from inner to the outer perimeter of the A319-20SiC FGMMC ring in the radial direction from inner region, transition and particle rich outer regions. Figure 4.16 (A, B) show the repeated microstructures of similar regions of centrifugally cast A319 and A319-10 wt % SiCp FGMMC castings processed in the same mould. The repeat casting and microstructures reconfirms the parameters fixed for casting conditions are suitable and repeatable. The density of the SiCp is 3.2 g/cc, and that of the aluminium alloy is 2.68 g/cc. Due to centrifugal effect the higher density SiC particles move radially from the inner region towards outer region

Figure 4.16C (a), the inner region of radial thickness 10-15mm, shows an area of the casting with very fine sized reinforcement particles, lower density impurities like slag inclusions and gas porosities. The centrifugal force and the solidification front will move the lighter gas bubbles and agglomerated particles, in the MMC melt, to diffuse and segregate towards inner regions of the FGM castings. Before the actual testing or applications, to get a dense porous free component, such areas can be removed by machining. Figure 4.16C (b) shows the transition region of 15-30mm radial thickness with a gradual increase in reinforcements from inner towards the particle rich region

(Figure 4.16C(c). These figures clearly depict the gradual changes in microstructure and composition leading to successful FGM casting. Further mechanical characterisations are done with standard test specimens and the results are compared.

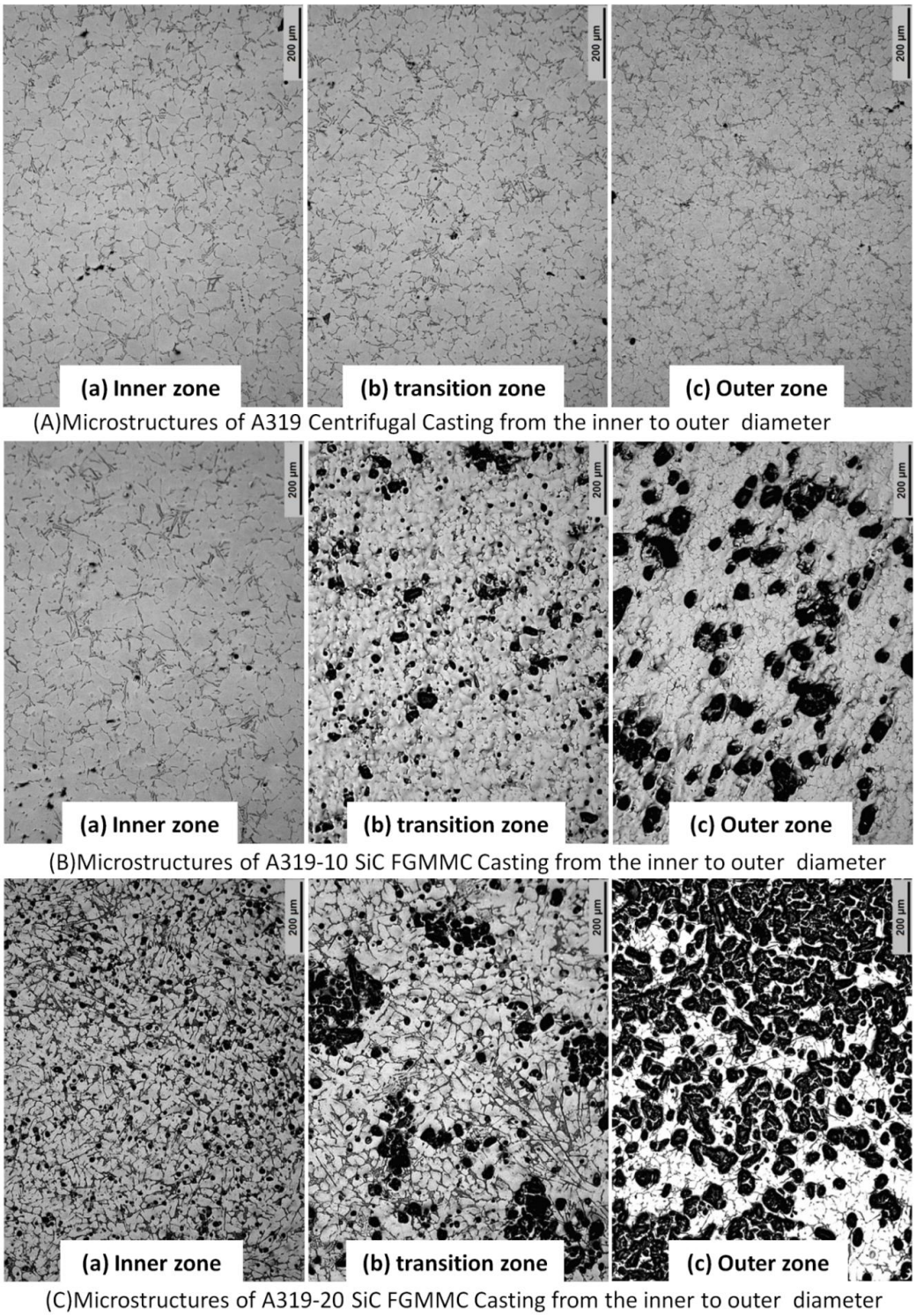

Figure 4.16(A-C): Microstructures of centrifugally cast A319, A319-10wt % SiC and A319-20 wt% SiC FGMMCs at different regions taken from inner to outer diameter

4.4.2 *Hardness Behaviour*

Table 4.3: Hardness of A319 Al alloy, A319-10 SiC and A319-20 SiC homogeneous gravity die casting under as cast and T6 heat treated conditions (in BHN)

Material specification	Gravity Castings In Brinell Hardness **BHN**	
	As Cast conditions	Heat Treated T6 conditions
A319	84	95
A319-10SiC	86	100
A319-20SiC	91	110

Table 4.3 shows the average Brinell hardness values of homogeneous gravity castings. A319 alloy gravity casting, the hardness value is 84 BHN in the as-cast condition and after the heat treatment it is raised to 95 BHN. The as cast condition hardness's of 86 and 91BHN of 10 and 20 SiC gravity cast MMCs are increased, respectively to 100 and 110 BHN after the heat treatment. Heat treated A319-20SiC composites shows higher value of hardness due to the presence of high volume fraction of reinforcements. Heat treatment improves the hardness as well as other mechanical properties due to the redistribution of Cu-Al_2 phases.

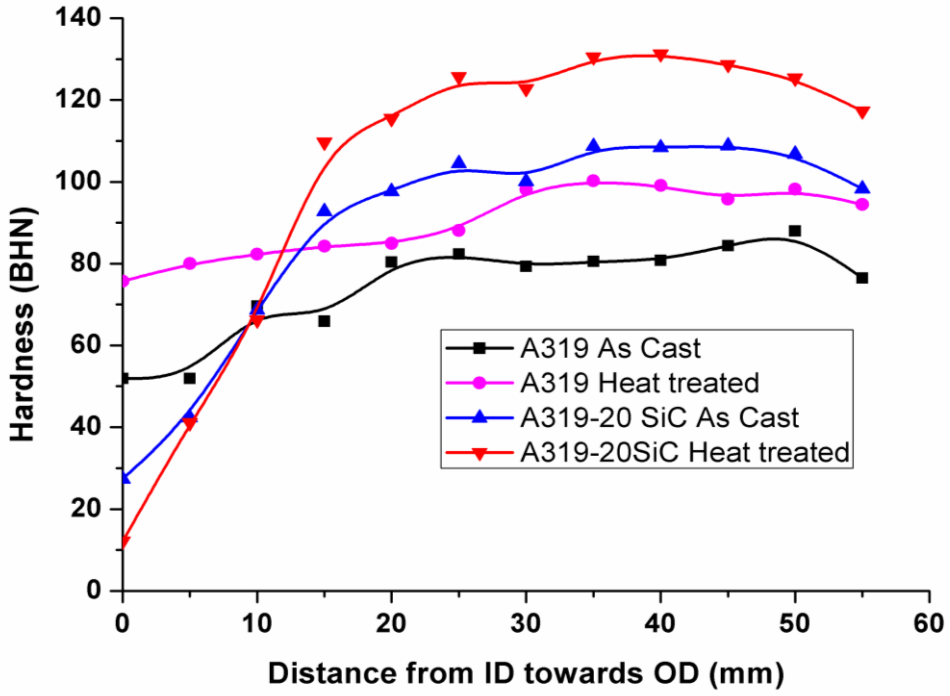

Figure 4.17: Hardness variation from inner towards outer diameter of the castings in as cast and heat treated conditions

Figure 4.17 displays the variations of the average hardness of FGM rings, from the inner towards the outer diameter in the radial direction of A319 alloy and A319-20SiC FGMMC in both as-cast as well as heat treated conditions. At the outer periphery of the A319 alloy centrifugal casting, the hardness value before and after the heat treatment is 76 BHN and 94 BHN respectively. There is neither addition of SiCp nor segregation of alloy phases, the variations in hardness are less from the middle region of the centrifugal casting towards the outer periphery in both conditions (as-cast and heat treated). In as-cast condition, the highest hardness value obtained is 87 BHN at a distance of 20 mm from the outer periphery towards inner, and after heat treatment the hardness increased to 100 BHN. For A319-20SiC FGMMC, at the outer periphery, the hardness value is 98 BHN in the as-cast condition and after heat treatment it is raised to 117 BHN. A maximum hardness value of 108 BHN in as-cast and 131BHN in the heat treated condition, at the particle rich region, was obtained. In the transition region, the hardness vary in the range of 100-108 BHN in as-cast and 122-131 BHN in heat treated conditions. The inner regions show very low hardness due to the presence of gas porosities and agglomerated particles, which are segregated by the combined effects of the centrifugal force and the solidification front.

4.4.3 *Wear Behaviour*

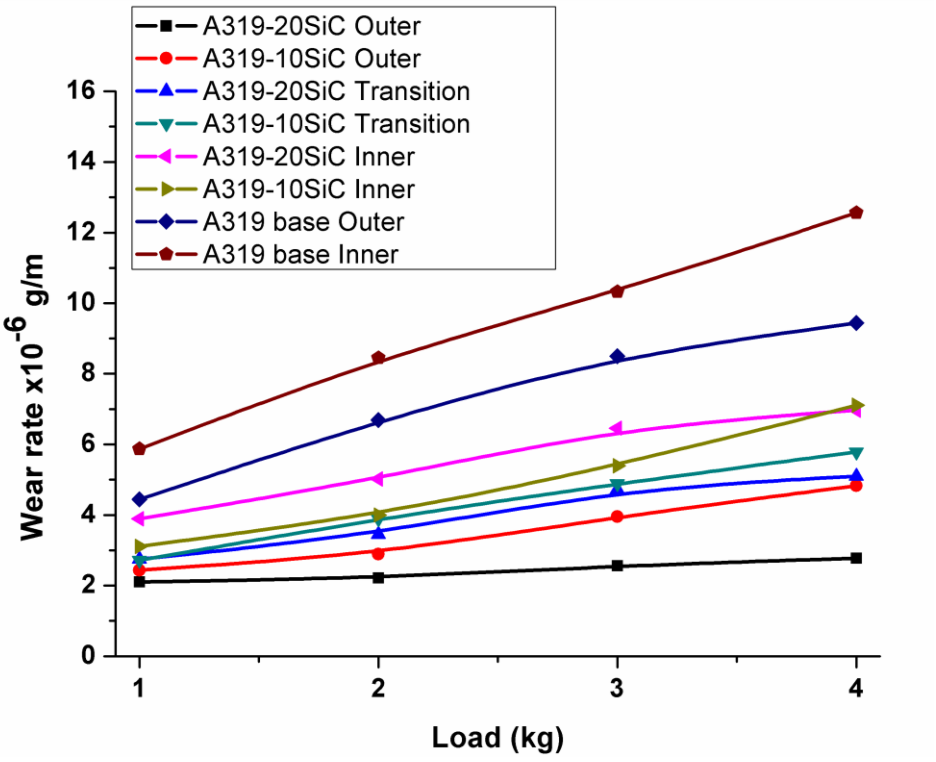

Figure 4.18: Wear rate of A319 and A319-20 SiC FGMMC at different regions

The pin samples of 6 mm diameter and 30 mm length are prepared from centrifugal castings and are heat treated at T6 conditions before the testing. Tests are conducted for a sliding distance of 1800 m with a relative velocity of 2 m/s, for 15 minutes duration at 1, 2, 3 and 4 Kg loading conditions. The weight loss method calculation is used to find out the wear rate behaviour of the FGM pins. Figure 4.18 shows the wear rate values A319 alloy and A319-20SiC FGMMC pins prepared from different regions of the rings. For A319 alloy centrifugal castings, since the variation in hardness value is marginal in the transition region, the inner and the outer pins are only prepared and tested. A319 alloy inner pin shows a minimum wear rate of 5.8×10^{-6} g/m at a load of 1kg and a maximum of 12.6×10^{-6} g/m at 4 kg. Both these values are the maximum in that loading condition in comparison with the wear rate of all other specimens. The A319 outer pin shows a wear rate of 4.4×10^{-6} g/m at 1kg and 9.4×10^{-6} g/m at 4 kg. These wear rate values are lesser than that of the inner pins of the same ring. The refined smaller grains of outer region of A319 centrifugal casting enhance the hardness and wear resistant properties than that of the inner region. In the case of A319-20SiC FGMMC castings, wear tests are conducted using pins prepared from three different regions namely particle free inner, transition and particle rich outer zones. Inner pin shows a wear rate of 3.1×10^{-6} g/m at a load of 1kg and 7.1×10^{-6} g/m at 4 kg. While the transition pins show a wear rate of 2.7×10^{-6} g/m, 5.7×10^{-6} g/m respectively at 1Kg and 4 Kg loads. The outer pins show a wear rate of, 2.4×10^{-6} g/m and 4.8×10^{-6} g/m respectively. At all conditions, the wear rate of FGMMC outer specimen shows the minimum than that of other specimens in the similar conditions. The graphs indicate that the SiC particles on the aluminium matrix alloy decrease the wear rate due to its higher hardness. The firm bonding of SiC particles with aluminium matrix protects the surface against the severe wear loading conditions. The strong interfacial bond plays a critical role in transferring the loading force between the matrix and the reinforcements resulting less wear. At lower load conditions, the SiC particles protrude from pin surface and protect the contact surface from any material loss by reducing the actual area of contact between the pin and disc.

4.4.4 *Wear Surface Morphology and SEM Analysis*

Figure 4.19 shows the surface morphology observed in stereo micrographs of the worn out surfaces A319 alloy inner, A319-SiC FGMMC inner and outer wear pins at

different loading conditions. Even in the 4 kg loading condition only the finer, abrasion grooves are visible.

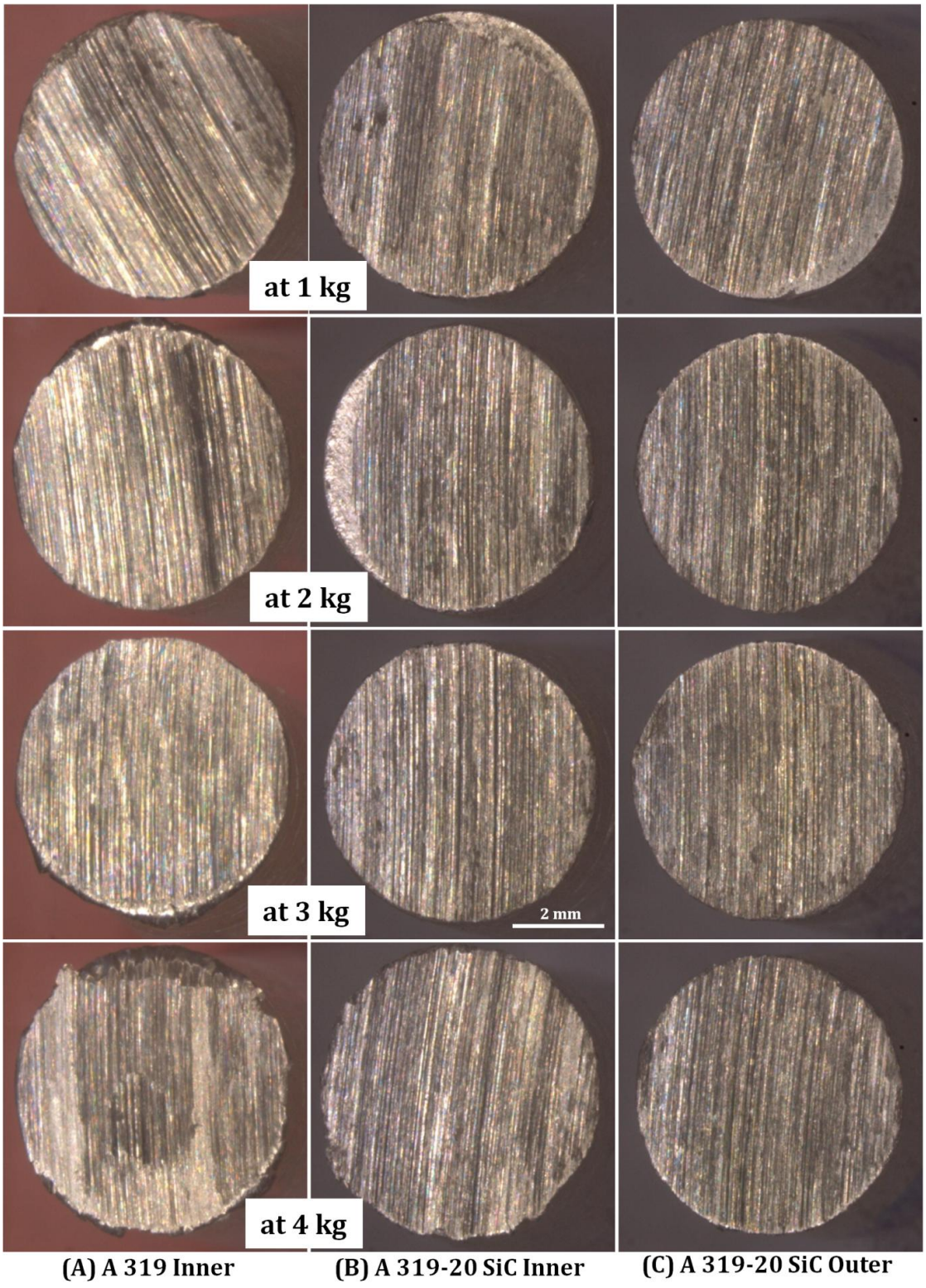

Figure 4.19: Worn out surfaces of A319 and A319-20 SiC FGMMC at different regions at different loads

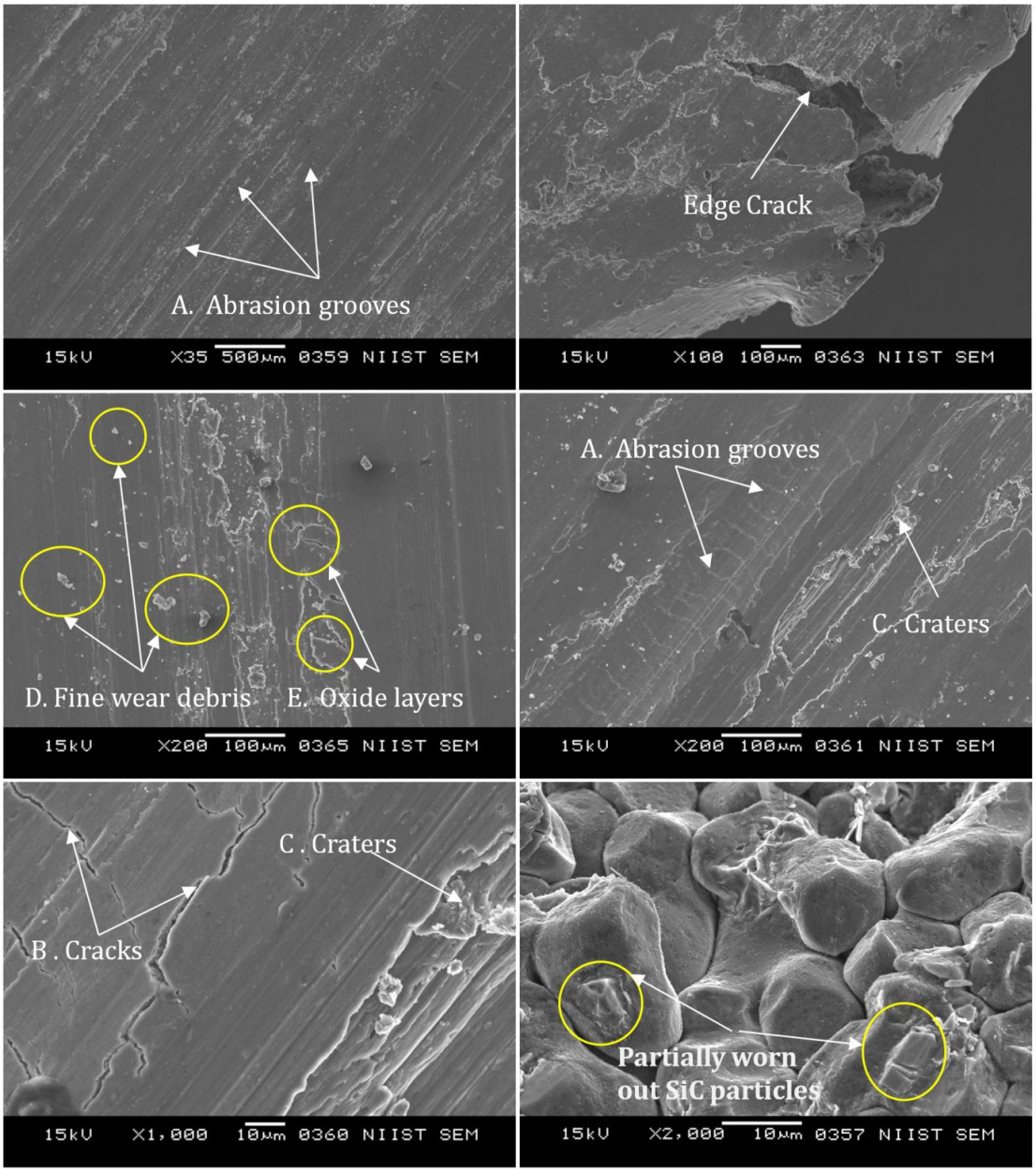

Figure 4.20: SEM microstructures of worn out surfaces of A319-20 SiC FGMMC pins from Outer region at 4 kg load [A- Abrasion grooves, B - Cracks, C - Craters, D - Fine wear debris and E - Oxide layers]

For further understanding of the wear the SEM microstructures of these surfaces are taken. Figure 4.20 shows the SEM micrographs of the worn-out surface of A319-20 SiC FGMMC outer subjected to 4 kg loading. The SEM micrographs, reveals the abrasion grooves (A), Cracks (B), Craters (C), Fine wear debris (D) and the Oxide layers (E) indicating the prominence of the mild abrasive wear conditions. The oxidized surface characteristics and scoring on surfaces suggests that they are the primary wear mechanisms responsible for material loss [164-166]. Fine debris generated during dry

siding has two contradictory roles. They may get locked in between the sliding surfaces, promote the three-body wear and enhance the volume loss in wear. On the other hand, the hard oxide particles in the debris may get locked between the sliding surfaces and get compacted to form a protective tribolayer so that there is neither further scoring on the surfaces nor scoring marks. During the dry abrasive wear sliding conditions, the tribolayers also flakes off along with the flakes of adhesion, micro-cutting and abrasion [167-169]. At higher magnifications, partially worn out protruding SiCp reinforcements are visible. Those well matrix bonded particles will protect the contact surfaces. The fine grains and grain boundaries indicate the tendency of delamination of grains along the boundary. The delamination produces edge cracks and flakes on the wear surface.

4.5 CONCLUSIONS

- A319 Aluminium functionally graded metal matrix composites (FGMMC) reinforced with different weight percentages SiCp (10, 15 and 20wt %) of average size 23 μm were processed successfully by liquid stir casting method followed by vertical centrifugal casting.
- The FGMMC microstructures reveal that centrifugal force has a greater influence in the formation of gradation in the system. The distribution curves of SiCp reinforcements in the radial direction show that the position and magnitude of concentration of SiCp depends on percentage of initial addition.
- There is a shift of the position of maximum concentration towards the outer directions for higher percentage of additions. With a radial shift, from 55 mm to 75 mm, for 15-FGM, the maximum of 28 wt % SiCp is obtained.
- The maximum density of 2.87 g/cm^3 and the lowest CTE value of 20.1 μm /mK are obtained in the particle rich zone of 15-FGM casting.
- Similarly the hardness and ultimate tensile strength show a graded nature in correlation with particle concentration and are higher at particle rich region.
- The maximum compressive strength of 15-FGM is 650 MPa in the particle rich region.
- The wear resistance is higher in the particle rich region of the FGMMC.
- The dry pin on disc wear test confirms that the mild abrasive wear is the major wear mechanism responsible for wear losses in these FGMMC castings.

Chapter 5

Processing and Characterisation of A390 Functionally Graded Metal Matrix Composites

5.1 INTRODUCTION

The functionally graded materials (FGMs) can achieve the target of location specific mechanical characteristics under service conditions, by virtue of its changing composition / microstructures, for various engineering and structural applications [170-178]. In the constructive approach, graded layers are processed through solid state powder metallurgy, sintering methods or by infiltration techniques. While in the transport aided approach a second phase is transported and diffused by one of the following driving forces like chemical gradient, gravitational, Thermal, or mechanical forces. Metal matrix composites (MMCs) are widely used in transportation and infrastructure industries due to their better high specific modulus, strength and wear resistance properties over the conventional materials. Functionally graded materials are relatively new class of inhomogeneous composite materials, where the composition or the microstructure is locally varied to alter the material properties in a component. These FGM are useful and economical in applications which demand different properties in a single component.

In the simplest Centrifugal casting methods the centrifugal radial force produced during the rotation of the mould containing the melt will transport and distribute the secondary particle or phases from outer to inner in the radial direction with respect to the axis of rotation in accordance of higher density to lower density compared with the density of matrix. And even though numerous processes are available for fabrication of FGM, centrifugal casting is the most economical and simplest of them. A390 (LM 30) with 10 and 20 wt % SiC composites were fabricated by stir casting and FGMMC by vertical centrifugal casting. The high density SiC particles formed gradation towards the outer periphery. The particles and porosities with lower density than the matrix material settled at the inner periphery of the component. The higher SiC particle concentration near the outer periphery tends to enhance the hardness of the casting at

this region. Compressibility, tensile strength and wear resistance were found to be higher at the outer periphery compared to the inner.

5.2 MATERIALS AND EXPERIMENTAL METHODS

The A390, hyper eutectic cast aluminum alloy, was used for FGMMC preparation and SiC particles of average particle size of 23 μm were used as reinforcements. The SiC particles were cleaned, dried and preheated to 600 °C for 3 hours. For improving the wettability of SiC with alloy, before the addition, 1 % Mg was added to the melt while the casting. The uniform addition of particles to a steady liquid vortex was done to ensure proper mixing and consistency of the MMC melt. Sufficient mechanical and hand stirring were also done before pouring. The melt at 760 °C is poured into metal mould, coated and preheated to 350 °C, which was rotating, at 1300 rpm, in vertical centrifugal casting machine. Standard specimens are cut for mechanical characterisation. The standard T6 heat treatment procedures, solution treatment at 495 °C for 8 hours, quenching in warm water and artificially aging at 175°C for 8 hours, were used for A390 FGMMC specimens.

Alloy chemical compositions were found out by SPECTRO MAXX Optical emission spectrometer. The DMRX Leica optical microscope was used to take microstructure. The volume fraction of the silicon carbide particles was measured by the Leica Qwin image analyser. The INDENTEC hardness tester was used for Brinell hardness measurements from the outer to the inner periphery of the specimens in both as-cast and heat treated conditions. Dry linear wear analyses were carried out in a DUCOM pin-on-disc tribometer. Wear surface morphology was taken by Zeiss stereo microscope. INSTRON 1195 – 5500R series tensile tester was used for tensile testings of the heat treated specimens taken from inner and outer zones of the cast.

5.3 STUDIES ON EX-SITU PARTICLE (SiC) ADDED Al FGM

5.3.1 *Microstructural Evaluation*

Figure 5.1 shows the microstructures of gravity cast A390 alloy, A390-10SiC MMC and A390-20SiC MMC. Polygonal shaped Primary Silicon particles (Phases) are clearly visible along with evenly spread grey coloured Al-Si eutectics in the gravity cast A390 alloy (Figure 5.1(a)). The aluminium matrix is visible as white background. In Figure 5.1(b) and (c) the evenly distributed SiC particles are visible as dark black, the

primary silicon particles are found to be finer in size and meanwhile the eutectic becomes thicker.

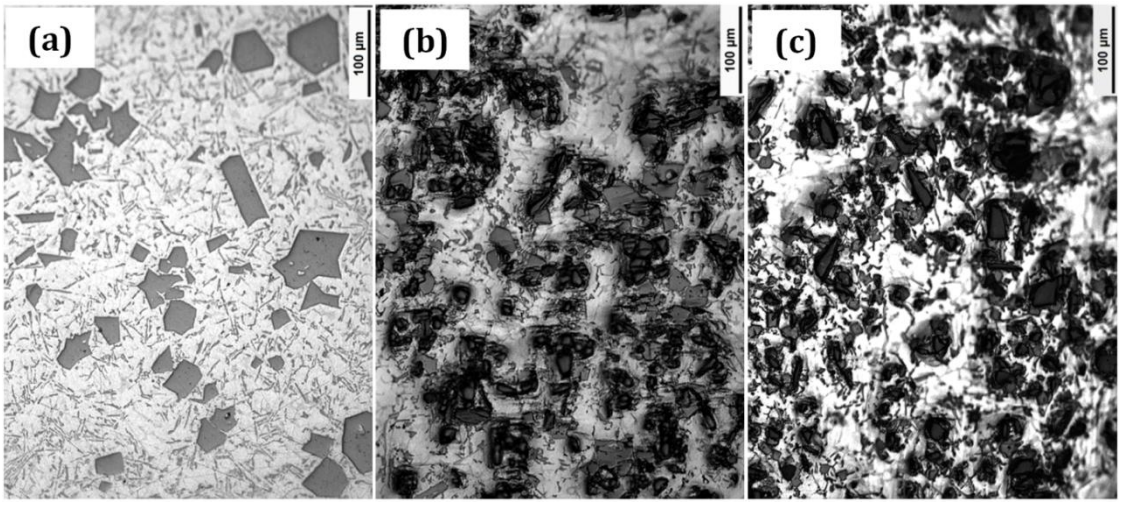

Figure 5.1: Microstructures of Gravity cast (a) A390 alloy (b) A390-10SiC MMC and (c) A390-20SiC MMC

Figure 5.2 shows the microstructure of A390 alloy centrifugally cast ring. The micrographs are taken from the outer to inner periphery in a radial direction. Since, in the alloy, volumes of Si and Cu were significant more volume of different phases formed and effective diffusions are visible in the microstructure. It was observed that the grain size at the outer periphery was smaller in size than that of inner periphery. This was due to the pressure force generated, during the centrifugal casting process, by the molten melt which comes in contact with solidification edge. The solidification edge moves from the mould outer periphery towards inner regions, while the pressure force acts from inner to outer in an opposing radial direction producing a squeeze effect. In the inner regions more primary silicon phases of less density are concentrated due to the centrifugal effect and coarse matrix grains are found with copper and silicon aluminium eutectic phases.

Figure 5.3 and 5.4 show the graded distribution of SiC particles in A390-10SiC and 20SiC FGMMC rings from outer towards inner periphery in a radial direction. The particle rich zone nearer to the outer periphery of the casting shows a higher concentration of SiCp than the inner and a clear transition region in between is also visible. The microstructural features of the matrix alloy also vary from outer to inner periphery. The grain size of the aluminum in particle enriched zone is very fine, which becomes coarser towards the interior. The presence of high volume

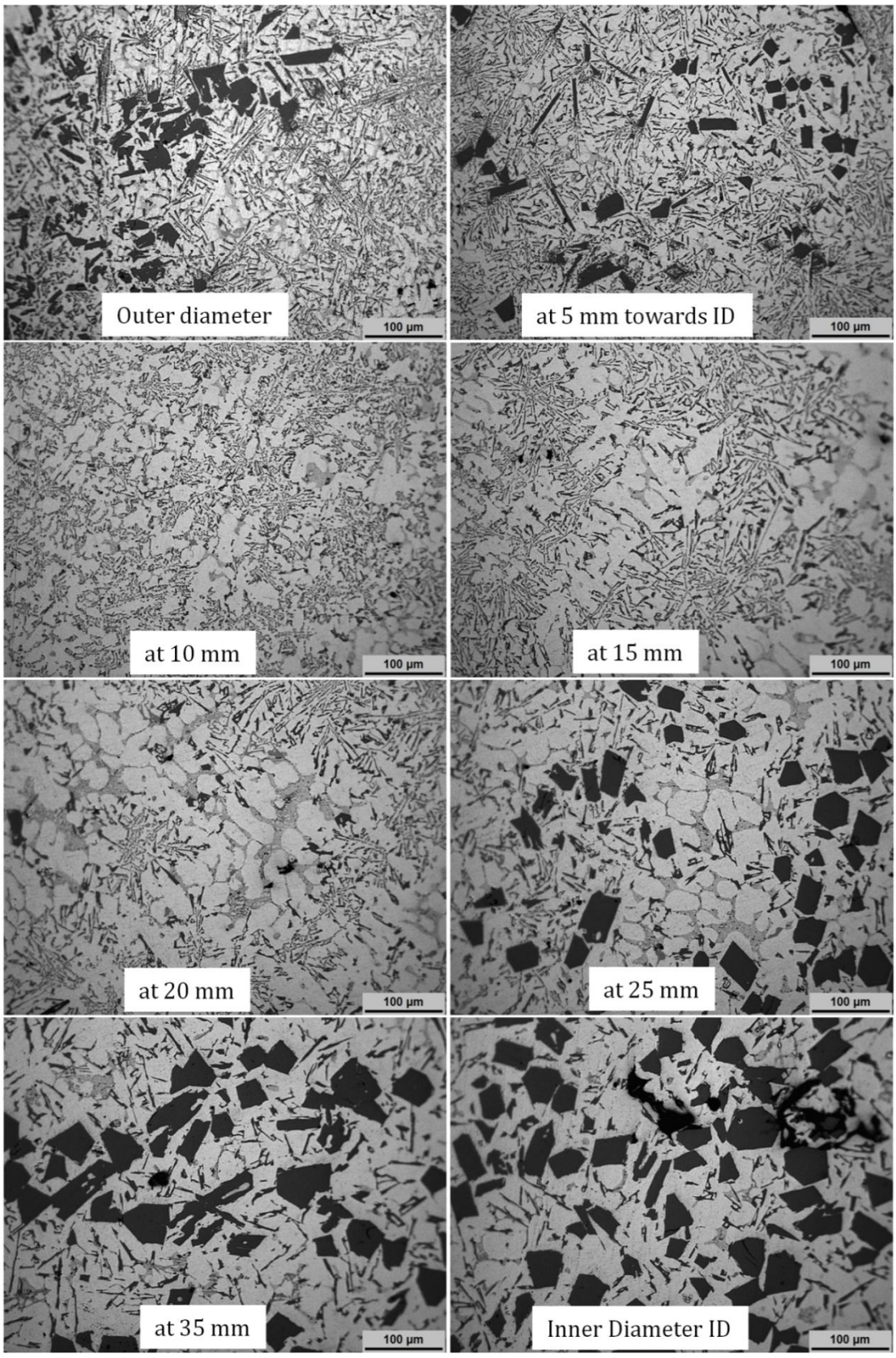

Figure 5.2: Microstructures of centrifugally cast A390 alloy taken from the outer to the inner periphery in a radial direction

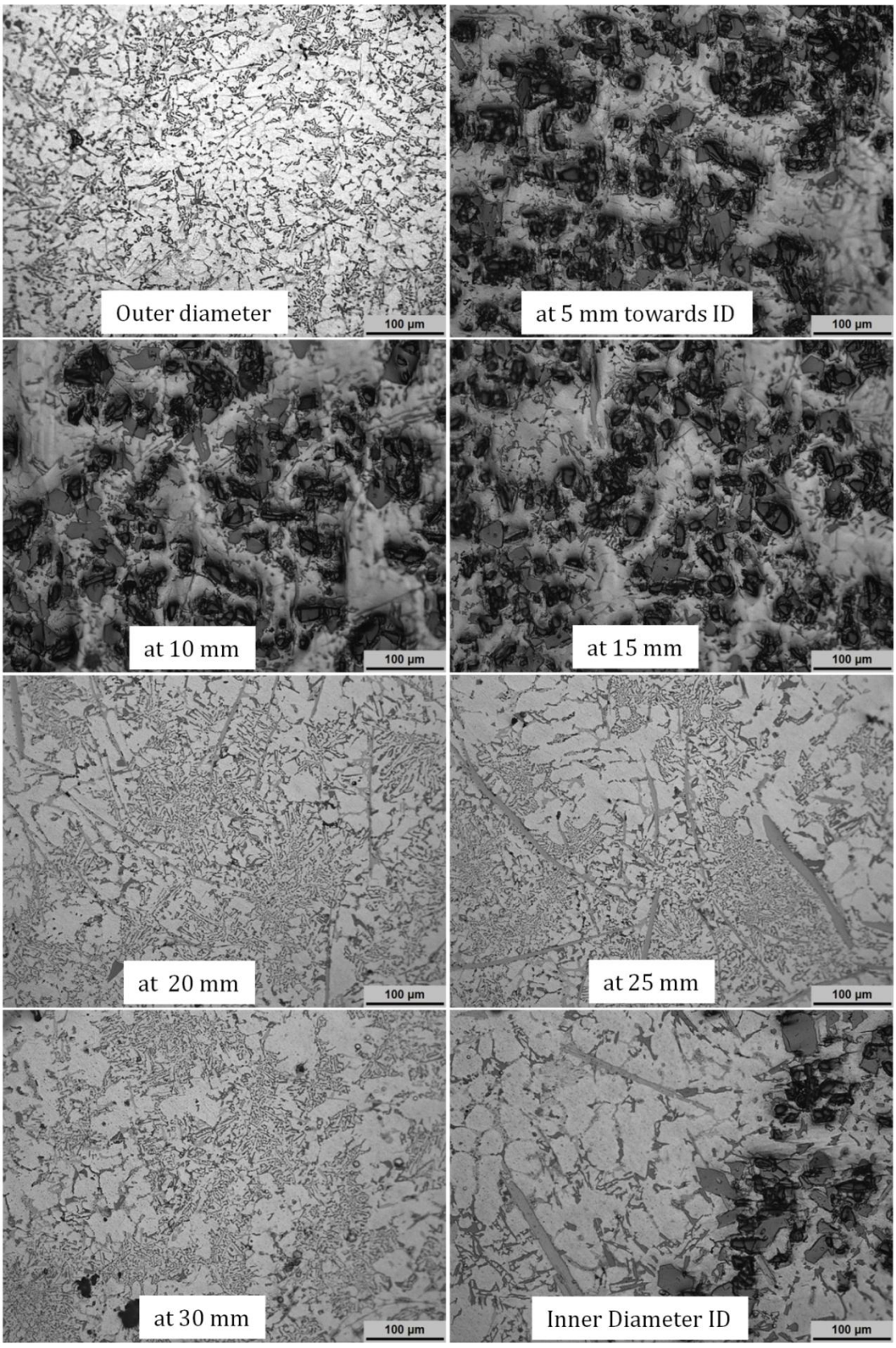

Figure 5.3: Microstructures of the A390-10 SiC FGMMC ring taken from the outer to the inner periphery in a radial direction

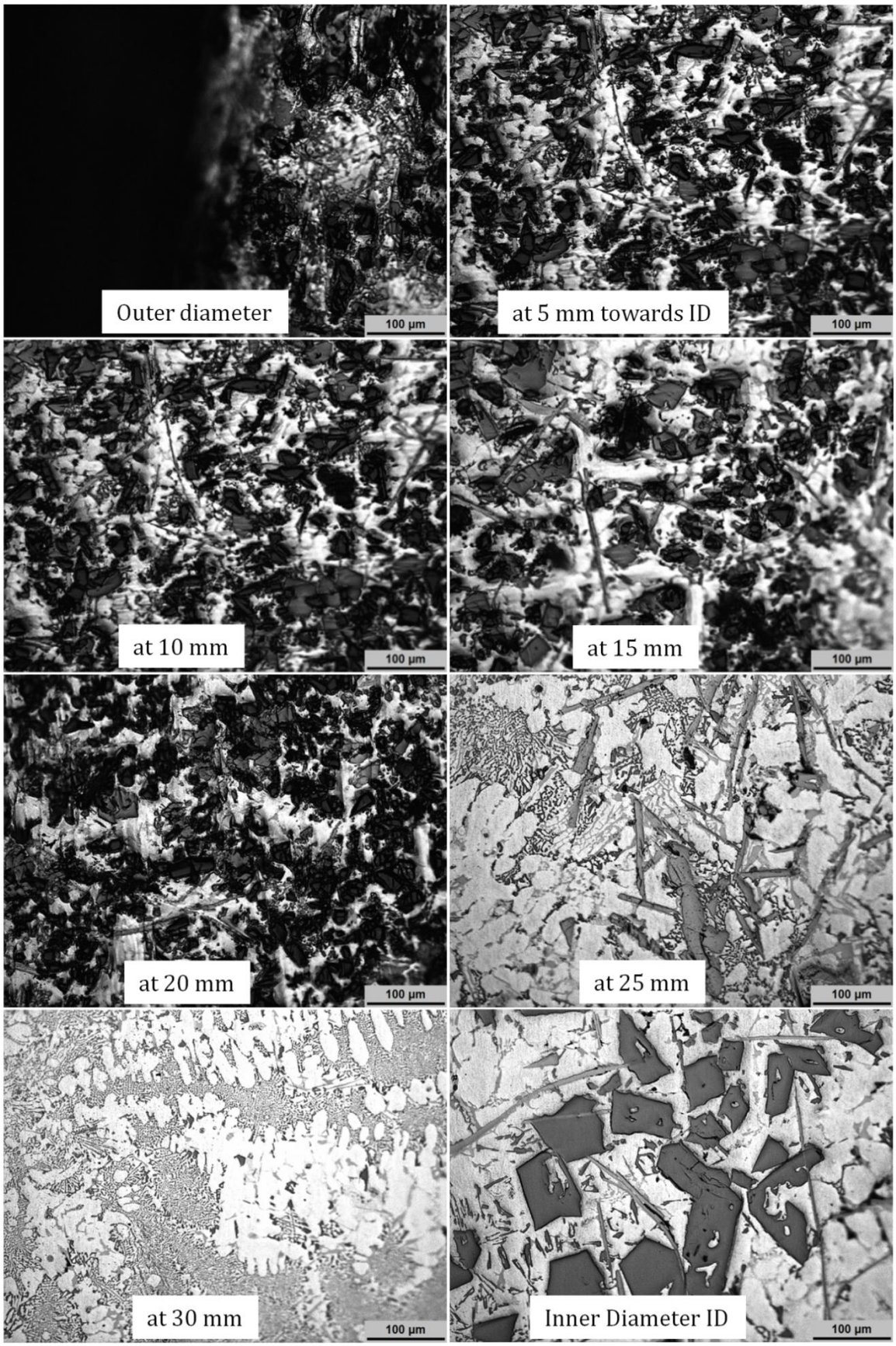

Figure 5.4: The micrographs of the A390-20 SiC FGMMC ring are taken from the outer periphery to the inner zones in a radial direction

fraction of SiC particles inhibits growth of primary aluminum and also the shear caused by movement of ceramic particles during solidification break the arms of dendrites to form fine structure [179- 181]. In both cases Al-Ferrite needles, which are formed by the iron that are diffused from the coated stirrer, baffles and other utensils (even graphite coated ones) during the MMC melt preparation, are visible in the transition regions (at 25 mm). Towards the inner regions as the melt gets more time for solidification, secondary dendrite arms also visible.

5.3.2 *Image Analysis*

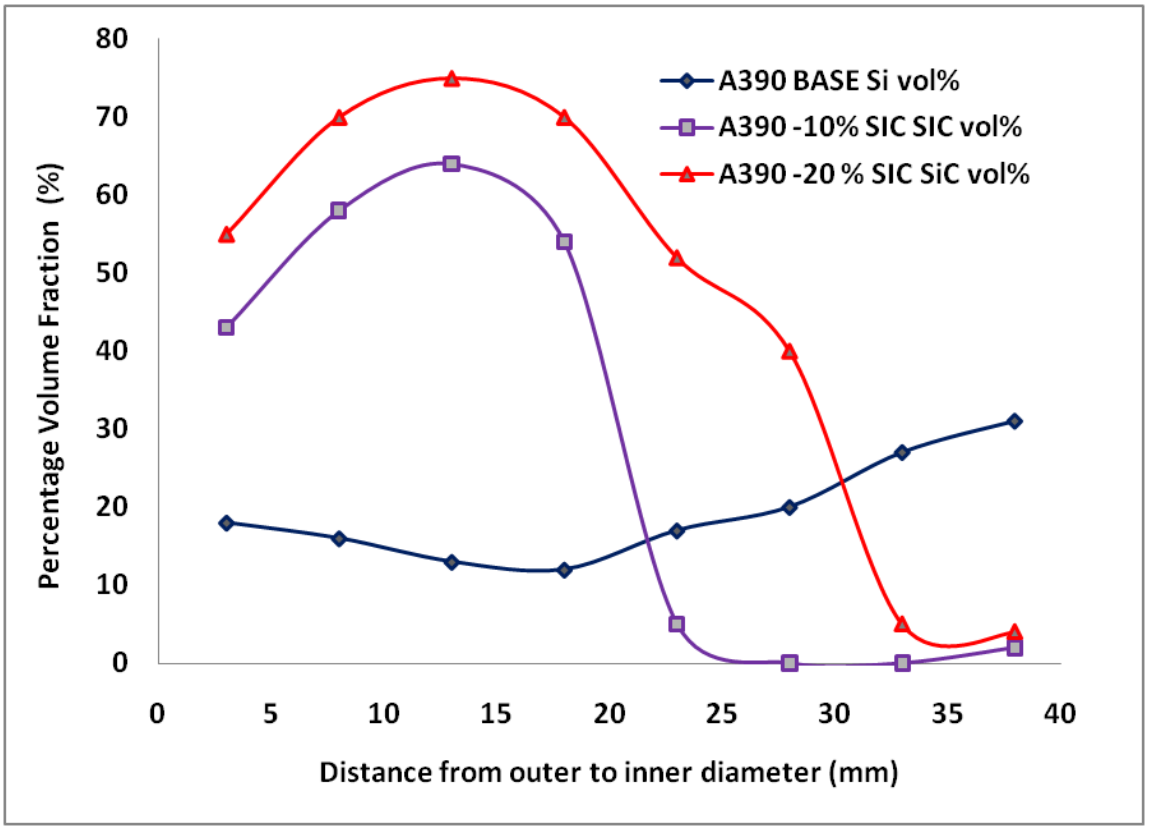

Figure 5.5: Volume Percentage Distribution of primary silicon (Si) and silicon carbide (SiC) in A390, A390-10SiC and A390-20SiC FGM castings from Outer Diameter towards Inner Diameter in radial direction

The image analysis results depicted in Figure 5.5 shows volume percentage distribution of primary silicon (Si) and silicon carbide (SiC) in A390, A390-10SiC and A390-20SiC FGM castings from outer diameter towards inner diameter in radial direction. For A390-20SiC at 3mm close to the outer region 55 vol. % is measured and it increases to 70 at the particle rich region. Then in the transition region it steadily decreases to 40 and then to 5% at matrix rich inner zone. In the inner most regions very

fine and agglomerated SiC particles entrapped in the gas porosity shows certain low volume percentages. For 10 SiC FGM, the SiC gets attached to the primary silicon particles and pulls them towards itself, thereby slows down the SiC particles from reaching the chill zone. Hence there are no SiC particles and can see only after a few millimeters away from the chill zone/outer periphery. The particle rich region of 10SiC FGMMC ring contains a maximum of 64 vol. % SiCp followed by a gradual reduction to lower levels towards the inner periphery. In the transition zone, between 15 mm and 25 mm away from outer periphery, the reduction SiC volume percentage were steep and reaches a value below 10 vol. % near the inner periphery. In the inner regions more primary silicon phases were concentrated in coarse matrix grains with copper and silicon aluminium eutectic phases rather than SiC particles. The inner most periphery regions of the casting show the presence of gas porosity and few agglomerated particles. The agglomerates constituting of partially wetted or non- wetted particles or both and gases, which are having a lower overall density, are pushed towards the inner periphery by the centrifugal force. These can be easily removed from components while machining.

The centrifugally cast A390 also shows a primary silicon phase distribution from outer periphery towards inner in radial direction which can be calculated by both image analysis and the optical emission spectra analysis. Since both results are confirming to each other image analysis results are shown in Figure 5.5. At the near outer a volume percentage of 18 Si is calculated, as expected in the close regions to chilled zone a composition that of base alloy A390. The volume percentage of silicon decreases to a value near to 12 % i.e. eutectic in the transition zone (confirmed by emission spectra) and increases to 31 % in the inner region. This is because the primary silicon is less dense than aluminium and on centrifugal casting they diffuse to inner rather than towards outer thereby enriching the inner regions.

5.3.3 *Hardness Behaviour*

The variations of the Brinell hardness values (BHN) in the as-cast and T6 heat treated samples from inner to outer zones of A390 FGM, A390-10 SiC and A390-20 SiC FGMMC rings were shown in Figure 5.6. The curves clearly depicts that the hardness value varies in proportion to the volume fraction of the primary silicon phase in both as cast and heat treated conditions for the A390 FGM ring. And the hardness value varies

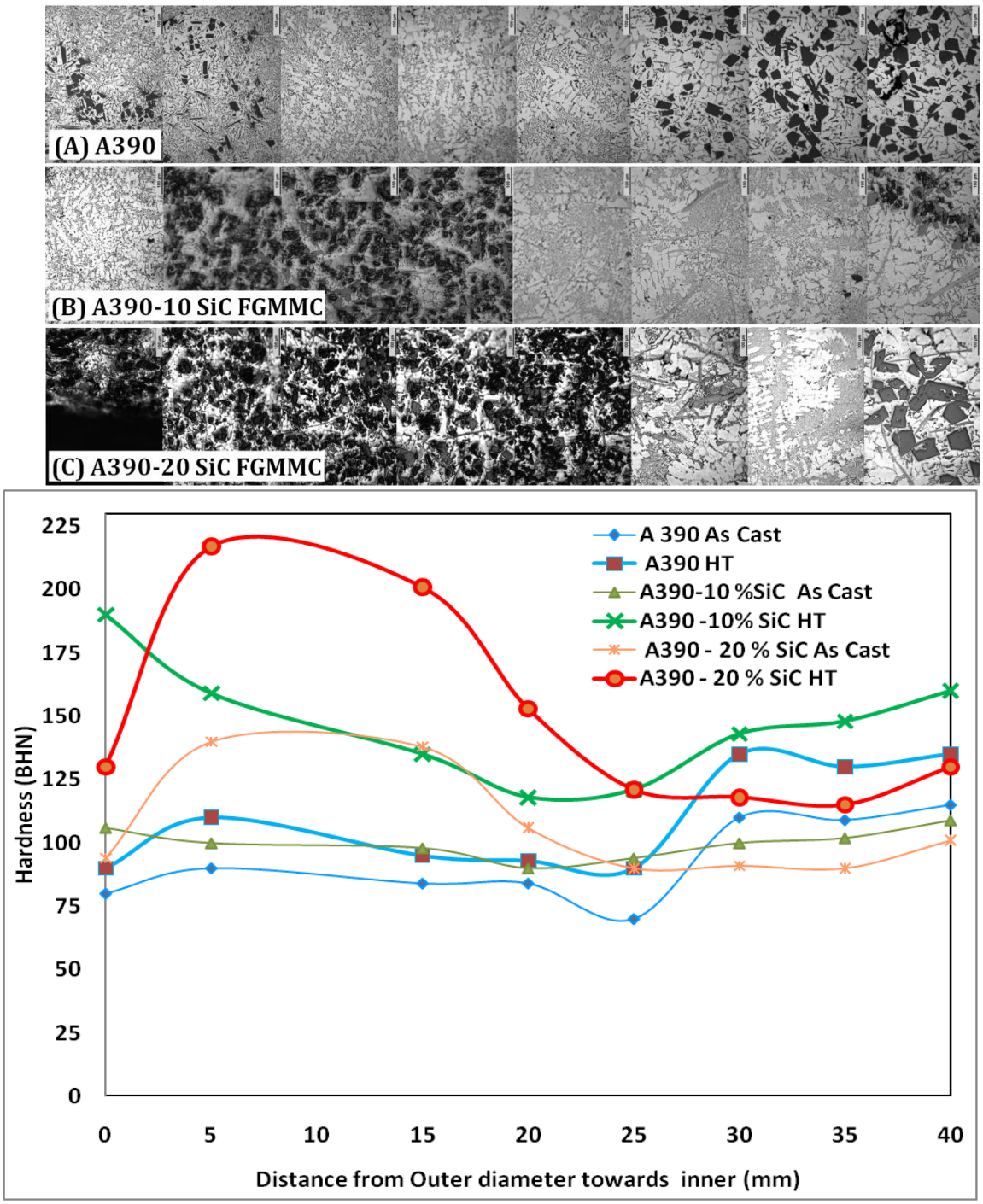

Figure 5.6: Brinell hardness values for the as-cast and T6 heat treated samples of A390, A390-10SiC and A390-20SiC FGM castings from Outer Diameter towards Inner Diameter in radial direction

in proportion to the total volume fraction of primary Si phase and SiC particles in both as cast and heat treated conditions for the A390-10 SiC and 20 SiC FGMMC rings. A390 is a hyper eutectic Al-Si cast alloy with 18 % Si. In these FGMs the less dense primary Si will diffuse towards the inner and high density SiC_p will move towards the outer regions during the centrifugal casting process creating two different gradations of opposite

nature. The diffusion will enrich inner regions with primary silicon and outer regions with SiC_p. The effective variation of a property at a location depends on the localized concentrations of each phase, the grain refinement achieved due to centrifugal pressure force and other parameters like porosity and agglomerations. In A390 FGM ring the maximum hardness, due to the presence of primary silicon phases in the inner regions, of 110 BHN in the as cast condition was observed and it raised to 135 BHN after heat treatment. From the transition zone towards outer zone the hardness value slowly increases from a lower value to moderate and reaches a maximum of 110 BHN (after heat treatment) then decreases to 90 BHN towards the extreme outer periphery. This was due to the combined effect of grain refinement in the outer zones and the lesser presence of primary silicon phase in these regions. The maximum hardness value in the particle rich zone was 106 BHN for 10 % SiC FGMMC in as cast condition and rose to 190 BHN after the heat treatment. For 10% SiC FGMMC in the transition region (15 to 25 mm away from the inner towards outer periphery) the hardness value changes between 90-98 BHN in as-cast condition and 118-135 BHN after the heat treatment. The region near the inner periphery shows high hardness of 160 BHN due to the presence primary silicon phases after heat treatment. In the case of 20SiC castings, the effect of both the presence of large volume of SiC particle and the grain refinement in the outer region provides a hardness 140 BHN in the as cast condition and 217 BHN in the heat treated condition. In the transition region, 20-35 mm away from outer periphery, a hardness of 90-106 BHN is observed in the as cast which increases to 115-121 BHN after the heat treatment. In the inner regions the hardness increases to 130 BHN (after heat treatment) due to the presence of primary silicon.

5.3.4 *Tensile Properties*

A390 and A390-10 SiC composites are used for tensile testing, since 20% SiC FGMMC castings possesses very high hardness leading to difficulty in specimen preparation. Figure 5.7 shows the ultimate tensile strength (UTS) and Yield Strength of Heat Treated specimens from Outer Region and Inner Region of A390 and A390-10 % SiC FGM castings. The ultimate tensile strength (UTS) value of 295 MPa and yield strength value of 178 MPa were obtained for the A390 FGM at the outer periphery. And for inner the values were 308 MPa and 172 MPa respectively. The higher values at the outer periphery are due to finer grain size and that at the inner are due to the large

concentration of primary silicon. The UTS and yield strength values of A390-10%SiC FGMMC at outer were 387 MPa and 176 MPa and in inner periphery 273 MPa and 180 MPa respectively. All yield strength values and UTS values of A390 FGM and FGMMC, at inner and outer periphery, are comparable except the UTS value of A390-10 SiC FGMMC outer. This was due to the presence of high volume fraction of SiCp.

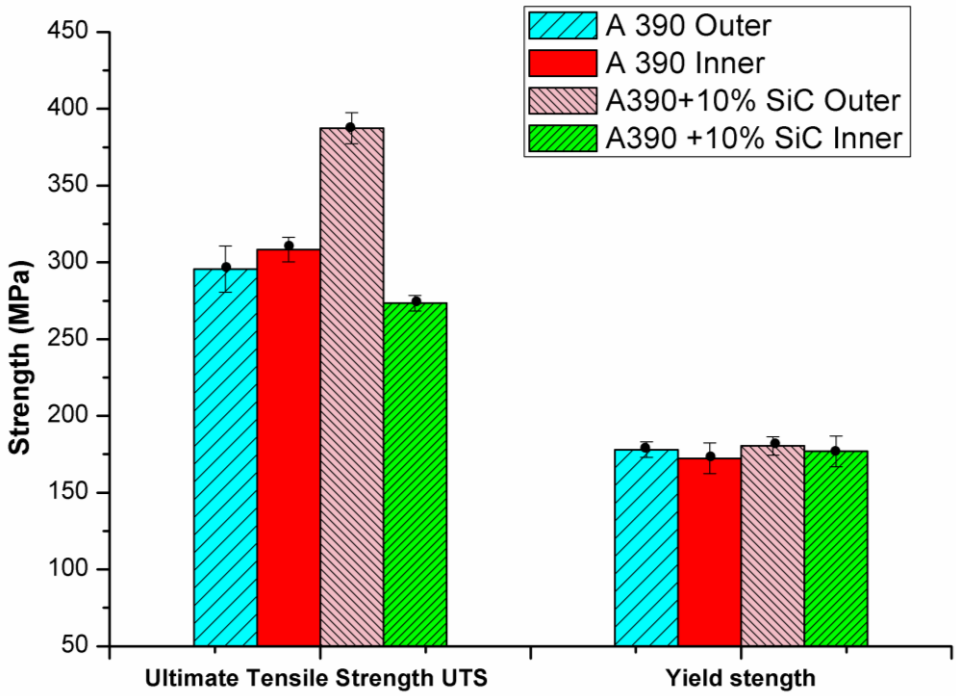

Figure 5.7: Ultimate Tensile Strength and Yield Strength of Heat Treated specimens from Outer and Inner Regions of A390 and A390-10 % SiC FGMs

5.3.5 *Wear Characteristics*

Figure 5.8 shows the wear rates of heat treated pins from inner and outer regions of A390 FGM, inner, outer and transition regions of FGMMC castings. For A390 alloy the wear rate at outer periphery was higher when compared to the inner periphery, due to the fine grain size of aluminum and the absence of primary silicon. At the inner periphery wear was less due the presence of primary silicon phase and coarser grain size. At increased loads, the wear rate increases by a large amount. A390-10 SiC FGMMC the wear rate at the outer periphery and the wear rate at the inner periphery of the A390 FGM ring was similar. The former was due to the presence of high volume fraction of SiC particles at the outer periphery, leading to higher wear resistance and the latter was due to the presence of high volume fraction of primary silicon in the inner of the FGM ring. In the transition region, lesser concentrations of primary silicon phases and SiC particles lower the wear resistance causing more wear loss.

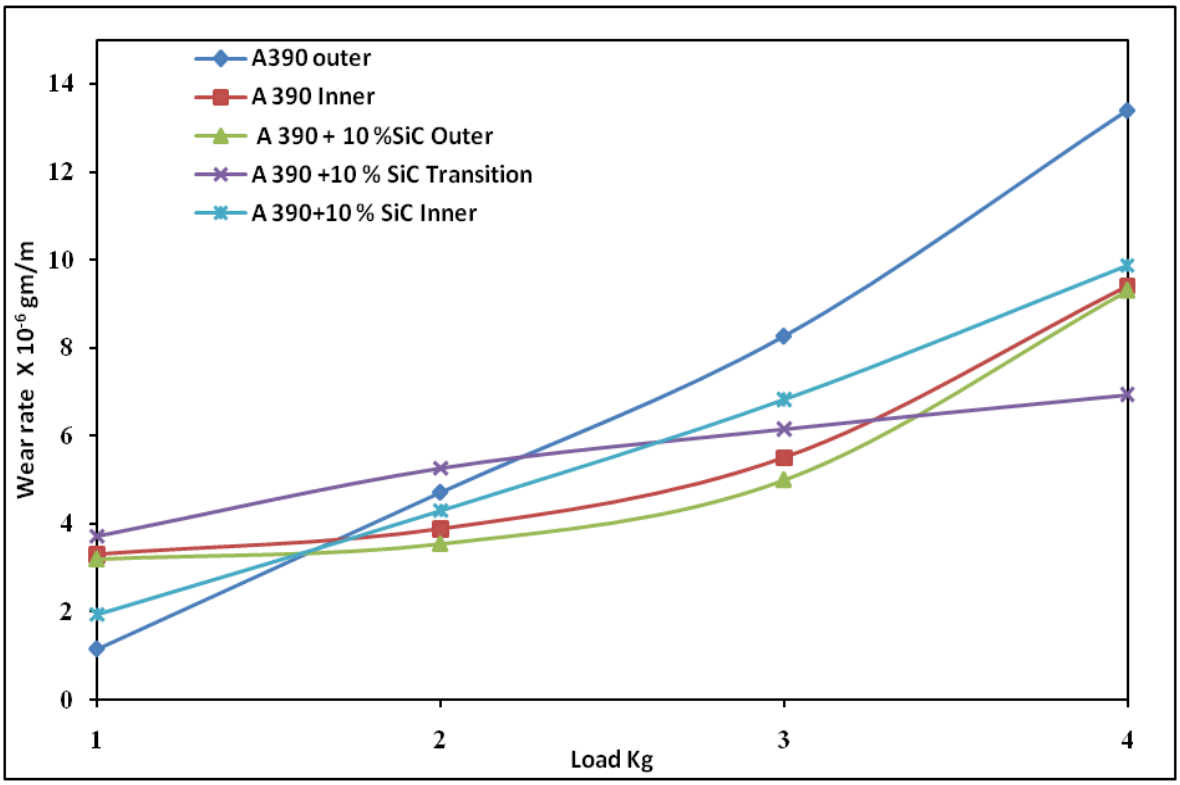

Figure 5.8: Wear rate of Heat Treated specimens from Outer Region, Transition and Inner Region of A390 and A390-10 % SiC FGM castings

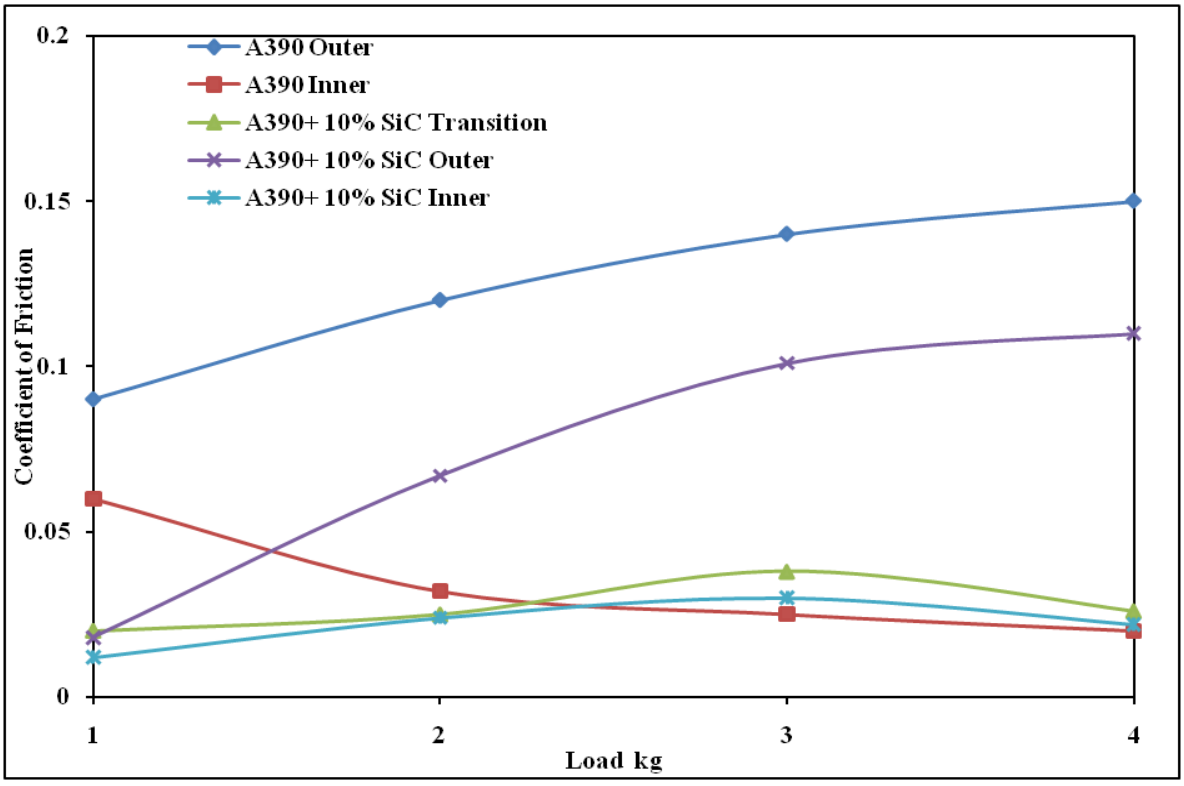

Figure 5.9: Coefficient of friction of Heat Treated specimens from Outer Region, Transition and Inner Region of A390 and A390-10 % SiC FGM castings

Figure 5.9 shows the coefficient of friction (COF) (μ) values as a function of loading. The frictional value increases as the load increases showing that the lesser wear resistance at higher loads for A390 FGM outer and A390-10 SiC FGMMC Transition heat treated wear pin samples. The microstructures taken from the respective regions clearly show that there were only aluminum matrix phase present in the region to protect matrix from more wear and neither primary silicon phase nor SiC particles were present (refer Figure 5.2 at 10,15 and 20mm and Figure 5.3 at 20 and 25mm). The COF value fluctuates over the time period for the load applied due to the heterogeneous nature of the FGM. While the test was being carried out for A390-10SiC FGMMC outer more SiC particles were exposed to the disc, then both the wear and coefficient of friction will be less. For both A390 FGM inner and A390-10SiC FGMMC inner instead of SiC particles more and more primary Si phase will expose to the disc and will in turn reduce wear and friction. Even though the general trend was as the load applied increases the COF value will also increase due to the increase in resistance to the relative motion. The COF value dependent on the frictional force, which varies with the operating temperature, in the dry sliding test, as the temperature of the pin and disc increase substantially which in turn decreases the wear resistance of the pin and thus changing the value of the coefficient of friction.

Figure 5.10 shows the stereo micrographs of the surface morphology of the wear specimens at different loads. From stereo micrographs it was clear that for all specimens even at the maximum load of 4 kg only wear scratches were visible, indicating that the mild abrasive wear mechanism was responsible for the wear loss. At 1kg load the wear scars were fine and evenly spaced. As load increases more coarse deep scars were found in the specimens. At higher loads, the interface contact surface temperature increases and weakens the interface bond between silicon particle and aluminium matrix. This is the main reason for the change in composite wear property under varying applied loads.The coarse wear scars at higher loads showing larger wear. It was seen that in A390-10SiC FGMMC inner and outer pins the wear scars at all the load are fine indicating less wear due to the presence of reinforcement particles. The ex-situ added SiC and in-situ formed primary Si particles are very hard and do not wear off easily and quickly, thus imparting higher wear resistance to the component. Si particles were present in the inner pins causing similar wear rate with that of particle rich outer pins.

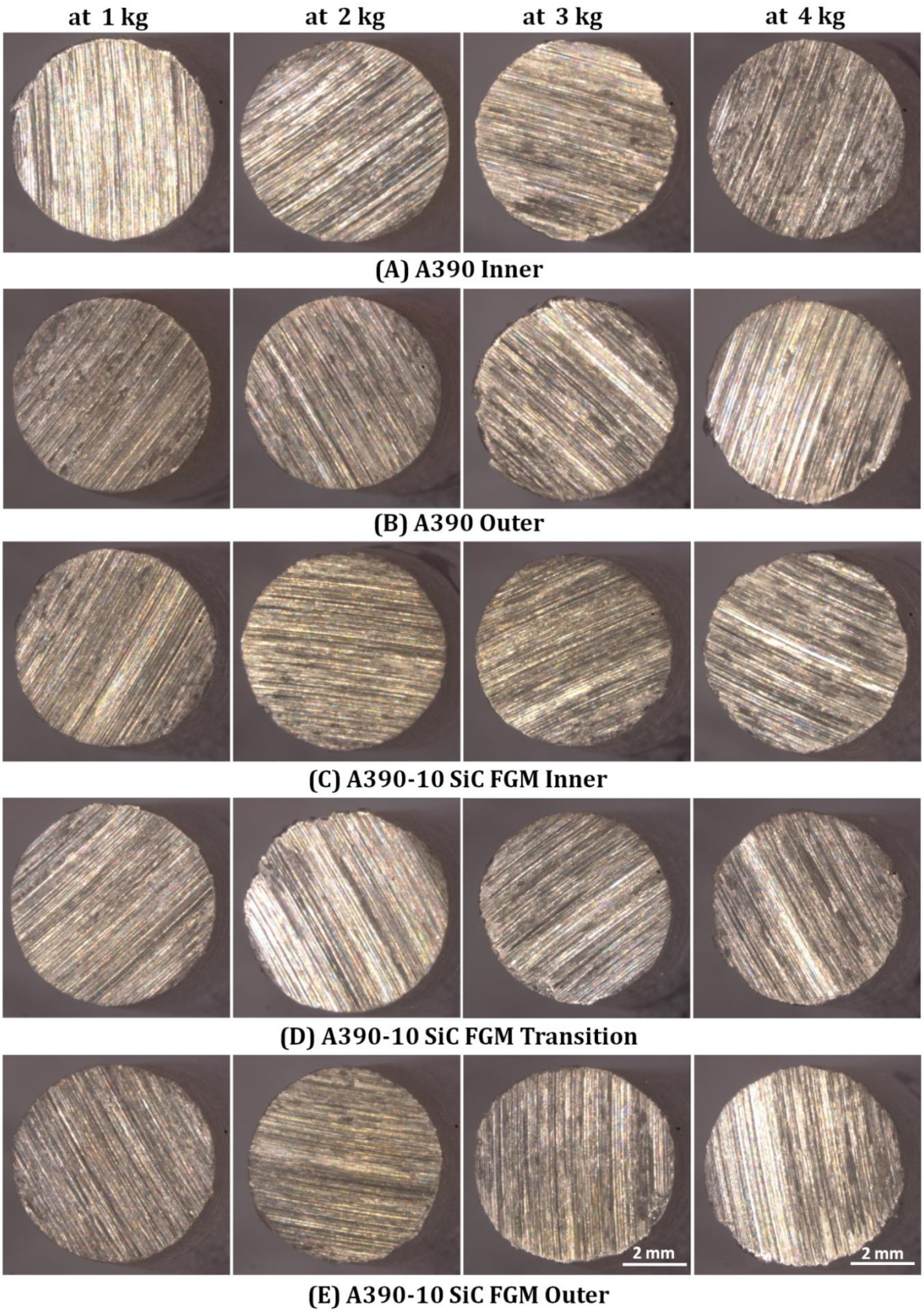

Figure 5.10 Stereo micrographs of the centrifugally cast (A) A390 Inner,(B) A390 Outer, (C) A390-10 SiC FGMMC Inner, (D) Transition and (E) Outer wear pins

5.4 STUDIES ON Mg MASTER ALLOY ADDED IN-SITU Al-Si FGM

Hypereutectic Al–Si alloys are used in components that require high resistance wear and corrosion, good mechanical properties, low thermal expansion and less density. The size and morphology of hard primary silicon particles present in Al–Si alloys greatly influences the mechanical properties. Addition of Mg leads to formation of intermetallic Mg_2Si phases, which contributes towards the properties of high silicon alloy as well as alters the nature and quantity of primary silicon formed [182-186]. The high silicon alloy subjected to centrifugal casting leads to the formation of functionally gradient material (FGM), which provides variation in spatial and continuous distribution of primary phases in a definite direction exhibiting selective properties and functions within a component. In A390 alloys by the addition of proper volume percentage of Magnesium, in-situ Mg_2Si particle phases can be formed during the MMC melt processing stage itself and can be effectively produce A390 FGMMC with Mg_2Si and Primary Silicon distributions. The Mg_2Si can be processed by two routes, either by the addition of Mg by using Al-Mg Master alloy or by direct pure Mg addition.

5.4.1 *Microstructural Evaluation*

A390 FGMMC with Mg_2Si and Primary Silicon distributions are prepared by adding calculated amount of Al-20 % Mg master alloy and the homogeneous melt is subjected to vertical centrifugal casting. The chemical compositions of homogenous castings of A390 base alloy and of all prepared alloys having pre-calculated percentage of magnesium are given in Table 5.1. The chemical composition was found out by optical emission spectra analysis. The sample preparation and experimental procedures are explained in the materials and methods (Refer chapter 3). It is observed that addition of Al-20 % Mg master alloy to obtain alloys with 1 % to 5 % Mg addition leads to change in the amount of Si, Cu and Mg in the resulting alloys.

The master alloy addition produces dilution of overall composition and is clear from the Table 5.1. The composition of minor alloying elements like Mn, Zn, Cr, Ni and Ti remains unaltered even after master alloy addition. But for Si, Cu and Fe the overall composition gradually decreases. For 1 % addition of Mg using Al-20Mg Master has reduced the Si content of A390 from 18.73 to 17.15 %. Similarly the 2, 3, 4 and 5 % Mg addition reduces the Si content in the base alloy to 16.35, 15.74, 14.89 and 13.69 % respectively. This change in composition of silicon has higher influence on the primary

silicon content in the alloy. Likewise, there is a shift in the composition of Cu towards lower percentage by the addition of Mg master alloy. The lower percentages of Cu will considerably reduced $CuAl_2$ phases in the microstructures.

Table 5.1: Chemical composition of alloys by Mg Master alloy addition

Details of Alloy	Major Alloying Elements in %				Minor Alloying Elements in %					Al in %
	Si	Cu	Mg	Fe	Mn	Zn	Cr	Ni	Ti	
A390as per standards	16 - 18	4 - 5	0.4–0.7	1.1 (Max)	0.3 (Max)	0.2 (Max)	0.1 (Max)	0.1 (Max)	0.2 (Max)	74-78
A390 ingot	**18.73**	4.09	**0.32**	0.43	0.06	0.06	0.01	0.01	0.01	76.21
A390+ 1Mg	**17.15**	2.80	**1.31**	0.35	0.06	0.04	0.01	0.01	0.01	78.16
A390+ 2Mg	**16.35**	2.81	**2.36**	0.32	0.04	0.04	0.02	0.01	0.01	78.04
A390+ 3Mg	**15.74**	3.67	**3.19**	0.37	0.06	0.05	0.02	0.01	0.01	76.79
A390+ 4Mg	**14.89**	3.11	**4.45**	0.36	0.05	0.07	0.01	0.02	0.02	76.79
A390+ 5Mg	**13.69**	2.96	**5.58**	0.37	0.04	0.06	0.01	0.01	0.01	77.13

Figure 5.11 gives the optical microstructures of gravity die cast A390 base alloy and with 1, 2, 3, 4 and 5 % Mg added alloys. The light grey phase is silicon, the dark phase is Mg_2Si and the white phase is α-Al. The base alloy shows the presence of higher percentage of primary silicon in the matrix (Figure 5.11a). It is observed that cuboidal primary silicon of average 50 µm sizes is evenly distributed. Needle/platelet type eutectic silicon is visible along the grain boundaries of aluminium matrix. No secondary dendritic arms are observed in the microstructure. As we proceed to (b) to (f) the Mg addition takes place and the formation of Mg_2Si occurs by the reaction of Mg with the silicon present in the melt. At 1 % Mg addition primary silicon percentage drastically reduces and more eutectics appears and at 2% there is no primary silicon appears in the microstructure and more evenly distributed eutectics are visible. At 3% Mg the addition give rise to a favourable condition to form maximum eutectic silicon rather than Mg_2Si and the residual primary silicon is also getting modified and more amount of eutectic silicon is observed. However in the 4 % and 5% Mg added alloys shows very less percentage of primary silicon. The excess primary silicon available, which are fine sized, after the formation of Al-Si eutectic gets reacted with the added magnesium to form

Mg_2Si. The primary Mg_2Si phases are observed in 4 and 5% Mg added alloys. As expected higher percentage of primary Mg_2Si phases is observed in 5%Mg added alloys.

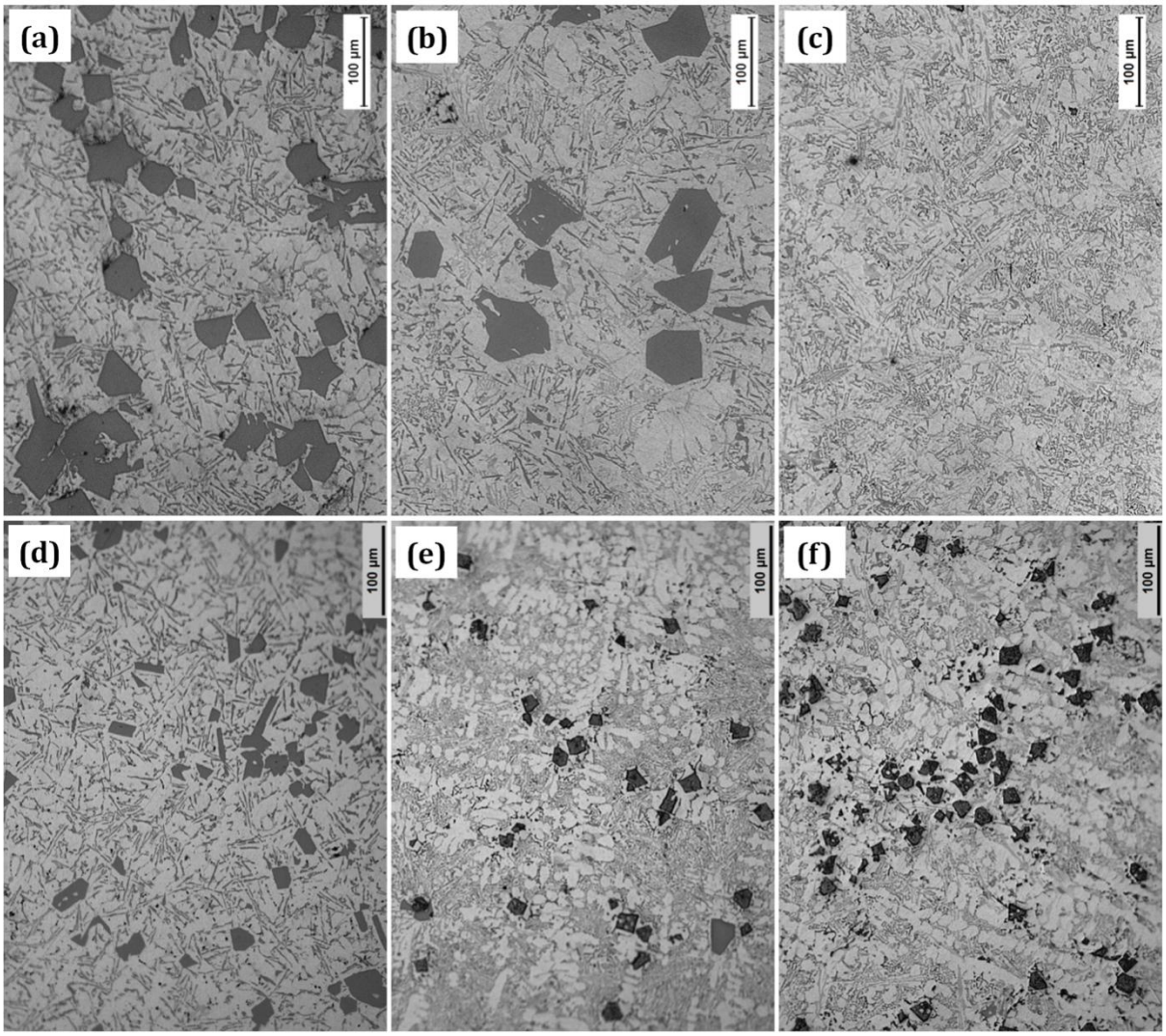

Figure 5.11: Microstructures of homogeneous gravity castings (The light grey phase is silicon, the dark phase is Mg_2Si and the white phase is α-Al) (a) A390,(b)+1% Mg,(c)+2% Mg,(d) +3% Mg,(e) +4 Mg and (f)+5 Mg by Al-Mg Master alloy addition

Functionally graded aluminium alloys have been successfully fabricated using centrifugal casting technique. Figure 5.12 gives the optical microstructures of as cast Al FGM from outer to inner periphery of the ring. The reinforcements formed are in-situ primary silicon and Mg_2Si phases. The densities of aluminium alloy matrix, the primary silicon and Mg_2Si are 2.6 g/cm^3, 2.33 g/cm^3 and 1.88 g/cm^3. Both the densities of primary silicon and Mg_2Si are less than that of the aluminium alloy matrix, they will diffuse

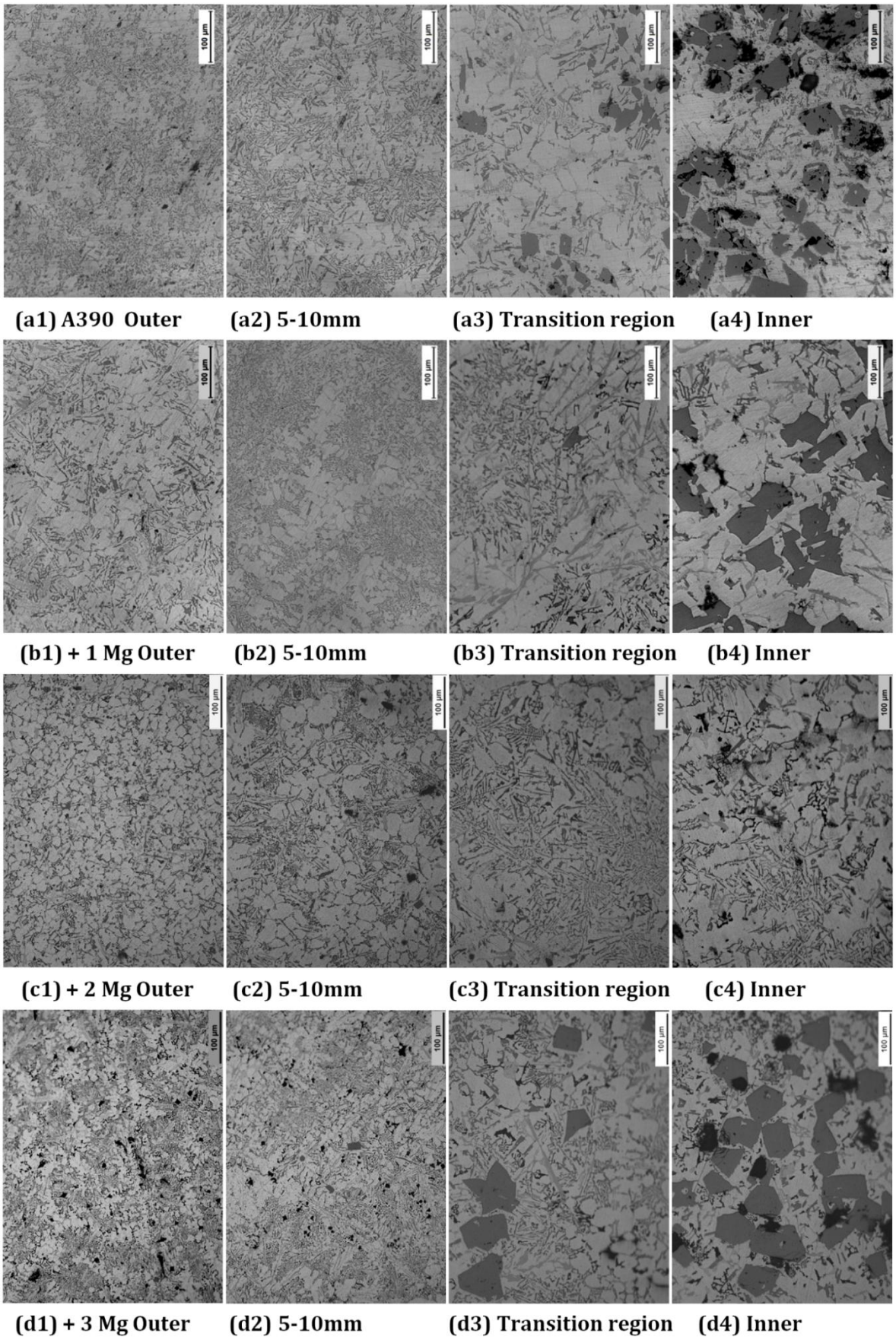

Figure 5.12A: Microstructures of FGM Mg Master addition from outer to inner

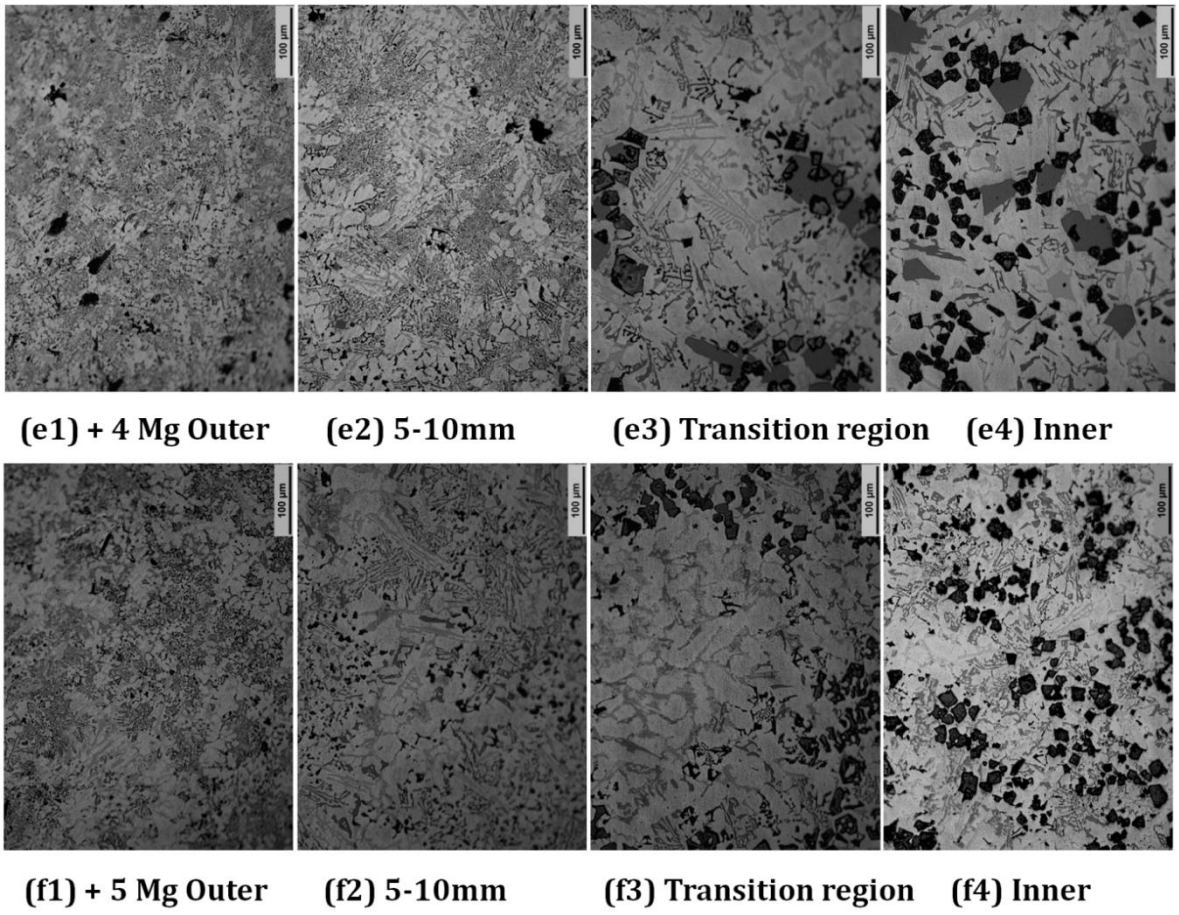

Figure 5.12B : Microstructures of centrifugal castings of alloy specimens from outer to inner periphery of the functionally graded casting (a) A390,(b)+1% Mg,(c)+2% Mg,(d) +3% Mg,(e) +4 Mg and (f)+5 Mg by Al-Mg Master alloy addition

towards the inner periphery during the centrifugal casting. In all castings four regions are observed. The four different regions formed in the Al-Si-Mg_2Si FGM are the chill zone, particle depleted/free region, transition /interface and region particle rich region. The chill zone is formed near the mould wall (outer region) due to the rapid solidification of the melt occurring by the contact of the molten metal with the mould wall. There is no sufficient time for diffusion or transportation of density different phases due to centrifugal force and the microstructure / composition will be similar to the gravity or homogeneous casting of the corresponding alloy composition. The average thickness of the chill zone is 2-3 mm. The second region is the particle free region which is formed by the movement of primary silicon and Mg_2Si towards the inner periphery and mostly primary aluminium (α-Al) and eutectic silicon phases are observed. The third region is the interface region / the transition region where the transition takes place from particle free to particle rich region. The fourth region is the

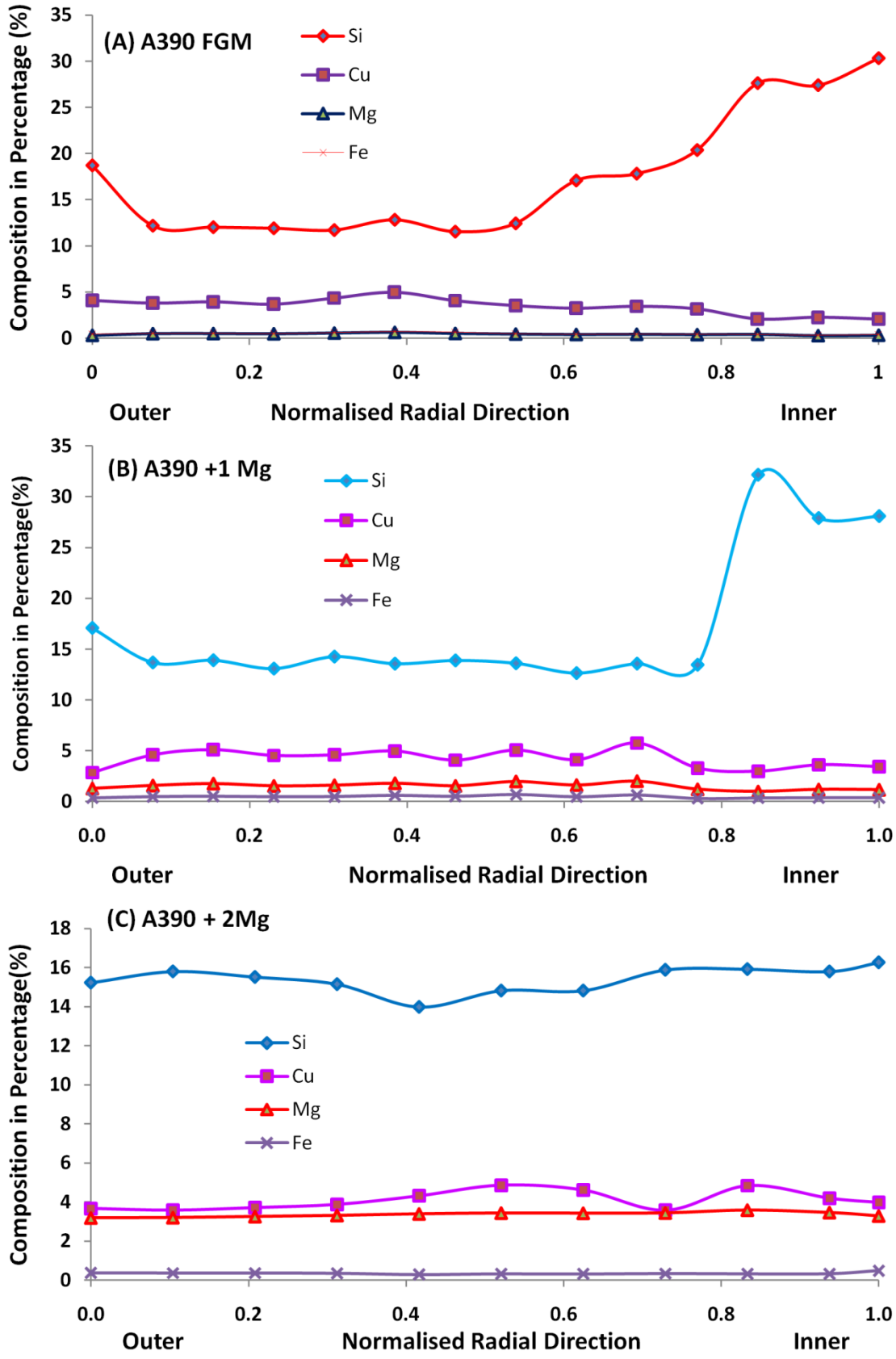

Figure 5.13A: Chemical composition variation of Major alloying elements (in %) along normalised radial direction (from outer to inner periphery) analysed using optical emission spectrometer

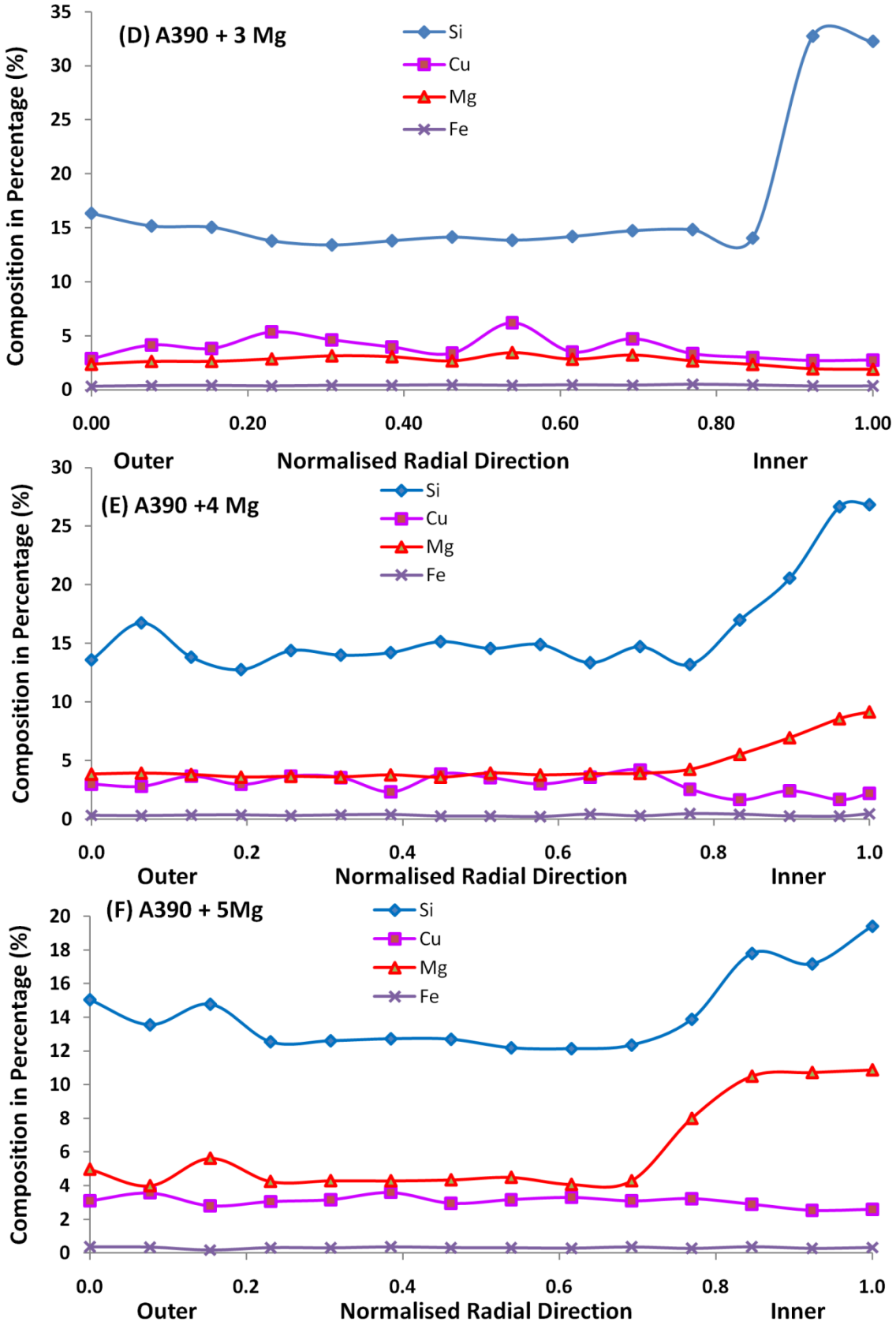

Figure 5.13B: Chemical composition variation of Major alloying elements (in %) along normalised radial direction (from outer to inner periphery) analysed using optical emission spectrometer

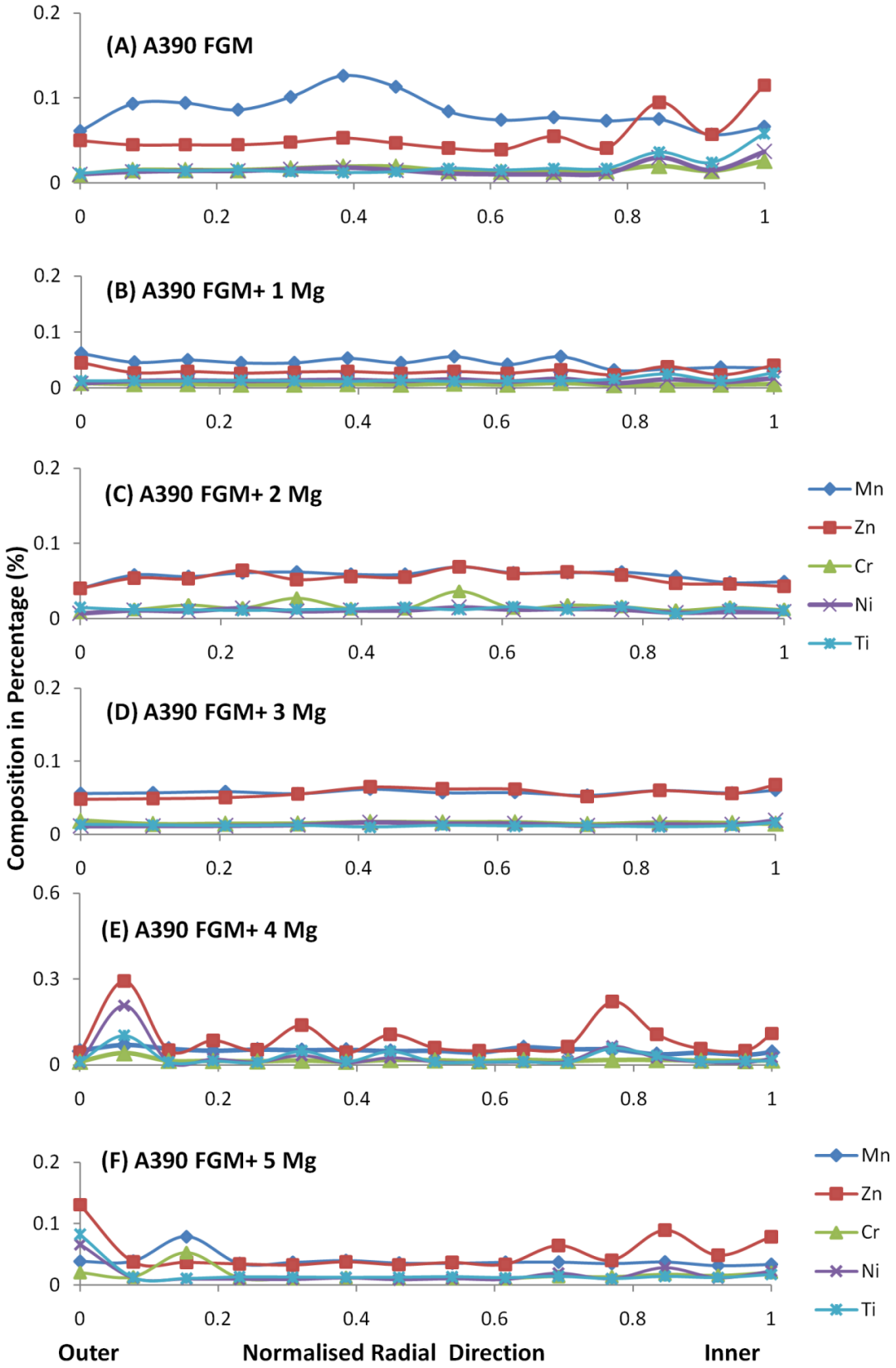

Figure 5.14: The variation in chemical composition of minor elements in the alloys along the normalised radial direction (Outer diameter towards the inner)

particle rich region where the Si and Mg_2Si phase get distributed and which enhances the overall hardness of the system. As the magnesium content increases more primary silicon is being converted to Mg_2Si and evenly distributed in the matrix. Moreover it is observed that the size of primary silicon reduces with increase in percentage of Mg added. The Mg_2Si phases are observed on the periphery of primary silicon phases during solidification. This is due to the formation of primary silicon at higher temperature than that of Mg_2Si during solidification.

5.4.2 Composition *Evaluation*

Figure 5.13 shows the chemical composition of centrifugally cast A390 alloys with 0, 1, 2, 3, 4 and 5% Mg processed by Al-Mg Master alloy addition. The FGM rings are analysed from outer to inner diameters in radial direction by using optical emission spectrometer. As observed in microstructures, the chemical composition analysis also shows gradation. There is a remarkable variation in chemical composition at different locations depending on the nature of segregation of phases and precipitates. The outer most region of the centrifugal casting shows a chemical composition (Figure 5.13) similar to that of respective homogenous alloy system (Table 5.1). This is due to the chilled zone formation in the centrifugal cast ring, where the metal gets solidified immediately reaching the mould surface and there is no time for segregation or migration of the phases. The microstructures also show a similarity in the structural features. The increase in Si content near the inner periphery is due to segregation of primary silicon particles and Mg_2Si phases. In 5% Mg added FGM, the presence of Mg_2Si is observed immediately after the chill zone. This is supplemented by the chemical analysis, where the Si and Mg percentages are also higher. In the transition regions a both Mg_2Si and Primary silicon are observed along with primary Al and eutectic silicon. (Figure 5.12 (a3), (d3), (e3) and (f 3)). Figure5.14 shows the variation in chemical composition of minor elements in the alloy. There is no remarkable variation in the chemical composition of minor elements in the FGM rings.

Once of the major observation is, on Al-Mg master alloy addition to A390 melt, the concentration of silicon gets diluted towards lower concentration and leading to presence of lesser primary silicon particles. The magnesium in the master alloy will have two different functions. At lower percentages, magnesium will act as a grain refiner / modifier with a little formation of Mg_2Si. And at higher percentage additions,

formation of Mg_2Si is predominant. The Mg_2Si formation requires modification or precipitation. In both microstructure and chemical composition, at lower percentage additions (1%), Al-Mg master addition resulted in the formation of a eutectic structure with less formation of Mg_2Si and a gradation of primary silicon towards the interior side from outer in the radial direction of the FGM casting is observed. The primary silicon phases formed are larger in particle size. In the 2% addition maximum formation of eutectic Al-Si is observed and is uniformly distributed in radial direction from outer to inner without forming a significant gradation, however there is no formation of primary silicon particles in this case both in gravity and centrifugal cast FGM. A few Mg_2Si phases are observed at the inner region. For higher percentage additions 3 to 5 % Mg additions, the excess Mg present in the system give rise to a favourable condition to form more and more Mg_2Si along with eutectic Al-Si and the residual primary silicon is also getting modified. The additions results in the formation of more Mg_2Si phases and are distributed towards the inner periphery during the casting of FGM. The primary silicon has a density of 2.33 g/cm^3 and that of Mg_2Si is 1.88 g/cm^3, they are lower than that of the aluminium alloy matrix i.e.2.6 g/cm^3. Due to the lower densities both primary silicon and Mg_2Si gets segregated towards the inner during the casting.

5.4.3 *Hardness Evaluation*

Table 5.2: Hardness of A390 alloy and A390- 1 Mg to 5 Mg alloys homogeneous gravity die casting under as cast and T6 heat treated conditions (in BHN)

Material Specification (By Al-Mg Master alloy addition)	Hardness of Gravity Castings in Brinell Hardness (**BHN)**	
	As Cast conditions	Heat Treated T6 conditions
A390 Base alloy	135	145
A390+1Mg	120	163
A390+ 2 Mg	124	146
A390+ 3Mg	136	151
A390+4 Mg	131	139
A390+5 Mg	138	147

Table 5.2 shows the hardness of homogeneous gravity castings prepared by the alloys and A390 base alloy in the as cast as well as heat treated conditions. For 1% Mg alloy gravity casting, after the T6 heat treatment, the best and the maximum hardness of 163 BHN is obtained. Other alloys have slightly higher or comparable hardness value of that of heat treated A390 base alloy.

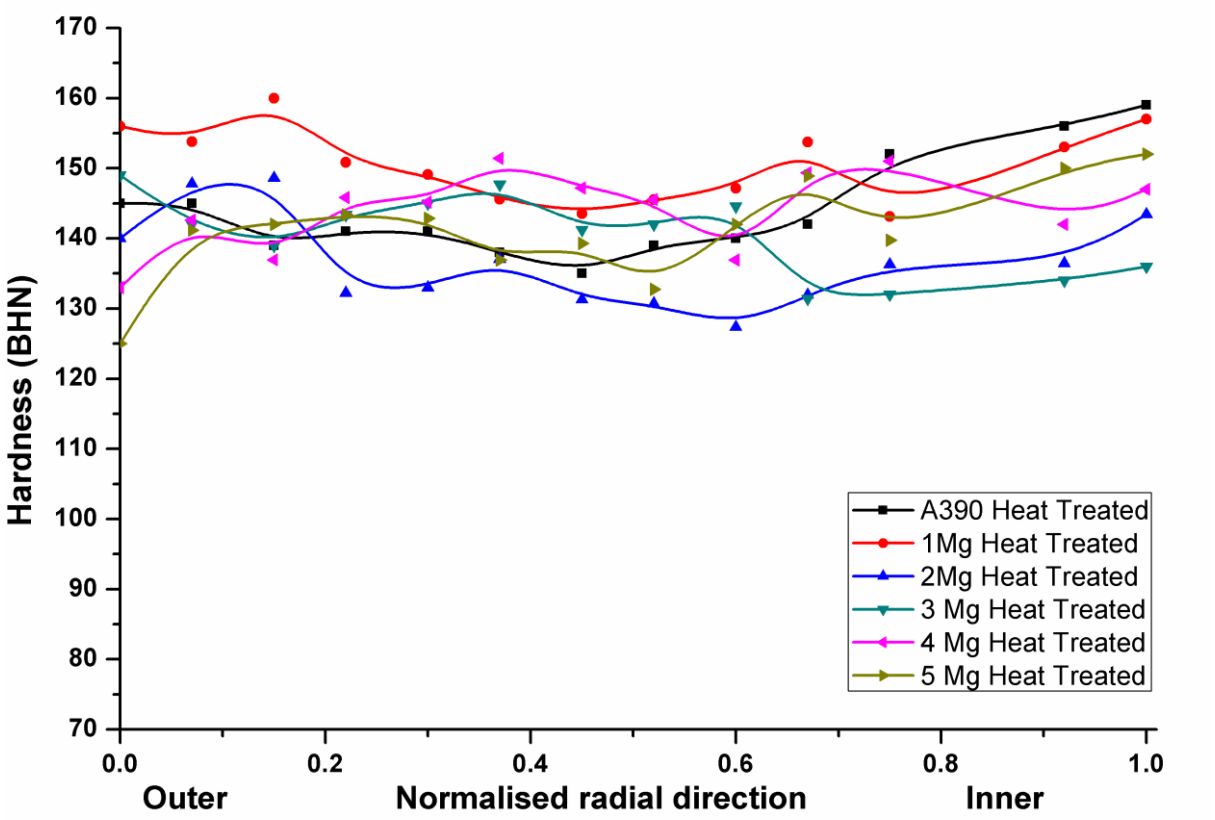

Figure 5.15: Hardness variation of heat treated alloys along normalised radial direction from outer diameter towards Inner in a radial direction

Figure 5.15 shows the hardness variation of all heat treated alloys along the normalised radial direction from outer diameter towards Inner in a radial direction. For all the castings the hardness value at the chilled zone is comparable with that of the alloy. The increase in volume percentage of silicon near the inner periphery is due to segregation of primary silicon particles and Mg_2Si phases. The 1% Mg alloy shows a higher hardness almost throughout the radial distances from the outer to the inner regions. Even though the composition of the 2% Mg modification doesn't initiate a gradation, the hardness shows a liner variation in a small range of 130-145 BHN. The 2% modified alloy shows almost the same or similar hardness values radially in all

regions. For A390 alloy and 4% Mg modified alloy the inner region have more phase concentration which resulted in a higher hardness value of 157-159 BHN, in A390 base alloy and for 4%Mg modified alloy a similar trend of 140-147 BHN at the inner regions. In 4% Mg alloy FGM, immediately after chill zone the hardness value increases from 133 to 142 BHN. This change is supported by the microstructural presence of Mg_2Si and is also supported by the chemical analysis that at this region the percentages of both Mg and Si are higher. In the transition regions, the hardness remains lower and fewer variations are experienced. This is also well supported by the local microstructures and the results of local chemical compositional analysis. It is also found that the remarkable variations in the chemical composition of minor elements in the FGM rings are limited to the chilled zone and particle free inner region.

5.4.4 *Wear Characteristics*

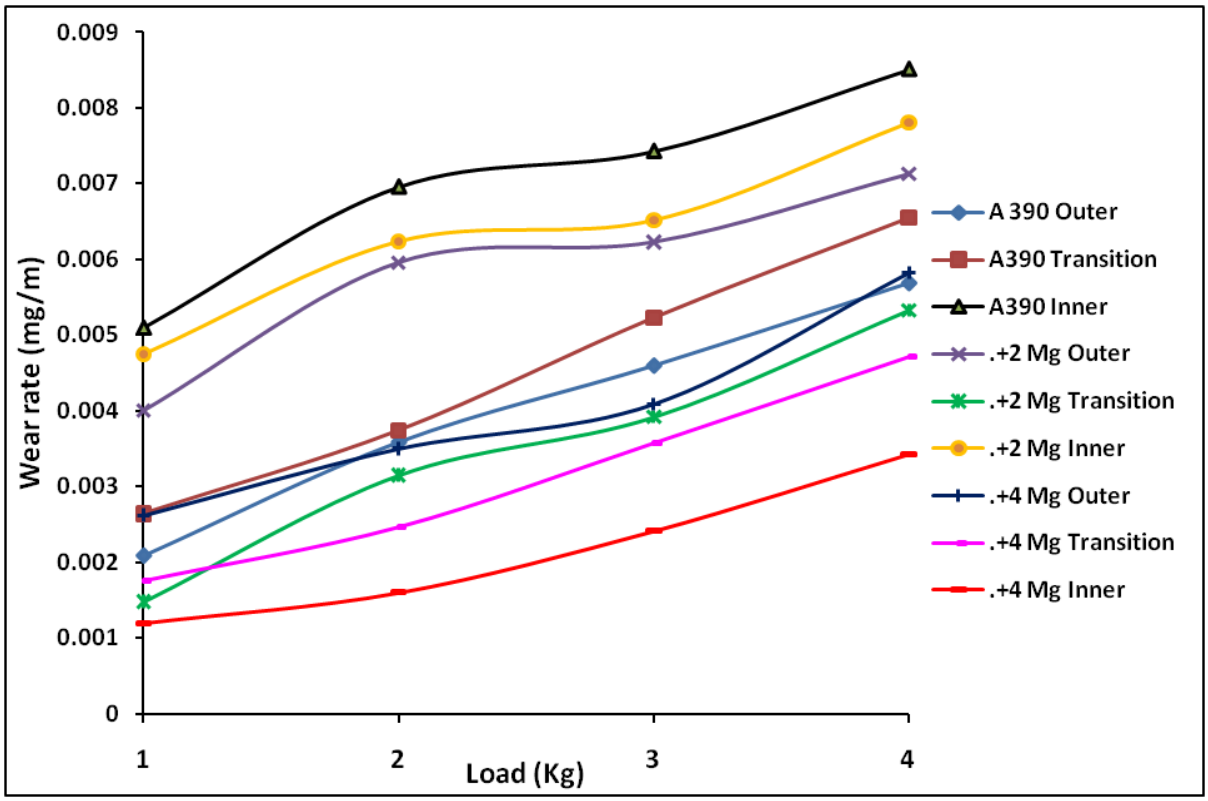

Reciprocating Dry Wear analysis: Wear rate in mg/m (Bidirectional)									
Load in Kg	A 390 Outer	A390 Transition	A390 Inner	+2 Mg Outer	+2 Mg Transition	+2 Mg Inner	+4 Mg Outer	+4 Mg Transition	+4 Mg Inner
1	0.00208	0.00264	0.0051	0.004	0.00148	0.00475	0.00262	0.00176	0.0012
2	0.00359	0.00374	0.00696	0.00596	0.00315	0.00624	0.0035	0.00247	0.0016
3	0.0046	0.00523	0.00743	0.00622	0.00392	0.00652	0.00409	0.00358	0.00241
4	0.00569	0.00655	0.00851	0.00713	0.00533	0.00781	0.00582	0.00472	0.00342

Figure 5.16: Reciprocating wear rate of heat treated alloy pins at different loads

Bidirectional wear test is carried out on a reciprocating wear test rig. The test was conducted on the A390, +2 Mg and+4Mg alloys with a sliding velocity of 0.6m/s for a total sliding distance of 500m at loads 1, 2, 3 and 4 Kg in a dry testing condition with a stroke length of 10 cm. The time of experiment was approximately 13 minutes. Pins of diameter 6 mm and length 30 mm are machined from the main three regions of FGM (outer, transition and inner). The counter surface was hardened and buffed EN31 steel. Wear rate as a function of weight loss are shown in Figure 5.16. The wear behaviour of hyper eutectic alloys depends on the hard phases present in them. So the primary silicon has a very crucial role in the wear behaviour of these alloys. The excess silicon segregated in the inner region carries away the direct load and transfer it to the aluminium matrix, there by reduces the wear compared to the outer regions. As the Si particles are strongly bonded with aluminium matrix, they protect the surface against severe destructive action of loading. The strong bond, which plays a critical role in transferring the loads from the reinforcements to the matrix, results in less wears.For 2 % Mg modification, all the regions namely, outer, transition and inner shows a similar type of variation in wear rate with inner pin maximum wear, outer pins in middle range and the transition pins have the minimum amongst. This behaviour is due to the presence of more eutectic Ai-Si phases present in the transition region giving less hardness at the same time more toughness/wear resistance property. Even though primary silicon is present in the inner, their contribution to wear resistance is much lesser than the effect that of grain refinement and eutectics present in the outer region. In the case of 4% Mg the order of wear is as the order expected as with outer in maximum followed by transition and in the inner at minimum wear rate condition. In this, the volume of Mg_2Si, Primary Silicon and eutectic Al-Si have an effective control along the radial direction which is well supported by the microstructure, hardness and compositional variations in the radial direction. As a result 4 Mg inner is having the lowest reciprocating wear rate at all loading conditions.

In order to compare the effects on wear characteristics of A390 alloy modification by Al-Mg master alloy addition, the unidirectional dry wear test on pin-on-disc is also conducted for the A390, +2 Mg and+4 Mg alloys with a sliding velocity of 0.6m/s for a total sliding distance of 500m at loads 1, 2, 3 and 4 Kg in a dry testing condition. (Even though the general Pin on Disc dry wear test conditions for aluminium and light metals are sliding velocity 2m/s, sliding distance 1800 m or more at loads 1 to

5 kg). Figure 5.17 shows the wear rates of alloy pins at different loads for the dry pin on disc wear testing. The wear is the minimum for 2% Mg transition zone and this is due to the presence of more eutectic Al-Si phases. The evenly distributed eutectic phases in the aluminium matrix will produce minimum grain boundaries and strong interface bonding between matrix grains than primary silicon or Mg_2Si particles. This bonding will reduce from abrasion wear which are prominent in unidirectional wear than in bidirectional wear. The fine grains produced by the centrifugal effect will help to reduce the wear rate of the specimens from the outer regions. But in the case of 2% Mg outer pins, the absence of eutectics and primary silicon results in high wear at higher loads.

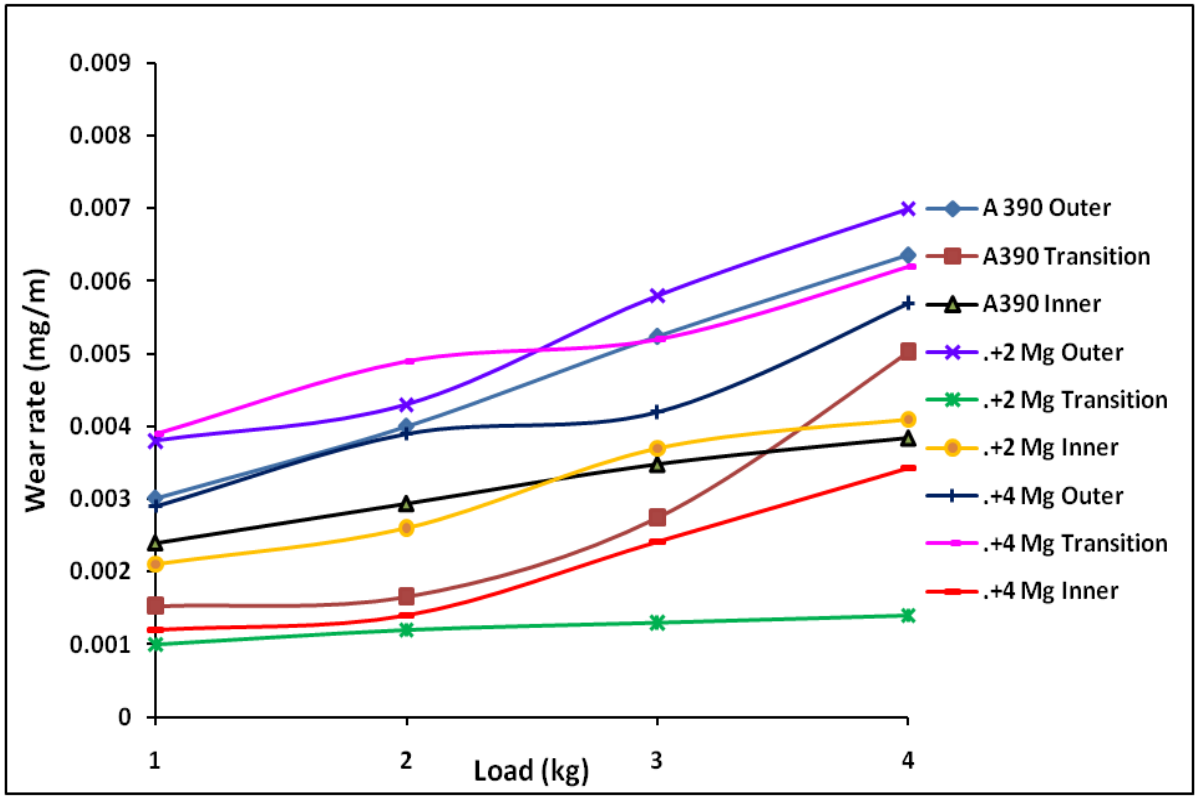

Pin on Disc Dry Wear analysis: Wear rate in mg/m (unidirectional)									
Load in Kgs	A 390 Outer	A390 Transition	A390 Inner	+2 Mg Outer	+2 Mg Transition	+2 Mg Inner	+4 Mg Outer	+4 Mg Transition	+4 Mg Inner
1	0.00301	0.00153	0.0024	0.0038	0.001	0.0021	0.0029	0.0039	0.0012
2	0.004	0.00166	0.00294	0.0043	0.0012	0.0026	0.0039	0.0049	0.0014
3	0.00524	0.00275	0.00348	0.0058	0.0013	0.0037	0.0042	0.0052	0.00241
4	0.00636	0.00503	0.00384	0.007	0.0014	0.0041	0.0057	0.0062	0.00342

Figure 5.17: Pin on Disc wear rate of heat treated alloy pins at different loads

The comparison of unidirectional pin on disc and bidirectional reciprocating wear tests on similar conditions reveals that in general bidirectional wear is more at all loading conditions. The wear micrographs of inner pins of the alloys at 4 kg loads in

both tests clearly shows that wear is more for bidirectional reciprocating wear (Figure 5.18). Since the sliding distance and relative velocities are lower than that of usual practices it is found that even after the full testing time at the maximum 4 kg loading condition, the contact surfaces are not fully and uniformly worn out. In the reciprocating wear delamination and adhesive wear are prominent mechanisms, which causes the material loss (wear rate), that can be effectively reduce by the surfacing hard phase/ particles on the contact surface by reducing the actual contact area to the minimum as possible. But in the case of unidirectional pin on disc rotating wear, the matrix interface bonding plays a major function in reducing the wear in addition to contact surfaces.

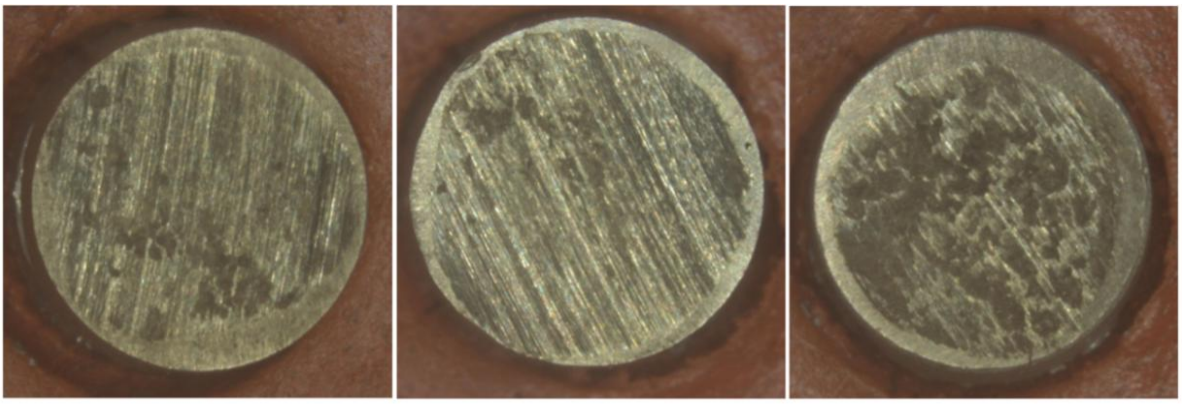

(A) Worn out surfaces of Inner region pins of alloys at 4 kg for Pin on Disc wear test

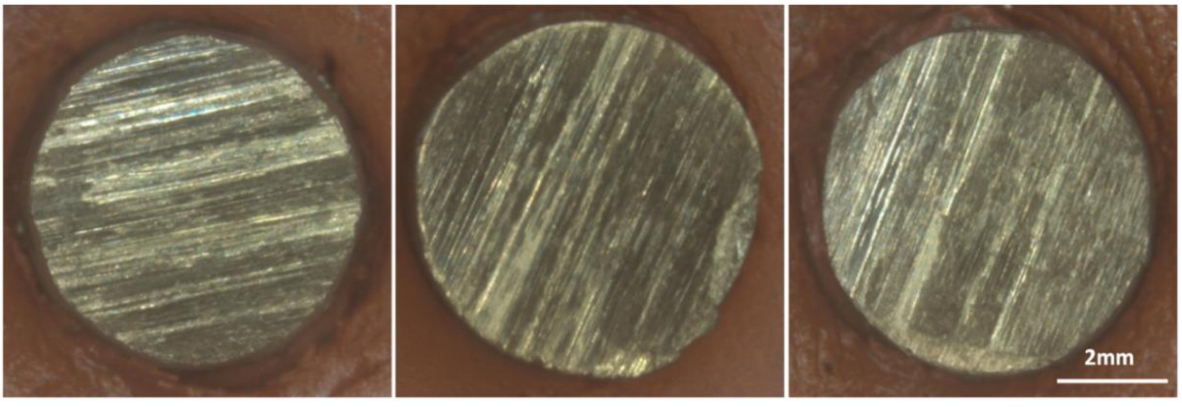

(B) Worn out surfaces of Inner region pins of alloys at 4 kg for Reciprocating wear test

Figure 5.18: Stereo micrographs of worn out inner pin surfaces of alloys at 4 kg load.

5.5 STUDIES OF PURE MAGNESIUM (Mg) ADDED IN-SITU Al-Si FGM

5.5.1 *Microstructural Evaluation*

A390 FGMMC with Mg_2Si and Primary Silicon distributions are prepared by adding calculated amount of pure Magnesium (Mg) and the homogeneous melt is subjected to vertical centrifugal casting. The chemical compositions of homogenous castings of A390 base alloy and of all prepared alloys having pre-calculated percentage of magnesium are given in Table 5.3. The chemical composition was found out by optical emission spectra analysis. The sample preparation and experimental procedures are explained in the materials and methods (Refer chapter 3). No dilution is observed, in the case of addition of 1% to 5% pure magnesium (Mg) to obtain different alloy compositions and is clear from the Table 5.3. The composition of minor elements like Mn, Zn, Cr, Ni and Ti remains unaltered along with that of the Si, Cu and Fe.

Table 5.3: Chemical composition of base alloy and alloys by Pure Mg addition

Details of Alloy	Major Alloying Elements in %				Minor Alloying Elements in %					Al in %
	Si	Cu	Mg	Fe	Mn	Zn	Cr	Ni	Ti	
A390as per standards	16 - 18	4 - 5	0.4–0.7	1.1 (Max)	0.3 (Max)	0.2 (Max)	0.1 (Max)	0.1 (Max)	0.2 (Max)	74-78
A390 ingot	**18.097**	3.26	**0.36**	0.426	0.08	0.04	0.01	0.01	0.01	77.59
A390+ 1Mg	**18.010**	3.18	**1.66**	0.35	0.04	0.05	0.01	0.01	0.01	76.55
A390+ 2Mg	**18.561**	3.81	**2.73**	0.39	0.04	0.12	0.04	0.03	0.01	74.04
A390+ 3Mg	**18.563**	3.01	**3.53**	0.22	0.06	0.11	0.05	0.02	0.02	73.88
A390+ 4Mg	**18.311**	3.74	**4.50**	0.415	0.05	0.05	0.01	0.01	0.01	72.79
A390+ 5Mg	**17.961**	2.94	**5.22**	0.43	0.08	0.04	0.01	0.01	0.01	73.12

Figure 5.19 gives the optical microstructures of gravity die cast A390 base alloy and with 1, 2, 3, 4 and 5% Pure Mg added alloys. The light grey phase is silicon, the dark phase is Mg_2Si and the white phase is α-Al. The base alloy shows the presence of higher percentage of primary silicon in the matrix (Figure 5.19a). It is observed that cuboidal primary silicon of average 40-50 μm sizes is evenly distributed. Needle/platelet type eutectic silicon is visible along the grain boundaries of aluminium matrix. No secondary dendritic arms are observed in the microstructure. As we proceed to (b) to (f) the Mg

addition takes place and the formation of Mg_2Si occurs by the reaction of Mg with the silicon present in the melt. At 1% Mg addition primary silicon percentage drastically reduces and more eutectics appear only very large sized primary silicon particles are visible. At 2% and 3 % there is a few primary silicon visible, with a relatively smaller size than the previous, in the microstructure and more evenly distributed eutectics are also visible. At 4% Mg the addition give rise to a favourable condition to form maximum Mg_2Si rather than eutectic silicon without any appreciable refinement in the residual primary silicon and lesser amount of eutectic silicon is observed. The primary Mg_2Si phases are observed in 4 and 5% Mg added alloys. As expected higher percentage of primary Mg_2Si phases is observed in 5%Mg added alloys.

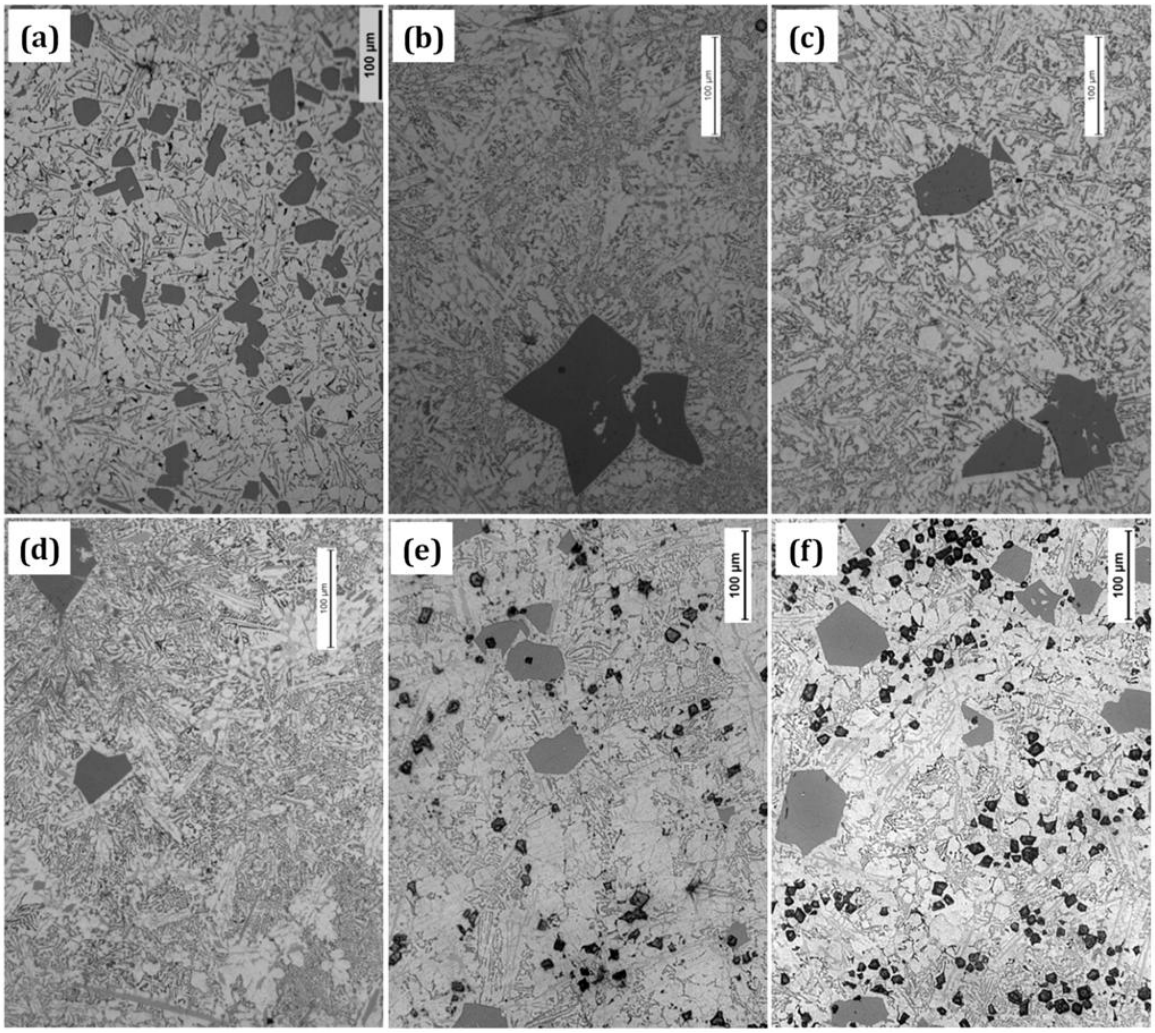

Figure 5.19: Microstructures of homogeneous gravity castings (The light grey phase is silicon, the dark phase is Mg_2Si and the white phase is α-Al) (a) A390,(b)+1% Mg,(c)+2% Mg,(d) +3% Mg,(e) +4 Mg and (f)+5 Mg by Pure Mg addition

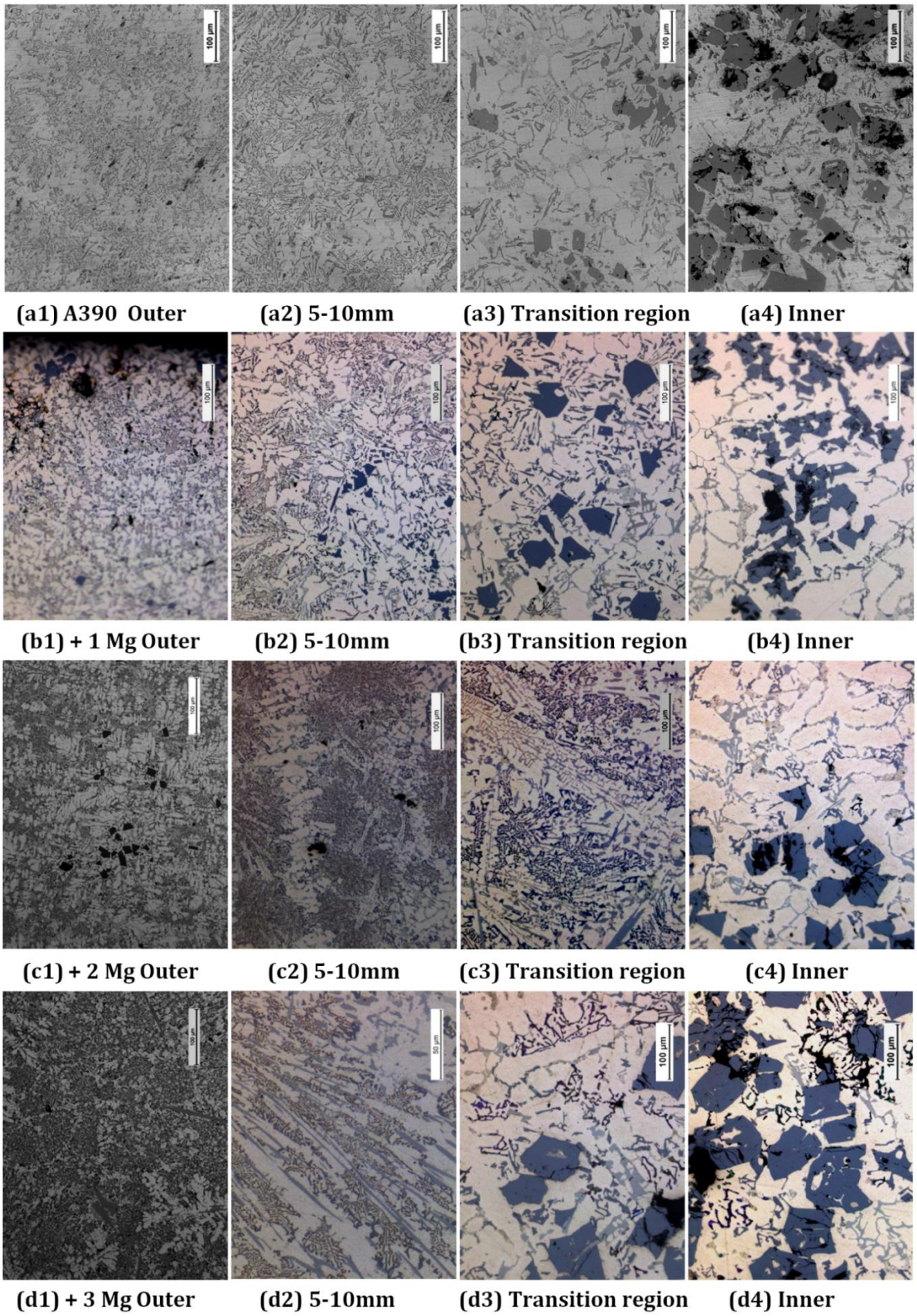

Figure 5.20A: Microstructures of Pure Mg added FGMs from outer to inner periphery

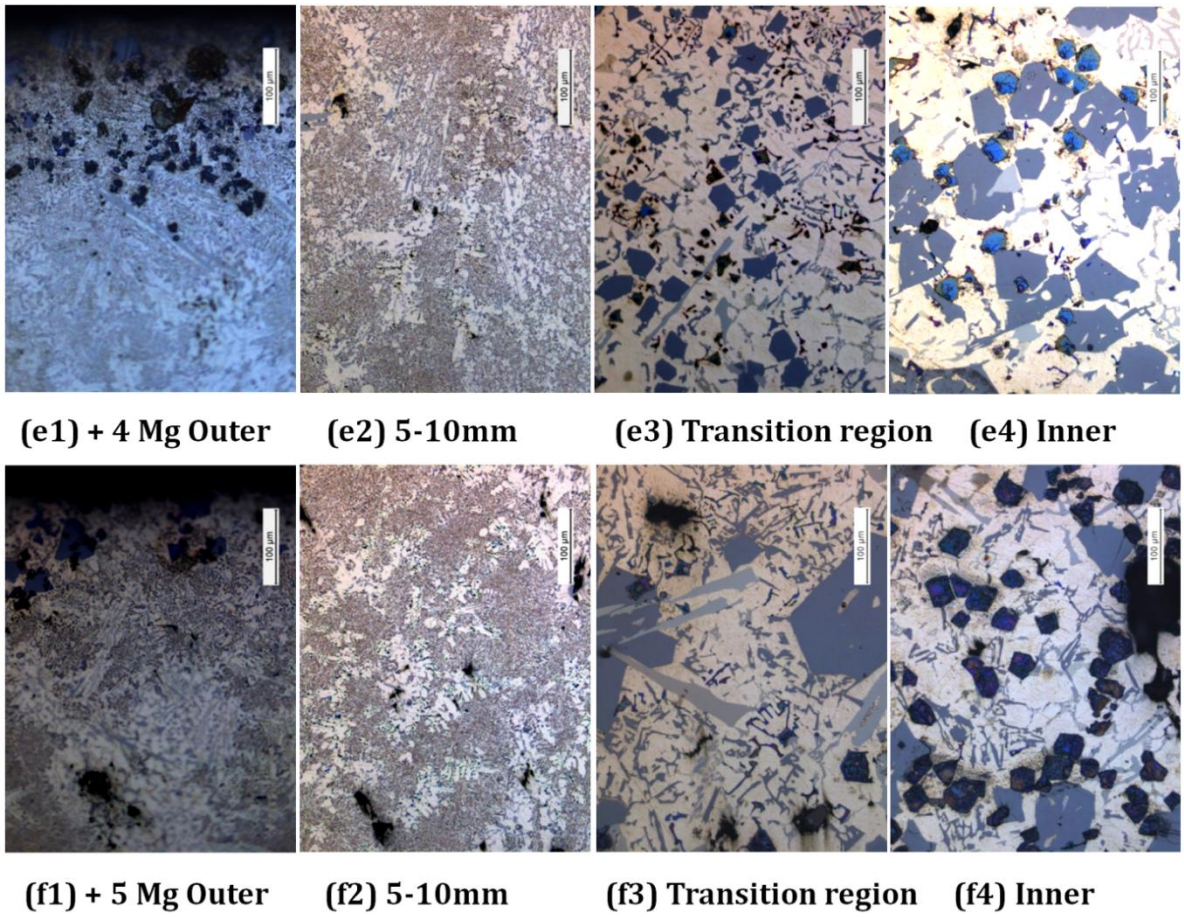

Figure 5.20B : Microstructures of centrifugal castings of alloy specimens from outer to inner periphery of the functionally graded casting (a) A390,(b)+1% Mg,(c)+2% Mg,(d) +3% Mg,(e) +4 Mg and (f)+5 Mg by Pure-Mg alloy addition

Functionally graded aluminium alloys have been successfully fabricated using centrifugal casting technique. Figure 5.20 gives the optical microstructures of as cast Al FGM from outer to inner periphery of the ring. The reinforcements formed are in-situ primary silicon and Mg_2Si phases and they, due to lower density than the matrix, will diffuse towards the inner periphery during the centrifugal casting. In all castings four regions are observed. The four different regions formed in the Al-Si-Mg_2Si FGM are the chill zone, matrix rich region, transition and particle rich region. The major differences in the microstructures from similar structures of master alloy additions are less eutectic are formed in the transition regions. The refinement of primary silicon is not observed in any region of the microstructures of pure mg added ones and the retained primary silicon phases are of larger sizes. The effective addition of magnesium is equal in both cases; there is no much variation in volume of Mg_2Si in the inner regions of higher percentage additions.

5.5.2 *Composition Evaluation*

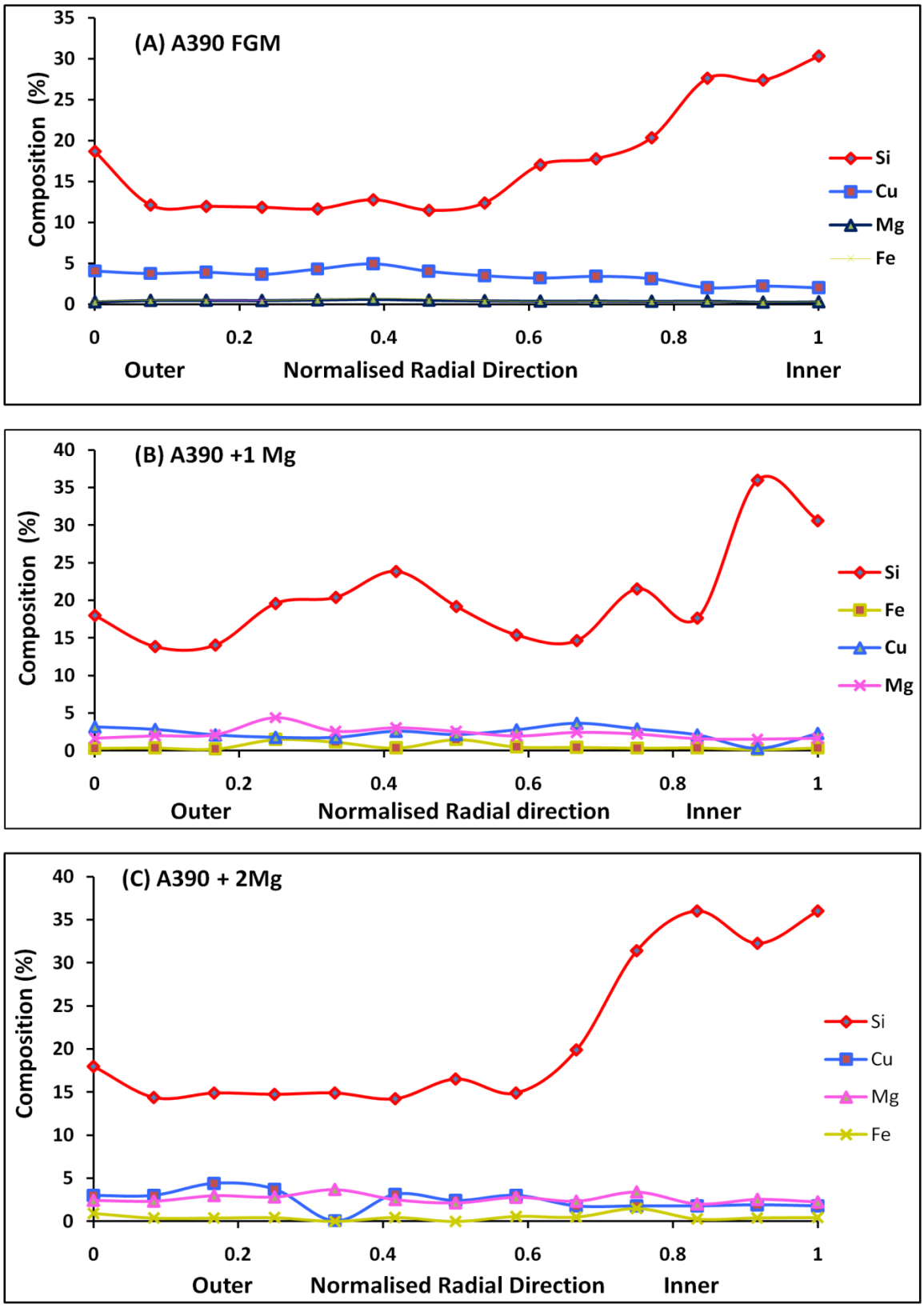

Figure 5.21A: Chemical composition of centrifugally cast A390 alloys with 0, 1, 2, 3, 4 and 5%Mg processed by pure Mg addition

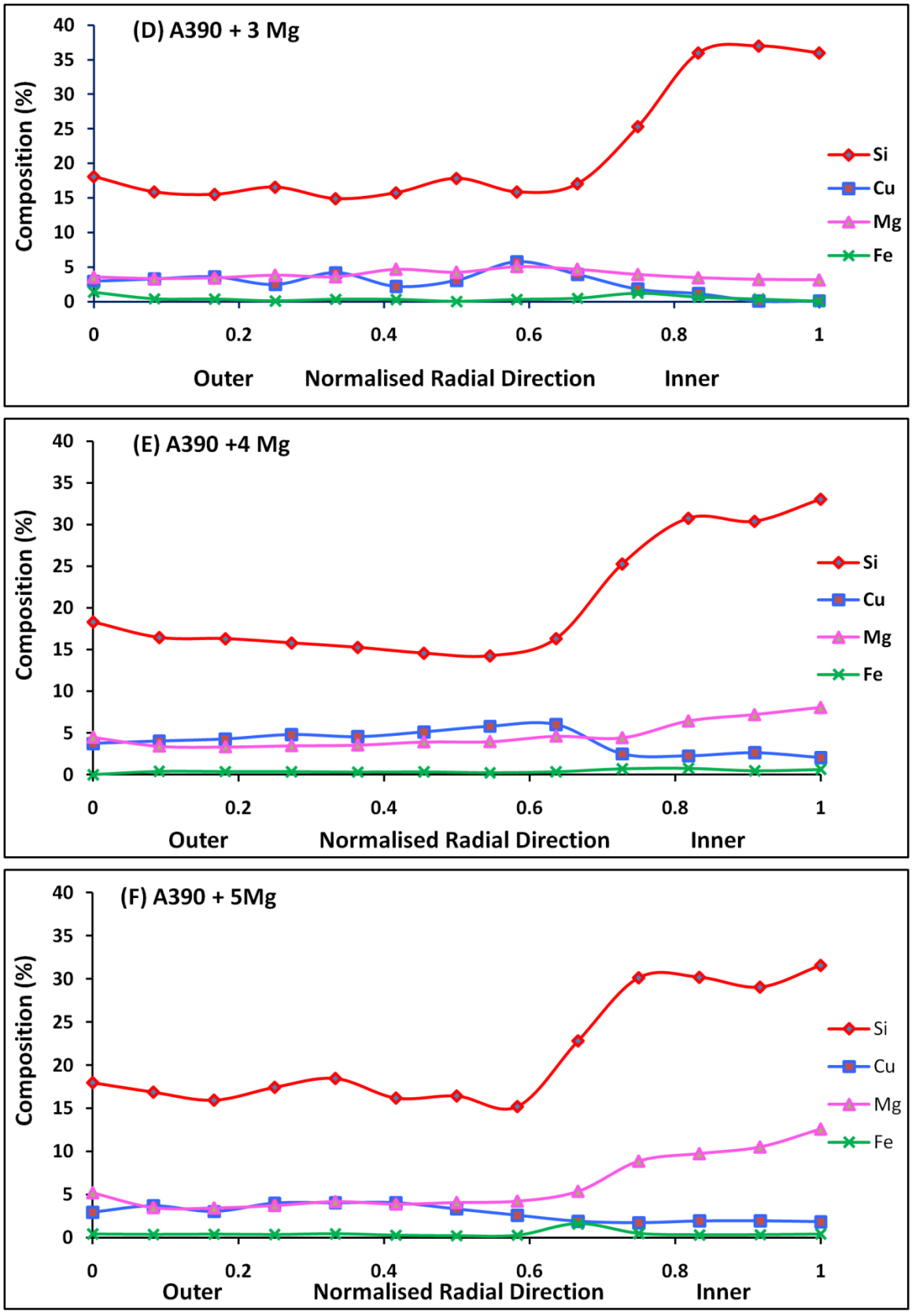

Figure 5.21B: Chemical composition of centrifugally cast A390 alloys with 0, 1, 2, 3, 4 and 5%Mg processed by pure Mg addition

Figure 5.21 shows the chemical composition of centrifugally cast A390 alloys with 0, 1, 2, 3, 4 and 5% Mg processed by pure Mg addition. The FGM rings are analysed from outer to inner diameters in radial direction by using optical emission spectrometer. As observed in microstructures, the chemical composition analysis also shows gradation. There is a remarkable variation in chemical composition at different locations depending on the nature of segregation of phases and precipitates. In 2, 3, 4 and 5% Mg additions the trends are very similar. Up to the starting of particle rich region the chemical compositions on major alloying elements do not have any variations remain almost same in the radial positions. Towards the inner region the volume percentage of both Mg and Silicon increase in a steady rate and reaches a maximum and there after remains almost same or have a light increase there after towards the inner. These observations are well confined with the observed microstructures. For 1% Mg addition, in addition to the latter part of early said behaviours of other alloys, there is some presence of primary silicon and Mg_2Si, which is indicated by the raising graphs of Si and Mg at certain transition regions. The variations of minor alloying elements along with Fe are negligible in radial direction. A marginal decrease in copper percentage is observed in the particle rich region towards the inner.

5.5.3 *Hardness Evaluation*

Table 5.4: Hardness of A390 Al alloy and A390-1 Mg to 5Mg alloys (by Pure Mg addition) gravity casting in as cast and T6 heat treated conditions (in BHN)

Material Specification **(By Pure Mg addition)**	Hardness of Gravity Castings in Brinell Hardness (**BHN)**	
	As Cast conditions	Heat Treated T6 conditions
A390 Base alloy	135	145
A390+ 1Mg	113	142
A390+ 2 Mg	113	141
A390+ 3Mg	125	138
A390+ 4 Mg	110	140
A390+ 5 Mg	126	142

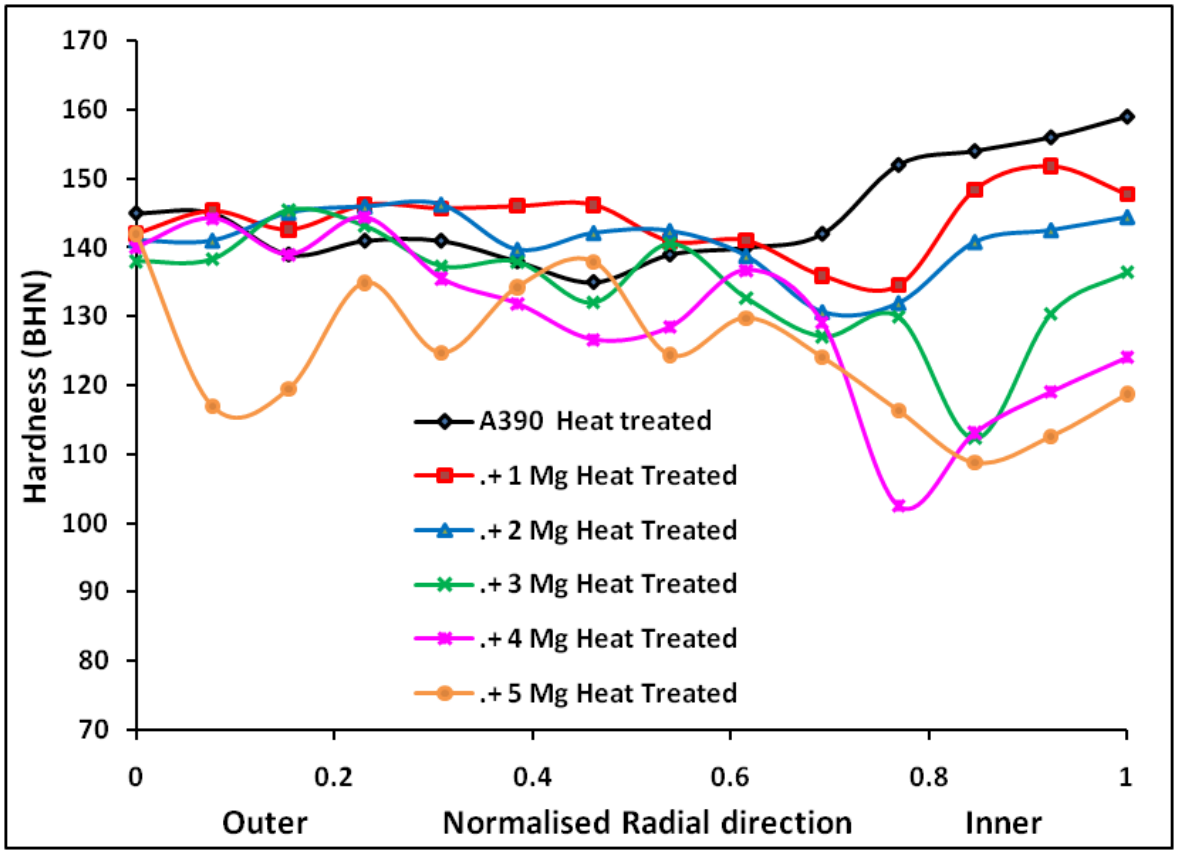

Figure 5.22: Hardness variation of heat treated Al FGM along normalised radial direction from outer diameter towards Inner in a radial direction

Table 5.4 shows the hardness of homogeneous gravity castings prepared by the alloys and A390 base alloy in the as cast as well as heat treated conditions. Only A390 alloy has got the maximum hardness after the heat treatment, i.e. a value of 145 BHN. All other alloys have slightly lower or comparable hardness value of that of heat treated A390 base alloy. Figure 5.22 shows the hardness variation of all heat treated Al-FGM along the normalised radial direction from outer diameter towards inner in a radial direction. For all the castings the hardness value at the chilled zone is comparable with that of the alloy and confines to a small range of 138-145. Similar to the Al-Mg master alloy addition there is an increase in volume percentage of silicon near the inner periphery and this is due to segregation of primary silicon particles and Mg_2Si phases. The 1% Mg alloy shows a maximum hardness of 150 BHN near the inner regions with a small depression in the transition region nearer to the starting of inner particle rich zone. The composition of the 2%Mg addition don't show a remarkable gradation as expected and the hardness shows a waviness variations in the range of 130-146BHN. The 3% Pure Mg shows a lower hardness towards the inner region. For A390 alloy

and 4% pure Mg modified alloy even though the inner region have more phase concentration the hardness value decreases from 136 BHN to 124 BHN, as we move radially towards the inner. In the case of 5%Mg modified alloy the hardness started dipping from the chilled zone itself and decreases in a zigzag manner to 118 BHN at the inner even though it has maximum primary silicon and Mg_2Si predicted by chemical composition analysis and microstructures. These results leads to a conclusion that, in A390 alloys, the Al-Mg master alloy addition is more effective to produce an FGM than the pure Mg addition and at the same time the volume of magnesium addition will be more effective up to 2 percentages.

5.6 STUDIES ON PROCESSING OF Al FGM I.C. ENGINE PISTON

5.6.1 *Prologue*

The internal combustion engines (IC Engines) have been a major power source throughout the history of automobiles, such as cars, tractors, agricultural machinery, construction machinery, and so on[187 -192]. Piston is one of the key components in the internal combustion engine, and it has a great role on the working reliability, drivability and the emission performance of the engine. The structure and working condition of the piston is complex. The force from combustion gas, inertial force from high-speed reciprocating motion, sidewall force and the frictional force acts to the piston periodically resulting in mechanical stress and deformations. Due to the high temperature of the burning gas, the temperature grads in whole piston are high, which make the piston to produce the thermal stress and the thermal deformation [193]. The main function of the IC Engine piston is to receive impulse from the expanding gas and to transmit the energy to the crankshaft through the connecting rod. The piston must also disperse a large amount of heat from the combustion chamber to cylinder walls.

The pistons for IC engines are usually of trunk type as shown in Figure 5. 23. Such pistons are open at one end and have the following parts: *Head or Crown:* The piston head or crown may be flat, convex or concave depending upon the design of combustion chamber. It withstands the pressure of gas in the cylinder. *Piston Rings:* The piston rings are used to seal the cylinder in order to prevent leakage of the gas past the piston. *Piston Skirt*: The skirt acts as a bearing for the side thrust of the connecting rod on the walls of cylinder. And the *Piston Pin:* It is also called *godgeon pin* or *wrist pin*. It is used to connect the piston to the connecting rod.

Aluminium–Silicon alloys have the potential for excellent cast-ability, good weld-ability, good thermal conductivity, high strength at elevated temperature and excellent corrosion resistance. They are, therefore, well suited for aerospace structural applications, automobile industry and military applications. The coefficient of thermal expansion positively decreases with increase of silicon content in the alloy composition. The solubility limit of silicon in aluminium is limited to 12 % (12.6 % exactly, i.e. eutectic composition), the excess silicon, present in hypereutectic alloys, will be retained as primary silicon granular forms. By proper heat treatments the mechanical properties can be improved. In automobile industry, at present two alloys with silicon content 12% (eutectic) and 22% (hyper-eutectic) are being used. And have the co-efficient of expansion of 21μm/mK and 17.5 μm/mK respectively in comparison with 24.5 μm/mK, that of aluminium [194-196]. A390.0 alloy is a hypereutectic aluminium-silicon alloy with 18% Si. The low coefficient of thermal expansion, high hardness and good wear resistance of this alloy make them suitable for internal combustion engine pistons and blocks and cylinder bodies for compressors, pumps and brakes.

FGM's ability to obtain two conflicting properties in a single component enables its functionally specific applications economically [197-200]. The functionally graded pistons are fabricated by vertical centrifugal casting method by using A390 and A390-0.5% Mg alloys along with their gravity castings. The microstructure, hardness and wear properties of FGMs at different regions are compared to that of specimens from the similar locations of the homogenous gravity cast pistons. A390 is a hypereutectic silicon cast alloy with 16-18 % Si. During the centrifugal casting the less dense Si (than alloy melt) will diffuse towards the inner diameter giving particle/phase strength to that regions. A permanent metal die suitable for FGM casting where the particle rich region is coming in the inner diameters is designed and fabricated. Figure 5.23 shows the designed mould having the facility for casting two piston at a time connected together by the runner and raiser of the casting. Figure 5.24 shows the pair of pistons (surface cleaned ones) produced in a single casting process. Figure 5.25 shows the typical schematic diagram of different regions formed in normal FGM ring casting and their respective positions in the newly designed piston. Figure 5.26 shows the cross sectional view of the piston with cut surface polished to 1000 grit size sand paper and slightly etched, for getting light contrast in the particle rich head region. On simple eye observation on the etched surface will give clear information that there is a distribution

of certain phases throughout the surface of the piston head region and penetrating into the piston interiors from the top side towards the skirt measuring about 15 mm thickness at the central line.

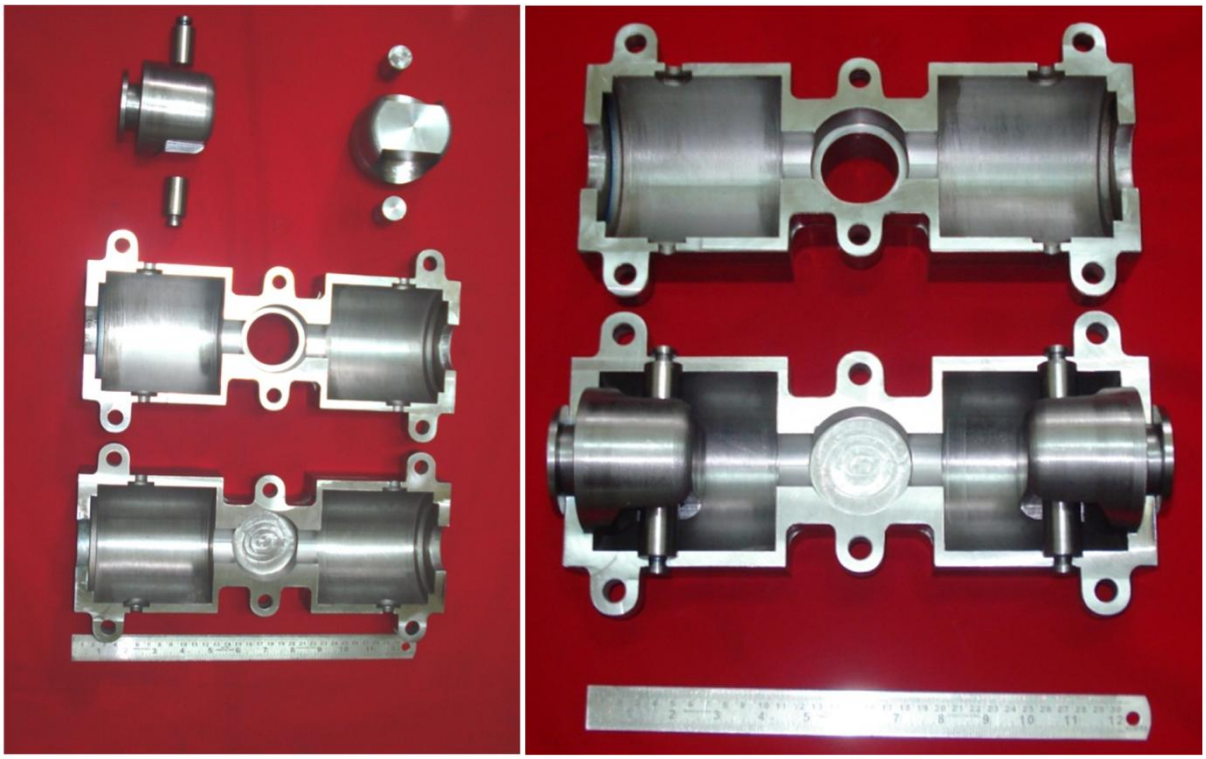

Figure 5.23: Mould having the facility to cast two pistons at a time

Figure 5.24: The pair of pistons (surface cleaned) produced in a single casting process

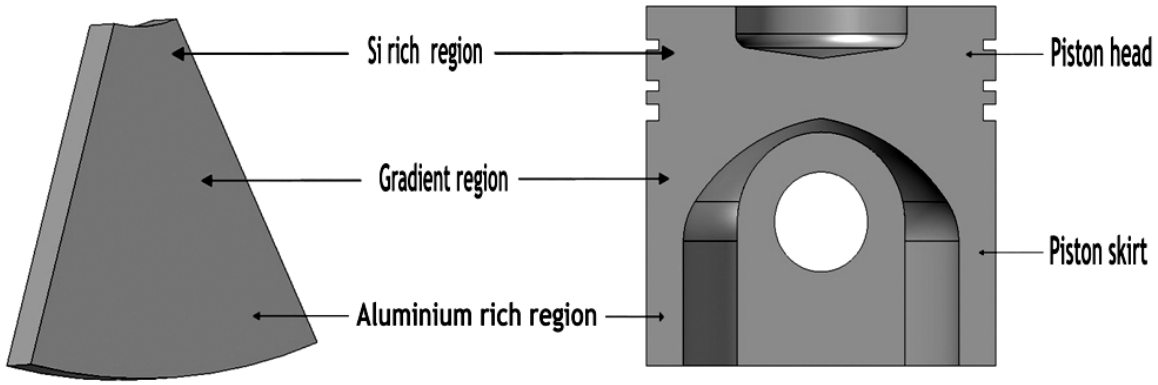

Figure 5.25: Schematic diagram of different regions formed in normal A390 FGM ring casting and their respective positions in the newly designed piston

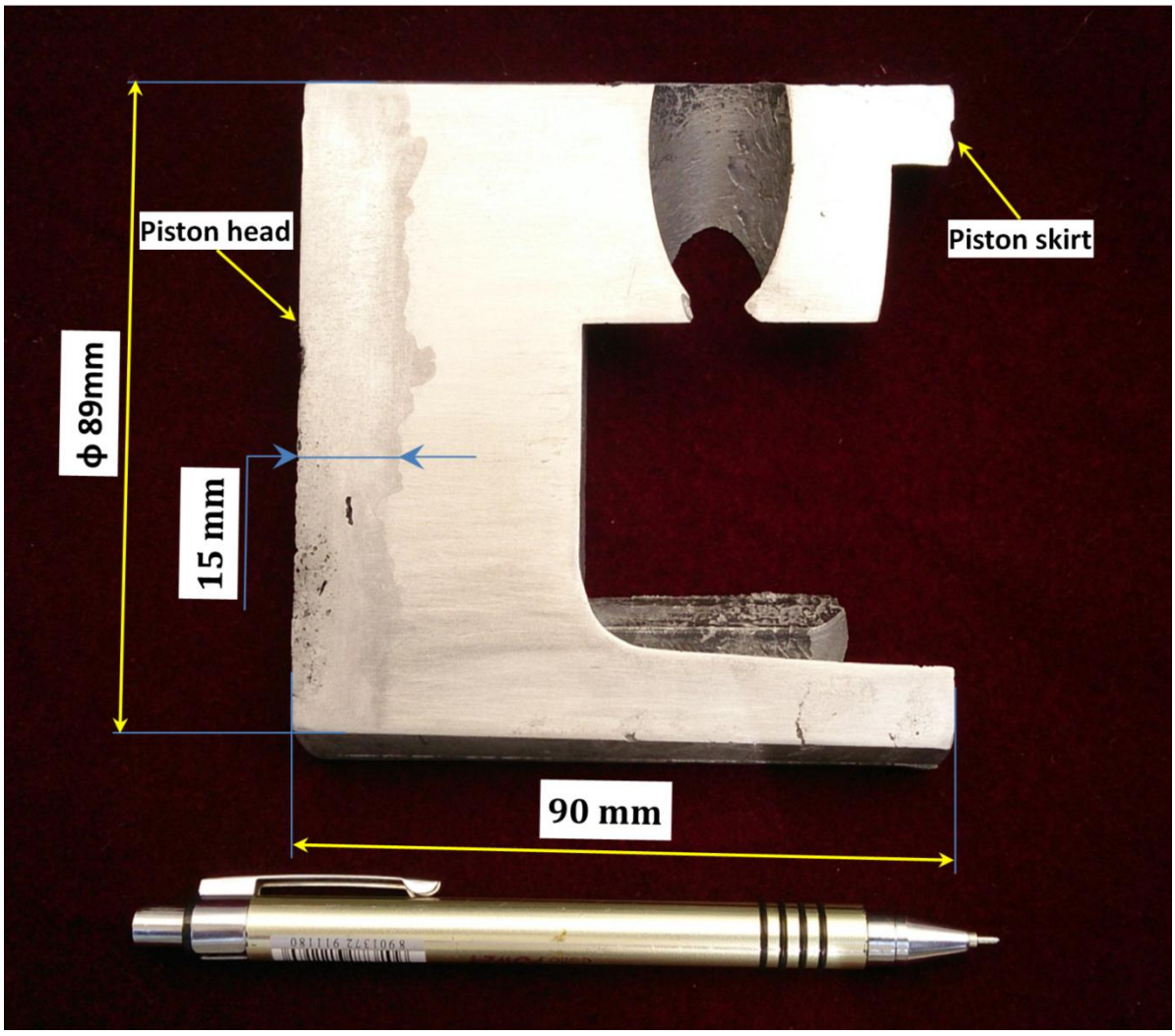

Figure 5.26: The cross sectional view of the piston with cut surface polished and etched showing the particle rich head region of approx. 15mm width from piston head towards the skirt of the piston.

5.6.2 *Microstructural Evaluation*

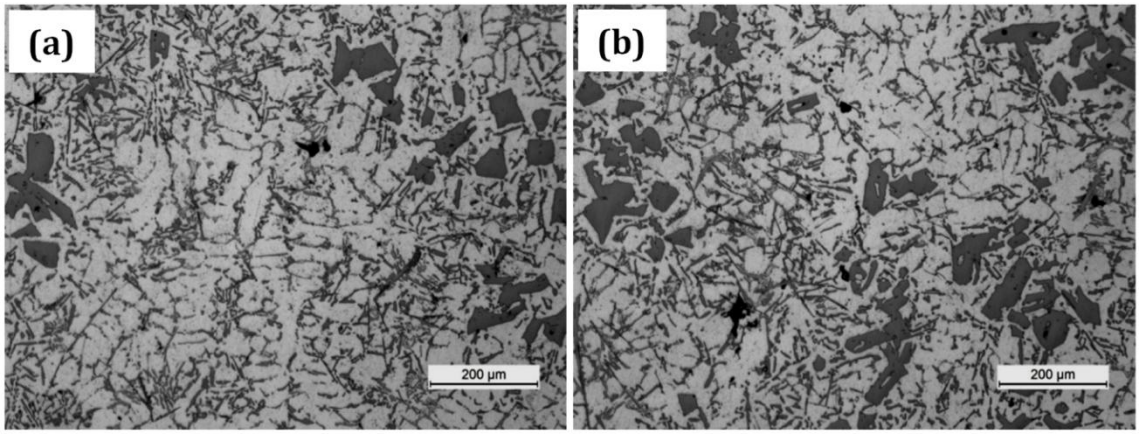

Figure 5.27: Microstructures of the gravity cast A390 piston (a) the head and (b) the skirt portions

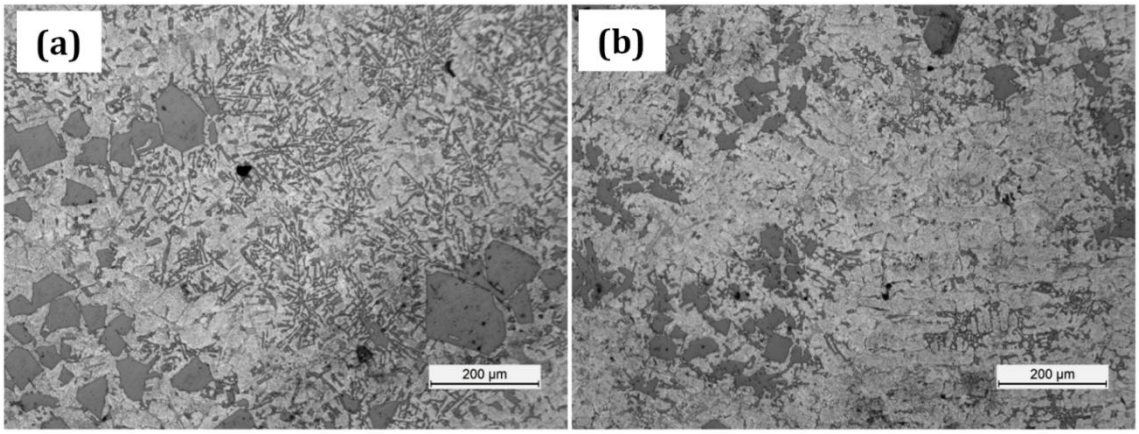

Figure 5.28: Microstructures of the gravity cast A390-0.5 Mg piston (a) the head and (b) the skirt portions

The optical microscopic studies carried on centrifugal and gravity cast A390 and A390-0.5% Mg pistons shows remarkable variation of microstructural characteristics. Figure 5.27 (a) and (b) show the microstructures of the head and skirt portions of the gravity cast A390 piston, with evenly distributed primary silicon particles and Al-Si eutectics in α-Al dendrites. Mg_2Si phases, formed by the Mg addition, will improve the mechanical properties during the age/precipitation hardening [201-203]. Figure5.28 shows microstructure of A390-0.5% Mg gravity cast piston in (a) head and (b) skirt portion showing uniform primary silicon. However compared to the A390 piston, the 0.5% Mg addition had refined the eutectic silicon phases in the casting. There are no α-Al dendrites observed either in head or skirt and a very few dark spots indicating the formation of Mg_2Si are visible. At high resolutions of the optical microscope these dark dots are deep blue in colours, simple colour identification of phases also indicate that

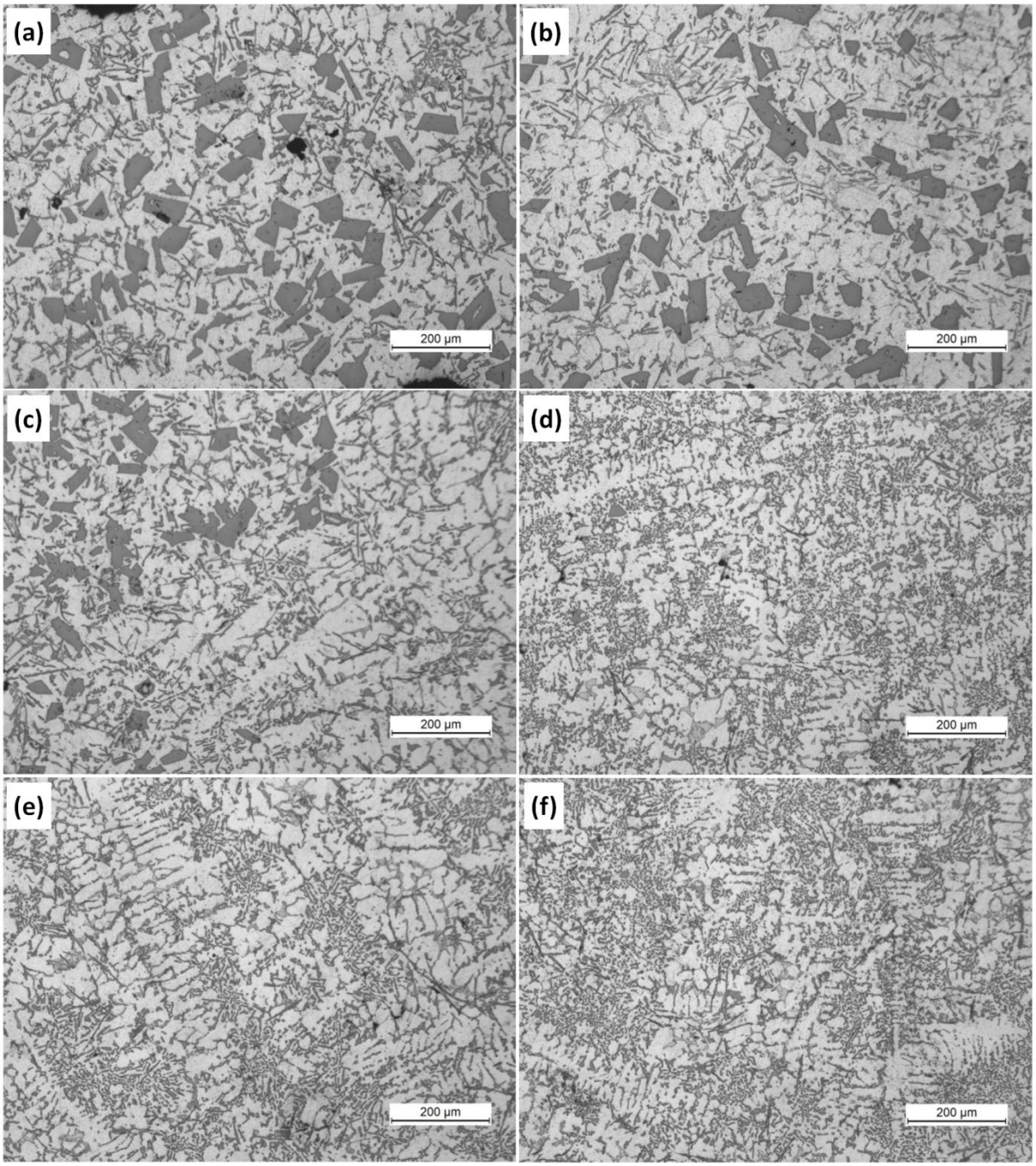

Figure 5.29: Microstructures of A390 centrifugally cast FGM piston. Head towards skirt at (a) 5mm (b) 10mm (c) 15mm (d) 20mm (e) 25 mm and (f) at 30 mm

they are nothing but Mg_2Si particles (refer Figure 5.20 e4). Figure 5.29 shows the microstructures at distances 5, 10, 15 and 20mm of A390 centrifugally cast piston along the axis of the piston from the piston head towards the skirt. The formation of a graded silicon structure is observed from head towards skirt of the piston with head region as particle rich zone. The primary silicon particle rich region of about 15 mm is observed towards the head portion of the piston (Figure 5.26). Figure 5.30 shows the

microstructures of A390-0.5% Mg centrifugal cast FGM piston from head to skirt region, where the gradation in the primary silicon is observed. By controlling the melt pouring temperature, preheat temperature and rotation speed of the centrifugal casting mould, the thickness of primary silicon particle rich region can be controlled. Towards skirt region less secondary dendritic arms and more eutectic Al-Si phases are observed than in the microstructures of A390 FGM piston from similar locations. It is also seen that the observed grains are more refined than the earlier A390 FGM piston microstructures.

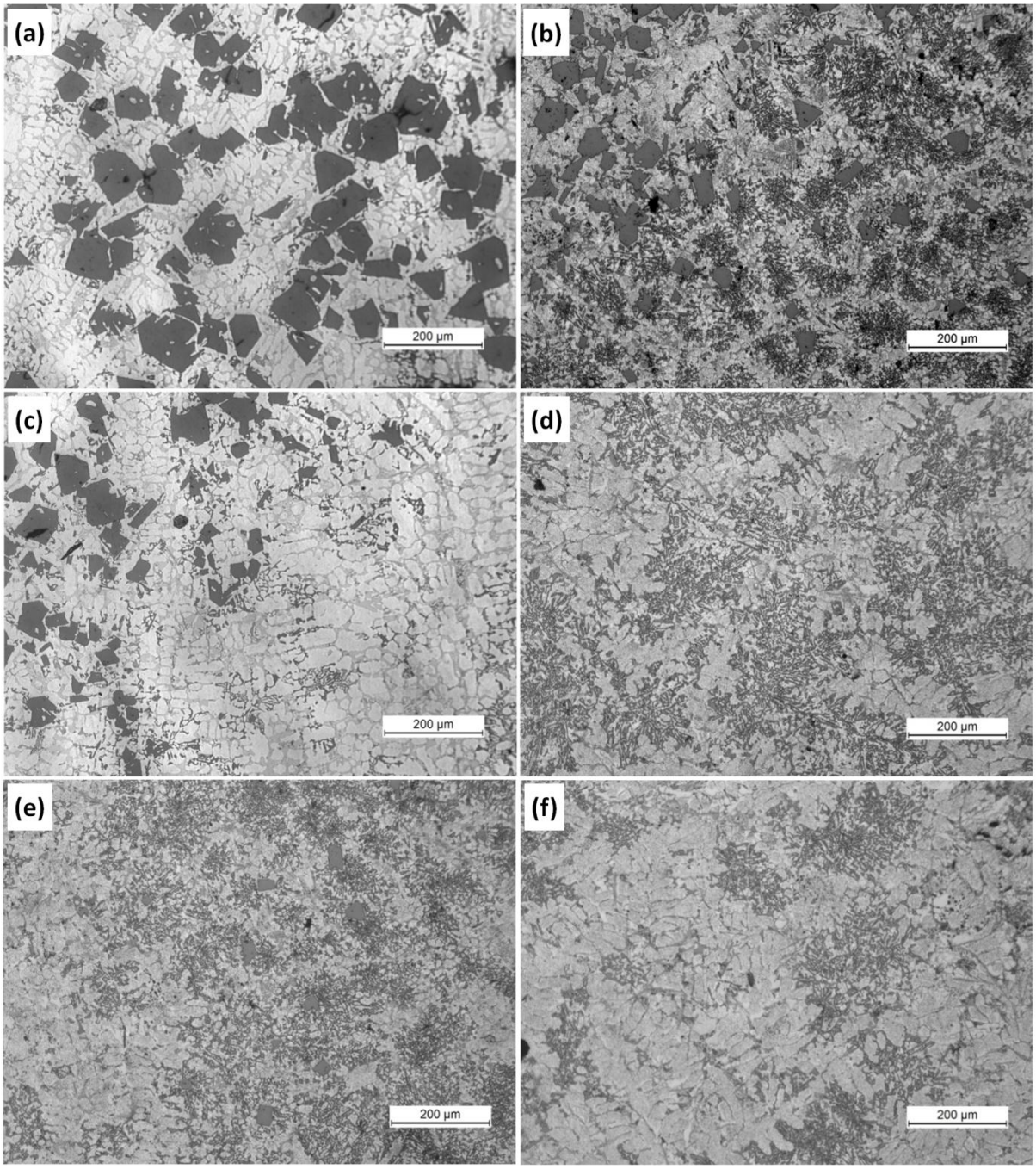

Figure 5.30: Microstructures of A390-0.5 Mg FGM piston. Head towards skirt at (a) 5mm (b)10mm (c)15mm (d) 20mm (e) 25 mm and (f) at 30 mm.

5.6.3 *Compositional Analysis*

Table 5.5: Chemical composition of A390 alloy ingot, gravity casted pistons and at specified locations of A390 and A390-0.5Mg FGM pistons from piston head towards skirt at 5mm (A, E),at 10mm(B, F),at 15mm(C, G) and at 20 mm (D, H)

Details of Alloy	Major Alloying Elements in %				Minor Alloying Elements in %					Al in %
	Si	Cu	Mg	Fe	Mn	Zn	Cr	Ni	Ti	
A390 standards	16 - 18	4 - 5	0.4–0.7	1.1 (Max)	0.3 (Max)	0.2 (Max)	0.1 (Max)	0.1 (Max)	0.2 (Max)	74-78
A390 ingot	18.735	4.09	0.32	0.43	0.06	0.06	0.01	0.01	0.01	76.21
A 390 gravity	19.141	3.28	0.621	0.42	0.057	0.047	0.010	0.014	0.001	76.412
A 390 FGM Piston A (at 5 mm)	**36.223**	3.48	0.54	0.44	0.077	0.056	0.021	0.032	0.002	59.352
B (at 10mm)	**28.465**	3.67	0.65	0.54	0.065	0.076	0.034	0.055	0.003	66.447
C (at 15 mm)	**23.663**	4.84	0.73	0.75	0.076	0.057	0.074	0.052	0.003	69.849
D (at 20mm)	**20.520**	4.76	0.66	0.52	0.025	0.051	0.085	0.047	0.008	73.324
A 390-0.5 Mg gravity	18.112	2.32	1.040	0.365	0.045	0.067	0.010	0.015	0.010	76.443
A 390-0.5 Mg FGM Piston E (at 5 mm)	**35.653**	2.52	1.037	0.328	0.052	0.042	0.053	0.274	0.012	59.42
F (at 10mm)	**29.289**	2.252	1.006	0.502	0.059	0.024	0.027	0.069	0.062	66.38
G (at 15 mm)	**20.891**	2.52	1.548	0.560	0.083	0.057	0.041	0.0353	0.047	74.021
H (at 20mm)	**15.881**	2.36	1.700	0.846	0.082	0.051	0.042	0.0138	0.015	79.770

Table 5.5 shows the chemical composition of gravity castings and FGM pistons processed by both A390 and A390-0.5% Mg alloys. The gravity cast pistons shows 18–20% of silicon throughout the casting. Optical emission spectrum (OES) results indicate that from the head towards the skirt portion, the chemical composition varies axially of the both centrifugally cast pistons of A390-0.5% Mg and A390 alloy. In the centrifugally cast pistons, in both cases, the concentration of silicon is about 36% at 5 mm from outer periphery. The concentration of silicon gradually reduces towards the skirt region. For

A390 FGM piston, at 10 mm from the piston head 28.4% of Si is observed and further it reduces to 23.6% at 15 mm and 20.5% at 20 mm. For the A390-0.5 Mg piston these values are 29.2, 20.8 and 15.8% respectively. These are in conformation with the variations of primary silicon as observed in optical microstructures of FGM. The enhancement in the concentration of Mg in gravity and centrifugally cast A390-0.5% Mg FGM piston is as expected, as in the alloy preparation; there is an addition of 0.5% Mg to the A390 alloy.

5.6.4 *Hardness Behaviour*

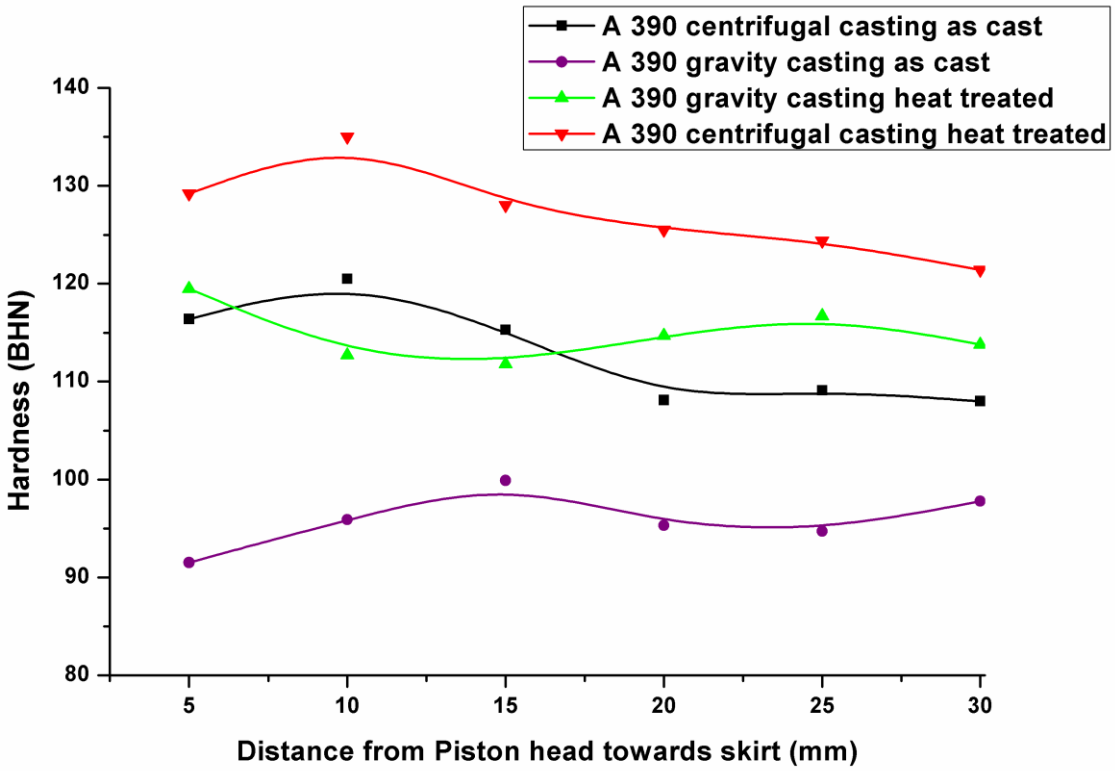

Figure 5.31: Hardness variations from the piston head to the skirt of A390 gravity casted and centrifugally cast FGM pistons in both as cast and in heat treated conditions

The hardness of both as cast and heat treated (T6 conditions) samples taken from the different axial locations of pistons from the piston head towards the skirt portion of A390 and A390-0.5 Mg alloy are shown in Figure 5.31. The minimum hardness value found is 94 BHN, which is similar to conventionally gravity as-cast piston having the hardness in the range 94–99 BHN. The heat treated hardness values of the gravity cast A390 piston is in the range 110–116 throughout the piston. In the case

of centrifugally cast A390 piston hardness gradually shows an decrease from the piston head towards the skirt portion with peak value of hardness obtained in the near head portion is 135 BHN, in the heat treated condition. The gradual gradation of hardness value from 135 to 120 BHN from head to skirt is due to the segregation of primary Si particles in the head region. It is evident that the hardness values of centrifugal cast pistons are higher than gravity cast piston. Figure 5.32 shows the hardness values of the A 390-0.5% Mg FGM pistons in as cast and heat treated condition. It clearly reveals that there is an increase in hardness values after heat treatment. The addition of 0.5% Mg had resulted in significant enhancement in the hardness values to 188 BHN in the piston head when compared to 135 BHN for the centrifugal cast 390 alloy. The significant improvement in the hardness by the addition of Mg is due to the formation more magnesium bearing phases like Mg_2Si in the matrix. The increase in the hardness towards the piston head is due to the presence of higher primary silicon particles. This higher hardness towards the head region contributes for an excellent wear resistance and high temperature capability of the FGM piston.

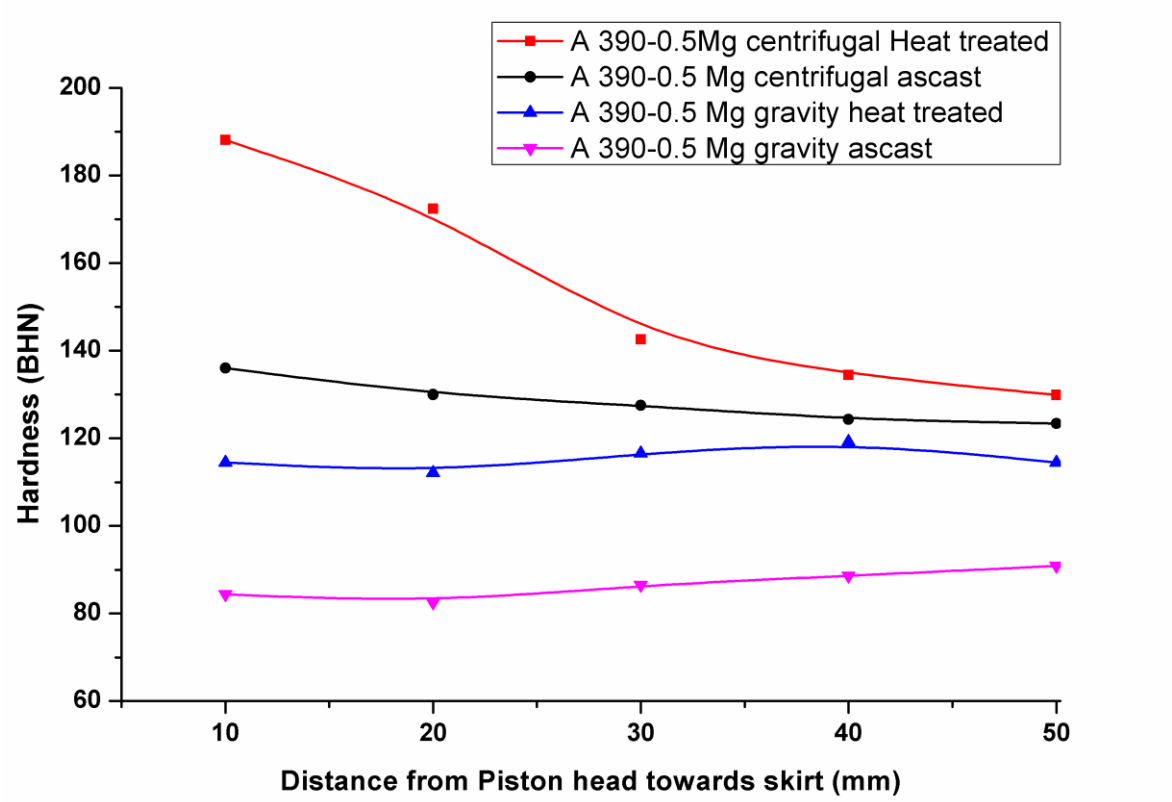

Figure 5.32: Hardness variations from the piston head to the skirt of A390-0.5 Mg gravity cast and centrifugally cast FGM pistons in both as cast and in heat treated conditions

5.6.5 *Tribological Characteristics*

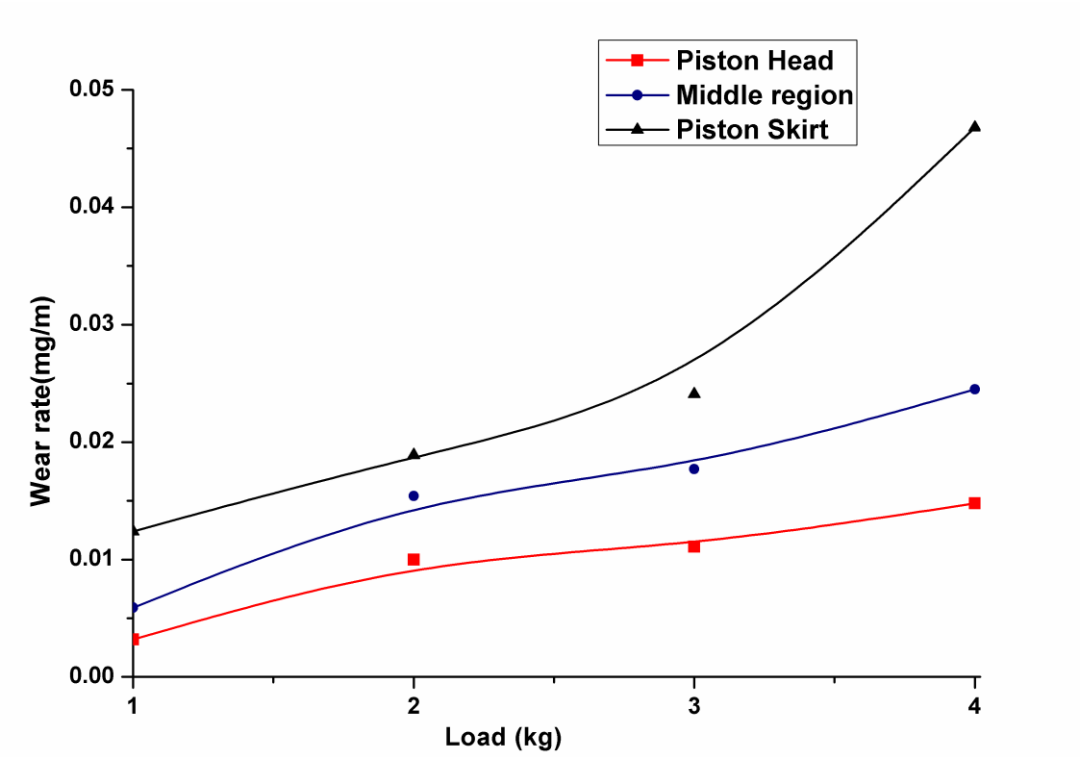

Figure 5.33: Wear rates of A390 centrifugal cast FGM Piston at Piston head, at Middle region of interface and at Piston Skirt.

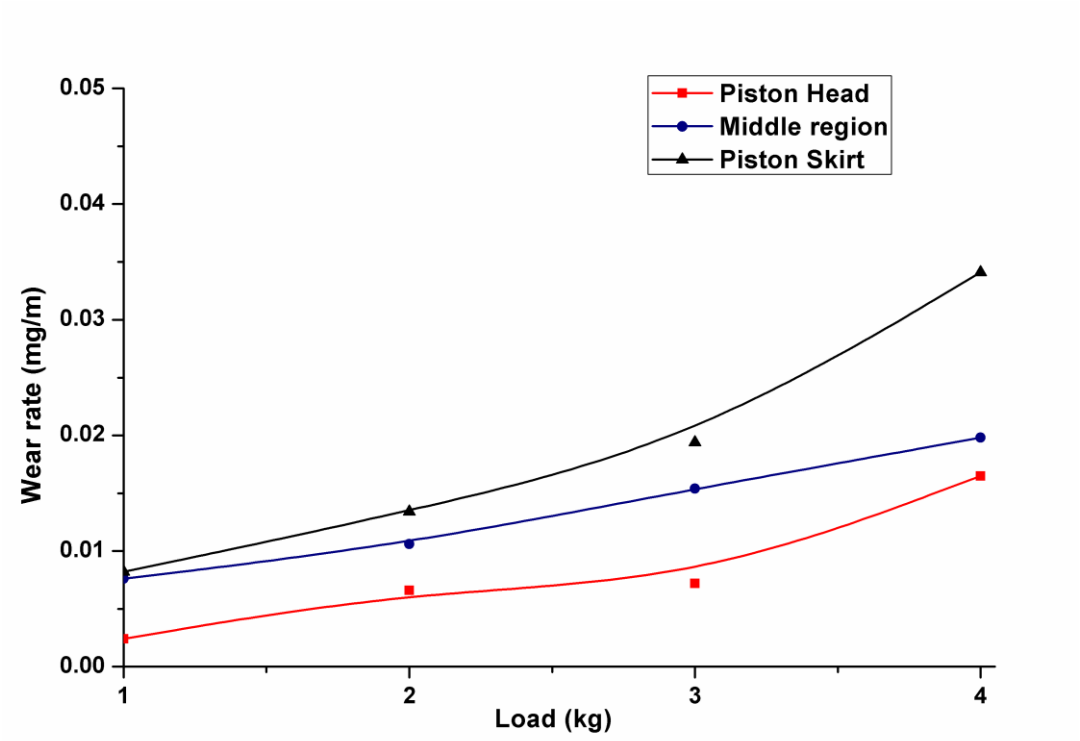

Figure 5.34: Wear rates of A390-0.5 Mg centrifugal cast FGM Piston at Piston head, at Middle region of Interface and at Piston Skirt.

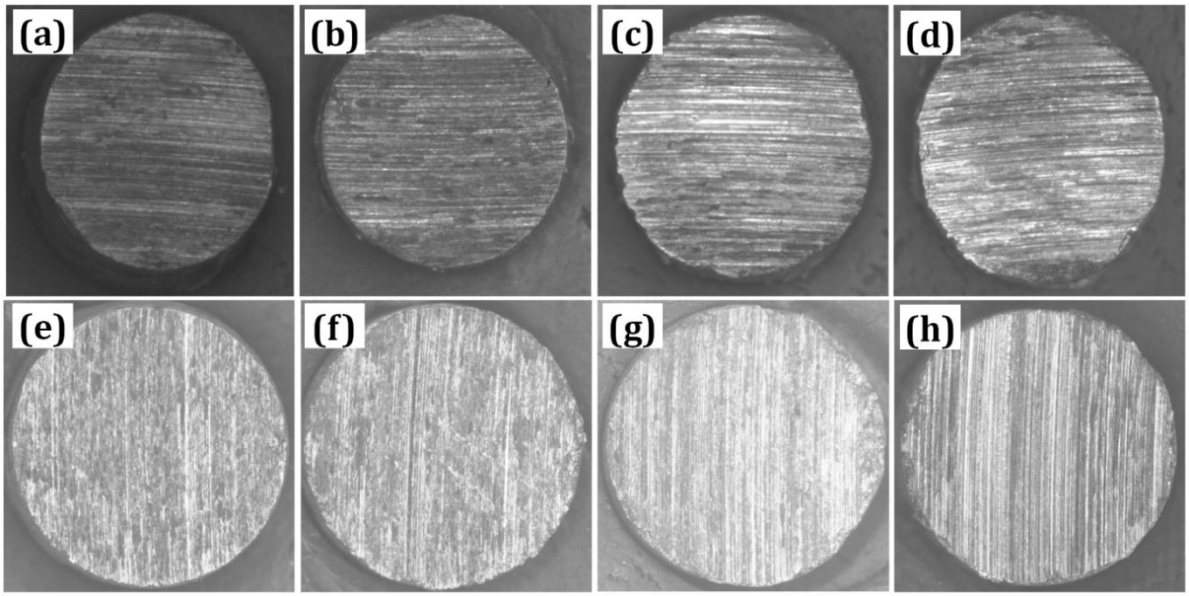

Figure 5.35: Stereo micrographs of worn out pins (a) , (e) at 1Kg, (b),(f) at 4Kg load of head portion, (c),(g) at 1Kg, (d),(h) at 4Kg load of skirt portion of A390 and A 390-0.5 Mg centrifugal casting pistons respectively

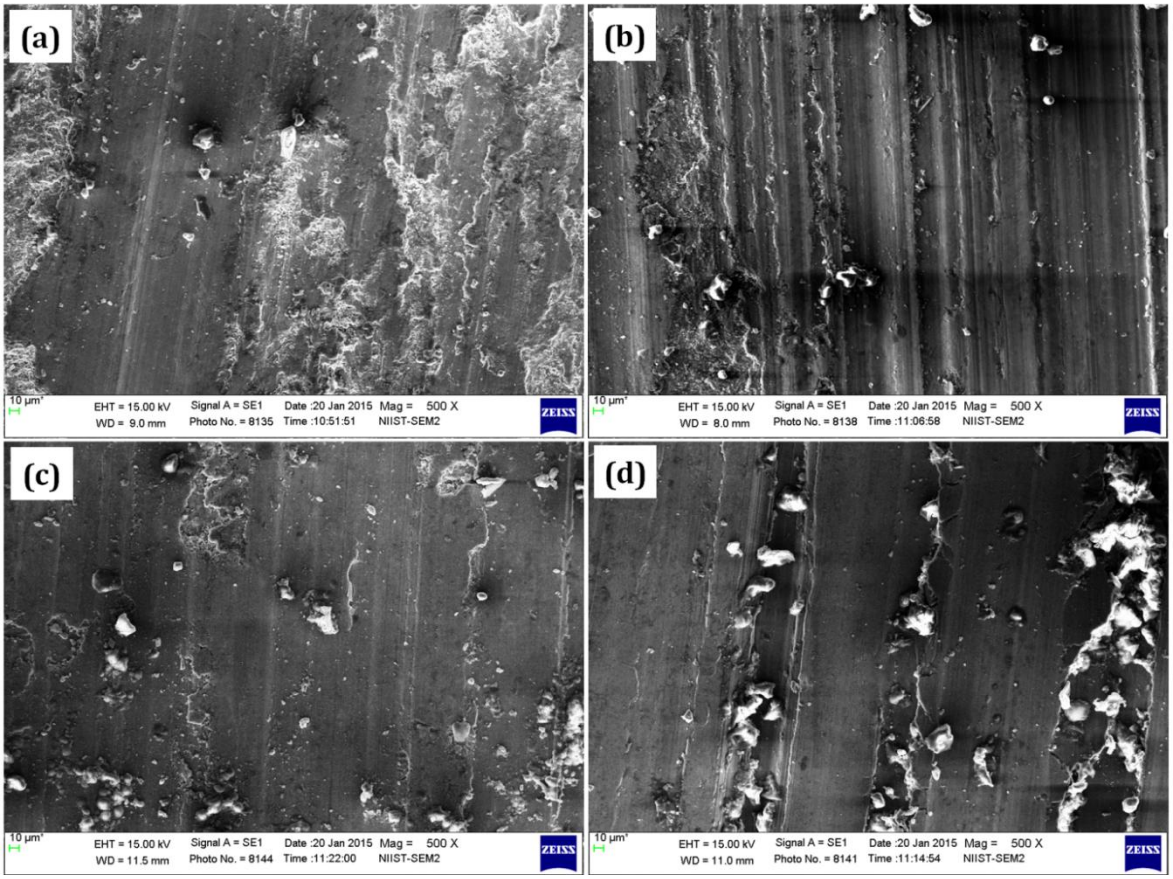

Figure 5.36: SEM photographs of worn out surface of centrifugal cast A 390- 0.5 Mg piston pins from piston head (a) at 1 kg (b) at 4 kg and from skirt region (c) at 1 kg and (d) at 4 kg loading conditions

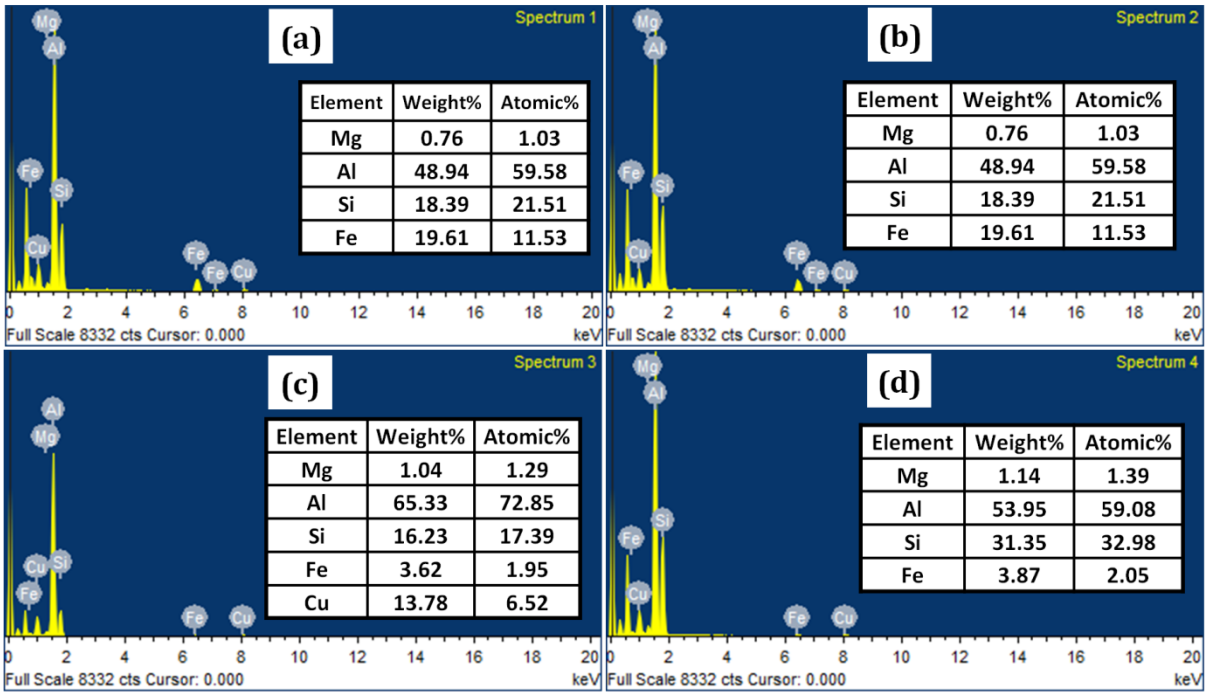

Figure 5.37: EDS of A 390-0.5 Mg FGM Piston worn out pin surfaces at piston head (a) at 1 kg, (b) at 4Kg and at skirt portion (c) at 1 kg and (d) at 4 kg load conditions

Figures 5.33 and 5.34 show the wear characteristics of centrifugally cast A390 and A390-0.5% Mg FGM pistons at the piston head, in the interface and at the skirt region. Dry wear test on a pin on disc tribometer is conducted with pins prepared from three different regions such as head, interface and skirt region of the piston. It is observed that A390-0.5% Mg Al FGM pistons exhibits lower wear rates when compared with pure A390 Al FGM pistons. This is due to the presence of more Mg bearing precipitates in the alloy and the hard in-situ primary silicon particles. The decrease in wear rate in centrifugal cast FGM piston head is due to the enrichment of primary Si particles and a gradual increase in wear rate is observed from piston head to skirt portion. Figure 5.35 (a-d) shows the wear tracks observed on the surface of the A390 alloy FGM piston in head and skirt portions at lower and higher loads. The detailed examination of wear tracks reveals the features associated with abrasive wear which causes scratches on the surface. The abrasive component of the wear mechanism is pointed out by the ploughed grooves inside the wear tracks, which are visible in Figure 5.35, are due to the harder (EN 31steel disc) surface scratching over the softer (pin) surface1[204-210]. Typical scanning electron micrographs of worn surface of centrifugally cast A390-0.5%Mg added FGM piston samples are illustrated in Figure

5.36. Fine grooves are observed in the head portion whereas the skirt portion shows wider grooves due to higher material removal by ploughing action during wear testing. Figure 5.37 shows the Energy dispersion Spectrum (EDS) analysis of the wear piston surfaces of the A 390-0.5% Mg FGM piston wear pin surface. The surface shows higher Fe peak in the head portion due to the more scratching of the disc surface by the hard primary silicon particle in the piston head. In general, the centrifugally cast functionally graded piston provides higher hardness and wear resistance towards the head region. The addition of 0.5% Mg had further enhanced the mechanical and tribological properties.

5.7 CONCLUSIONS

- A390-SiC FGMMC with 10 and 15 wt % SiCp particles, 23μm size, was successfully processed by the centrifugal casting.
- Microstructure evaluation and image analysis shows the formation of functional graded SiCp particle distribution from outer to inner periphery of the casting.
- The hardness of different regions largely depended on the concentrations of SiC particles and primary silicon. The SiC rich outer zone and the Si rich inner region show higher hardness and lesser wear rate in comparison with the transition region.
- The variation of wear rate with respect to applied load is linear. The addition of SiC particle and heat treatment provide comparable improvements in the wear resistance.
- Also by the distribution of primary silicon phase in the A390 alloy by centrifugal force the wear and structural property can be effectively tailored.
- The study clearly depicts that the gradient nature of the structure and properties of the FGM rings can be controlled by particle addition as well as by phase distributions.
- Aluminium FGM with in-situ primary Si and Mg_2Si reinforcements have been fabricated successfully by the centrifugal casting process using A390 commercial Al alloy and Mg addition.
- Both primary silicon and Mg_2Si phases segregate gradually towards the inner periphery of the casting due to lower density of these phases compared to the

matrix. Increase in Mg content increases the concentration of Mg_2Si whereas percentage of primary silicon decreases.

- The size of the Mg_2Si, reinforcement phase is smaller and distributed in the edges of primary silicon particles and also individually in the matrix.
- The *in-situ* Mg_2Si and primary silicon can significantly increase the properties of the inner periphery of the casting in the specific system.
- In-situ functionally graded Al composite pistons were successfully designed and fabricated by vertical centrifugal casting technique.
- Two different zones of primary Si rich and depleted zones were observed.
- Higher concentration of primary Si particles gets gradually distributed towards the head region of the piston providing enhanced properties.
- Magnesium provides substantial strengthening and improvement of precipitation hardening phases of aluminium alloy.
- Centrifugally cast FGM pistons provide high hardness, thermal resistance and wear properties than that of conventionally gravity cast pistons.
- Heat treated samples were found to provide superior properties than that of as-cast samples. A higher hardness of 188 BHN was observed in 0.5% Mg added FGM piston head region.
- The head portion of the 0.5% Mg A390FGM piston shows remarkable reduction in wear rate even at high load of 4 kg compared to skirt region and gravity cast piston.

Chapter 6

Processing and Characterisation of A6061–SiC Functionally Graded Metal Matrix Composites

6.1 INTRODUCTION

Metal matrix composites (MMCs) reinforced with ceramic or metallic particles are widely used in transportation sector, recreational and infrastructure industries due to their better high specific modulus, strength and wear resistances properties over the conventional materials. Aluminium matrix composites (AMCs) possess higher wear resistance and lower friction coefficient with increasing volume fraction of reinforcement particles, compared to aluminium alloys and are preferred over monolithic metals or alloys in a number of specialized applications [211-212]. MMCs can be tailored through appropriate selection of constituents to meet specific requirements and for specific application. Since properties of matrix and reinforcements vastly differ from each other, the properties of MMCs can be varied over a very broad range that spans from those characteristic of metals to those of the ceramics by appropriate adjustment of reinforcement volume fraction, morphology and distribution. FGMs are new class of advanced two component composite characterized by a compositional gradient of one component to another along a certain direction. FGM's ability to obtain two conflicting properties in a single component enables its functionally specific applications economically [213]. Centrifugal casting route is easy and the best economical technique utilized successfully among the numerous available FGMs processing techniques [214-215]. Two steps FGM processing includes the synthesis of MMC by liquid stir casting followed by pouring melt into the rotating moulds fitted in a vertical centrifugal casting machine. Depending on the density of reinforcement particles and matrix phase, subjected to centrifugal force and particle diffusion, different regions are formed during the solidification namely; outer surface chilled zone, particle rich, transition and particle depleted/matrix rich zones. The centrifugal force causes the lighter particles segregate towards the axis of rotation and the denser ones move away from axis of rotation the positions and size of different

zones and its gradation inside the component depends on parameters like the densities of the particle and matrix, melt temperature, centrifugal pressure, metal viscosity, particle size, cooling rate and magnitude of centrifugal acceleration [216].

A6061 FGMMC with 10 wt% and 20 wt% silicon carbide particles (SiC_p), of 23 μm sizes, reinforced composite is processed by liquid metal stir casting method followed by vertical centrifugal casting to obtain the FGM rings. The SiC_p due to their higher density than the matrix diffuse towards the outer periphery giving a graded structure. While the porosities, impurities and agglomerates with lower densities accumulate towards the inner periphery and can be removed by machining. Microscopic image analysis shows higher volume percentage of SiC near the outer periphery of 45 % volume. The various mechanical characterisations confirm the presence of three different graded regions, namely particle rich, transition and particle depleted/ matrix rich regions. It is also found that the outer regions have better hardness, wear resistance and tensile properties compared to the inner region due to superficial reinforcement concentrations.

6.2 MATERIALS AND EXPERIMENTAL METHODS

The wrought aluminium alloy, A6061, is used for synthesizing FGMMC with green SiC particles of 23 μm average particle size (APS) and density 3.2 gm/cm^3 is used as the particulate reinforcements (refer chapter 3 sections 3.4 and 3.5 for detailed material properties and composite melt preparation). The MMC melt is synthesized by liquid metal stir casting method and later poured into rotating mould of vertical centrifugal casting machine to obtain the FGMMC component. The SiC particles were preheated to 600^{o}C and 1% Mg was added to the melt while stir casting before the SiC addition to improve the wettability. Steady liquid vortex and uniform addition of particles is used to ensure proper mixing and consistency of MMC melt. Sufficient mechanical and hand stirring are also done before pouring. The melt at 780 °C is poured into metal mould, coated and preheated to 300 °C, which is rotating, at 1300 rpm, in vertical centrifugal casting machine. Figure 6.1 shows the picture of the FGM casting with 25 mm thickness, fixed outer diameter of 230 mm, average inner diameter of 140 mm and weighs about 2.5 kg.

Standard specimens are cut for mechanical characterisation. The standard T6 heat treatment procedures, solution treatment at 535 °C for 4 h, quenching in warm

water and artificially aging at 175 °C for 8 h, is used for A6061 FGMMC specimens. Optical Emission spectrometer, SPECTRO MAXX LMM05, is used for chemical composition analysis. Microstructural characterization is carried out by using DMRX Leica optical microscope and Leica Qwin image analyser is used for the measurement of volume fraction of the silicon carbide particles in the matrix. INDENTEC hardness tester is used for Brinell hardness measurements from outer to the inner periphery in the as-cast and heat treated conditions. Dry linear wear analysis is carried out by using DUCOM pin-on-disc tribometer. Wear surface morphology is taken by Zeiss stereo microscope. Tensile test is carried out on INSTRON 1195 – 5500R series tensile and compression tester for specimens taken from both inner and outer zones of the cast.

Figure 6.1: FGMMC cast ring

6.3 STUDIES ON A6061-10 Wt % AND 20 Wt. % SIC FGMMC

6.3.1 *Microstructural Evaluation*

Figure 6.2 shows the microstructures of A6061 alloy on gravity casting at different magnifications. The chemical composition of the alloy is given in Table 3.1 (refer the section 3.2 of chapter 3). The optical emission spectrum analysis reveals that only 0.82 vol. % Si, 0.259 % of Cu and 0.646 % of Mg are present in the alloy ingot. Corresponding to this, the volume of different phases like Mg_2Si and primary silicon flakes formed in the alloy melt are also less. The smaller percentage phases produce less effective diffusions. At higher magnifications the Mg_2Si phases and primary silicon flakes are clearly visible in the microstructures. The microstructures of centrifugally cast ring of A6061 alloy without any SiC addition are shown in Figure 6.3(A, B). The micrographs are taken from outer periphery to inner zones in a radial direction.

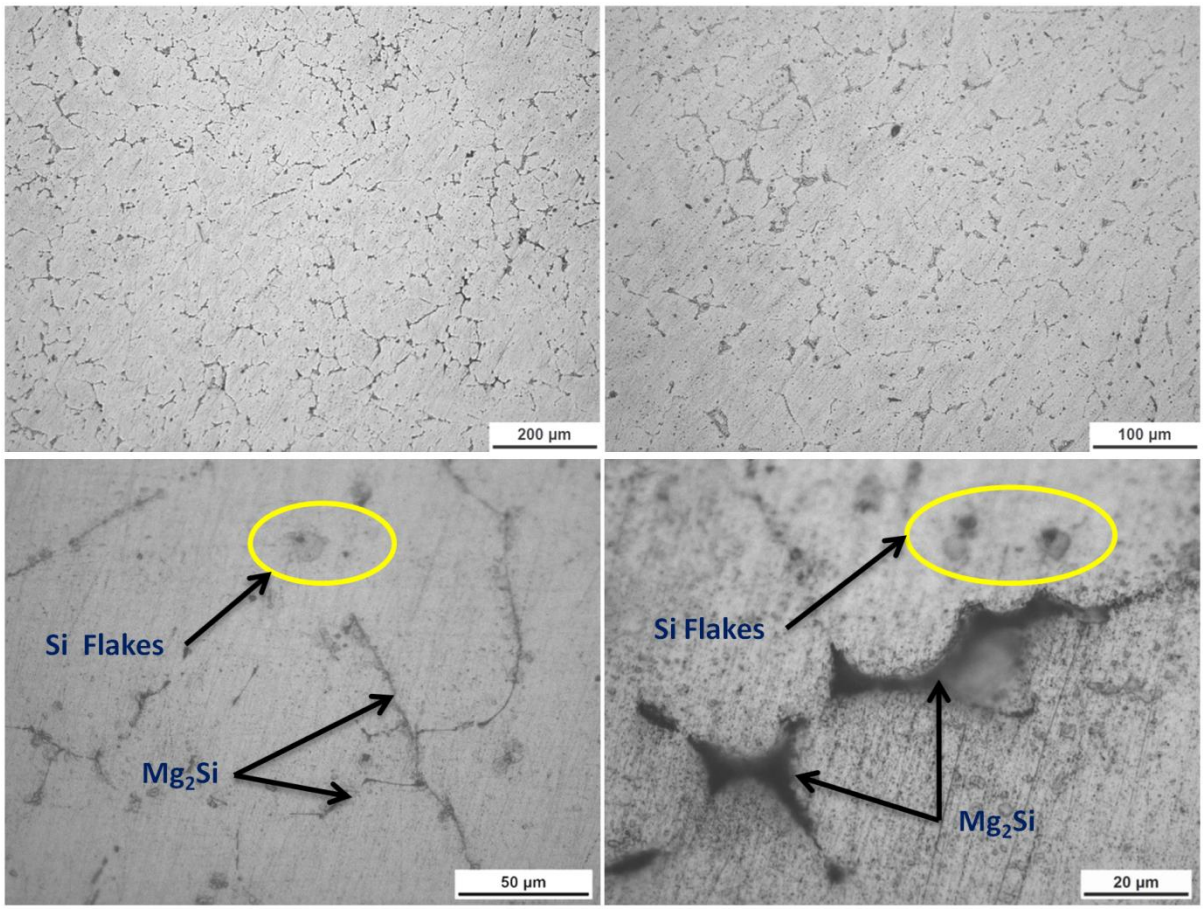

Figure 6.2: Microstructures of A6061 alloy on gravity casting at different Magnifications showing Mg_2Si and Primary Silicon flakes.

It is observed that the grain size towards the outer periphery is smaller in size than that towards the inner periphery. A pressure force developed on the molten melt which comes in contact with solidifying edge during the centrifugal casting process. The solidification edge moves from mould outer periphery towards inner regions and the pressure force acts from inner to outer in an opposing radial direction. These opposing forces create a squeeze effect on the melt during solidification and produce grain refinement. Due to the centrifugal effect the less dense gas porosities, slag inclusions and agglomerates will diffuse towards the inner diameter and are observed at the inner periphery regions. These can be easily removed from components while machining. The grain refinement effect is clearly reflected later on the hardness measurements. The hardness variation for the heat treated A6061FGM is mainly contributed by the grain refinement due to centrifugal effect. Figure 6.4 shows the graded distribution of 10 wt % SiC particles in A6061 alloy FGMMC ring from particle rich outer periphery to matrix rich inner periphery through a transition region. The outer periphery of the

casting shows a higher concentration of SiC particles than the inner. A clear transition region in between is also visible. The presence of high volume fraction of SiC particles inhibits growth of primary aluminium in addition to the break the arms of dendrites by the shear caused by movement of ceramic particles during solidification can also help to form the fine structure [217]. Figure 6.5 shows the graded distribution of 20 wt % SiC particles in A6061 alloy FGMMC ring at different regions namely particle rich outer, transition and matrix rich inner periphery respectively. The outer periphery of the

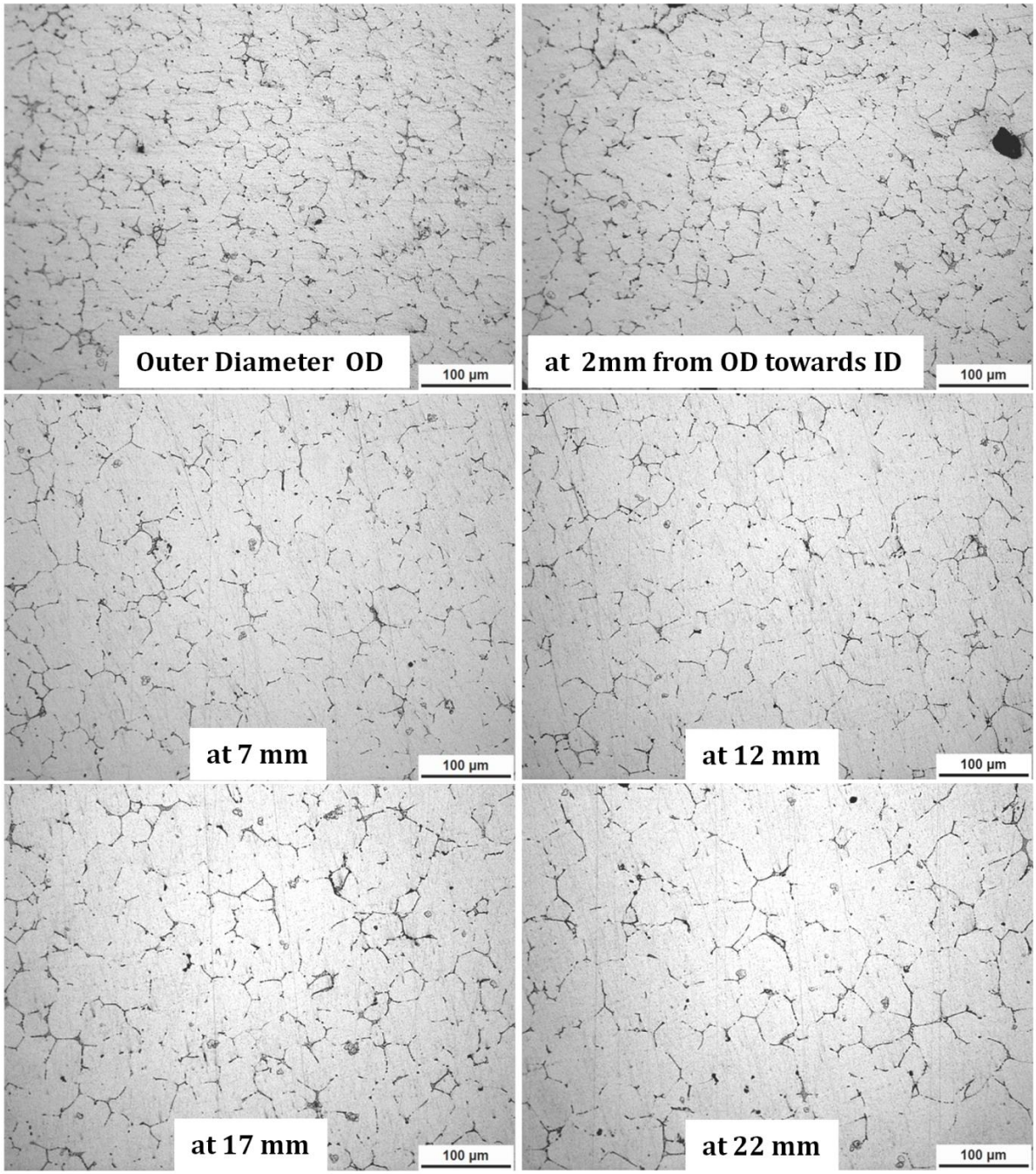

Figure 6.3 A: Optical microstructures of A6061 centrifugal cast ring

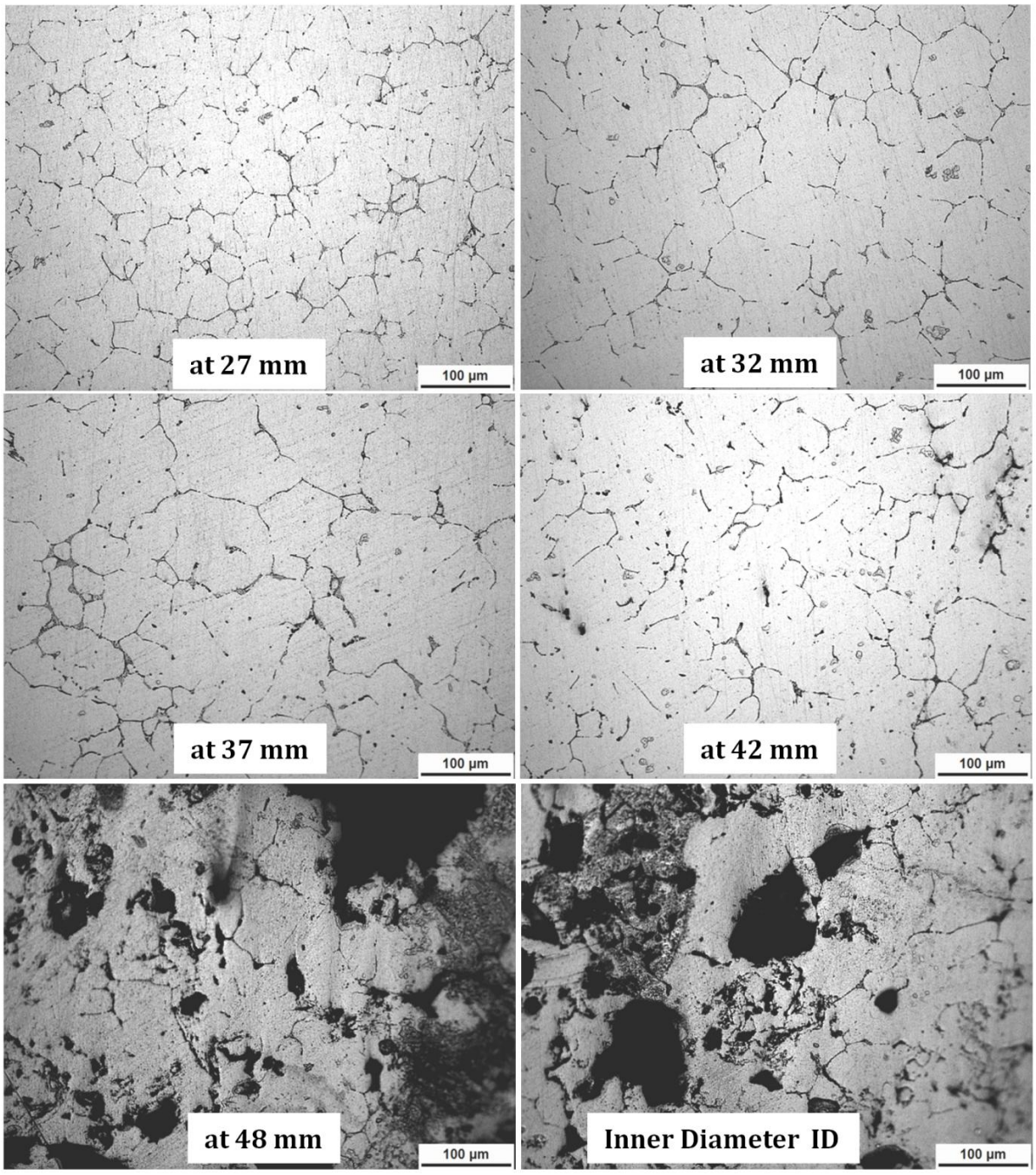

Figure 6.3 B: Optical microstructures of A6061 centrifugal cast ring taken at different locations starting from outer periphery towards inner periphery at 20x (100 µm)

casting shows a higher concentration of SiC particles than the inner and a clear transition region in between is also visible. The microstructural features of the matrix alloy also vary from outer to inner periphery. The grain size of the aluminium in particle enriched zone is very fine, which becomes coarser towards interior. The particle distribution is more diffused in nature in A6061 alloy matrix compared to earlier studies of A319 due to higher solidification temperature and the lesser eutectic phases / region which restricts for particle movement during solidification.

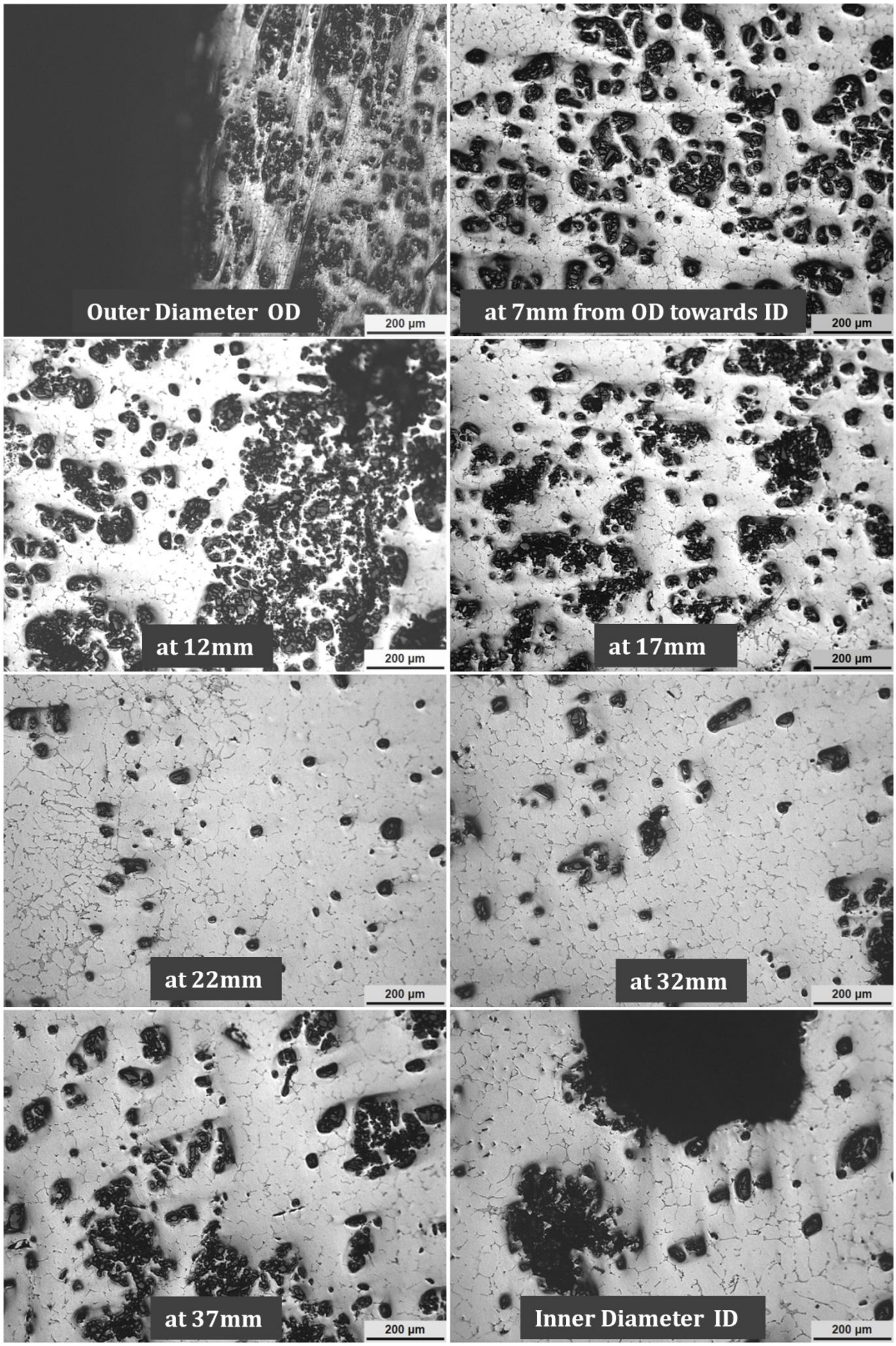

Figure 6.4: Microstructures of A6061–10% SiC FGMMC ring from OD to ID

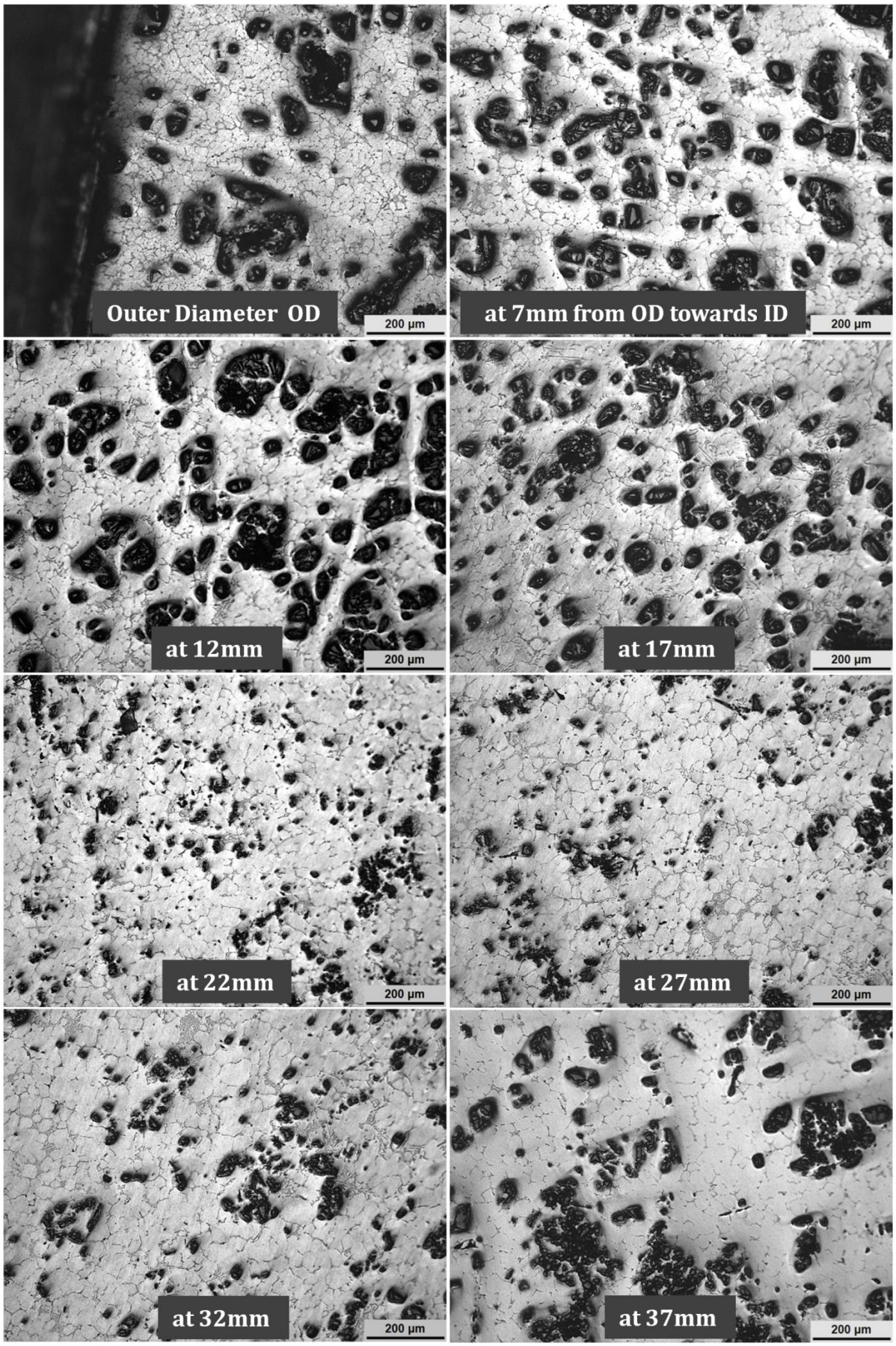

Figure 6.5 A: Optical micrograph of A6061–20% SiC FGMMC ring from OD to ID

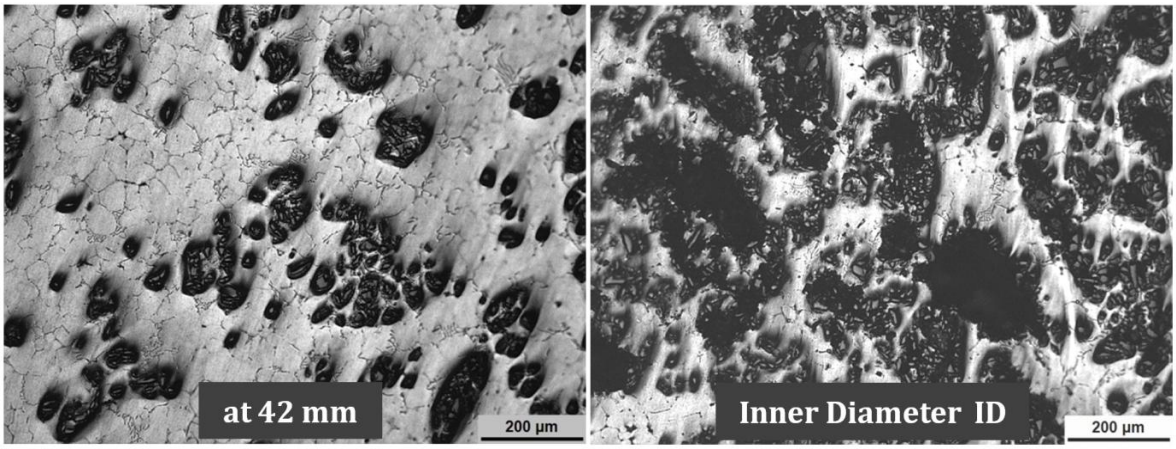

Figure 6.5B: Optical micrograph of A6061–20% SiC FGMMC ring taken at different regions starting from outer periphery towards inner periphery

6.3.2 *Image Analysis*

The image analysis results depicted in Figure 6.6 shows the volume fraction of SiC particles at different locations of both 10 and 20 wt % FGMMC castings from outer to inner diameter. The outer region of 20% SiC FGMMC ring contains a maximum of 55 vol.% SiCp followed by a reduction to lower levels. In the transition zone, between 12mm and 22 mm away from outer periphery, the reduction in SiC volume percentage reaches to a value of 11 and then increases to 15 near the inner periphery. The outer region of 10% SiC FGMMC ring contains a maximum of 45 vol. % SiCp followed by a gradual reduction to lower levels. In the transition zone, between 20mm and 30 mm away from outer periphery, the reduction SiC volume percentage is steep and reaches a value below 10 near the inner periphery. By subjecting a homogenous MMC melt of A6061 and10 wt % SiC to centrifugal force, a maximum volume fraction of 45% is obtained at the outer periphery leading to selective improvement in specific properties such as hardness, wear resistance and tensile properties. Similarly for 20wt% addition a maximum of 55 % is obtained. In comparison, it is observed that more particles are diffused towards outer for 20% addition than in 10% addition and along transition region of less particle concentration is also observed. This may be due to the free paths created by the leading SiCp, which are having high thermal capacity than the aluminium matrix leading to more thermal energy content, enabling more time of diffusion by increasing the solidification duration. The inner most periphery regions of the casting show the presence of gas porosity and few agglomerated particles. The agglomerates constituting partially wetted or non- wetted particles or both and gases having lower

overall density are also pushed towards the inner periphery by the centrifugal force. Further, the movement of gas bubbles from the outer periphery towards the inner during the rotation can hinder the particle movement in the opposite direction and carry away few particles.

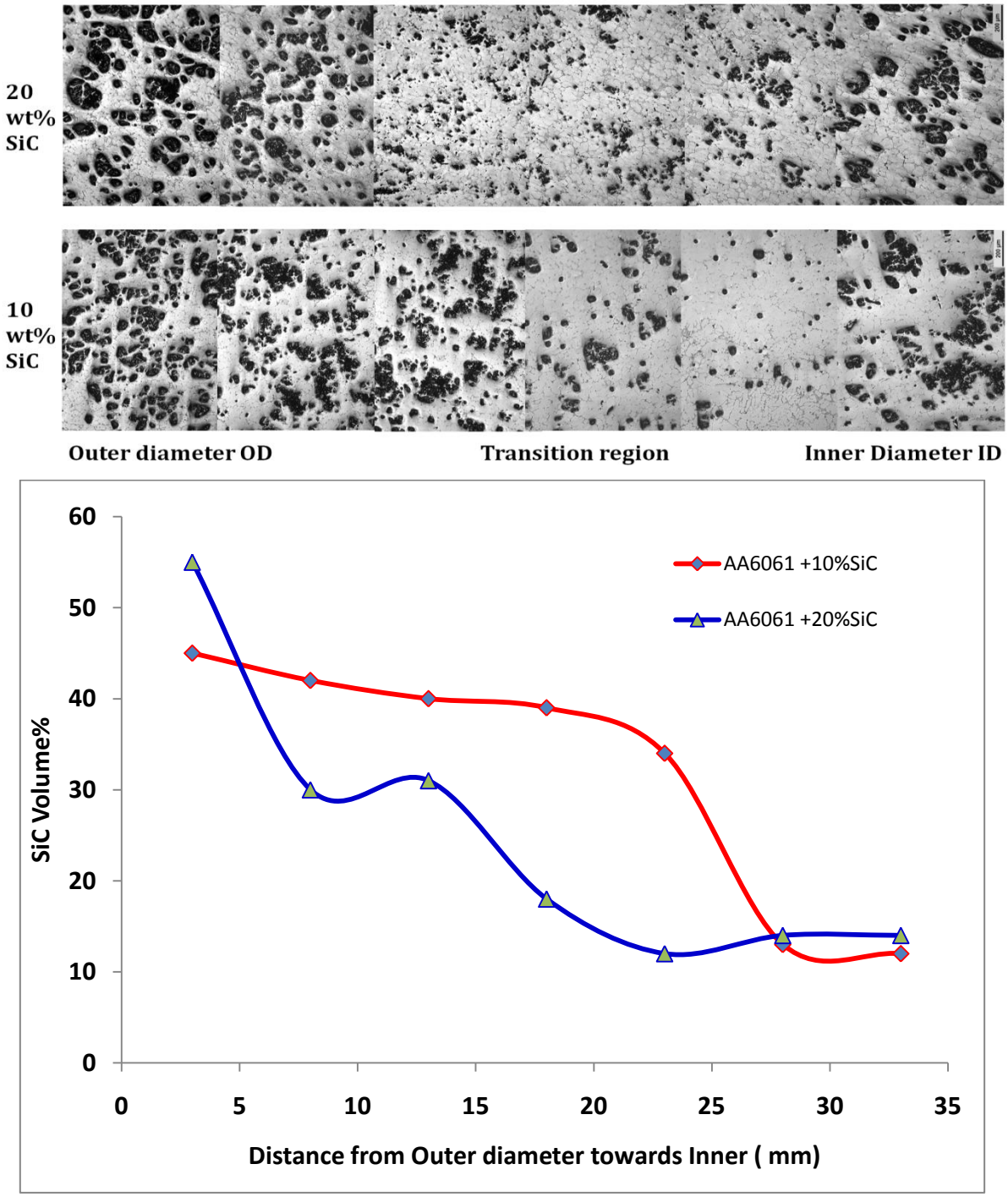

Figure 6.6: Volume Percentage Distribution of Silicon Carbide (SiCp) in A6061-10 % SiC and A6061-20% SiC FGM castings from Outer Diameter towards Inner Diameter in radial direction

6.3.3 *Hardness Behaviour*

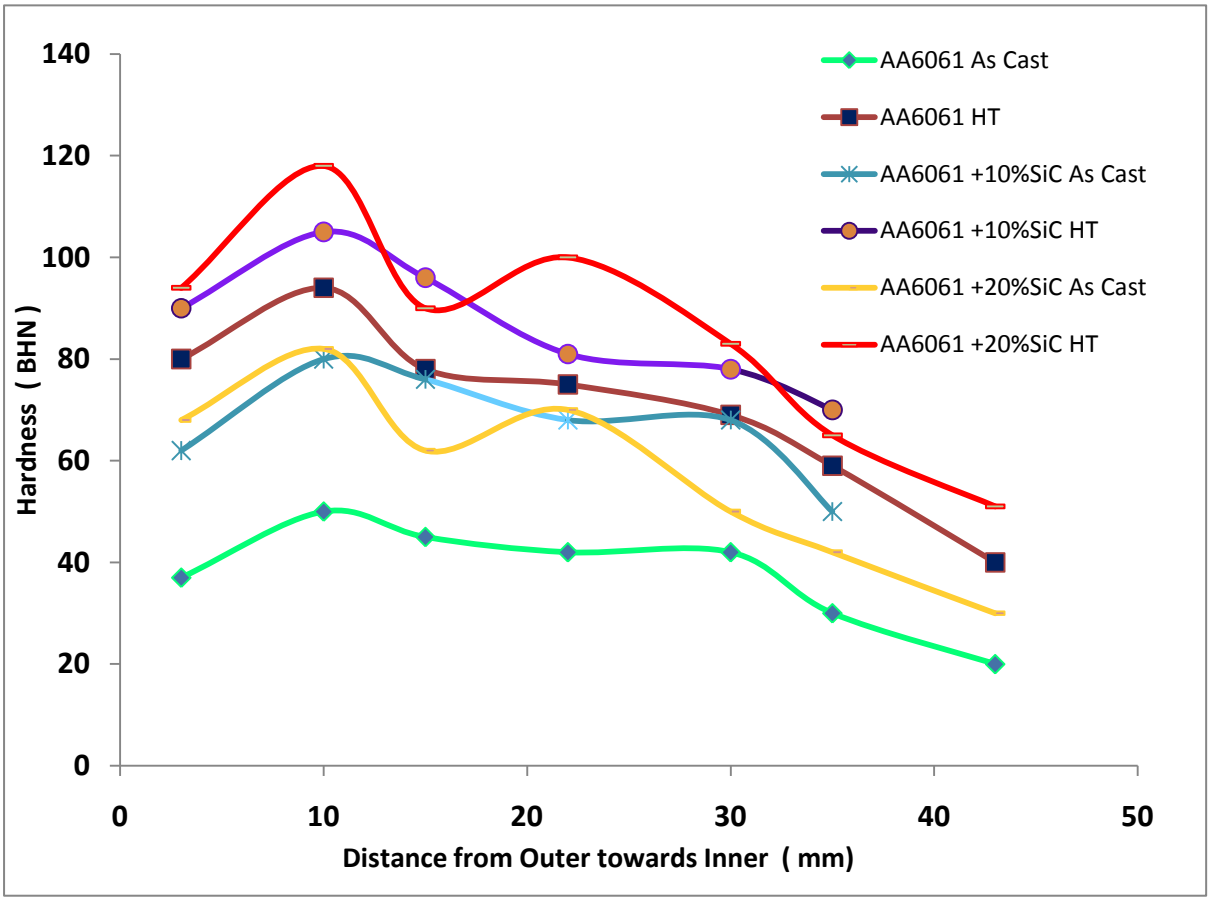

Figure 6.7: Hardness Variation in A6061, A6061-10 % SiC and A6061-20% SiCp FGM castings from Outer Diameter towards the Inner Diameter in radial direction for as cast as well as Heat Treated Conditions

The variations of the Brinell hardness values (BHN) for the as-cast and T6 heat treated samples of the FGMMC rings and centrifugally cast A6061ring in radial direction, from outer towards inner diameter, are shown in Figure 6.7. The curves clearly show that the hardness value varies in proportion to the volume fraction of SiC particles in both as cast and heat treated conditions for all compositions. It is also found that the heat treated ones have far better hardness than the as cast ones. The A6061 cast ring also shows similar trend because of grain refinement happened in outer zones compared with inner zones in addition to the densification caused by centrifugal force. A systematic improvement in hardness is visible from base A6061 FGM as cast to 10wt % SiCp and to the as cast 20wt % SiCp. For A6061 as cast condition, the maximum hardness obtained at particle rich zone was 50 BHN and it rose to 94 BHN after heat treatment. The maximum hardness values in the particle rich zone is 80 BHN for 10 %

SiC FGMMC in as cast condition and is raised to 105 BHN in heat treated condition. Similarly for 20 % SiC the values are 82BHN and 118 BHN respectively. In the transition region the hardness changes between 42-45, 68-76 and 62-50 BHN in as-cast and 78-69, 78-96and 83 -90 BHN in heat treated for A6061, 10% and 20% SiCp FGM Castings respectively. The transition region is observed from 15 to30 mm away from the outer periphery towards inner. The region near the inner periphery shows very low hardness of 20, 50 and 30BHN in as cast and 40, 70 and 51 BHN after heat treatment, due to the presence of porosities and agglomerated particles. Because of high hardness of 20 % SiCp FGMMC, the specimen preparations became difficult and the specimens are too brittle at smaller dimensions, further tensile and wear studies are limited to 10 % FGMMC and the base A6061.

6.3.4 *Tensile Properties*

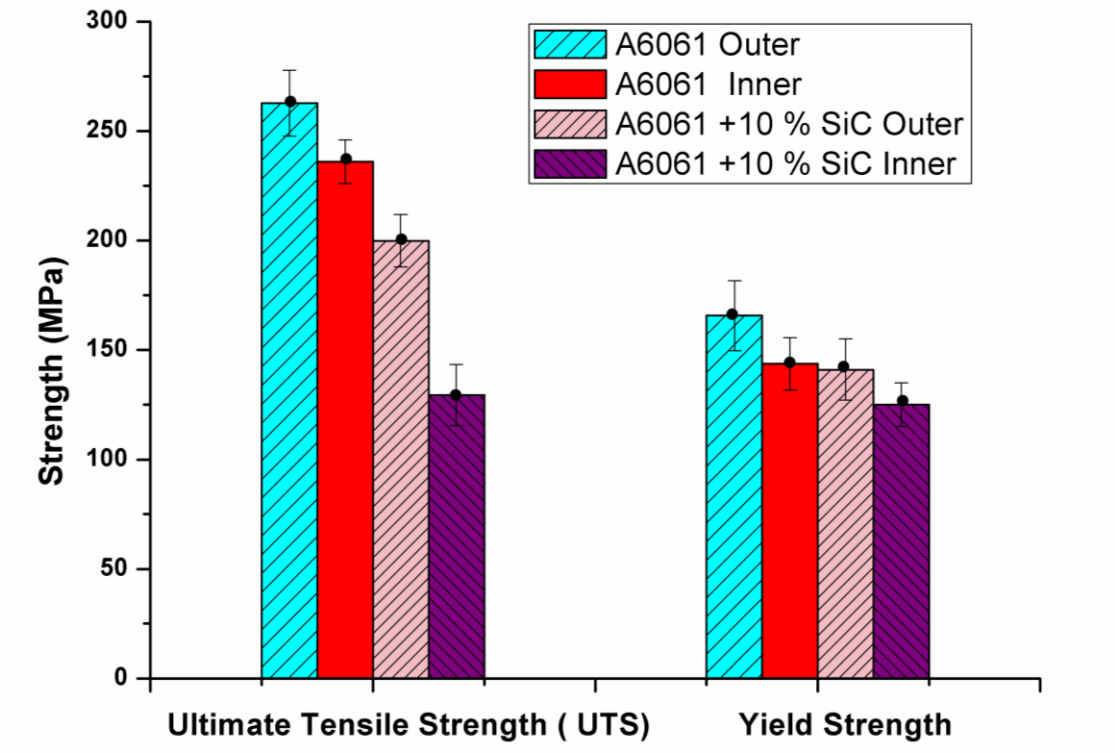

Figure 6.8: Ultimate Tensile Strength and Yield Strength of Heat Treated specimens from Outer Region and Inner Region of A6061 and A6061+10 % SiC FGM castings

The ultimate tensile strength (UTS) value of 262 MPa and yield strength (yield) value of 165 MPa has been obtained for the A6061 base alloy at outer periphery and for inner the values are 236 MPa and 143 MPa respectively (Figure 6.8). The higher values

at the outer periphery are due to finer grain size. The inner periphery specimens may also have porosities in them in addition to the coarser grain which lead to lesser tensile values. The UTS and yield strength values of A6061-10 % SiC at outer and inner periphery. Both the values at inner and outer periphery are comparably lesser than that the values of base alloy. At the outer periphery the decrease is due to presence of high volume fraction of SiC particles which means there is less matrix material to yield leading to lower UTS and yield strength. In the case of inner specimens the presence of porosities and agglomerates contribute to the lower UTS and yield strength values.

6.3.5 *Wear Characteristics*

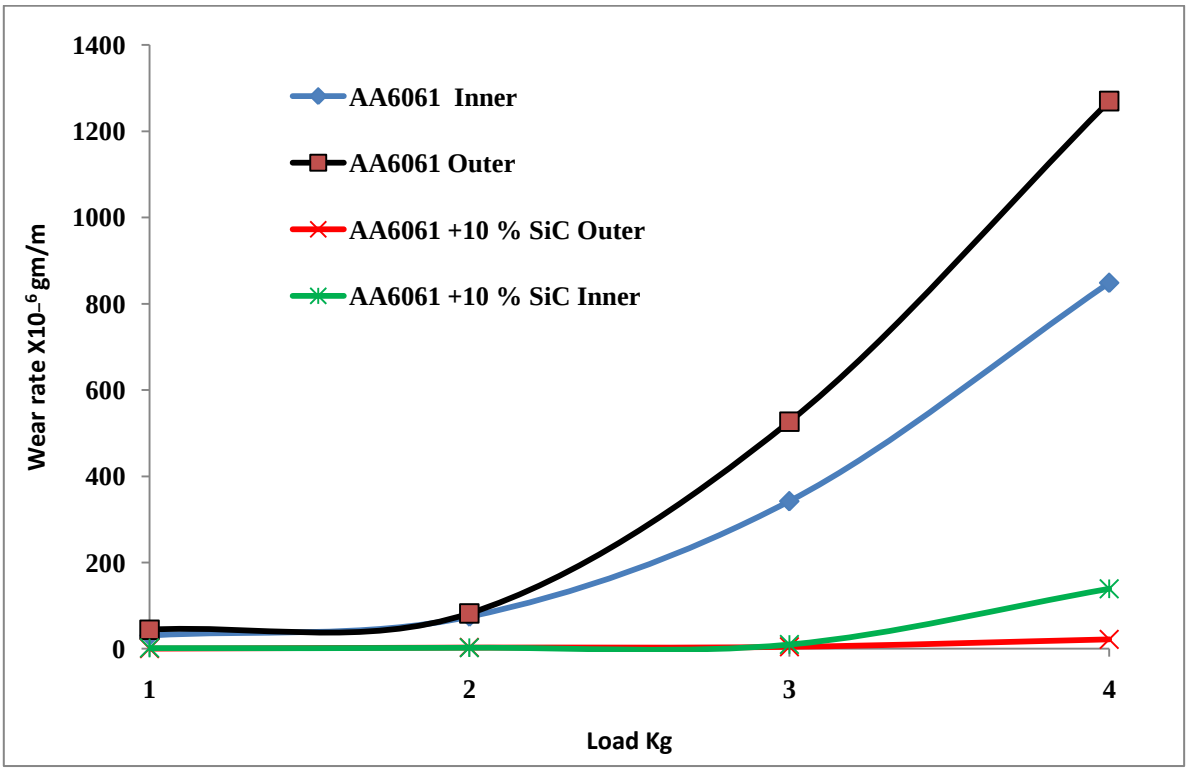

Figure 6.9: Wear rate of Heat Treated specimens from Outer Region and Inner Region of A6061 and A6061-10 % SiC FGM castings

The dry pin on disc wear tests are conducted with pins, of diameter 6mm and 30mm long, from inner and outer regions. Figure 6.9 shows the wear rate versus load as a function of weight loss per meter. For A6061 alloy, from the graph, it is seen that the wear rate at outer periphery is lower when compared to the inner periphery which is due to the finer grain size of aluminium at the outer periphery when compared to coarser grain size at the inner periphery leading to lower wear resistance at the inner periphery. The wear rate increases by a large amount at increased loads. A6061-10%

SiC FGMMC the wear rate at the outer periphery is much lesser than both the wear rate at inner periphery of the same ring as well as A6061 ring. This is due to the presence of high volume fraction of SiC particles at the outer periphery leading to higher wear resistance and the SiC particle concentration gradually decreases towards the inner periphery which leads to lower wear resistance at the inner periphery.

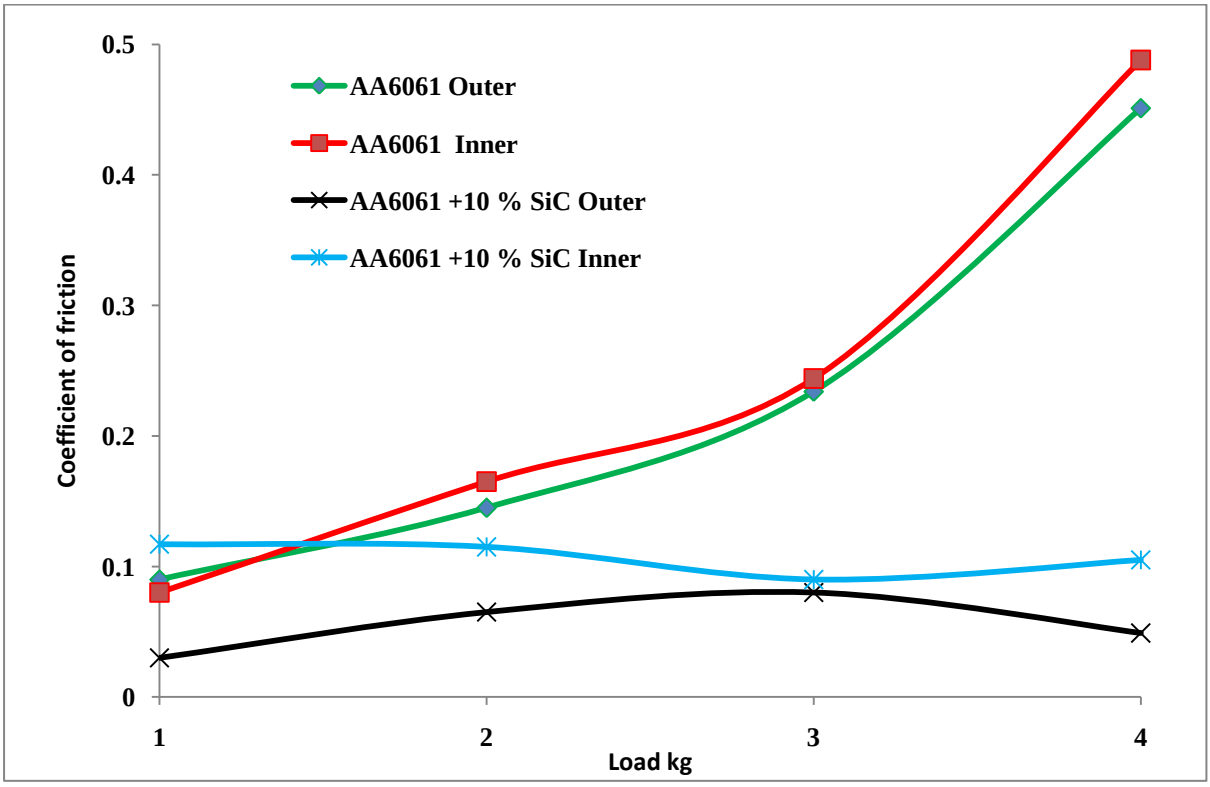

Figure 6.10: Coefficient of friction of Heat Treated specimens from Outer Region and Inner Region of A6061 and A6061-10 % SiC FGM castings

Figure 6.10 shows the coefficient of friction (μ) values as a function of loading. The frictional value increases as the load increases showing that the wear resistance at higher loads is less. For A6061 rings frictional value ranges from 0.09 to 0.451 at outer periphery and 0.08 to 0.488 at inner periphery for loads 1 to 4kg. The frictional values for A6061-10% SiC FGMMC at outer and inner periphery varies from 0.03 to 0.049 at outer and 0.117 to 0.105 at inner. The μ value fluctuates over the time period for the load applied due to heterogeneous nature of the FGM. While the test is being carried out if more SiC particles are exposed to the disc then both the wear and coefficient of friction will be less and when more of the matrix materials are in contact with the disc both will be high. General trend is as the load applied increases the frictional (μ) value will also increase due to the increase in resistance to the relative motion. The μ value dependent on the frictional force, which varies with the operating temperature, in the

dry sliding test, as the temperature of the pin and disc increase substantially which in turn decreases the wear resistance of the pin and thus changing the value of the coefficient of friction.

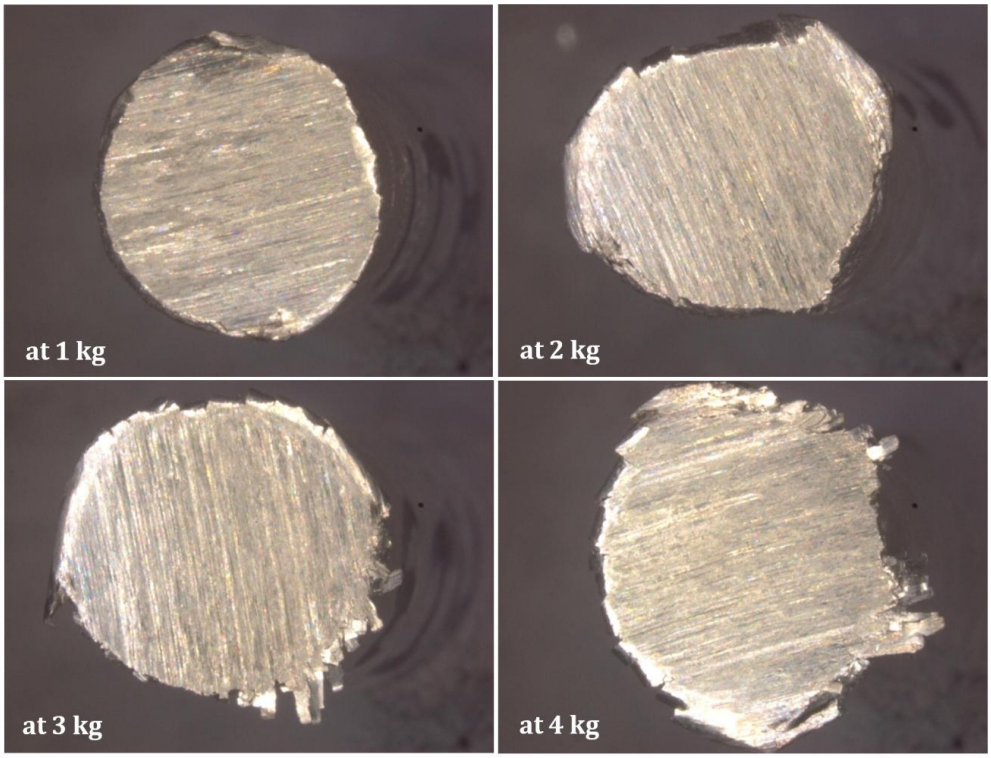

A) A6061 inner pin wear surfaces at different loads

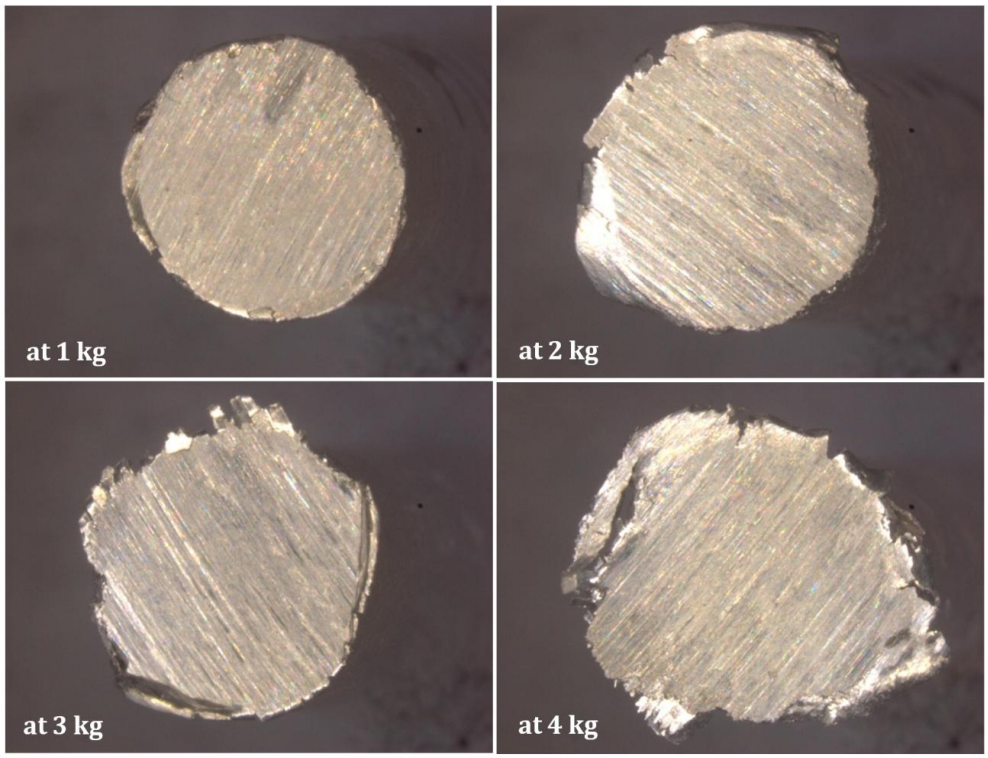

B) A6061 outer pin wear surfaces at different loads

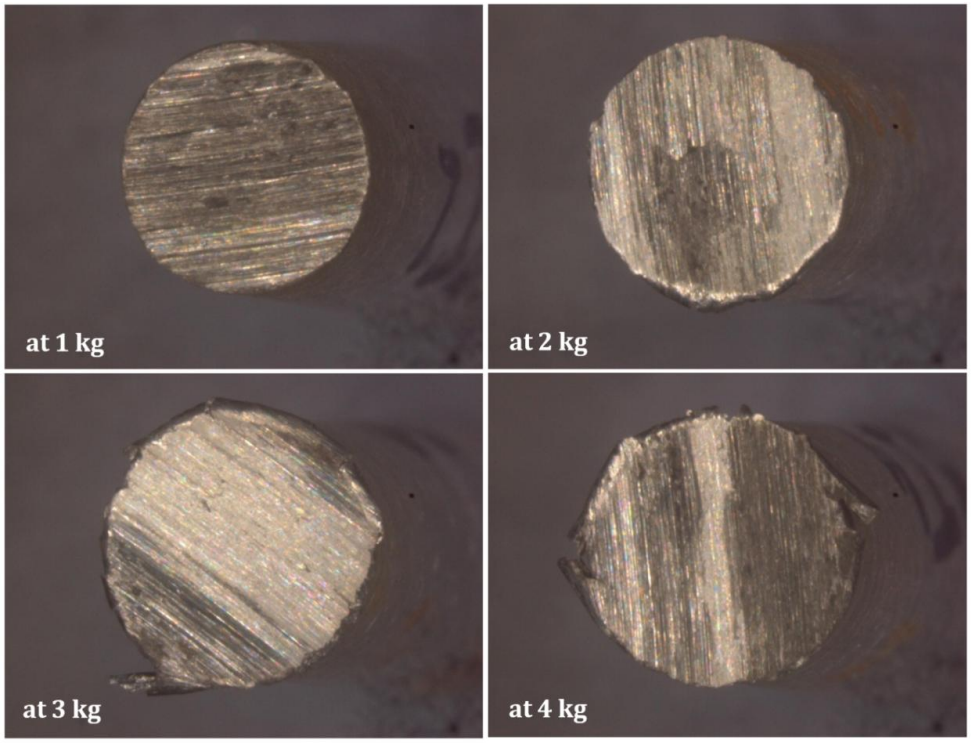

C) A6061-10% SiC FGMMMC inner pin wear surfaces at different loads

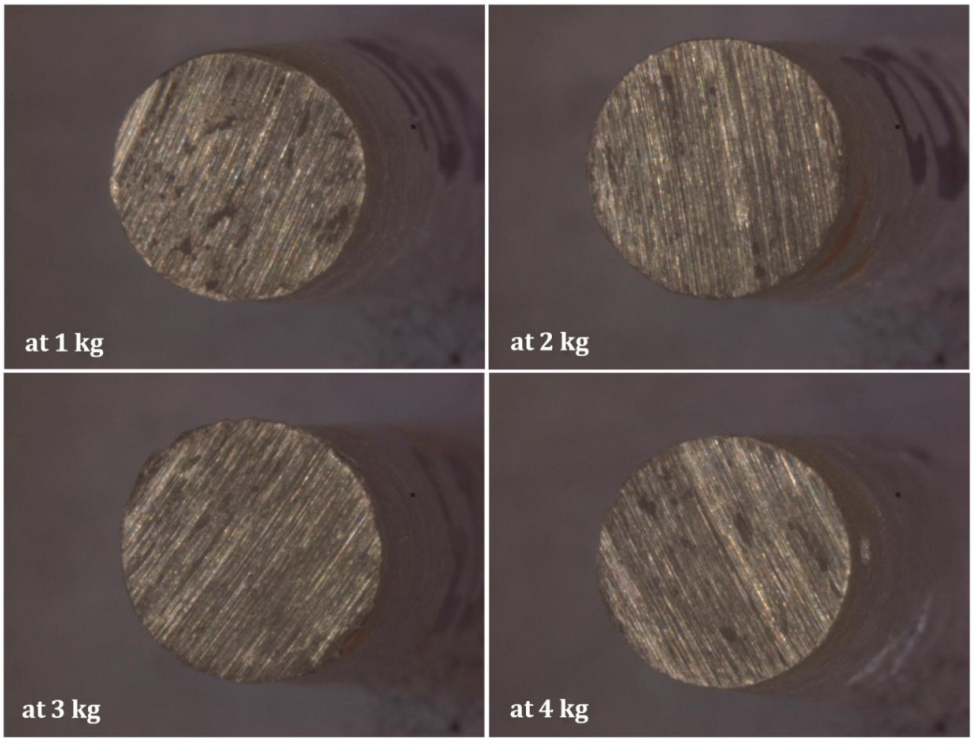

D) A6061-10% SiC FGMMMC outer pin wear surfaces at different loads

Figure 6.11 Stereo micrographs of wear surfaces A6061 and A6061-10% SiC FGMMC

Figure 6.11 shows the stereo micrographs of the surface morphology of the wear specimens at different loads. From Figure 6.11(A, B) for A6061 both inner and outer

specimens the wear scars, at 1kg load, are fine. As the loading increases the interface temperature between the pin and the steel disc increases and soften the aluminium matrix. The softened matrix will stick to the rotating disc and later they will be thrown out by the smudging phenomenon leading to more adhesive wear. Because of this, at higher loads and at severe wear conditions the wear surface show only less fine wear scars. It is seen that in A6061-10 % SiC FGMMC inner and outer pins, Figure 6.11(C,D), at all the load conditions, the wear scars are fine indicating less wear due to the presence of SiC particles. These SiC particles are very hard and do not wear off easily and quickly, thus imparting higher wear resistance to the component. Few SiC particles are only present in the inner pins causing higher wear rate with that of particle rich outer zone pins.

6.4 CONCLUSIONS

- Wrought aluminium A6061 FGMMC with SiCp reinforcements have been fabricated successfully by the centrifugal casting process.
- The microstructure evaluation and image analysis reveals the functional gradation of SiCp particles distribution from outer to inner as the particles are of high density material compared with aluminum matrix.
- The particle distribution is more diffused in nature in 6061 Al alloy matrix compared to earlier studies of 319 Al due to higher solidification temperature and the lesser eutectic phases / region which restricts for particle movement during solidification.
- The hardness of three regions of particle rich, transition and matrix rich regions largely depends upon the concentration of SiC particles. SiC rich outer zones show lesser wear rate in comparison with other regions.
- The variation of wear rate with respect to applied load is linear. The weak interface bond between silicon carbide particle and aluminium matrix at higher load and enhanced interface temperature is the main reason for the change in composite wear property under varying applied loads.
- Addition of SiC particle and heat treatment provide comparable improvements in the wear resistance.
- The study clearly depicts the gradient nature in the structure and properties of the FGM rings.

Chapter 7

Processing and Characterisation of Epoxy– SiC Functionally Graded Polymer Matrix Composites

7.1 INTRODUCTION

Polymeric Gradient material (PGMs) are a class of functionally graded material in which at least one of the constituent phases, mostly matrix is a polymer. Centrifugal casting helps in providing a continuous grading in the Functionally Graded Polymer matrix composite (FGPMC) being produced. In this method the difference in the material densities and the spinning of the mould aids in the formation of functionally graded material. The diffusion of the reinforcement particles are affected by several factors like centrifugal force, shape, the size of the reinforcements, density difference of reinforcement and the matrix.

Epoxy resins form the common matrix for a wide range of applications owing to their properties of low shrinkage, excellent adhesion, high strength, processing versatility and good corrosion resistance. They have got a range of operating temperature 353K- 413K (80-140^0 C), which is better than polyesters and also have an added advantage that their processing does not evolve any toxic gases like styrene [218]. In PGMs the location specific concentration change and graded distributions can be achieved by controlling the centrifugation time [219-221]. The increase in hardness, wear resistance and the rheological behaviour of PGMs can be achieved by proper reinforcement's addition [222-226]. The wear of polymers based on the environment, lubrication, third body factor (which appears in the form of transfer film) and the different wear mechanisms have been reported with the effects of size of the fillers, sliding velocity and sliding distance on the wear rate and, coefficient of friction [226-229]. The PGMs are generally prepared by centrifugation at 4000 to 6000 rpm, gravity settling or by very slow rpm of 2-5revolutions per minutes of the mould. In all the above, processing time and other controlling parameters like speed and curing time is too high and not economically viable for commercial application. Only a very few research is being conducted and available in the area of FGPMC processing at 100-1000

rpm with reinforcements, especially ceramic particles, and very less curing time of 40-50minutes, instead of 24 - 48 hours. In the present work, FGPMC disc with epoxy- 5 wt% SiC_p are processed by vertical centrifugal casting method and characterised by evaluating microstructure, hardness and tensile testing

7.2 MATERIALS AND EXPERIMENTAL METHODS

Thermosetting epoxy resin having a low curing temperature of 363K (90°C) of Shell Epon 828(XY 100) is used as resin and HY 951 IN from Petro Araldite Pvt. Ltd is used as the hardener with a hardener to resin ratio of 1:10. 5 wt. % green SiC_p of 23 μm average particle size (APS) and density 3.2 gm/cm^3 is used as the particulate reinforcements (refer chapter 3 sections 3.4 and 3.5 for detailed material properties and composite melt preparation). After the preparation of the composite, the mix is poured into the rotating mould which fitted in the vertical centrifugal casting machine and the machine is run for 30 to 35 minutes until the curing is completed. FGM with epoxy-5wt. % SiC_p is prepared by centrifugal casting at 500 rpm in metal mould of size (110mm diameter x 55mm height).

Perkin Elmer Pyris 6 DSC, differential scanning calorimeter is used to study variations in curing temperature of different compositions (refer chapter 3 sections 3.6 for detailed specification of experimental instrumentation and experimental conditions). The viscoelastic behaviours of the composite system are studied by using a parallel plate rheometer, Physica MCR 150. DMRX Leica optical microscope was used to observe and capture the microstructures. Vickers hardness (HV3) was tested by INDENTEC hardness tester with a Vickers diamond pyramidal indenter having a square base and pyramidal angle of 136˚. The specimens are subjected to a load of 3 kgf with a dwell time duration of 20seconds. INSTRON 1195-5500R series tensile and compression tester was used for the tensile and compression testing. Dry wear tests were conducted in a DUCOM (LR20E) pin on disc tribometer with EN31 hardened steel disc. With a sliding velocity of 3 m/s for a sliding distance of 3000 m with a pin of 6mm diameter and 30mm length. The worn out surface morphology were taken by Prog Res C5, Zeiss stereo microscope. Zeiss EVO 18 Scanning Electron Microscope was used to take SEM images of worn out surfaces.

Parameter optimization is initially done to get the information about the setting of the processing variables and parameters for the castings. Initially experiments were

conducted to find out the glass transition temperature of epoxy by differential scanning calorimetry (DSC). Rheology tests were conducted to find out the variation in viscosity, gel point (curing point) of both epoxy and the composite by measuring storage modulus and loss modulus. The laboratory scale 10 ml experiments were conducted to find out the effects of epoxy hardener ratio on time of curing and the effects of percentage of reinforcements (particle loading) on the ratio, time and thereby optimizing these parameters.

7.3 PARAMETER OPTIMIZATION

DSC scans were performed using a differential scanning calorimeter in nitrogen atmosphere at a heating rate of 10 °C/min to find the glass transition temperature. By observing the difference in heat flow between the sample and reference, differential scanning calorimeters are able to measure the amount of heat absorbed or released during such transitions. In case of epoxy hardener mix, after an initial deflection near the temperature region 44 - 50 ^{0} C the curve shows a clear deviation from 90 ^{0} C to around 120 ^{0} C (Figure 7.1) and this corresponds to glass transition temperature region of the mix, Generally the epoxy polymers shows a band rather a specific point of temperature at which the phase transition or the curing of the epoxy occurs.

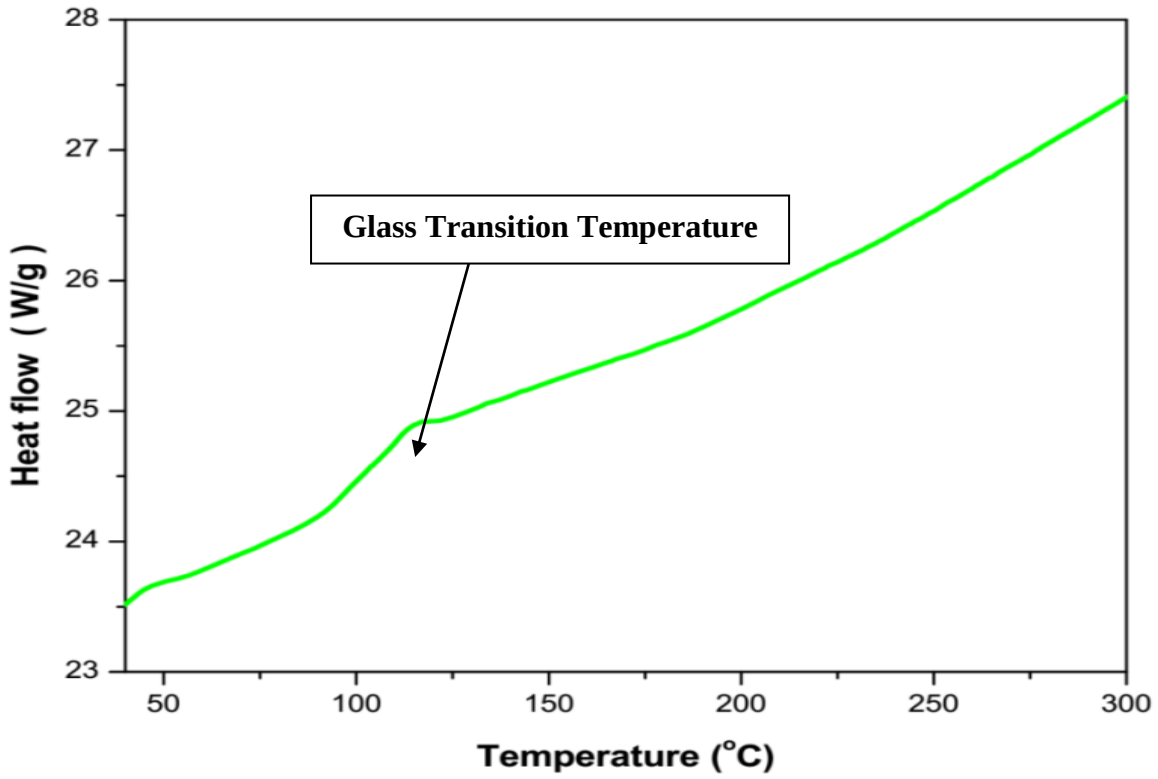

Figure 7.1: DSC Result for Epoxy Resin showing the Glass Transition Temperature

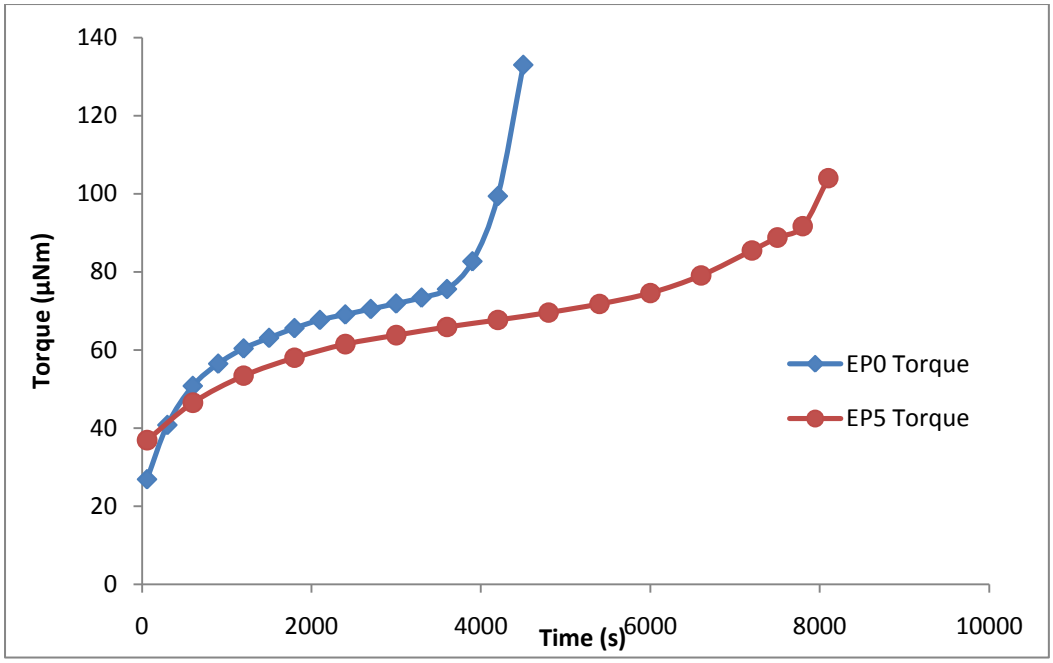

Figure 7.2: Torque variations for epoxy with reinforcements 0 wt. % SiC (EP0) and 5wt. % SiC (EP5) with an optimised epoxy to hardener ratio of 10:1

The viscoelastic behaviour of the composite system is studied using parallel plate rheometer. A rheometer measures the material responds to an applied force in terms of torque, from which we will get information about curing time, viscosity, storage and loss modulus variations during the curing period. The rheology is done for epoxy and with 0 wt.% SiCp (EP0) and 5wt.% SiCp (EP5) reinforcement with an optimised epoxy to hardener ratio of 10:1 . The variation of torque with respect to time is shown in (Figure 7. 2) and other results are discussed in the following sections in detail.

It is observed that during curing of the blend of epoxy and hardener alone EP(0) sample the torque on parallel plate is at 25 µNm and slow and steadily increased to 60 µNm at around 1750 seconds and thereafter shows a very slow increment in torque until 3800 seconds of the experiment. At around this period the torque values increased sharply from 80 to 135 µNm indicating the completion of curing (polymerisation) process. In the case of epoxy with 5 wt % SiC (EP5) the initial torque itself is at 35 µNm as expected (SiC addition increases the blend viscosity and offers more resistance to the plates for turning) The rate of curing process is also slower due to the presence of SiC reinforcement particles and as a result the change in torque readings until 8000 seconds of the experiment is slow and it increases to 90 µNm. After that, there observed a sharp increase in torque value indicating particle loading has an influence on curing

time. With the addition of SiC to the epoxy (EP5), the time for curing of the epoxy increased by a considerable amount and this is due to the hindrance of the active sites of the epoxy and the absorption of the heat generated during the exothermic curing process by the reinforcement SiC particles

From the DSC and rheology results, we get information about the glass transition temperature, gel point and the viscosity variations happening in the blend of epoxy, hardener and SiC during the curing reactions. Since there were no literatures available, before doing the centrifugal castings, it was necessary to get more information about the optimum ratio of mixing of blending and its curing time in room temperature and gravity conditions. This is very much need for the setting of the casting parameters like pouring time, machine running time, cast removal and to get the total time of a centrifugal experiment. To begin with, the hardener and SiC particles are taken in a 10 ml container (Figure 7.3) and mixed properly for 10 minutes so that a proper wetting of the reinforcement with the hardener is ensured. Then the resin is slowly added and stirred for another 15-20 minutes. The blend is kept undisturbed, observed and evaluated at regular intervals by doing piercing test.

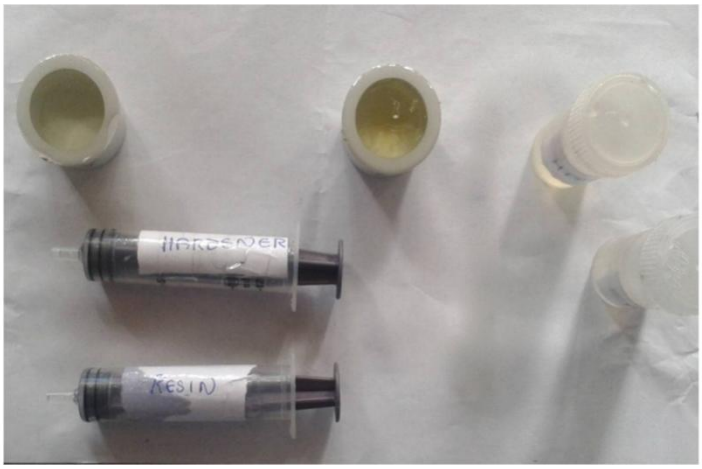

Sample no	Ratio of Hardener: Epoxy Resin
1	1:1
2	1:2
3	1:3
4	1:4
5	1:5
6	1:6
7	1:7

Figure 7.3: Epoxy and Hardener in syringes. Various blends of hardener and epoxy as per table in 10ml containers

Starting from a mixing ratio, hardener to epoxy, 1:2 various proportions of the resin and hardener are taken and conducted gravity curing test at room temperature. Figure 7.4 shows the curing time of various mixing ratios. The samples 4, 5 and 6 cured within 40 - 60 minutes (the preferred period of rotation, chosen for a centrifugal casting process.) As the next step in the optimization, the effect of SiC particle addition on the time of curing of epoxy – hardener blend was analysed (Figure 7.5). The effect of

reinforcement loading was evident and as the percentage (wt %) addition increases for samples with mixing ratio 1:5 and 1:6 experiences large variations in curing time and the blend with 1:4 shows minimum changes.

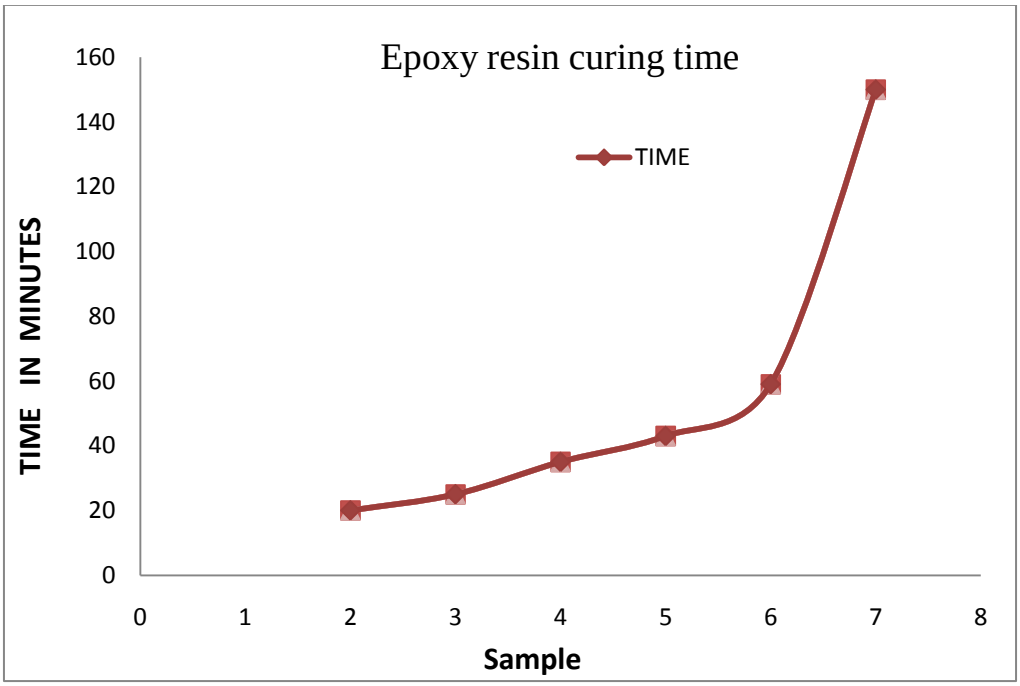

Figure 7.4: Epoxy resin curing time at various mixing ratios of hardener with resin

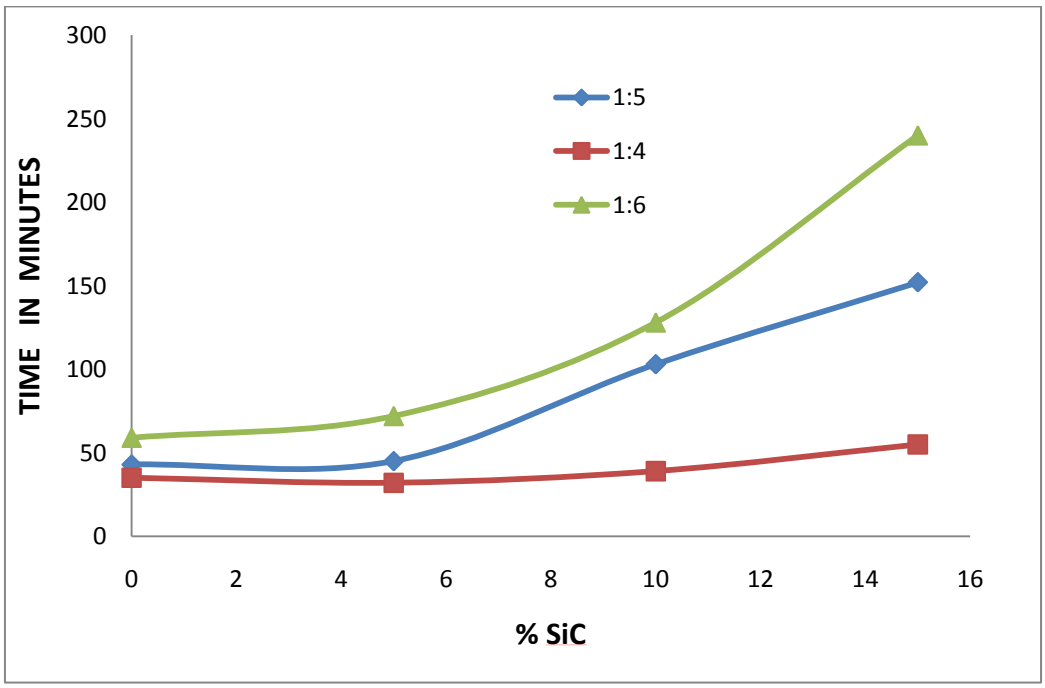

Figure 7.5: Effect of addition of SiC reinforcement particles on the curing time of epoxy with different hardener to epoxy mixing ratios

Based on Figure 7.4 and 7.5, it was decided to start centrifugal castings with mixing ratio 1:4 (hardener to resin) since there were minimum variations in curing time with and without particle addition. Also there were minimum effects of particle loading observed in the curing time of the blend. Initial gravity castings were done with a mixing ratio (hardener to epoxy) of 1:4 with addition of 5 wt. % SiC particles, and with the same composition the centrifugal castings were done at speed of 500rpm. The castings are removed and visually inspected. A systematic observation and refined the processing parameter (basically mixing ratio) were done. Figure 7.6 show the images of the castings with different mixing ratios. On inspection of the ring with ratio 1:4 (Figure 7.6 a) it was observed to have 2-3 huge vertical cracks, the casting was unable to stay as a single unit and were independent pieces. The inner surfaces were having high roughness and gas porosities. A SiC particle rich layer of 3-5 mm thickness was also observed nearer to the outer periphery. The cracks formed may be due to uneven curing of the epoxy resin under the centrifugation effect or it might be due to larger volume effects. Increased amount of hardener to resin can also be a possible cause for this behaviour.

The possibility of volume effects and the uneven curing during centrifugal casting process are omitted after a through literature study and decided to reduce the amount of hardener (1:5 ratio, i.e. dilution of hardener in the blend) in expectation of reduction in the cracks. Figure 7.6(b) resulted in a cast with smoother inner surface, lesser gas porosities, partial vertical and a fine horizontal crack along the inner surface. More castings were done with further reduction in hardener ratio to epoxy (i.e. 1:6 to 1:8) and as expected the castings obtained were with lesser and lesser defects. A successful casting was obtained with a hardener to epoxy ratio of 1:9. Then experiment was extended to ratios 1: 10 and 1:11, a defect free, flawless casting was obtained for ratio 1:10 within a running time of 45 minutes. But for 1:11 even after 60 minutes the curing was not complete and attempt of casting was unsuccessful. Thus the parameter of mixing ratio hardener to epoxy was fixed to 1:10. Final casting are done with a hardener to epoxy resin mixing ratio 1:10, 5 wt.% SiC particles of average particle size of 23 μm and centrifugal speed of 500 rpm for a centrifugal run time of 45 minutes. Thus centrifugal castings without SiC particles (EPC0), centrifugal castings with 5 wt % SiC particles(EPC5) and the gravity castings with 5 wt % SiC (EPG5) were processed

(Figure 7.7). Standard samples are prepared from the castings for the microstructural evaluation and for other mechanical characterisations.

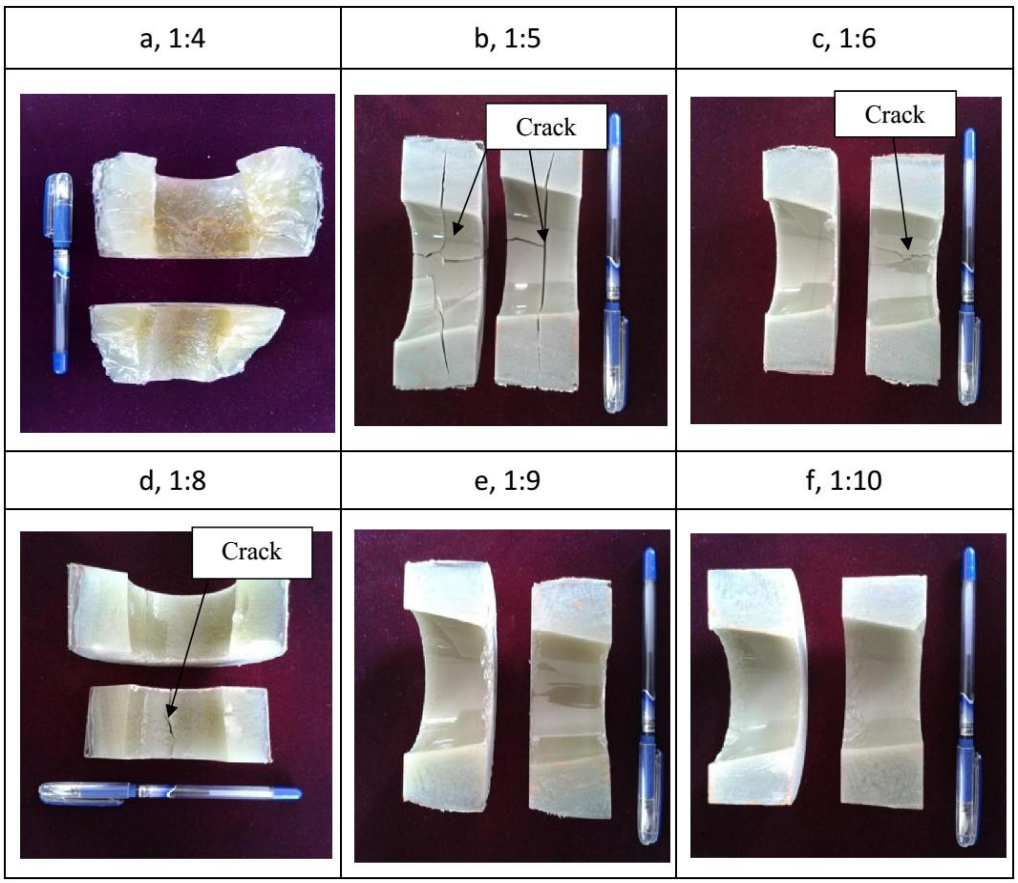

Figure 7.6: Centrifugal castings with different mixing ratios of hardener to epoxy with 5 wt% SiC particles

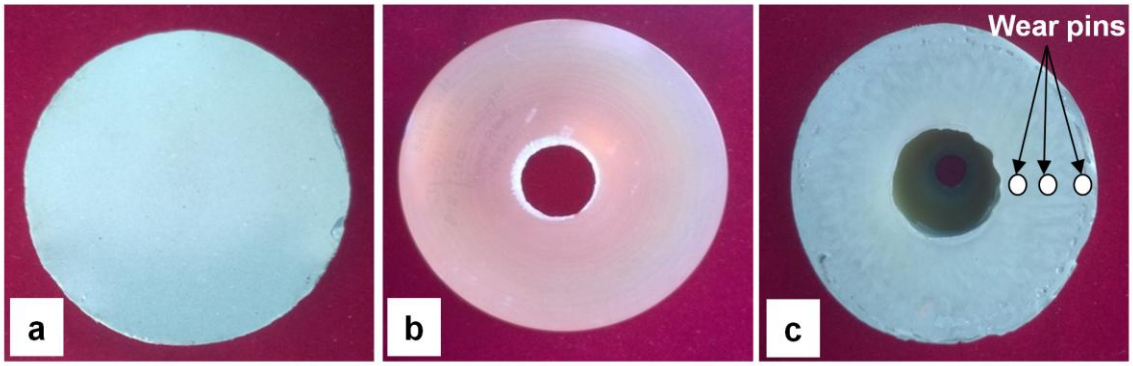

Figure 7.7: Castings (a) Homogeneous (Gravity casting) of epoxy-hardener with 5wt %SiC_p, (b) Centrifugal casting of epoxy-hardener alone and (c) Centrifugal casting of epoxy-hardener with 5wt %SiC_p showing the inner, transition and outer positions of wear pins produced

7.4 RESULTS AND DISCUSSION

7.4.1 Differential Scanning Calorimetry (DSC)

The DSC scans of epoxy with hardener (10:1) alone and epoxy-hardener with different wt. % SiC_p are shown in Figure 7.8. The results indicate that there is no variation in glass transition temperature (curing temperature) of different composition. However, the energy band peak becomes more sharpened with less change in bandwidth and lower heat flow due to the reduction in energy released during curing from unit area caused by increased particle concentration as well as the absorption of heat by the cold reinforcing particles. Similarly, the increase in SiC particle loading enhances the thermal conductivity of the system and above certain percentage the heat flow increases. Hence the study indicates that the addition of 5 wt % SiC_p to epoxy does not affect the curing temperature and the chemical reactions that occur between the polymer and the hardener during the curing process.

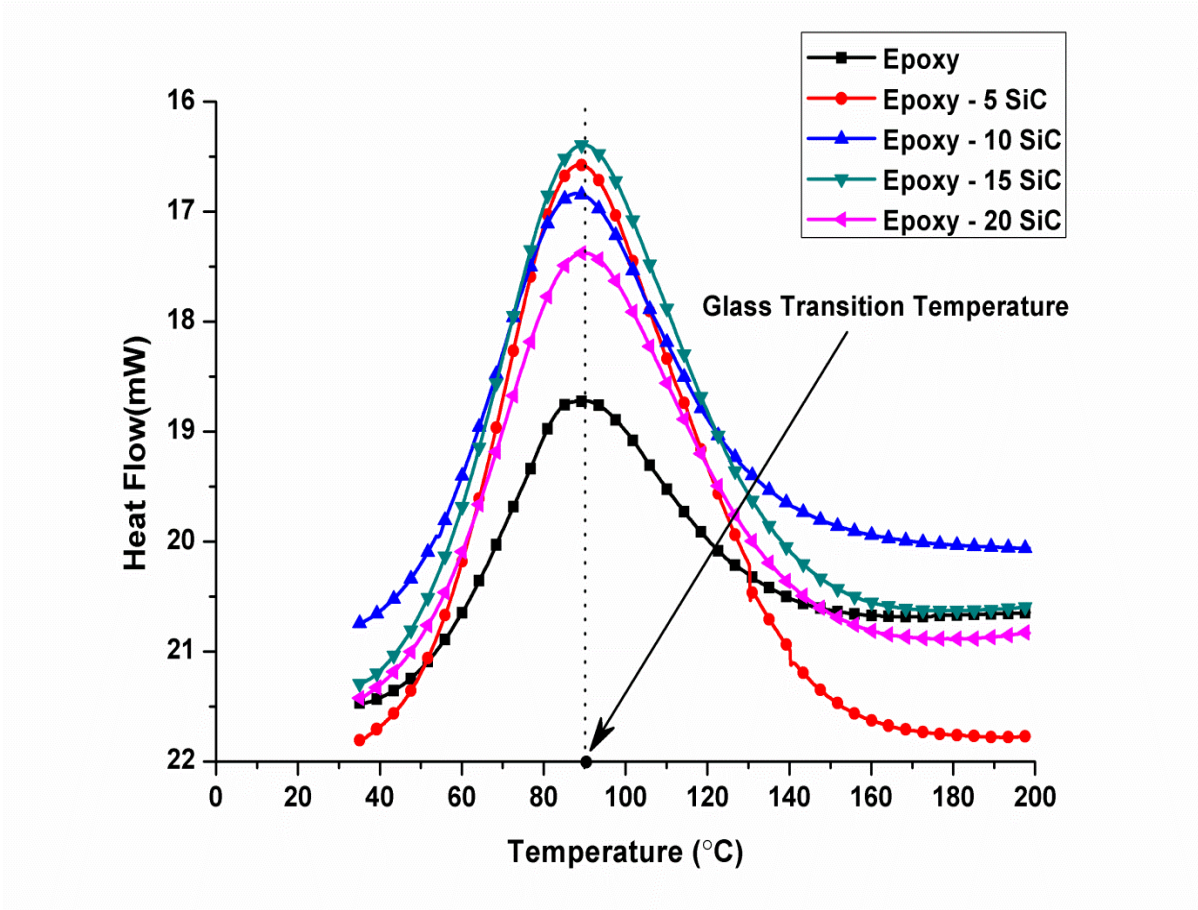

Figure 7.8: Differential Scanning Calorimetry for Epoxy-hardener with different wt% of SiCp

7.4.2 *Rheology*

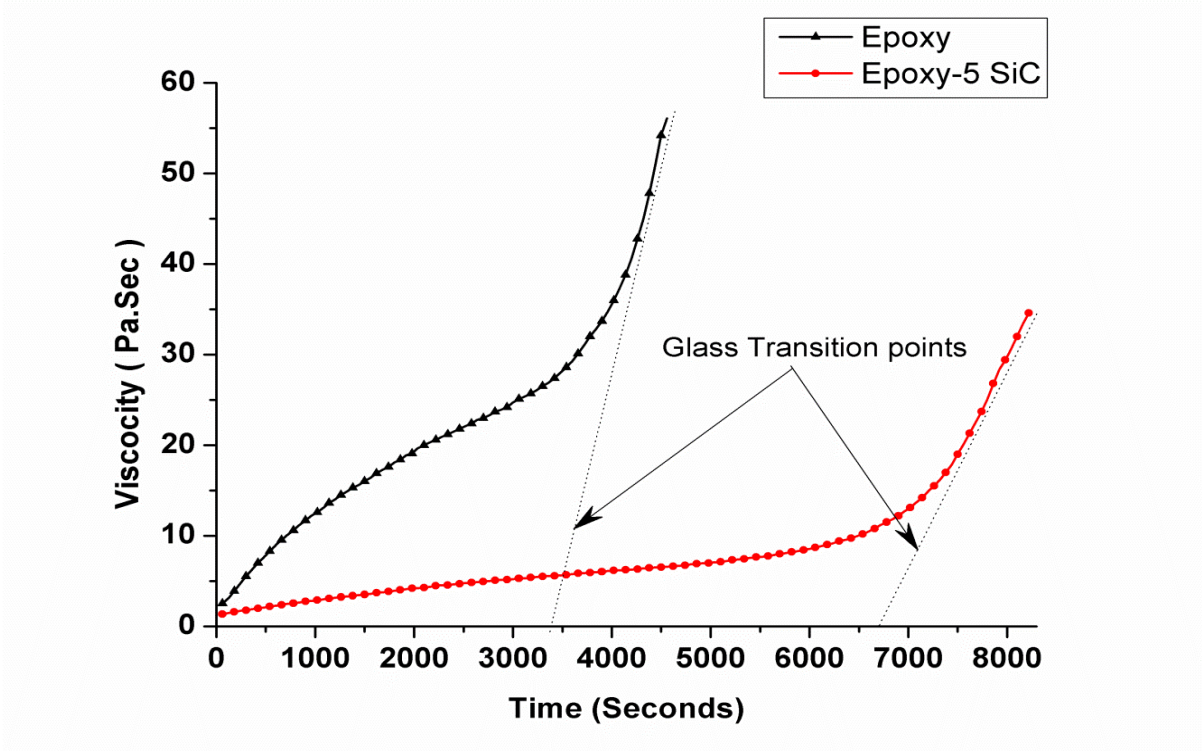

Figure 7.9: Rheology, viscosity variations of Epoxy-hardener and Epoxy-hardener with 5 wt % SiC_p

The Rheology tests are conducted with SiCp as filler material and epoxy resins with hardener as the matrix phase. The viscosity measurement during curing was conducted for 0 and 5 wt. % SiC reinforcement in epoxy-hardener mix at room temperature. Results of viscosity variations as a function of time are shown in Figure 7.9. It can be observed that the viscosity of epoxy shows a rapid transition from 25 to 55 Pa.sec at 3500 sec indicating that the curing completes at this stage. The similar rapid transition in viscosity for epoxy-5 wt. % SiC_p (EP5) happens around 6500 seconds. This asserts that the addition of SiC particles has resulted in a lower viscosity variation and the epoxy retains its fluidity for longer time. This shows that the addition of SiC particle has increased the curing time of the epoxy-5 wt. % SiC_p composite. The increase in curing time by the addition of particles is due to the inhibition provided by the particle for the continuous polymerisation. The higher curing time of the composite is beneficial for the radial diffusion of particle and formation of gradation in the FGM castings. Figure 7.10 shows the variations in storage modulus and loss modulus of both compositions. The cross over point of these curves determines the curing time of a composition more accurately. For epoxy-5 wt. % SiCp (EP5) the curing time is 6200 seconds and for epoxy

alone (EP0) is 4000 seconds, which are closely matching the tangent intercept values obtained from viscosity variations curve(Figure 7.9).

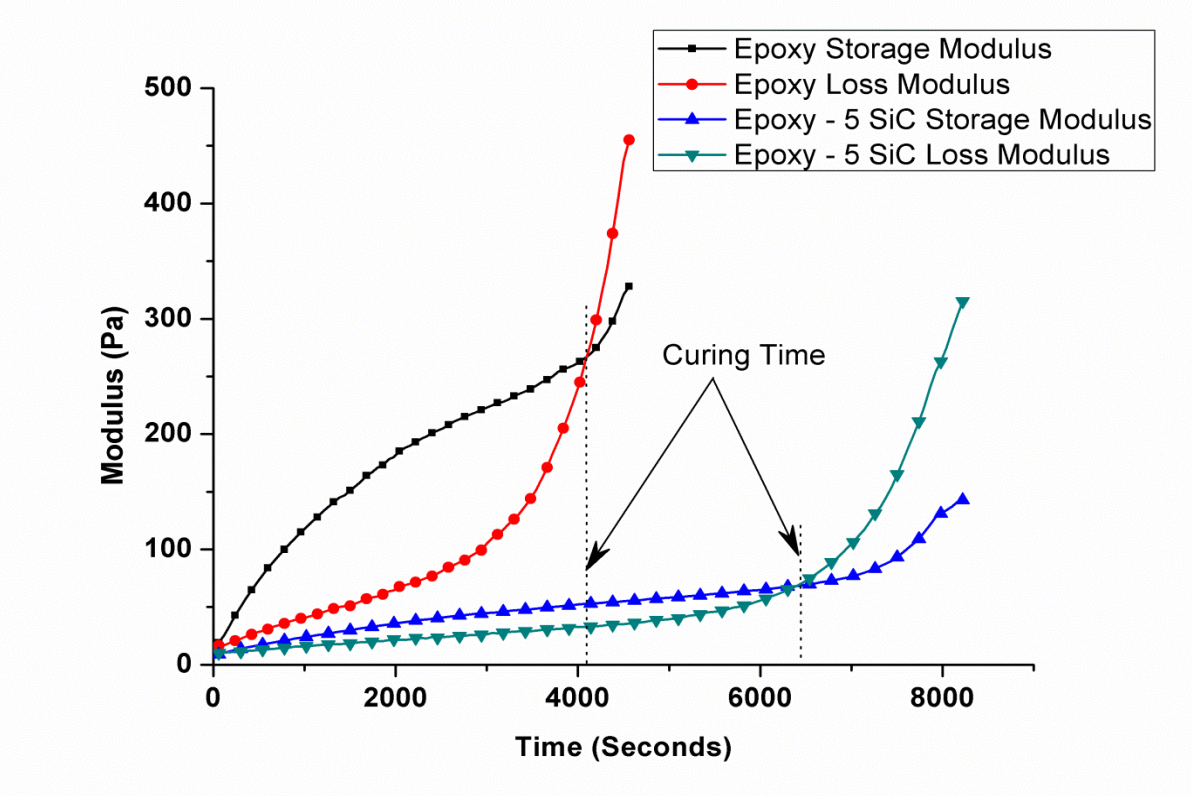

Figure 7.10: Rheology test showing the variations of storage and loss modulus of Epoxy-hardener and Epoxy-hardener with 5 wt % SiC_p

7.4.3 *Microstructural Evaluation*

The prepared mix is poured into the rotating moulds and after giving sufficient rotating time ensuring the complete curing of polymers, the machine is stopped and the moulds are removed. The inner side wall of the metal mould was covered with double sided gum tapes for the easy release of the casting. The casting are removed from the mould (Figure7.7) and cleaned before specimen preparations. The specimen along the axial direction for taking microstructure and hardness are cut along a direction parallel to the centrifugal force in the form of thick slabs of around 1cm thickness (Figure 7.11).

The microstructures of gravity cast Epoxy (EP0) and homogeneous gravity cast Epoxy-hardener with 5 wt % SiCp (EPG5) are shown in Figure 7.12. The reflection mode microstructures of gravity cast Epoxy-5wt % SiC produced by stir casting, taken by using Leica optical microscope, show homogeneous distribution of SiC particles (Figure 7.12 a-e). SiC particles are observed as polygonal shaped white structures in the optical image as observed in (Figure7.12d&e). The SiC particles are well bonded in the particle-

matrix interface and no porosity is observed in the composite. The microstructure of gravity cast Epoxy (EP0) is shown in Figure 7.12f. A clear semi-transparent surface is obtained at all magnifications. The centrifugally cast epoxy (EPC0) also shows a similar microstructure as that of gravity cast EP0 (Figure 7.13). The macroscopic observation shows the outer regions are more transparent and inner regions are light reddish yellow in colour.

Figure 7.14 (A,B) shows the microstructure of the functionally graded epoxy-5 wt % SiCp (EPC5) from inner to outer diameter obtained by centrifugal casting method, taken at a uniform radial distance at different magnifications. The micrographs are taken from inner to outer periphery of the casting along a radial line at mid height of the casting. The region very close to the outer periphery (30 mm OD) shows a thick layer of SiC_p particle about 2mm thickness with very high concentration. A particle graded transition region of 5 to 28 mm thickness is formed between the inner particle depleted region and the outer region. The inner clear zone is almost free from SiC particle, only a very few suspended particles can be observed in this inner region (0 to 5 mm).

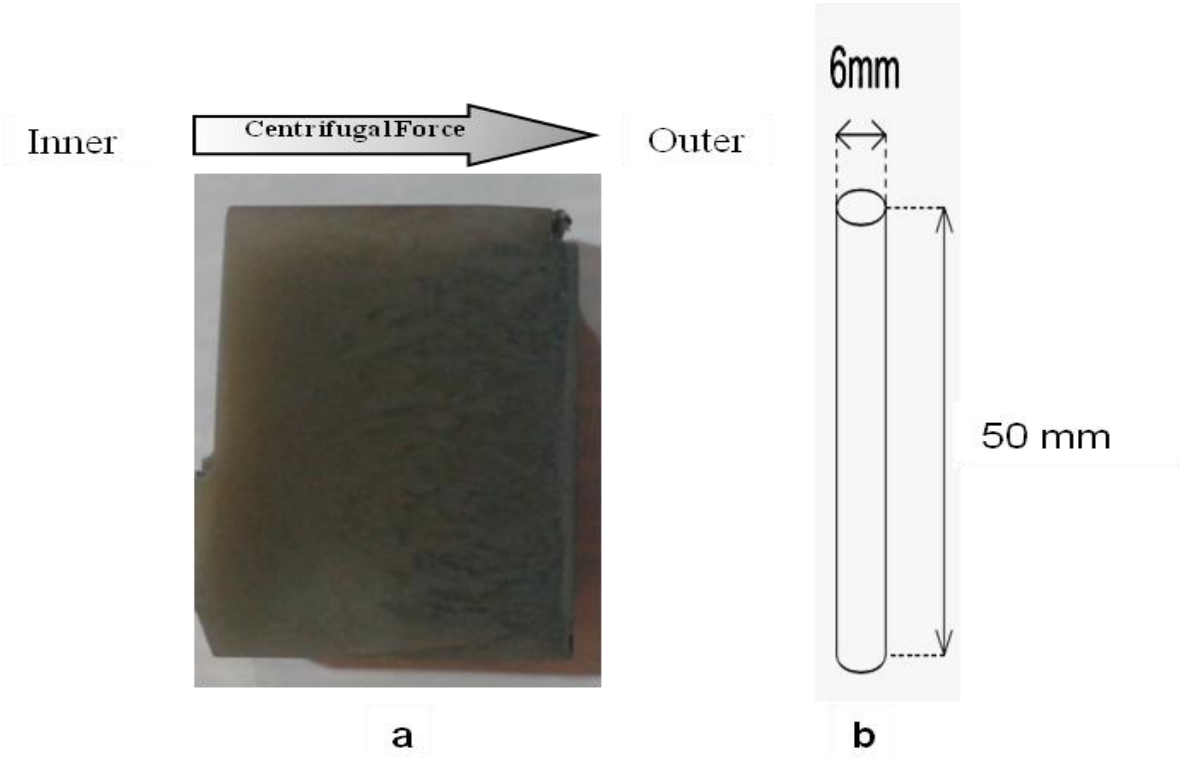

Figure 7.11: specimens (a) Macrograph of microstructure specimen showing different regions of SiCp concentrations from inner to outer diameter with a thick outer layer of SiC_p,(b)Full length wear pin sample prepared along the thickness

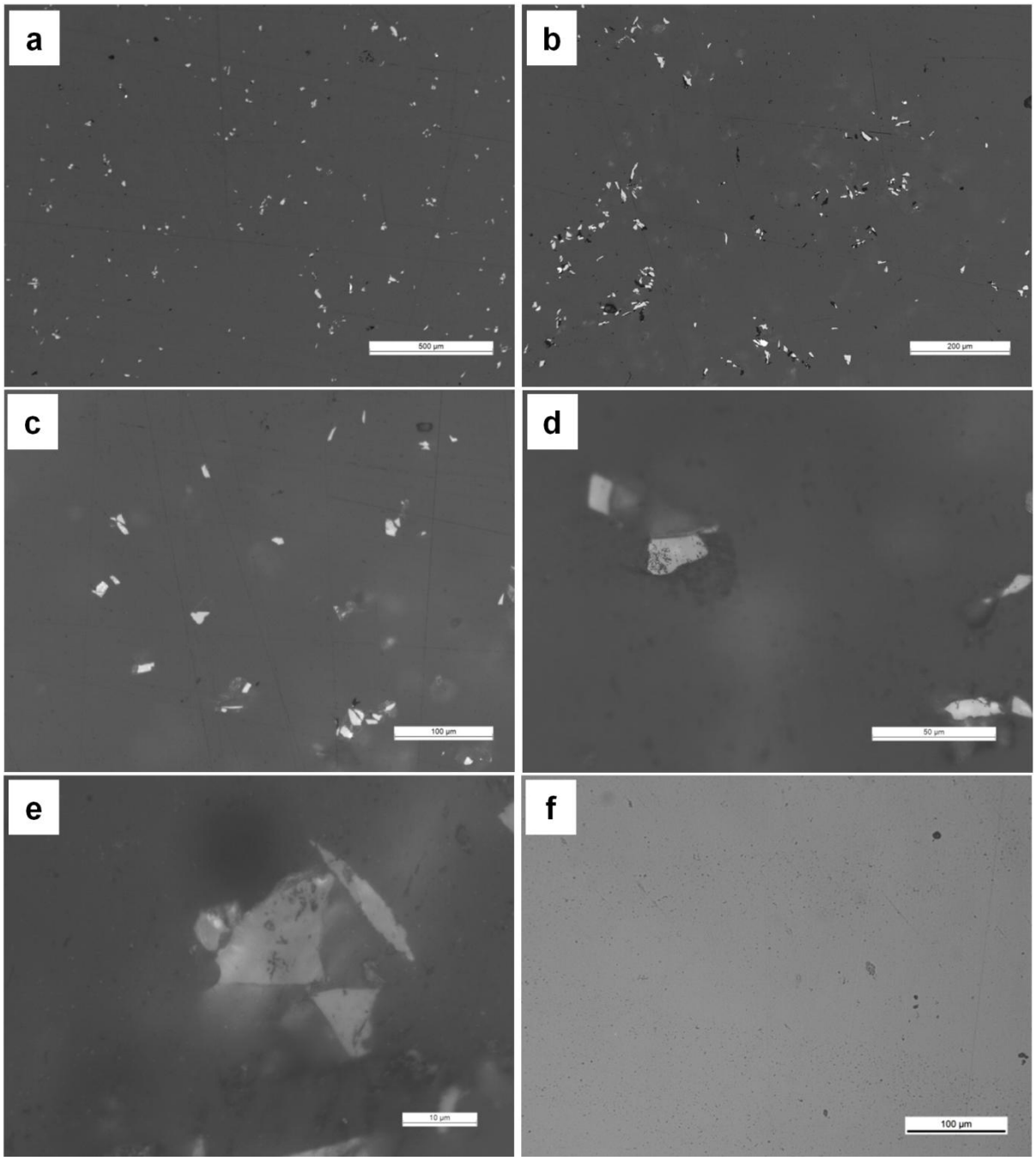

Figure 7.12 Microstructures of (a-e) Homogeneous gravity cast Epoxy- 5 wt % SiCp (EPG5) at different magnifications and (f) Gravity cast Epoxy (EP0)

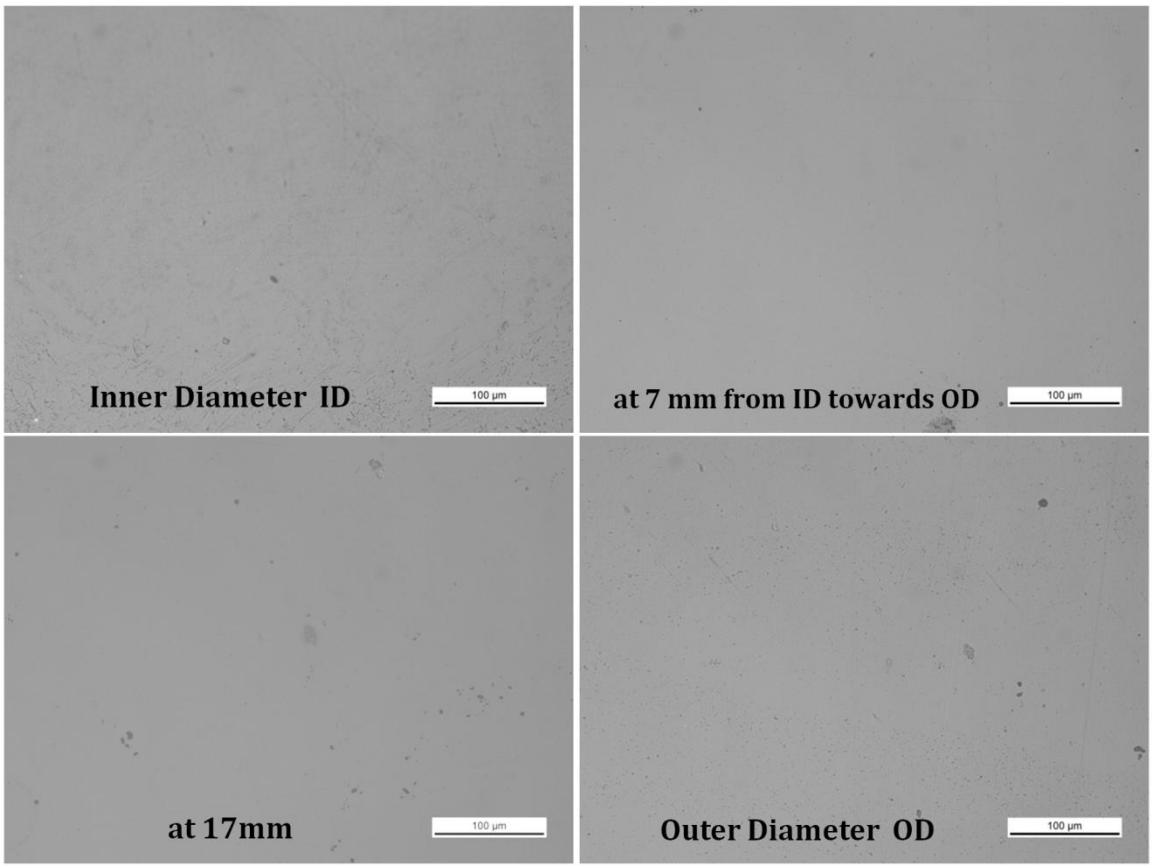

Figure 7.13 Microstructures of Centrifugally cast Epoxy (EPC0) from ID to OD

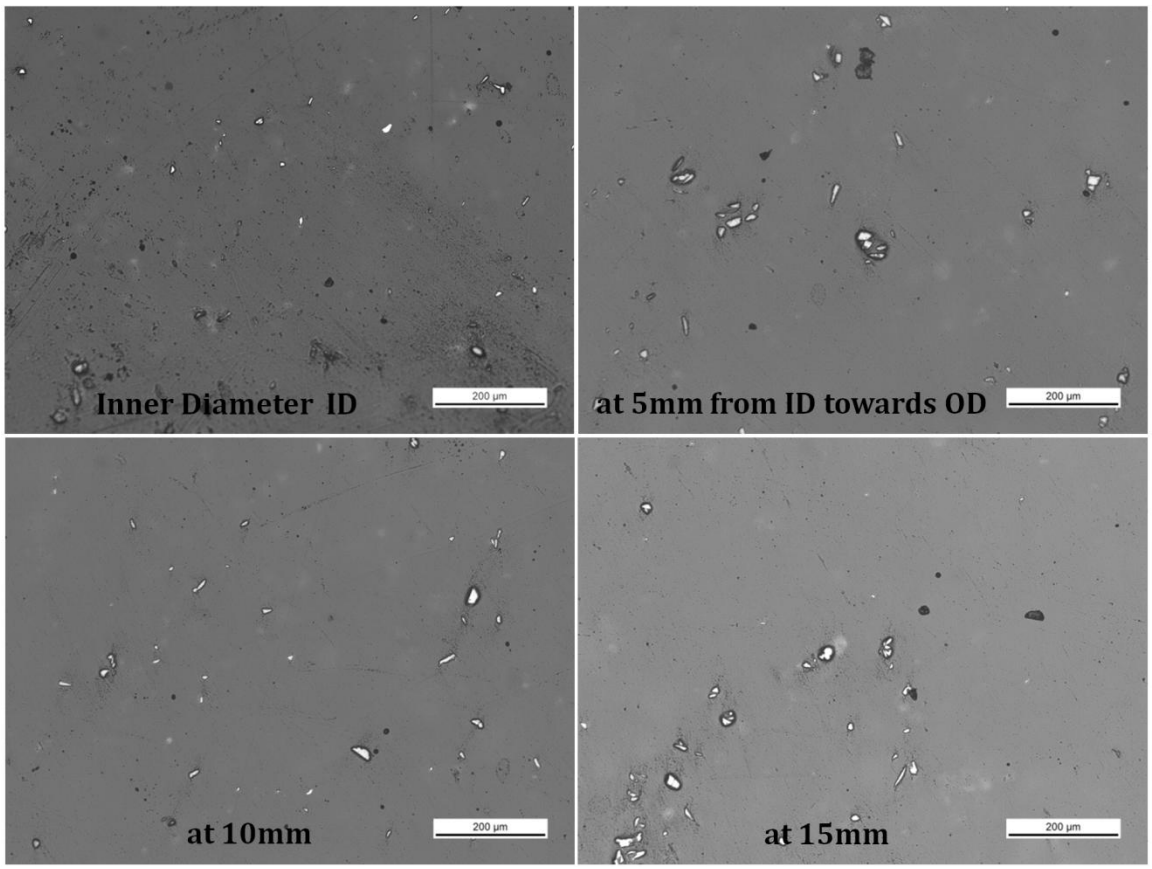

Figure 7.14A: Microstructures of Epoxy- 5 wt % SiCp FGM (EPC5) from ID to OD

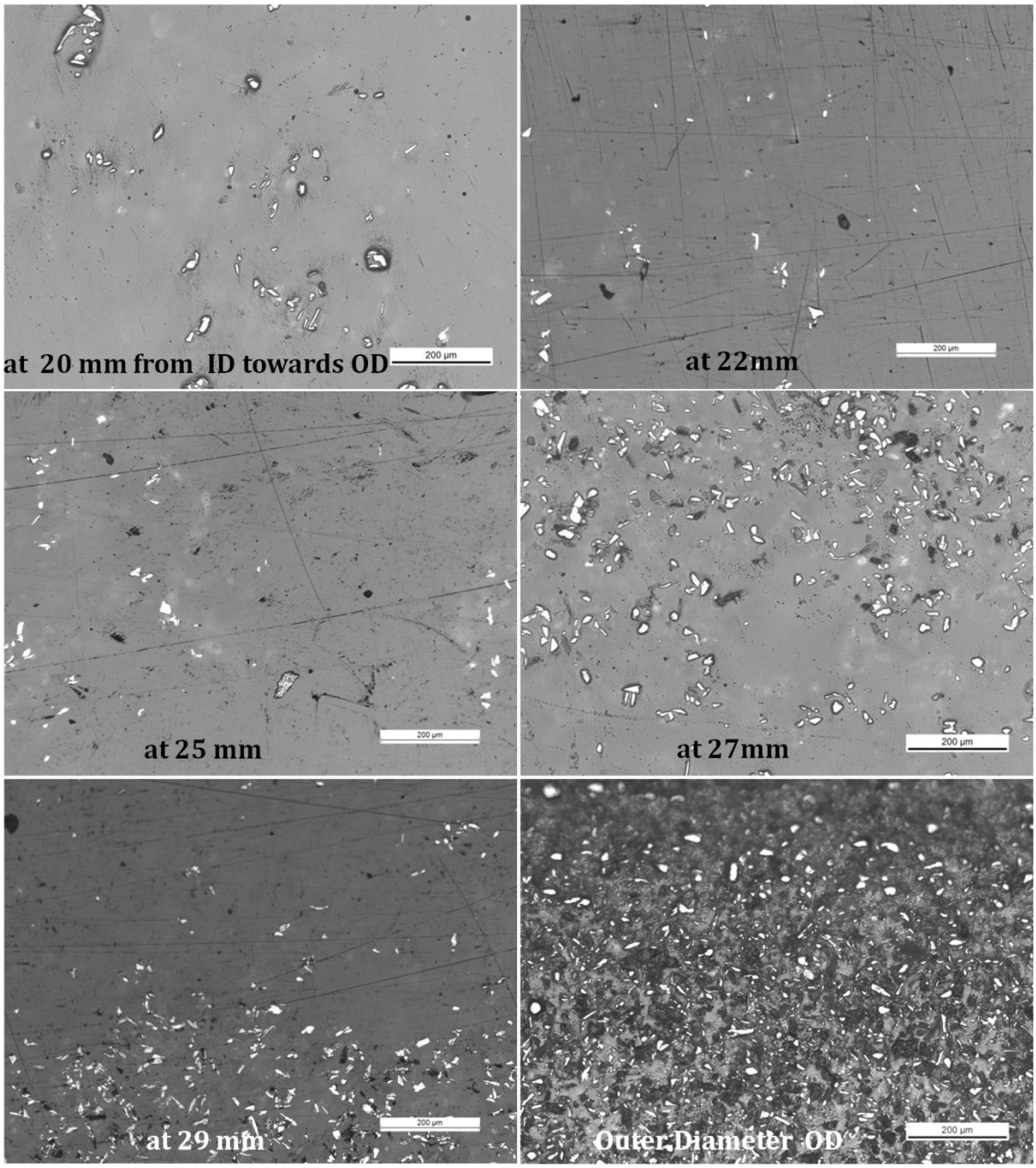

Figure 7.14B: Microstructures of centrifugally cast Epoxy- 5 wt % SiCp (EPC5) from inner diameter to the outer diameter at different magnifications at a uniform radial distance

7.4.4 *Hardness Behaviour*

The Vickers (HV3) hardness values are measured in the radial direction along a line at mid height of the casting at a distance of 3 mm from inner to outer periphery. In the case of epoxy gravity cast with 5 wt.% SiC reinforcement (EPG5), Figure 7.15 clearly shows that the hardness value remains almost same and is minimum. It is due to visco-

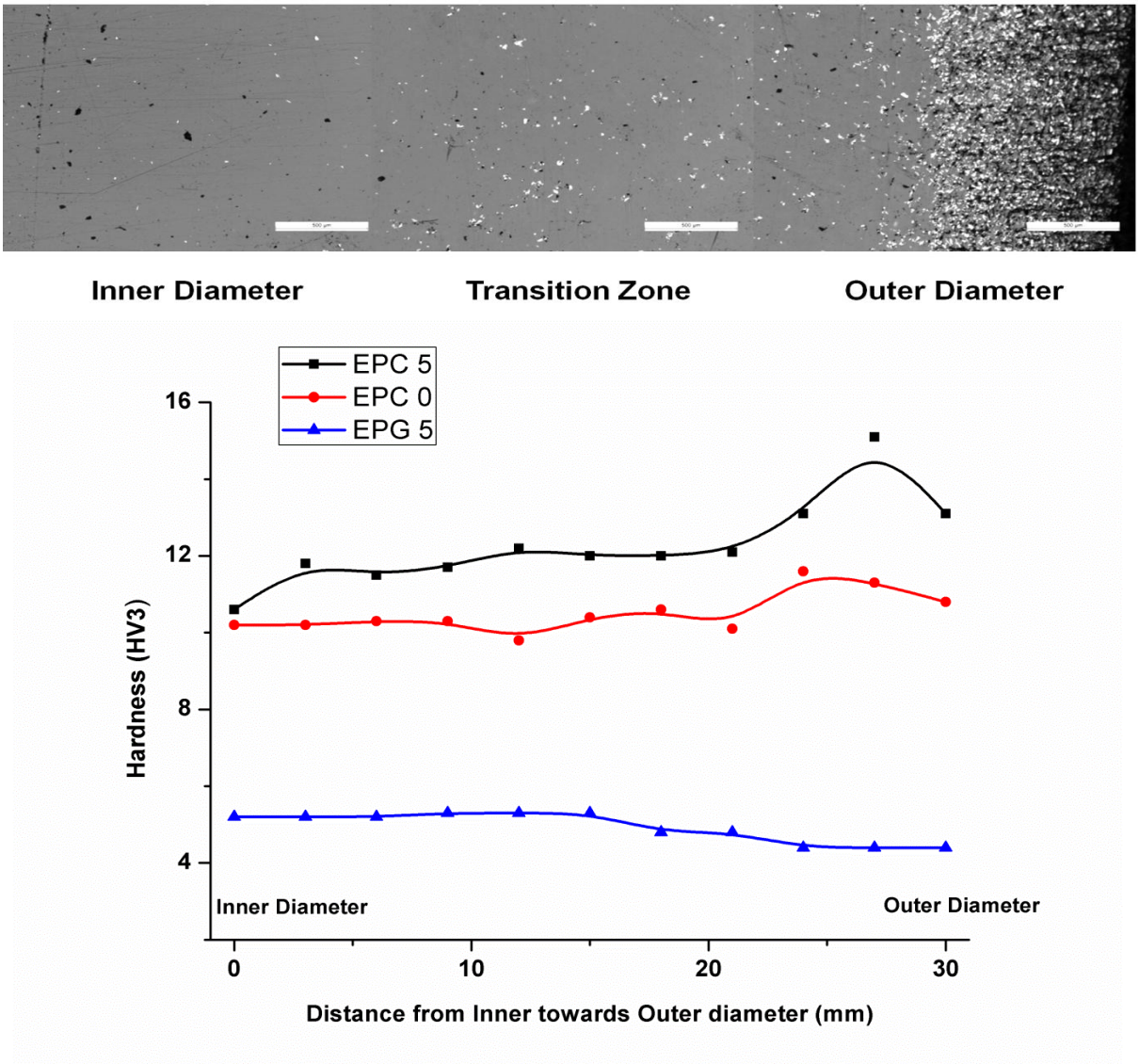

Figure 7.15: Vickers hardness (HV3) variation in radial direction from inner to outer diameter of the castings. EPC5 – Centrifugally cast epoxy-5 wt% SiCp FGM casting, EPC0-Centrifugally cast epoxy casting without SiCp and FPG5-Homogeneous Gravity cast epoxy-5 wt% SiCp casting

elastic flow or the cushioning of the SiC in the epoxy matrix. Rather than resisting the tip indentation during the hardness test the polymer cushions and produces less indentation and returns to normal as the load releases. The value of hardness for centrifugally cast epoxy alone (EPC0) is greater than gravity cast epoxy with 5 wt. % SiC reinforcement (EPG5). The hardness value of homogeneous gravity cast epoxy with 5 wt. % SiC reinforcement (EPG5) is low throughout and varies between 4 HV to 5 HV. The centrifugal force on the polymerization reaction produces effects that are similar to directional solidification i.e. as and when the epoxy monomers link together to form

dense polymer chains they are oriented and pushed radially towards outer regimes making a dense region with change in transparency/ colour. As polymerization approaches towards the inner region the centrifugal effect reduces resulting in lower hardness. The maximum hardness of 11.5 HV3 is observed in the outer region of EPC0 and is gradually decreases to 10 HV3 towards the inner regions. The centrifugal effect is evident in EPC0. There is a clear increase in hardness value just because of processing method change; i.e. from gravity to centrifugal casting the hardness values gets doubled due to the centrifugal effect ,compaction and orientation. The highest value of 15HV3 hardness is observed for outer region of EPC5 due to the greater concentration of SiC particles in this region. Towards inner region the hardness value decreases to a value 10 HV3 through a large transition region.

7.4.5 *Tensile Properties*

Figure 7.16 illustrates the variations in ultimate tensile strength (UTS) for the gravity (EPG5) and centrifugal cast EPC0 and EPC5 samples taken from inner (I), transition (T) and outer (OD) regions. The ultimate tensile strength of the matrix material is higher than that of the composite materials. The maximum value of 43 MPa is obtained for the inner zone of centrifugal cast epoxy with 0 wt. % SiCp (EPCO(I)) and the value gradually decreases to 40MPa at the outer (EPCO(O)). In the case of centrifugal casting with 5 wt. % SiCp (EPC 5), the inner specimen (EPC5(I)) has an ultimate tensile strength value of 37 MPa which decreases to 32 MPa at the outer (EPC5(O)). The homogeneous gravity cast specimen with 5 wt.% SiCp(EPG5) has a value 37.5 MPa. The influence of centrifugal force on tensile property is also clearly evident with the effects of reinforcement additions.

Figure 7.17(A, B) shows the SEM fractograph for the surface of tensile samples taken from different regions of the casting. Figure 7.17A (b) shows fracture surface with dimples of specimen taken from the inner region of EPC0(I). Figure 7.17A (d) shows the sand beach patterns of plastic deformations, which are generally observed in brittle failures and are similar to chevron marks in metals (signatures of brittleness). The crack initiation and the direction of propagation indicate the inner specimens which are less populated with reinforcements have brittle failure with higher ultimate strength values. Figure 7.17B (h, j and l) shows the SEM fractograph of outer region specimens of EPC5(O). Delaminated SiCp particles, fractured resin debris and cleavage failure

surfaces indicate the brittle nature of failure. Sharp cleavage edges are clearly visible in Figure 7.17B (h). The presence of hard ceramic reinforcements in SEM confirms brittle failure with the lower UTS values obtained at the outer region. Similar brittle failure is observed in the outer region specimens of EPCO(O) Figure 7.17B (g, i and k). Fractured resin debris 7.17B (k) confirms more brittleness.

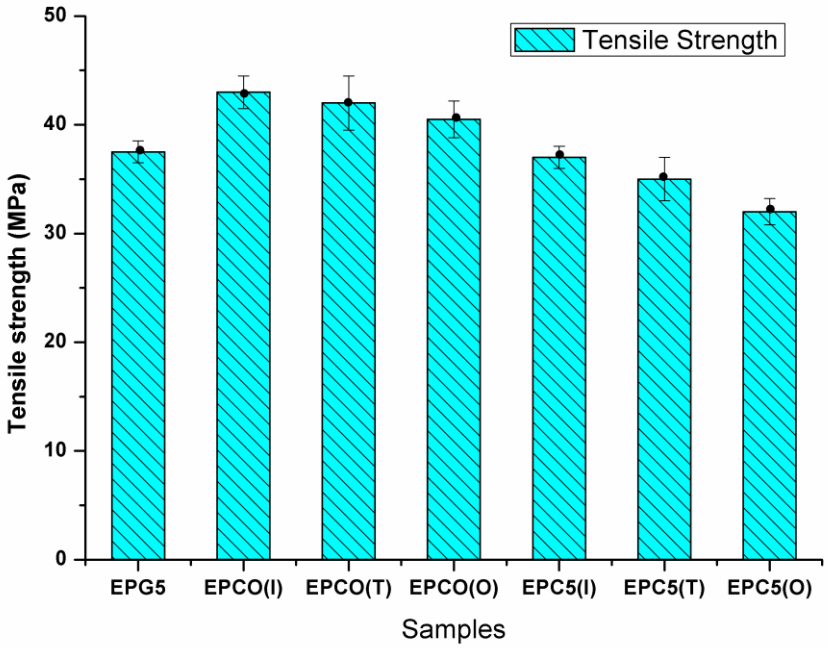

Figure 7.16: Ultimate Tensile Strength (UTS) variations in radial direction from inner to outer diameter of the castings. Specimens are taken from inner (I), Transition (T) and outer regions (O) of the FGM casting. EPG5- Homogeneous Gravity cast epoxy-5 wt%, EPC0-Centrifugally cast epoxy casting without SiCp and SiCp EPC5 – Centrifugally cast epoxy-5 wt% SiCp FGM casting.

7.4.6 *Wear Characteristics*

Wear is the unpreventable consequence of friction in a sliding contact and is computed in terms of loss of mass during a sliding contact. In polymers, wears due to a sliding contact against a hard counter face can be of abrasive, cohesive, interfacial, adhesive or chemical nature. Thermosetting polymers show high coefficient of friction and high wear rate despite of their high values of strength and hardness among other polymers. FGM's have paved way for modification of wear properties in case polymeric materials. Dry wear tests are carried out on wear specimens taken from different location of the composite and the results are compared with the homogeneous castings.

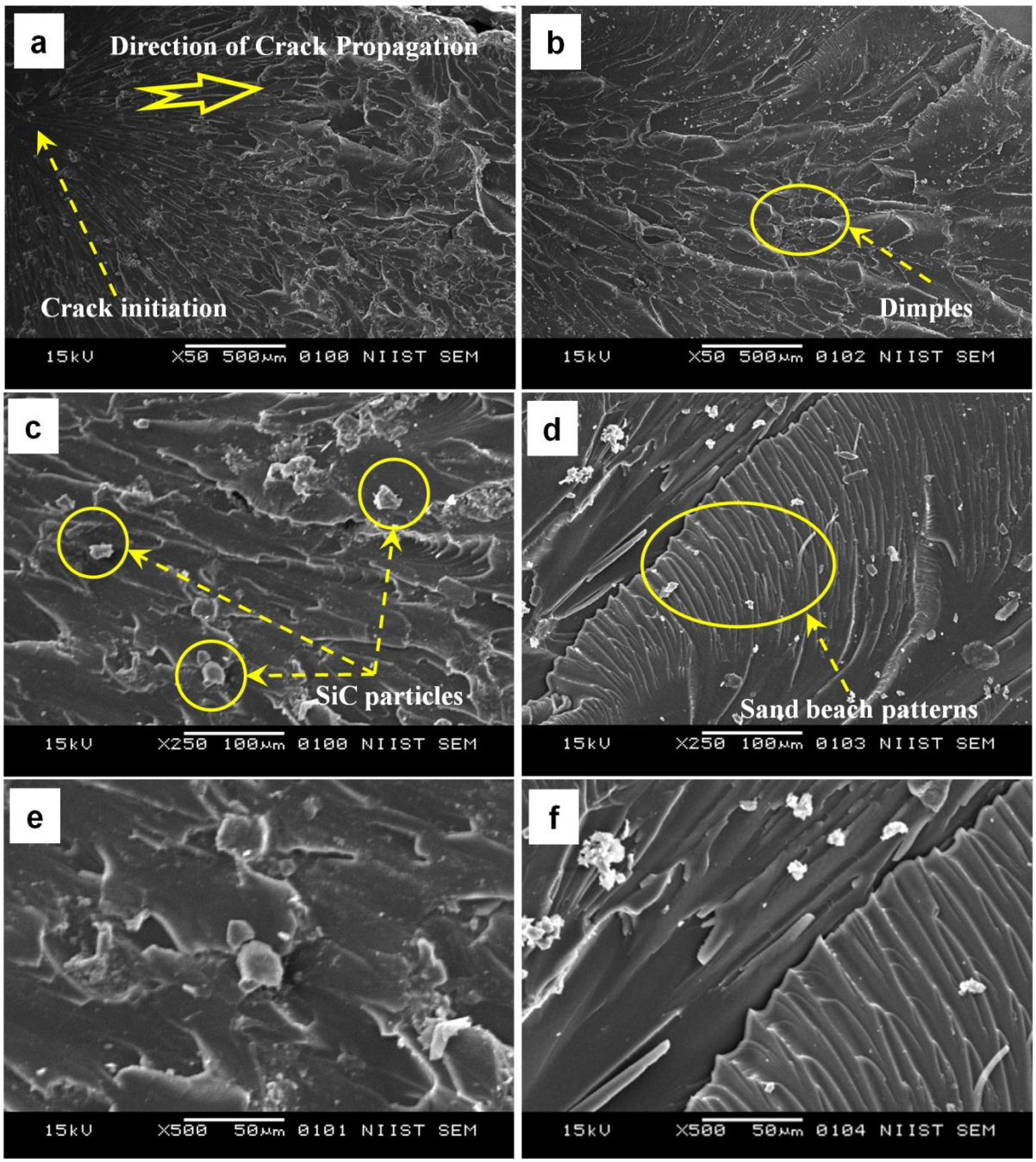

Figure 7.17A: SEM Fractograph of tensile specimens. EPG5- Epoxy-5wt%SiCp gravity casting (a,c,e), EPC0(I)-Centrifugally cast epoxy without SiCp inner region specimen (b,d,f)

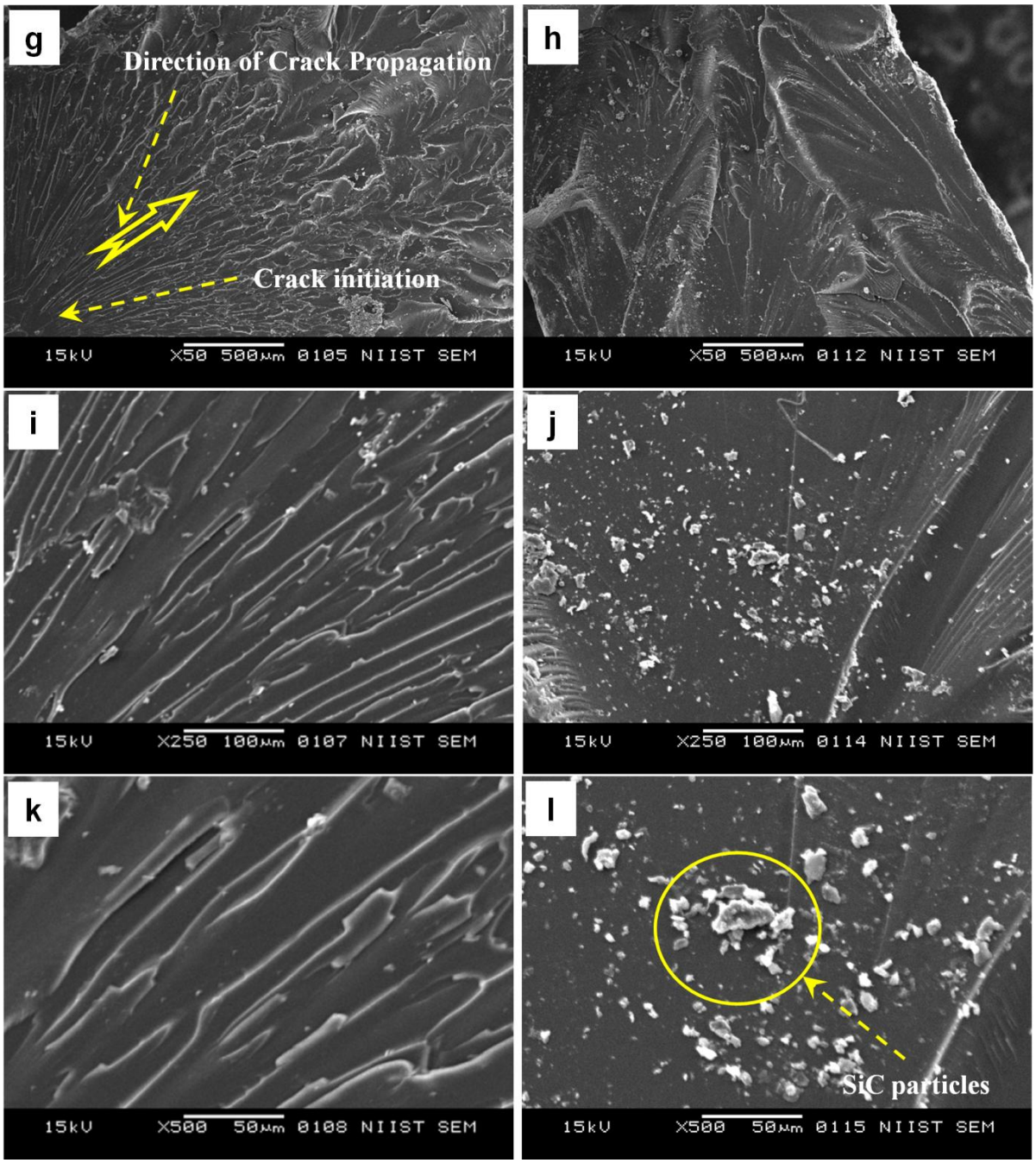

Figure 7.17B: SEM Fractograph of tensile test specimens. EPC0(O)-Centrifugally cast epoxy casting without SiCp outer region specimen (g,i,k) EPC5(O) – Centrifugally cast epoxy-5 wt% SiCp outer specimen (h,j,l)

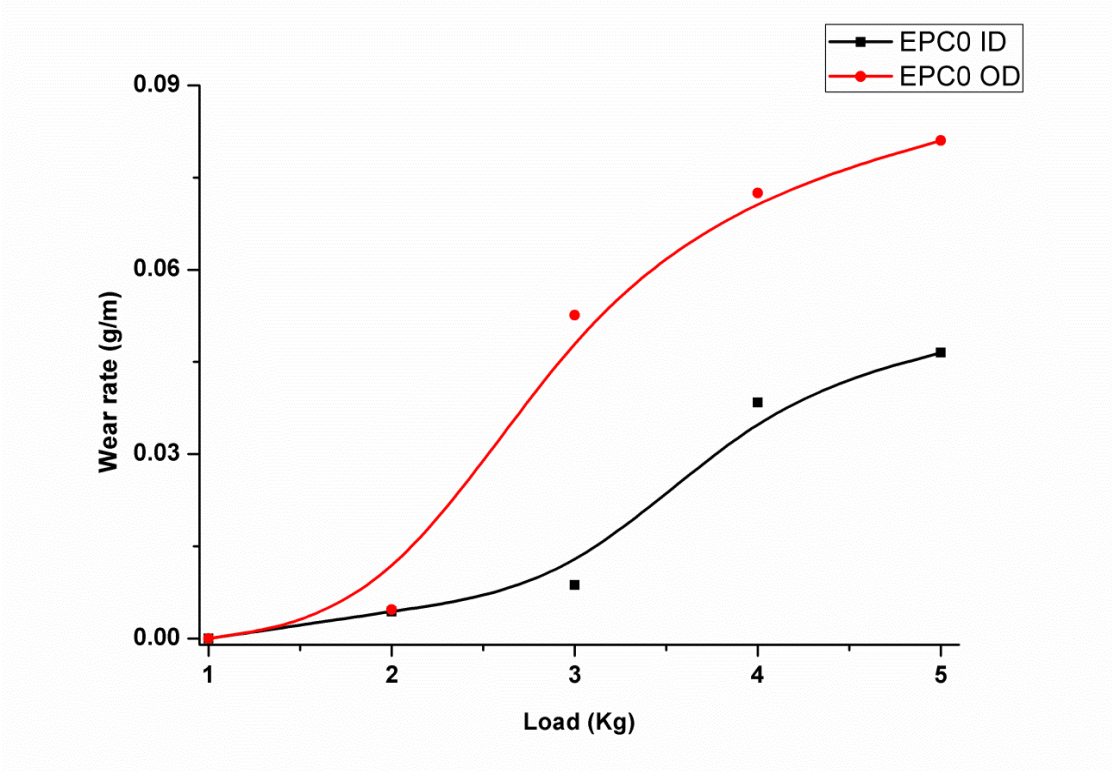

Figure 7.18: Wear loss of pins of EPC0- centrifugally cast epoxy casting without SiCp. Specimens taken from inner and outer regions of the castings

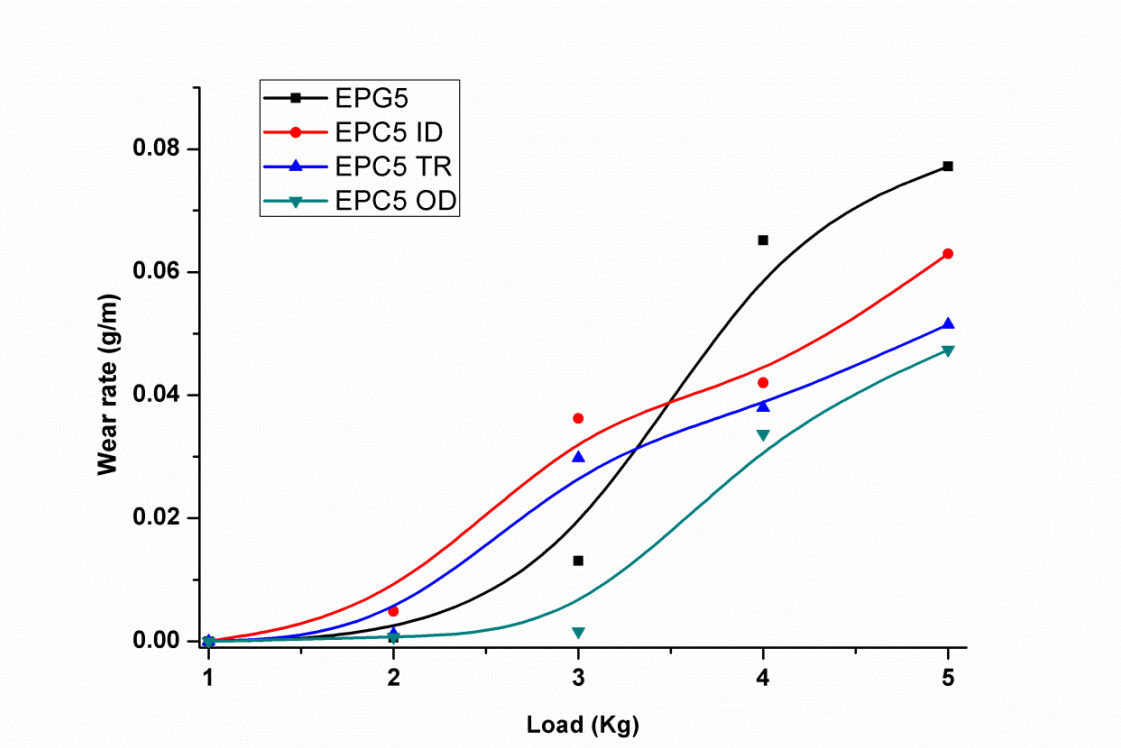

Figure 7.19: Wear loss of pins from inner (ID), transition (TR) and outer regions (OD) of the EPC5-Centrifugally cast epoxy-5 wt% SiCp FGM casting, and EPG5-Homogeneous Gravity cast epoxy-5 wt% SiCp casting

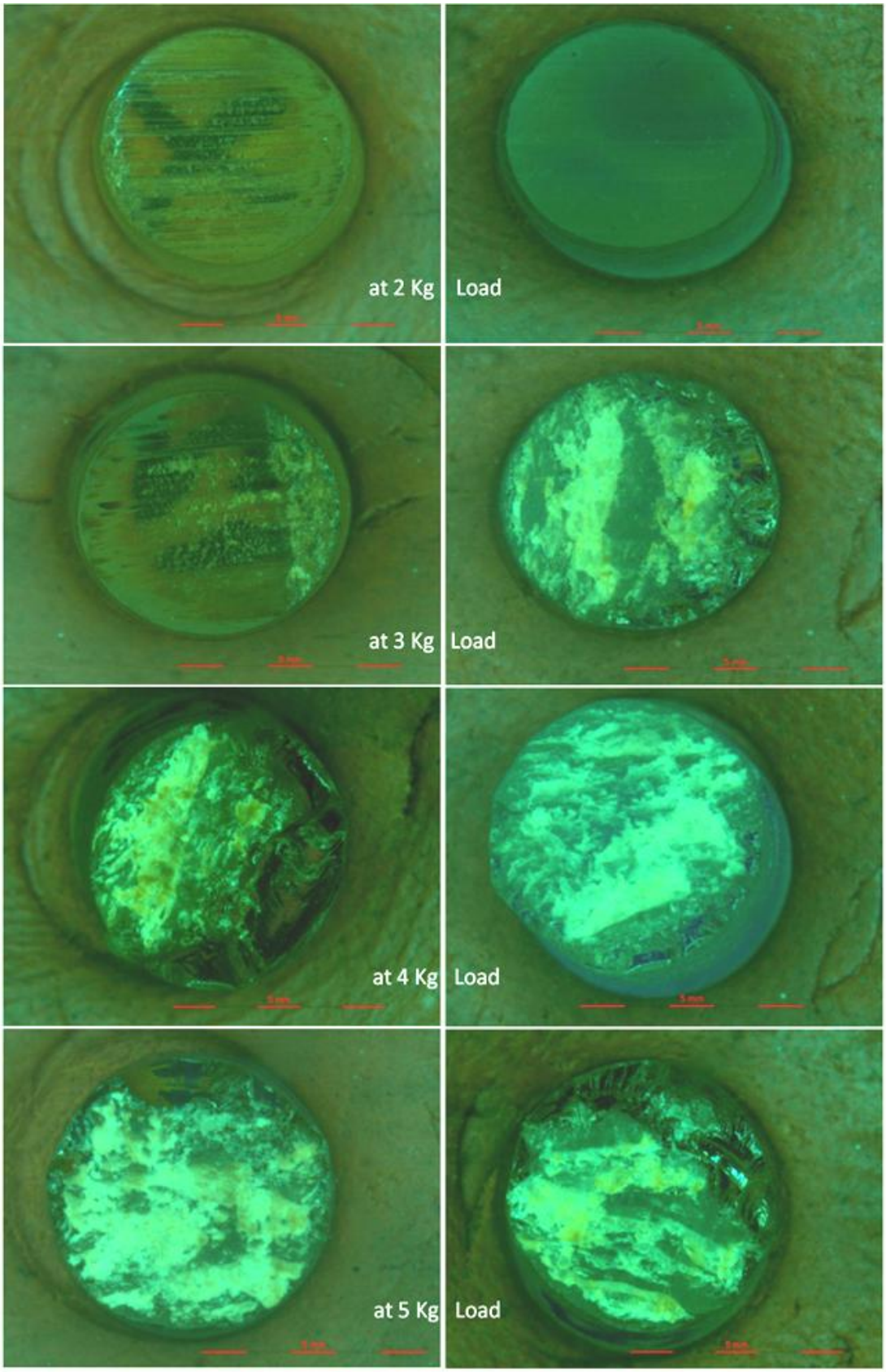

Figure 7.20: shows the wear scars formed on the surface of the pin taken from the inner and outer region of EPC0 at different loads

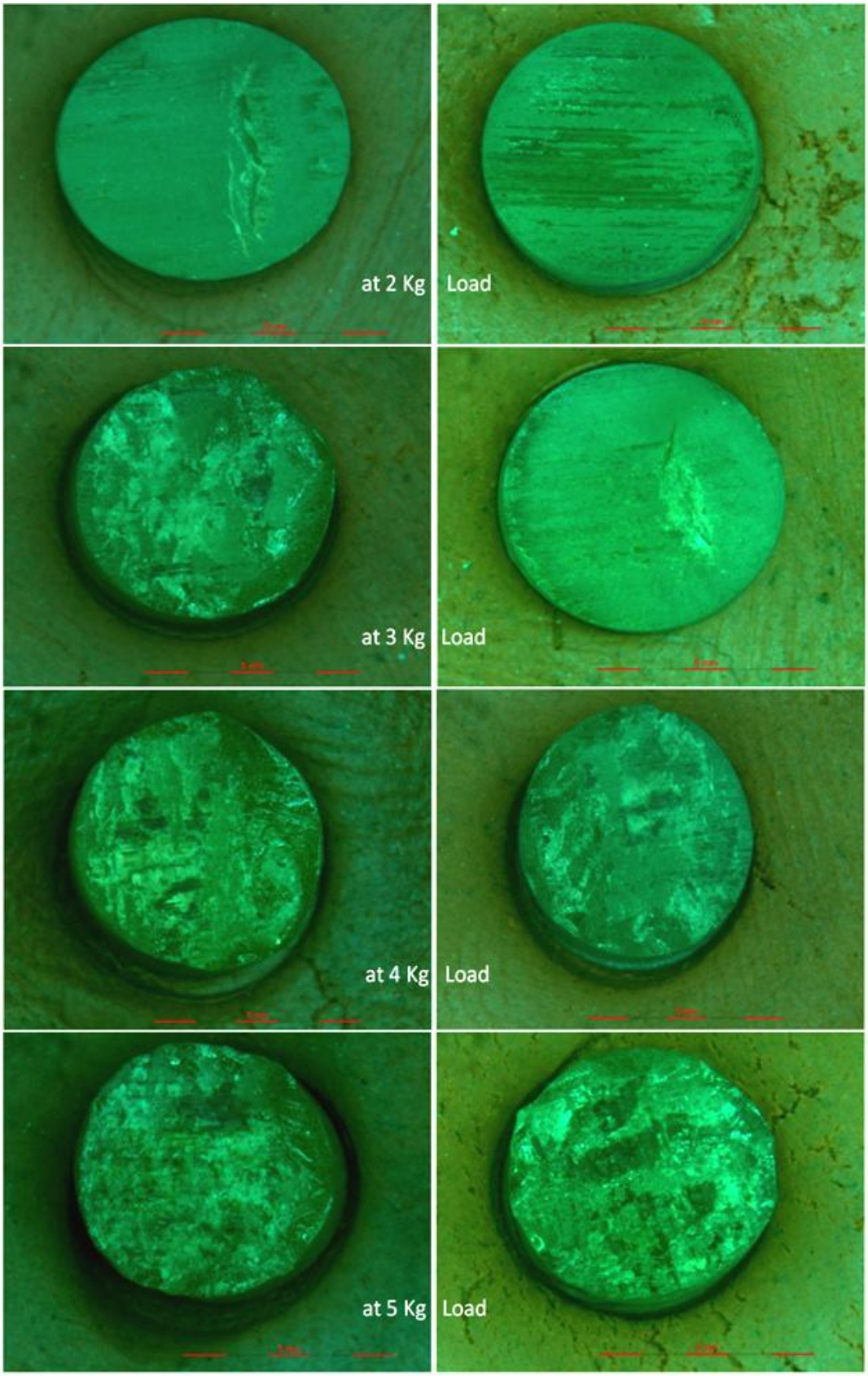

Figure 7.21A: shows the wear scars formed on the surface of the pin taken from the inner and outer region of EPC5 at different loads

With a sliding velocity of 3 m/s for a sliding distance of 3000 m with a pin of 6mm diameter and 30mm length on pin on disc tribometer for a load variation of 1 kg to 5 kg. Figure 7.18 shows the wear rate values for the inner and outer region of the centrifugal cast epoxy with 0 wt. % SiCp (EPC0). Wear rate is maximum in case of outer periphery of EPC0(OD) at a load of 5 kg and a minimum for the pin taken from the inner portion of EPC0(ID). Figure 7.19 shows the wear rate values in pin on disc for the composite specimens from the inner, transition and outer region of the centrifugally cast epoxy-5 wt% SiCp FGM casting (EPC5). The outer region of the EPC5 ring is enriched with SiC particles meanwhile the concentration of SiC particle to the inner periphery is minimum all specimens show almost no wear at 1 kg load. The outer pin (EPC5 OD) has a minimum wear rate of 0.0007 g/m at a load of 2 kg and a maximum of 0.0474 g/m at a load of 5 kg. The inner pin (EPC5 ID) shows 0.0049g/m and 0.063 g/m respectively, which are higher when compared to the outer pins. It is evident that the specimen from the outer part of the EPC5 ring shows better wear resistance than the specimen from the inner part of the ring.

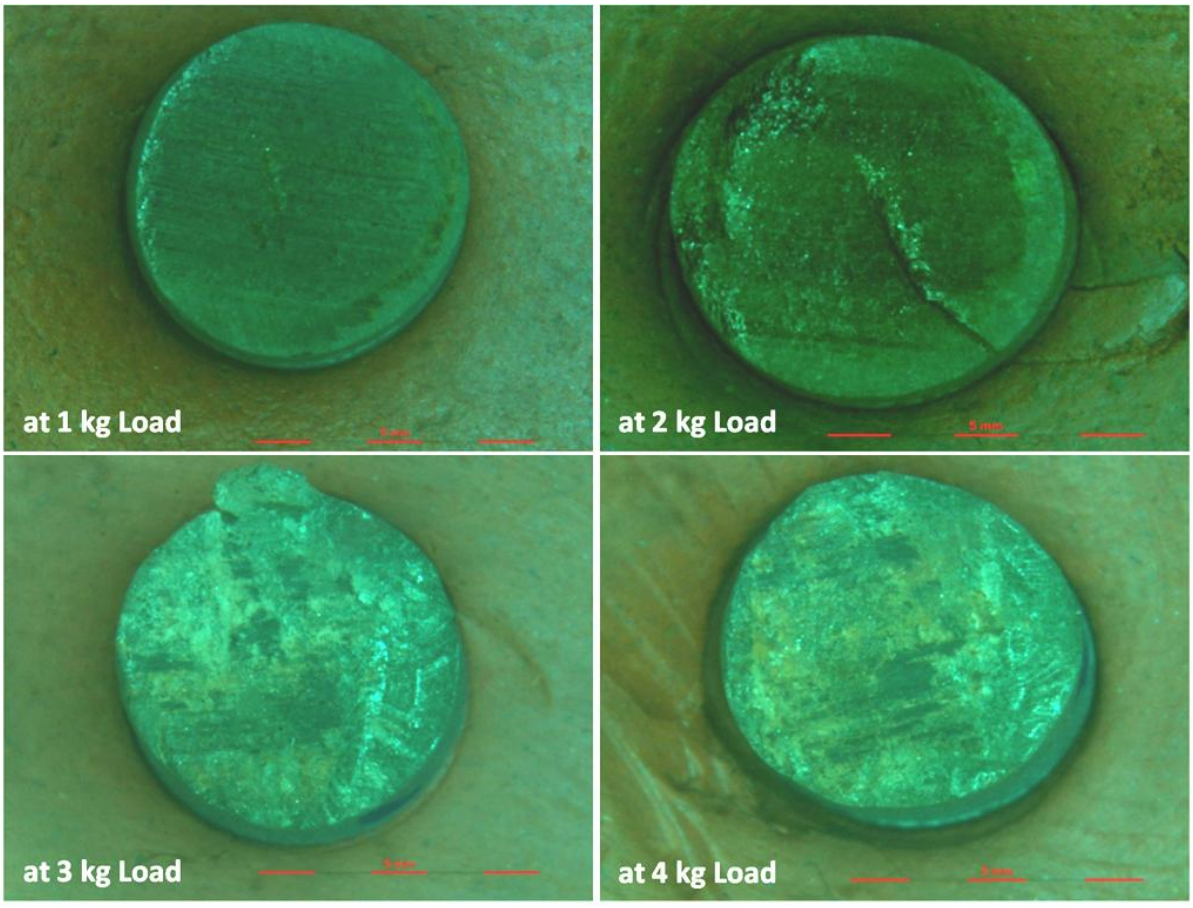

Figure 7.21B: shows the wear scars formed on the surface of the pin taken from the inner and outer region of EPG5 at different loads

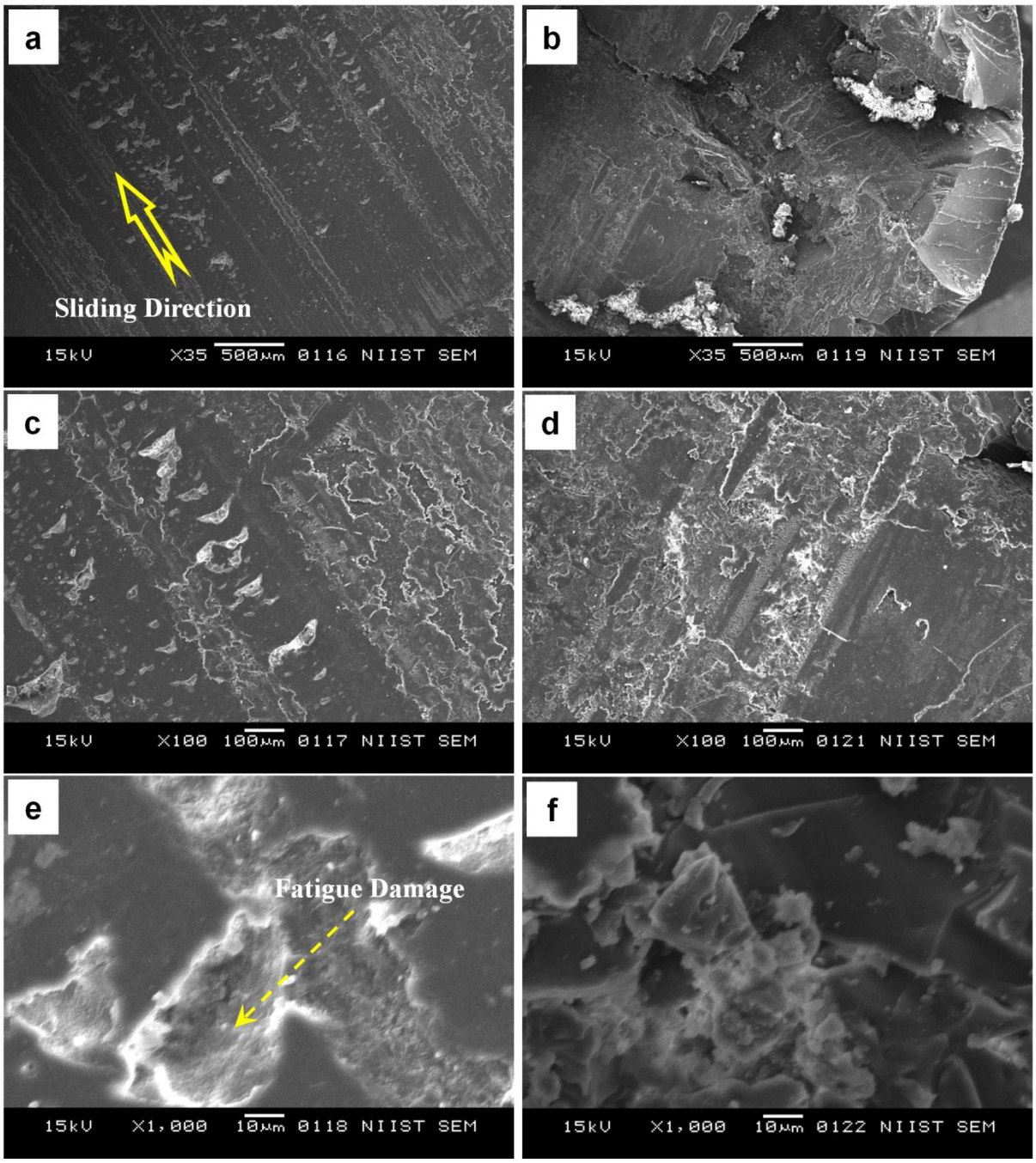

Figure 7.22A (a-f) shows the SEM observations of worn surface of pin from the inner region of EPC0 at 2 kg (a,c,e) and outer pin of EPC5 (b,d,f) to a load of 5 kg

This is because there is much higher concentration of SiC particles in the outer diameter due to the centrifugal action during the casting process. For the gravity castings (EPG5) the value of wear rate is comparatively less for 2 and 3 kg but there is a considerable increase in the wear rate when the load is increased to higher values (4 kg and 5 kg), where a mild to severe wear transition is observed. Figure 7.20 shows the wear scars formed on the surface of the pin taken from the inner and the outer region of EPC0 at different loads. Material removal is more in case of the outer pin and some part of the

material sheared off from the surface at loads 3kg and 5 kg. But in case of outer pin of the FGM casting EPC5OD, at similar loads, the material removal from the pin surface is lesser as there is higher concentration of SiC particles, which provide an extra abrasion resistance to the epoxy material (Figure 7.21A). Figure 7.21B shows the worn out surfaces of epoxy with 5wt % SiC gravity casting at various loads. A transition is observed at 4 kg load and uniform wear without any break off is experienced. In addition to vertical pins at a radial position, radial pins with axis parallel to radial rays of the casting are also wear tested. Wear surface of the radial pins are observed with the outer particle rich region being the rubbing surface. In this case very fine wear scars are detected on the surface of the wear pin even at a load of 5kg with negligible weight loss.

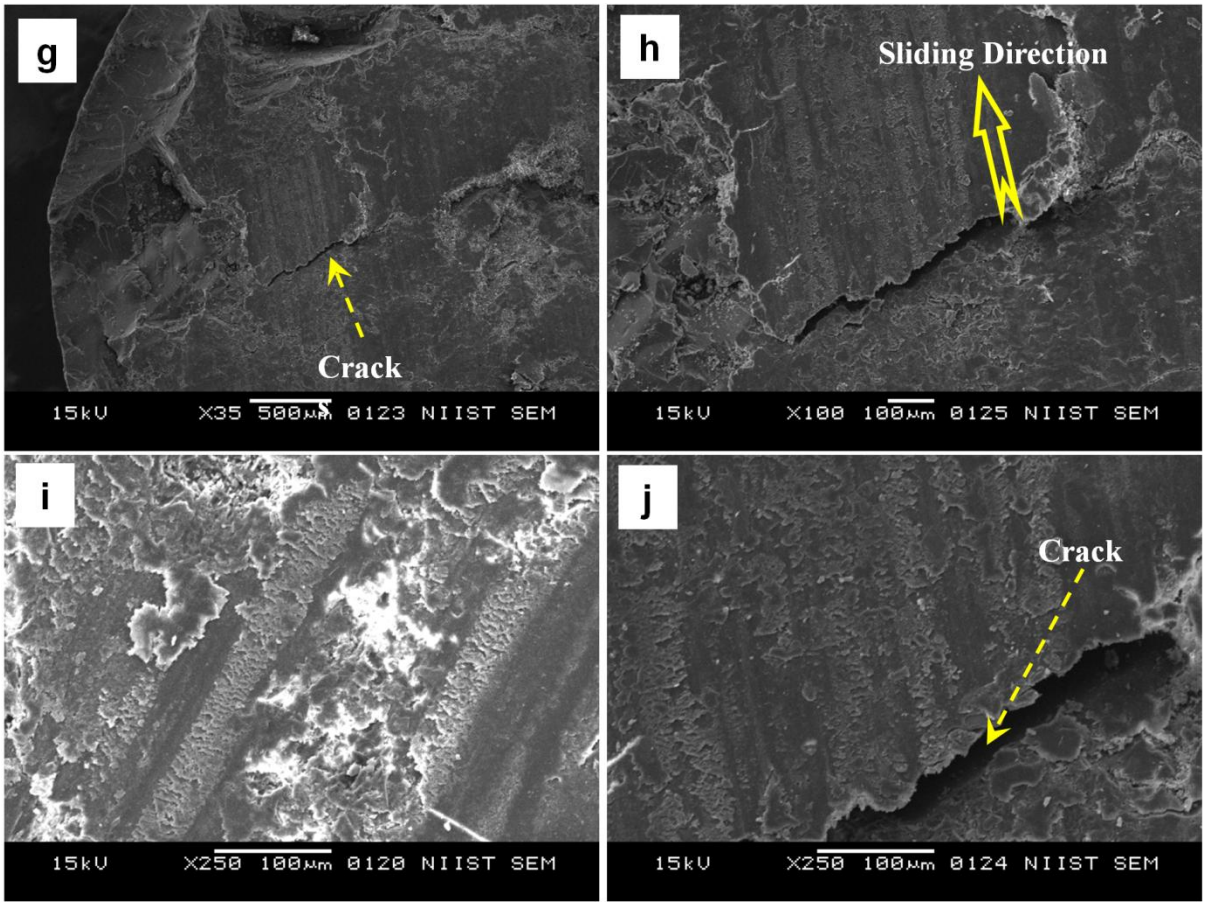

Figure 7.22B (g,h,i and j) shows the SEM observations of worn surface of pin of EPG5 corresponding to a load of 5 kg

Figure 7.22A (a-j) shows the SEM observations of worn surface at room temperature and a few white lines which corresponds to fatigue damage are observed perpendicular to the sliding direction along the worn track [230]. The protruding SiC particles covered with epoxy resins are clearly visible in Figure7.22A (f). These surfacing SiC particles protect the epoxy matrix from further contact and minimising the

wearing material loss. The top layer disintegrated causing severe wear damage in case of filled epoxy gravity cast specimen at contact pressures of 5 Kg (Figure 7.22B (g)). Even macro cracks can also observed normal to the sliding direction indicating the parting off tendency of pin surfaces (Figure 7.22B (h, j)). The higher contact pressure leads to more massive material loss and this proclaims that abrasive wear mechanism plays the major role. Higher frictional temperature at the surface occurs due to higher contact pressure and hence more severe abrasive wear occurs. SEM image for the wear surface of outer pin of EPC5 predicts minimum material removal rate.

7.5 CONCLUSIONS

- Functionally graded polymer matrix composites (FGPMC) reinforced with 5 wt. % SiCp, of average size 23 μm were processed successfully by liquid stir casting method followed by vertical centrifugal casting at a lower speed of rotation of 500 rpm.
- The microstructure analysis shows a higher concentration of SiC particles towards the outer periphery of the FGM casting with different regions while the gravity casting shows a uniform distribution of reinforcements.
- Three regions are formed, namely particle rich outer zone, transition and polymer rich inner zones.
- The hardness testing shows that the centrifugal casting method itself had improved the hardness of polymer to a measurable level by Vickers scale (HV3). The hardness value maximum of 15 HV3 is obtained at the outer periphery of the FGM casting due to higher concentration of SiC particles.
- The maximum value of ultimate tensile strength (UTS) of 43 MPa is obtained for the inner zone of centrifugal cast epoxy with 0 wt. % SiCp and the value gradually decreases to 40MPa at the outer. A clear transition from mild brittle nature to more and more brittle is observed and confirmed by the SEM images.
- The functional gradation in SiC particles is strongly appraised from the results of the wear test.
- The dry pin on disc wear test confirms that the abrasive wear is the major wear mechanism responsible for wear losses in these FGPMC castings.

Chapter 8

Summary and Scope of Future Studies

The present investigation has successfully demonstrated the application and capability of centrifugal casting technique in tailoring the functionally graded microstructure and properties in aluminium metal and epoxy polymer composites using silicon carbide particles as the ex-situ reinforcement. The study also explored the use and effectiveness of centrifugal casting in forming functionally graded structures and components by in-situ primary silicon and Mg_2Si particle reinforcement in hypereutectic Al-Si alloys. A prototype functionally graded IC engine piston, was fabricated by centrifugal casting method, shows enhanced structural, mechanical and tribological properties.

The major findings of the present investigation are summarised below.

A319 – SiC reinforced FGM

- A319 Aluminium functionally graded metal matrix composites (FGMMC) reinforced with different weight percentages SiC (10, 15 and 20wt %) of average size 23 μm were processed successfully by liquid stir casting method followed by vertical centrifugal casting.
- There is a shift of the position of maximum concentration of SiC particles towards the outer directions for higher percentage of additions. With a radial shift, from 55mm to 75 mm, for 15-FGM, the maximum of 28 wt % SiC is obtained.
- The density maximum of 2.87 g/cm^3 along with the lowest CTE value of 20.1 μm /mK are also obtained in the particle rich zone of 15-FGM casting.
- The maximum compressive strength of 15-FGM is 650 MPa in the particle rich region.
- Particle rich region shows enhanced wear resistance.

A390 Ex-situ and In-situ particles reinforced FGM

- A390-SiC FGMMC with 10 and 15 wt % SiCp particles, 23μm size, was successfully processed by the centrifugal casting.

- Aluminium FGM with in-situ primary Si and Mg_2Si reinforcements have been fabricated successfully by the centrifugal casting process using A390 commercial Al alloy and Mg addition in pure and master alloy state.
- In-situ functionally graded Al composite pistons were successfully designed and fabricated by vertical centrifugal casting technique. Two different zones of primary Si rich zone and eutectic silicon rich zones were observed. Higher concentration of primary Si particles gets gradually distributed towards the head region of the piston providing enhanced properties.
- Magnesium provides substantial strengthening and improvement of precipitation hardening phases of aluminium alloy. Centrifugally cast FGM pistons provide high hardness and wear properties than that of conventionally gravity cast pistons.

A6061 – SiC reinforced FGM

- Wrought aluminium A6061 FGMMC with SiCp reinforcements have been fabricated successfully by the centrifugal casting process.
- The FGMMC microstructures reveal that centrifugal force has a greater influence in the formation of gradation in the system. The distribution curves of SiCp reinforcements in the radial direction show that the position and magnitude of concentration of SiCp depends on percentage of initial addition.
- The study clearly depicts that the gradient nature of the structure and properties of the FGM rings can be controlled by particle addition as well as by phase distributions
- Similarly the hardness and ultimate tensile strength show a graded nature in correlation with particle concentration and are higher at particle rich region.
- The wear resistance is higher in the particle rich region of the FGMMC.

Epoxy – SiC reinforced FGM

- Functionally graded polymer matrix composites (FGPMC) reinforced with 5 wt. % SiCp of 23 μm average particle size were processed by liquid stir casting method followed by vertical centrifugal casting at a lower speed of rotation of 500 rpm.
- The microstructure analysis shows a higher concentration of SiC particles towards the outer periphery of the FGM casting with different regions while the gravity casting shows a uniform distribution of reinforcements. Three regions

are formed, namely particle rich outer zone, transition and polymer rich inner zones.

- The hardness testing shows that the centrifugal casting method itself had improved the hardness of polymer to a measurable level by Vickers scale (HV3). The hardness value maximum of 15 HV3 is obtained at the outer periphery of the FGM casting due to higher concentration of SiC particles.
- The maximum value of ultimate tensile strength (UTS) of 43 MPa is obtained for the inner zone of centrifugal cast epoxy with 0 wt. % SiCp and the value gradually decreases to 40MPa at the outer.
- The functional gradation by SiC particles provides enhanced the wear resistance.
- The dry pin on disc wear test confirms that the abrasive wear is the major wear mechanism responsible for wear losses in these FGPMC castings.

Scope of Future Studies

The centrifugal castings have so many advantages like it is a coreless production process for cylindrical parts which can be made into rapid production type economically. They can be used for both ferrous and non-ferrous metals and alloys. The inner periphery containing slag and other impurities can be machined off easily. Functionally graded components with engineered transitions in microstructure and/or compositions promote the functional performance requirements that vary with location within the component.

The present work can be extended further

- FGMMC can be prepared by the ex-situ additions with Al_2O_3, TiB_2, TiO_2, TiC, B_4C, and graphite.
- Short and long fibre additions of glass and carbon fibres in FGM is also an interesting area to be explored since the fibre orientation in preferred direction can improve the tensile properties and strength of cylindrical components and pressure vessels.
- FGMMC can also be prepared by the in-situ additions with Al_3Ni, TiB_2, TiO_2, $CuAl_2$.
- Similar to Magnesium modification by master alloy addition and pure Mg addition other alloying elements like Cu, Cr, Mn and Ti can be studied.

- Very few studies are reported with fibre orientation and with other particle reinforcements in Functionally Graded Polymer composites.
- Similar to FGMMC IC engine Piston other automobile components like brake disc, cylinder liner and gears, which need either inner or outer surface property enhancements can be produced.
- The gradation studies in chemical composition to FGM components are rarely reported. So detailed studies on the already developed materials can also be conducted along with new materials.

References

1 W.D. Callister, Material Science and Engineering - An Introduction, Sixth edition, John Wiley & Sons. Inc, River street, Hoboken, NJ-783, 2003.

2 A. Jacobs James, Engineering Material technology, Prentice Hall, 2004, ISBN-10:0130481858.

3 Josmin P. Jose, Sant Kumar Malhotra, Sabu Thomas, Kuruvilla Joseph, Koichi Goda and Meyyarappallil Sadasivan Sreekala, Advances in Polymer Composites: Macro- and Micro composites – State of the Art, New Challenges, and Opportunities, 2012

4 M. S. Bhatnagar, Epoxy Resins (Overview), The Polymeric Materials Encyclopedia CRC Press, Inc,1996.

5 H. Lee and K. Neville, HandBook of Epoxy Resins, McGraw Hill, New York, NY, 1982.

6 Darrel R. Tenney, NASA Langley Research Center, Advanced Composite Materials: Applications and Technology Needs, presentation to the Metal Properties Council, Inc., Miami, FL, Dec. 5, 1985.

7 Tim Paluka and Bernadette Bensaude, Composite Overview, History of Recent Science and Technology, www.authors.library.caltech.edu.

8 Friedrich Raether, Ceramic Matrix Composites – an Alternative for Challenging Construction Tasks, Ceramic Applications , 2013, 1 [1], pp 45-49.

9 G. Akovali, Handbook of Composite Fabrication, Rapra Technology Ltd., 2001, ISBN-1-85957-263-4

10 K.K Chawla, Composite materials-Science and Engineering, Springer science and Businees media, Newyork, 2102.

11 Nikhilesh Chawla, Krishan K. Chawla. Metal Matrix Composites. Springer; 1 edition (September 28, 2005). ISBN-10: 0387233067

12 D. B. Miracle, Metal matrix composites – From science to technological significance. Composites Science and Technology, 2005, Vol. 65, 15-16, pp 2526 - 2540.

13 ASM Handbook Vol. 15, Casting, ASM International, 1988. ISBN-10: 0871700212 &1992 ISBN ISBN-10-87170-007-7

14 ASM Handbook Vol. 10, Materials Characterization, ASM International, 1986. ISBN-10: 0871700166

15 Composite Materials Handbook - Metal Matrix Composites, 4, 2002,pp 34-35

16 F. C. Campbell, Manufacturing Technology for Aerospace Structural Materials, Elsevier Ltd., First Edition, 2006

17 Karl U. Kainer, Metal Matrix Composites: Custom-made Materials for Automotive and Aerospace Engineering, Wiley-VCH,2006,ISBN-3-527-313600

18 Todd Johnson, History of Composites: The Evolution of Lightweight Composite Materials, www.researchgate.net.

19 Sufei Wei, ASM Handbook, Volume 15: Casting, ASM Handbook Committee, pp 667-673, DOI: 10.1361/asmhba0005257

20 Suong.V.Hoa, Principles of the manufacturing of composite materials, DEStech Publications Inc., 2009.

21 High Performance Composites, Source Book 2001, Ray Publishing, www.composites world.com.
22 American Foundry men's society, Inc. Des plaines, Illinois, USA. ISBN 0-87433-121-8.
23 Bryan Harris, Engineering Composite Materials, The Institute of Materials, London, Applications of Composites ,6, 1999,pp192-193.
24 Degarmo E. Paul, J.T. Black, Kohser, A Ronald, Materials and Processes in Manufacturing (9th Ed), Wiley. 2003, p. 133. ISBN 0-471-65653 4.
25 ASM Metals Handbook Vol. 2, Properties and Selection of Nonferrous Alloys and Special Purpose Materials, ASM International, p 222.
26 John E Gruzleski, Bernard M Closset, The Treatment of Liquid Aluminium-Silicon alloys.
27 A Guide to Aluminium Casting Alloys. Mid Atlantic Casting Services. www.Mid-AtlanticCasting.com
28 J. Polmear, Arnold, Light Alloys, 1995, ISBN 9780340632079
29 Dr. Catrin Kammer, Aluminium Handbook Vol. 1: Fundamentals and Materials, Beuth Verlag, 1999, ISBN-10:3410220232
30 Gilbert Kaufman, Aluminium Alloy Castings: Properties, Processes and Applications, ASM International, 2004, 0-87170-803-5
31 G. Dieter, Tribological study of al-si eutectic alloy used in automotive application, Mechanical Metallurgy, vol. Third edition,1998, pp. 301–304.
32 K. Ludema, Friction and wear applications, ASM Handbook, vol. 18, 1992, pp. 257–271.
33 Gwidon W. Stachowiak, Andrew W. Batchelor, Engineering Tribology, Second edition, Butter worth-Heine mann, 2001, ISBN 0-7506-7304-4
34 Prasantha sahoo, Engineering Tribology, 2009, ISBN 978-81-203-2724-5
35 M. Gasik, Mater. Sci. Forum, 2003, Vols. 423-425, p.11.
36 Gururaja Udupa, S.Shrikantha Rao, K. V. Gangadharan, Procedia Materials Science,2014, 5 , pp 1291 – 1299
37 B. Kieback, A. Neubrand, H. Riedel, Materials Science and Engineering A, 2003, 362, pp 81–105, DOI:10.1016/S0921-5093(03)00578-1
38 S. Suresh and A. Mortensen, International Materials Reviews, 1997, Vol. 42, No.3, pp 85-116.
39 M. S. EL-Wazery, A. R. EL-Desouky, Mater. Environ. Sci., 2015, 6 (5), pp 1369-1376 ISSN : 2028-2508
40 T. P. D. Rajan , R. M. Pillai And B. C. Pai, Indian Foundry Journal, 2007, Vol. 53, No 6, pp 79 – 86.
41 Y. Fukui, The Japan society of Mechanical Engineers, JSME Journal Series III, 1991, Vol. 34, No-1, pp 144-148
42 C. G. Kang, P. K. Rohatgi , C. S. Narendranath, and G. S. Cole, ISIJ International, 1994, Vol. 34 , No. 3, pp. 247-254.
43 A. Mortensen and S. Suresh, International Materials Reviews, 1995, Vol. 40, No.6, pp 239-265.
44 Wang Qudong and Jin Junze, Trans. Nonferrous Met. Soc. China, 1997, vol.1, No. 7, pp-125-130.
45 Akira Kawasaki, Ryuzo Watanabe, Ceramics International,1997, 23, pp 73-83, 0272-8842(95)00143-3

46 Yoshimi Watanabe, Noboru Yamanaka and Yasuyoshi Fukui, Composites Part A,1998, 29A ,pp 595-601, PII: S1359-835X(97)00121-8

47 J. K. Kim, P. K. Rohatgi, Journal Of Materials Science, 1998, 33, pp 2039- 2045.

48 J.W. Gao, C.Y. Wang, Materials Science and Engineering A, 2000,292 , pp 207–215, PII: S0921-5093(00)01014-5

49 Yoshimi Watanabe, Akihiro Kawamoto , Koichi Matsuda, Composites Science and Technology, 2002, 62, pp 881–888, PII: S0266-3538(02)00023-4

50 Yoshimi Watanabe and Yasuyoshi Fukui, FORMATEX 2004, Current Issues on Multidisciplinary Microscopy Research and Education , pp 189- 198

51 Yoshimi Watanabe, Shin Oike, Acta Materialia, 2005, 53, pp 1631–1641, DOI:10.1016/j.actamat.2004.12.013

52 Z. Humberto Melgarejo , O. Marcelo Suárez , Kumar Sridharan, Composites: Part A, 2008, 39 ,pp 1150–1158, DOI:10.1016/j.compositesa.2008.04.002

53 T.P.D. Rajan and B.C. Pai, Transactions of The Indian Institute of Metals, August-October 2009, Vol. 62, Issues 4-5, TP 2300,pp. 383-389.

54 T.P.D. Rajan And B.C. Pai, 59-IIF-Congress-Chandigarh-2011

55 Thomas C Chamlee, US Patent, Patent Number 5980792, date of Patent Nov 9,1999

56 P. D. Sequeira, Yoshimi Watanabe, Hiroyuki Eryu, Tetsuya Yamamoto, Kiyotaka Matsuura, Transactions of the ASME, April 2007,Vol. 129, pp 304- 312 , DOI: 10.1115/1.2712467

57 T.P.D. Rajan, R.M. Pillai, B.C. Pai, Journal of Alloys and Compounds ,2008, 453, L4–L7

58 S.C. Ferreira , A. Velhinho , L.A. Rocha and F.M. Braz Fernandes, Materials Science Forum, 2008, Vols. 587-588, pp 207-211

59 Xuedong Lin , Changming Liu, Yanbo Zhai, Kai Wang, J. Mater Sci, 2011, 46,pp1058–1075, DOI :10.1007/s10853-010-4874-9

60 R. Rodriguez-Castro , M. H. Kelestemur, Journal Of Materials Science , 2002, 37, pp 1813-1821

61 F. Bonollo, A. Moret, S. Gallo, C. Mus, Materiali Composite, La Metallurgia Italina , 6/2004 , pp 49 – 55.

62 Xie Yong, Liu Changming, Zhai Yanbo, Wang Kai, and Ling Xuedong, Rare Metals, Aug 2009, Vol. 28, No. 4, pp 405-411

63 P. G. Mukunda , Shailesh Rao A , and Shrikantha S Rao, Met. Mater. Int., 2010, Vol. 16, No. 1, pp 137- 143.

64 Adelakin, Tunde Kingsley and Suárez, Oscar Marcelo, Materials and Manufacturing Processes,2011, 26, 2, pp 338- 345,DOI: 10.1080/10426910903124829

65 Y. Fukui., K. Takashima, C. B. Ponton, Journal Of Materials Science, 1994, 29, pp 2281-2288

66 G. Chirita, I. Stefanescu,D. Soares, F. S. Silva, Anales De Mecánica De La Fractura, 2006, Vol. I, pp 317 -322

67 G. Chirita , I. Stefanescu , J. Barbosa , H. Puga, D. Soares and F. S. Silva, International Journal of Cast Metals Research, 2009, Vol 22, No 5, pp 382-389.

68 G. Chirita, D. Soares, F.S. Silva, Materials And Design , 2008, 29, pp 20–27

69 Yoshimi Watanabe, Noboru Yamanaka, and Yasuyoshi Fukui, Metallurgical and Materials Transactions A, December 1999,Volume 30A, pp 3253-3261

70 J.R. Gomes , A.R. Ribeiro , A.C. Vieira , A.S. Miranda , L.A. Rocha, Report of Program POCTI, contract POCTI/CTM 46086/2002, FCT-Portugal.
71 Zenón Humberto Melgarejo, Master of Science In Mechanical Engineering University Of Puerto Rico Mayagüez Campus 2006
72 Z. Humberto Melgarejo, O. Marcelo Sua´rez and Kumar Sridharan, Scripta Materialia, 2006, 55,pp 95–98 , DOI:10.1016/j.scriptamat.2006.03.031
73 A.C. Vieira, P.D. Sequeira, J.R. Gomes, L.A. Rocha, Wear ,2009, 267,pp 585–592, DOI:10.1016/j.wear.2009.01.041
74 Shimaa El-Hadad , Hisashi Sato , Yoshimi Watanabe, Journal of Materials Processing Technology, 2010, 210,pp 2245–2251, DOI:10.1016/j.jmatprotec.2010.08.012
75 S.C. Ferreira, L.A. Rocha,, E. Ariza, P.D. Sequeira, Yoshimi Watanabe, J.C.S. Fernandes. Corrosion Science, cs 4327,19 Feb 2011 doi: 10.1016 / j.corsci. 2011.02.010
76 Nairobi B Duque , Z. Humberto Melgarejo , O. Marcelo Sua´Rez, Materials Characterization, 2005, 55 , pp 167– 171
77 X. H. Qin, W. X. Han, C. G. Fan, L. J. Rong, Y. Y. Li, Journal Of Materials Science Letters, 2002, 21, pp 665– 667
78 T. P. D. Rajan , R. M. Pillai And B. C. Pai, International Journal Of Cast Metals Research, 2008, Vol. 21, No 1–4, pp 214 – 218.
79 Yoshimi Watanabe, Ick Soo Kim and Yasuyoshi Fukui, Metals and Materials International, 2005, Vol. 11, No. 5, pp. 391-399.
80 Wang Kai, Xue Han-Song, Zou Mao-Hua, Liu Chang-Ming, Trans. Nonferrrous Met. Soc. China, 2009, 19, pp 1410-1415, DOI: 10.1016/S1003-6326 (09) 60042-X
81 T.P.D. Rajan , R.M. Pillai, B.C. Pai, Material Characterization, 2010, 61, pp 923 – 928, DOI:10.1016/j.matchar.2010.06.002
82 Hao Xuhong, Liu Changming, Pan Dengliang, Chinese Journal of Mechanical Engineering, 2011, Vol. 22, No. 5, DOI: 10.3901/Cjme.2011.05
83 W.Q. Zhang, Y.S. Yang, Y.F. Zhu, Q.M. Liu and Z.Q. Hu , Metallurgical And Materials Transactions A , January 1998,Volume 29A, pp 404 -408
84 A. Velhinho , P.D. Sequeira , Rui Martins , G. Vignoles , F. Braz Fernandes , J.D. Botas , L.A. Rocha, Nuclear Instruments and Methods in Physics Research B, 2003, 200 , pp 295–302
85 Francisco Braz Fernandes, Luís Augusto Rocha, Alexandre Velhinho, ESRF, Experiment number: ME-461, Date of report 07/03/2005
86 Yoshimi Watanabe, Masahito Kurahashi , I.-S. Kim , Shinya Miyazaki , Shinji Kumai , A. Sato , Shunichiro Tanaka, Composites: Part A Applied Science and Manufacturing , 2006, 37, pp 2186–2193
87 Weimin Wang, Xiufang Bian, Jingyu Qin, And S.I. Syliusarenko, Metallurgical and Materials Transactions A , September 2000, Volume 31a, , pp2163- 2168.
88 Jian Zhang , Yu-Qing Wang, Ben-Lian Zhou, Xing-Qiang Wu, Journal Of Materials Science Letters,1998, 17, pp 1677-1679.
89 Yasuyoshi Fukui, Hiroshi Okada, Noriyoshi Kumazawa and Yoshimi Watanabe, Metallurgical and Materials Transactions A, 2000, vol. 31A, pp 2627 – 2636.
90 Yoshimi Watanabe, Satoru Watanabe and Kiyotaka Matsuura, Metallurgical and Materials Transactions A, May 2004, Volume 35A, pp 1518 – 1524.
91 P.D. Sequeira , Yoshimi Watanabe , Yasuyoshi Fukui, Scripta Materialia, 2005, 53, pp 687–692

92 Yoshimi Watanabe , Yoshifumi Inaguma , Hisashi Sato and Eri Miura-Fujiwara, Materials, 2009, 2, pp 2510-2525
93 A.G. Rao, M. Mohape, V.A. Katkar, Gowtam, D. S. , Deshmukh, V. P. and Shah, A. K., Materials and Manufacturing Processes, 2010, 25, 7, pp 572 - 576.
94 Shimaa El-Hadad , Hisashi Sato , Eri Miura-Fujiwara and Yoshimi Watanabe, Materials, 2010, 3, pp 4639-4656, ISSN 1996- 1944, DOI:10.3390/ma3094639
95 S. Kumar, V. Subramaniya Sarma and B.S. Murty, Metallurgical And Materials Transactions A, January 2010, Volume 41A,pp 242-254
96 M. Sánchez , J. Rams, A. Ureña, Composites: Part A, 2010, 41 ,pp 1605–1611 , DOI:10.1016/j.compositesa.2010.07.014
97 Hiroshi Okada , Yasuyoshi Fukui , Ryoichi Sako, Noriyoshi Kumazawa, Composites Part A, 2003,34,pp 371–382, DOI:10.1016/S1359-835X(03)00023-X
98 Prem E. J. Babu, T.P.D. Rajan, S. Savithri, U.T.S. Pillai And B.C. Pai, International Symposium Of Research Students On Materials Science And Engineering December 20-22, 2004, Chennai, India , Department Of Metallurgical And Materials Engineering, Indian Institute Of Technology Madras.
99 Gustavo Gutierrez , O. Marcelo Suárez and Mauricio A. Giordano, Mecanica Computacional, October 2007,Vol XXVI, pp 2612-2622, Sergio A Elaskar,Elvio A.Pilotta, German A .Torres(Eds) Cordoba, Argentina,
100 Zhang Wei-Qiang, Lou Chang-Sheng, Trans. nonferrous Met. Soc. China, 2010, 20, pp 870-876, DOI: 10.1016/S1003-6326(09)60228-4
101 N. J. Lee, J. Jang, M. Park, C. R. Choe, Journal of Materials Science,1997, 32, pp 2013- 2020
102 Mashiro Funabashi, Composites Part A ,1997, 28A, pp 731–737, PII: S1359-835X(97)00016-X
103 C. Klingshirn, M. Koizumi, F. Haupert, H. Giertzsch, K. Friedrich, Journal Of Materials Science Letters, 2000, 19, pp 263– 266
104 M. Krumova, C. Klingshirn, F. Haupert and K. Friedrich, Composites Science and Technology, 2001, 61, pp 557-563,
105 P. Tsotra , K. Friedrich, Composites: Part A,2003, 34, pp 75–82
106 V. Goncharov, V. A. Ivanov and S. P. Zakharychev, ISSN 1068-798x, Russian Engineering Research, 2009, Vol. 29, No. 3, pp. 259–263.
107 M. Szczepanik, J. Stabik, M. £azarczyk, A. Dybowska, Archives of Materials Science and Engineering, 2009, 37/1, pp 37-44.
108 Siddhartha, Amar Patnaik , Amba D. Bhatt, Materials and Design, 2011, 32 , pp 615–627
109 S. A. R. Hashmi, U. K. Dwivedi, D. Jain, Ajay Naik, Navin Chand, Journal of Applied Polymer Science,2005, Vol. 96,pp 550–556 ,DOI: 10.1002/app.21478
110 S. A. R. Hashmi, U.K. Dwivedi, Navin Chand, Wear,2007, 262, pp 1426–1432 DOI:10.1016/j.wear.2007.01.014
111 S. A. R. Hashmi, U. K. Dwivedi, Navin Chand, Journal of Applied Polymer Science, 2009, Vol. 113, pp 3840–3846, DOI 10.1002/app
112 J. Stabik, A. Dybowska, M. Chomiak, Journal of Achievements in Materials and Manufacturing Engineering, November 2010, Vol.- 43, 1, pp 153 - 161
113 J. Stabik, A. Dybowska, J. Pluszyñski, M. Szczepanik and £. Suchoñ, Archives of Materials Science and Engineering International Scientific Journal , January 2010,Vol. 41, 1, pp 13-20

114 J. Stabik, M. Chomiak, Archieves of Materials Science and Engineering, January 2011, Vol.47, 1,pp 48-56
115 J. Stabik, A. Chrobak, G. Haneczok, A. Dybowska, Archives of Materials Science and Engineering, 2011, 48/2,pp 97-102.
116 Chul Rim Choe, C. Klingshirn and K. Friedrich, Macromolecular Research, 2002,Vol. 10, No. 4, pp 236-239
117 P. Tsotra , K. Friedrich, Composites: Part A ,2003, 34 ,pp 75–82
118 P. Tsotra , K. Friedrich, Composites Science and Technology ,2004, 64, pp2385–2391, DOI:10.1016/j.compscitech.2004.05.00
119 Cavus Falamaki , Jamileh Veysizadeh, Ceramics International, 2008, 34,pp 1653–1659
120 S. A. R. Hashmi, Journal of Applied Polymer Science, 2006,Vol. 99, pp 3009–3017
121 S.A.R. Hashmi, U.K. Dwivedi, Polymer Engineering and Science-2006,pp 1660-1666, DOI: 10.1002/pen.20648
122 S.A.R. Hashmi and U.K. Dwivedi, Journal of Polymer Research, 2007, DOI:10.1007/s10965-006-9083-5
123 S.A.R. Hashmi, U.K. Dwivedi, Polymer Composites, 2009, pp 162-168, DOI 10.1002/pc
124 J. Stabik and A. Dybowska, Journal of Achievements in Materials and Manufacturing Engineering, November 2007,Vol. 25, 1, pp 67 - 70
125 J. Stabik , M. Chomiak, A. Dybowska, Ł. Suchoń and K. Mrowiec, Journal of Achievements in Materials and Manufacturing Eng., 2012, 54/2 , pp 218-226.
126 F.J. Tavitas-Medrano, J.E. Gruzleski, F.H. Samuel, S. Valtierra, H.W.Doty, Materials Science and Engineering A , 2008, 480, pp 356–364
127 J. Gauthier, P. R. Louchez, F. H. Samuel, Cast Metals, 1994, vol. 8(2), pp 91–106
128 K.R. Ravi, V.M. Sreekumar, R.M. Pillai, Chandan Mahato, K.R. Amaranathan, R. Arul kumar, B.C. Pai, Materials and Design, 2007, 28, pp 871–881
129 J. Barresi, M J. Kerr, H. Wang, M. J. Couper, 2000, AFS Trans 2000, pp 563–570
130 J. Hashim, L. Looney, Journal of Materials Processing Technology, 2001, 119, pp 324-328
131 P.S. Robi, B.C. Pai, K.G. Satyanarayana, S.G.K. Pillai, P.Prabhaker Rao, Materials Characterization,1991, Vol. 27, 1, pp 11–18
132 Z. Trojanova, M. Pahutova, J. Kiehn, P. Lukac, and K.U. Kainer: in Proceedings of the 1st International Conference, San Sebastian, Spain, Sept 1996, p. 1001
133 V. R. Rajeev, D.K. Dwivedi and S.C. Jain, 4th International conference on recent advances in composite materials, ICRACM-2013, February 18-21, 2013, India.
134 Miyamoto, Y; Kaysser, W.A; Rabin, B.H; Kawasaki, A.; Ford, R.G. Functionally Graded Materials. Kluwer Academic Publishers, Boston 1999.
135 Y. Wanatanab and, H. Sato: Materials, 2009, vol. 2, pp 2510-2525, DOI:10.3390/ma2042510
136 C.Ponzi, Metal matrix composites fabrication processes for high performance aerospace structures, Composite Manufacturing, 1992, 3, pp 32-41.
137 W. Hunt and D. Miracle, Composites, 2001, vol. 21, pp. 1029–1032.
138 B. K. Yen and T. Ishihara, Composites, 1996, vol. 198, pp. 169–175.

139 O. Carvalho, M. Buciumeanu, S. Madeira, D. Soares, F.S. Silva, G. Miranda: Mater. Design, 2015, Vol. 80, pp. 163–173
140 A.G. Arsha, E. Jayakumar, T.P.D. Rajan, V. Antony, B.C. Pai, Mater. Design, 2015, Vol. 88, pp. 1201-1209.
141 Xuedong Lin , Changming Liu, Haibo Xiao, *Composites Part B,* 2013 ,vol. 45, pp 8 – 21
142 Ramazan Kayikci, Ömer Savaş, J. Compos. Mater., 2015, vol. 49(16), pp 2029-2037
143 S.L. Pramod, Srinivasa R Bakshi, and B.S. Murty: J. Mater. Eng. and Performance, 2015, vol. 24(6), pp 2185-2207
144 C.Saravanan, K. Subramanian, V. Ananda Krishnan, R. Sankara Narayanan: Mechanics and Mechanical Eng., 2015,vol. 19 (1), pp 23-30
145 Himanshu Kala, K.K.S Mer, Sandeep Kumar: Procedia Mater. Sci., 2014, vol. 6, pp. 1951 - 1960.
146 L. R.A. Saravanan, Metall. Mater. Trans.A, 1999, vol. 30, pp. 2523 -2538.
147 W. Kai and S. Wenju, J. Compos. Mater, 2004, vol. 26(3), pp. 71–72.
148 A. Divecha and S. Fishman, Developments in the centrifugal casting technology, Journal of metals, 1981, vol. 33(9), pp 12.
149 Michael Oluwatosin Bodunrin, Kenneth Kanayo Alaneme, Lesley Heath Chown: J. Mater. Res. Technol. 2015, vol. 4(4), pp 434-445.
150 M.C. Gowri Shankar, P.K. Jayashree, Raviraj Shetty, Achutha Kinia and S.S. Sharma: Inter. J. Current Eng. Technol., 2013, Vol. 3(3), pp 922-934
151 Halvaee, A. Talebi, J. Mater. Process. Technol., 2001, vol. 118,1-3, pp 122–126.
152 F. H. Samuel, J Mater Sci., 1998, 33, pp 2283–97.
153 P.S. Wang, S. L. Lee, J. C. Lin, M. T. Jahn, J Mater Res, 2000,15(9), pp 2027–35.
154 C. Villeneuve, A.M Samuel, F. H. Samuel, H. W.Doty, S. Valtierra, AFS Trans, 2001, pp 287–300.
155 J. Gauthier, P. R. Louchez, F.H. Samuel, Cast Metals, 1994, 8(2), pp 91–106.
156 Z. Li, A.M. Samuel, F.H. Samuel, C. Ravindran, S. Valtierra, H W. Doty: AFS Trans, 2003, vol. 2, pp 241–254.
157 J. M. Boileau, S. J. Weber, R. H. Salzman , J. E. Allison, AFS Trans, 2001, pp 419-432.
158 P N. Crepeau: AFS Trans, 1995, 103, pp 361–366.
159 D.K. Dwivedi: Mater. Design, 2010, vol. 31, pp 2517 – 2531.
160 R.L. Deuis, C Subramanian & j. M. Yellup, Composites Science and Technology, 1997, 57, pp 415-435.
161 V.R. Rajeev, D.K. Dwivedi and S.C. Jain: Mater. Design, 2010, vol. 31, pp 4951–4959.
162 K. M. Jasim and E. S. Dwarakadasa, Wear, 1987, pp 119–130.
163 J. Sun Zhiqiang, Zhang Di, Li Guobin, Materials and Design, 2005, 26, pp 454–458.
164 S. Sawla, S. Das, Wear, 2004, 257, pp 555–561.

165 E. Jayakumar, Jibin C Jacob, T.P.D. Rajan, M.A. Joseph, B.C. Pai: Mater. Sci. Forum, 2015, Vol. 830-831, pp 456-459.
166 M.B. Karamis, A. Alper Cerit, Burhan Selcuk, Fehmi Nair, Wear, 2012, 289, pp 73-81.
167 Akhil S Karun, T.P.D. Rajan, U. T.S. Pillai, B.C.Pai, J. Composite Materials, 2015, pp 1-15, DOI: 10.1177/0021998315602946.
168 Md. Aminul Islam, Zoheir N. Farhat, Tribology International, 2011, 44, pp 498–504.
169 Jeong.H , G.H.Paulino, International Journal of Solid and Structures 40. 2003, 3967-4001.
170 A. Mortensen, C. Sanmarchi, Glossary of terms specific to Metal Matrix Composites by H.P.Degischer. MMC- Assess Thematic Network, August 2000
171 M. V. Gandi, B. S. Thompson, Materials and Design, 1990, 11, pp 235-242
172 Barbara Previtali, Dante Pocci, Composites: Part A, 2008,39, pp 1606–1617
173 M K Surappa, Sadhana, 2003, 28, pp 319-334.
174 W. C. Harrigan, Materials Science and Engineering A, 1998, 244, pp 75–79.
175 D. J. Lloyd, International Materials Reviews, 1994, 39, pp 1–23.
176 G. B. Veeresh Kumar, C. S. P. Rao, Journal of Minerals and Materials Characterization and Engineering, 2010, Vol. 9 No. 1, pp 43-55.
177 R.M. Mahamood, E.T. Akinlabi, M. Shukla, S. Pityana, Proceedings of the World Congress on Engineering WCE (2012), 2012, Vol III, pp 4–6.
178 Tamer Ozben, Erol Kilickap, Orhan C akır, Journal of materials processing technology, 2008, 198, pp 220–225.
179 S. Balasivanandha Prabu, L. Karunamoorthy, S. Kathiresan, B. Mohan, Journal of Materials Processing Technology, 2006, 171, pp 268–273.
180 Rong Chen, Akira Iwabuchi, Tomoharu Shimizu, Wear, 2000, 238, pp110 – 119.
181 Chang-Jiang Song, Zhen-Ming Xu, Jian-Guo Li, Composites: Part A , 2007, 38, pp 427–433.
182 Jian Zhang, Zhongyun Fan, Yuqing Wang, Benlian Zhou, Materials and Design, 2000, 21, pp 149-153.
183 S. Raghunandan, Jasim Akber Hyder, T.P.D. Rajan, K. Narayan Prabhu and B.C. Pai, Materials Science Forum, 2012, 710,pp 395-400.
184 Alireza Hekmat-Ardakan, Frank Ajersch and X.-Grant Chen, J Mater Sci, 2011, 46, pp 2370–2378.
185 Chang-Jiang Song, Zhen-Ming Xu, Jian-Guo Li, Trans. Nonferrous Met. Soc. China, 2010, 20, pp 361−370.
186 S. Nafisi, light metals, 2004, vol. 32(2).
187 S. Das, D.P. Mondal, O.P. Modi, R. Dasgupta, Wear, 1999, 231, pp195–205.
188 Haizhi Ye, ASM International, JMEPEG (2003), 12, pp 288-297.
189 M. Gupta, S. Ling, Journal of Alloys and Compounds, 1999, 287, pp 284–294.
190 N. Gravier and Y. C. E.C. Cutiongo, Tribol. Trans., 1995, pp 168–172.

191 C.M.L. Huang, L. Xunjia, G.F. Li, J. Mater. Process. Technol., 2008, 211, pp 1540–1546.
192 M.M. Haque, A. Sharif, J.Mater. Process. Technol., 2001, 118, pp 69–73.
193 Z. J. Wen, W. U. Shu-sen, Trans. Non-ferrous Met. Soc. China, 2010, 20, pp 754–757.
194 A. H. Ardakan, F. Ajersch, Acta Mater. , 2010, 58, pp 3422–3428.
195 N. A. Nordin, A.Sfaota. Bakar, E. Hamzah, Mater. Charact., 2013, 86, pp 97–107.
196 M. Zuo, J Mater Sci., 2009, vol. 44, pp 1952–1958.
197 T.P.D. Rajan, B.C. Pai, Acta Metall. Sci. 2014, 27, pp 825–828.
198 M.F. Forster, R.W. Hamilton, R.J. Dashwood, P.D. Lee, J. Mater. Sci. Technol., 2003, 19, pp 1215–1219.
199 R. S. Rana, Rajesh Purohit, S. Das, Int. J. Sci. Res. Publ.,2012, 63,pp 90–97.
200 C. H. Caceres, I. L. Svensson, J. A. Taylor, Int. J Cast Metals Res, 2003, 15, pp 531–543.
201 G. K. Sigworth, S. Shivkumar, D. Apelian, , AFS Trans ,1989, pp811–824.
202 Z.Y. Ma, A.L. Pilchak, M.C. Juhas, J.C. Williams, Scr. Mater, 2008, 58, pp 361–366.
203 S.A. Alidokht, A. Abdollah-zadeh, S. Soleymani, T. Saeid, H. Assadi, Mater. Charact., 2012, 63,pp 90–97.
204 Z. Yan-bo, Liu, C. ming, W. Kai, Z. Mao-hua, X. Yong, Trans. Non-ferrous Met. Soc. of China, 2010, 20, pp 361–370.
205 L. Wu, X. Guo, J. Zhang, Lubricants, 2014, 2, pp 66–89.
206 M. Elmadagli, T. Perry, A.T. Alpas, Wear, 2006, 243, pp 456-462.
207 S. Das, Y.L. Saraswathi, D.P. Mondal, Wear, 2006, 261, pp 180–190
208 D. K. Dwivedi and D. Kumar, Materials and Design, 2006, vol. 27, pp 610 - 616.
209 M. A. H. Goto, wear,1987, vol. 116, pp 141–155.
210 B. C. Pai. V.C. Srivastava, and R.K. Mandal, Trans. Indian Inst. Met, 1991, vol. 34, pp. 29–40.
211 J.R. Gomes, A. Ramalho, M.C. Gaspar, S.F. Carvalho, Wear, 2005, 259, pp 545–552.
212 V. R. Rajeev, D. K. Dwivedi, S. C. Jain, Tribology International, 2010, 43, pp 1532–1541.
213 J.R. Gomes, A.S. Miranda, D. Soares, A. E. Días, L. A. Rocha, S. J. Crnkovic., Ceramic Transactions, 2000, 114, pp 579-586.
214 M.H. Korkut, Materials Science and Technology, 2004, 20, pp 73-81.
215 Serope Kalpakjian, Steven R.Schmid, Manufacturing engineering and technology, fourth edition, 2004.
216 T.P.D. Rajan, R.M. Pillai, B.C. Pai, Indian Foundry J., 2003, 49 (9), pp 19–30.
217 R. Rodr´iguez-Castro, R.C. Wetherhold, M.H. Kelestemur, Mater. Sci. Eng. A , 2002, 323, pp 445 -456.

218 J. Hashim, L. Looney, M. S. J. Hashmi, Journal of Materials Processing Technology, 2001,119, pp 329-335.
219 P. Rohatgi, R. Asthana, Journal of minerals, metals and materials society, 1991, 43, pp 35 – 41.
220 U.K. Dwivedi, Journal of Polymer Research , 2006, pp 75-81
221 Suong .V. Hoa, Principles of the Manufacturing of Composite Materials, DEStech Publications, Inc (2009).
222 J. Zhang, Express Polymer letters, 2009, vol.3, no.9, pp 534–554
223 J. Cho, M.S. Joshi, 2005, Composites Science and Technology, Volume 66, 13, pp 1941-1952.
224 X.S. Xing, X.S. Xing, R.K.Y. Li, Wear, 2004, 256,pp 21–26.
225 J. Stabik, A. Dybowska, M. Szczepanik, Ł. Suchoń, Archives of Mater. Sci. and Eng.,2009, 38, 1.
226 L.S. Silva, Maria Madalena De Camargo Forte, J. Mater. Sci., 2004, 39.
227 B. J. Briscoe and S. K. Sinha, Wear of polymers, Proc Instn Mech Engrs, Part J, Tribology Int., 2002,216, pp 401-413.
228 Oscar Olea-Mejia, Witold Brostow, Eli Buchman, Journal of Nano-science and Nanotechnology, 2010, Vol.10, pp 524-530.
229 Witold Brostow, Vera Kovacevicb, Journal of Materials Education, 2010, Vol.32, (5-6), pp 273 -290.
230 Klaus Friedrich, K. Alois, Tribo. Interface Eng. Series, 2008, 55.

List of Publications

1. Processing and Characterisation of Functionally Graded Aluminium (A319) - SiCp Metallic Composites by Centrifugal Casting Technique,
   E. Jayakumar, Jibin C Jacob, T. P. D. Rajan, M. A. Joseph , B.C. Pai , Metallurgical and Materials Transactions A, 2016, 47(8), 4306-4315, DOI: 10.1007/s11661-016-3558-8
2. Processing and Characterization of Hypoeutectic Functionally Graded Aluminium – SiC Metal Matrix Composites,
   E. Jayakumar, Jibin C Jacob, T.P.D. Rajan, M.A. Joseph, B.C. Pai:, Mater. Sci. Forum, 2015, Vol. 830-831, pp. 456-459, DOI: 10.4028/www.scientific.net/MSF.830-831.456
3. Design and fabrication of functionally graded in-situ aluminium composites for automotive pistons,
   A.G. Arsha, **E. Jayakumar,** T.P.D. Rajan, V. Antony, B.C. Pai, Materials and Design, 2015, Vol. 88, pp. 1201-1209, DOI:10.1016/j.matdes.2015.09.099
4. Effect of Mg on Solidification Microstructures of Homogenous and Functionally Graded A390 Aluminum Alloys,
   E. Jayakumar, T. P. D. Rajan and B.C. Pai, Transactions of the Indian Institute of Metals, 65(6) 2012, pp.531-537, DOI: 10.1007/s12666-012-0198-6
5. Processing and Characterization of Functionally Graded In Situ Aluminum Composite,
   A.G. Arsha, **E. Jayakumar**, T.P.D. Rajan, B.C. Pai, Materials Science Forum 830-831:485-488, 2015, DOI: 10.4028/www.scientific.net/MSF.830-831.485.
6. Developments in Solidification Processing of Functionally Graded Aluminium Alloys and Composites by Centrifugal Casting Technique,
   T. P. D. Rajan, **E. Jayakumar** and B.C. Pai, Transactions of the Indian Institute of Metals ,65(6), 2012, DOI: 10.1007/s12666-012-0191-0.
7. Processing and characterization of SiCp reinforced functionally graded AA 6061 aluminium metal matrix composites,
   Ramakrishna Vikas S., Manjunath Maiya U., **E. Jayakumar**, T. P. D. Rajan, B. C. Pai and Nagaraja, The Inter.Journal for Advancements in Mechanical and Aeronautical Eng.-IJAMAE, vol.1 (2),2014. DOI: 10.13140 / RG .2. 1.1877. 6161
8. Centrifugal Casting and Characterisation of Primary Silicon and Mg_2Si Dispersed Aluminium Functionally Graded Materials,
   P. Midhun Krishnan, S. Hari, **E. Jayakumar**, T.P.D. Rajan and K. Narayan Prabhu, Materials Science Forum, 2015,Vols. 830-831 , pp 11-14
9. Processing of Functionally Graded Aluminium alloy and Composite Engineering Components by Centrifugal and Squeeze Casting Techniques,
   T. P. D. Rajan, **E. Jayakumar ,** K. M. Sree Manu, Akhil S Karun and B.C. Pai, Indian Foundry Journal , April 2016, Vol. 62, No.4, pp 21-25.

List of International/National Conference Presentations

1. Study of SiC Reinforced Functionally Graded Hyper-Eutectic Aluminium Composites,
   E. Jayakumar, U. Manjunath Maiya, S. RamakrishnaVikas, T.P.D. Rajan,B.C. Pai and Nagaraja, International Conference on Aerospace and Mechanical Engineering (ICAME'15), 14-16 December, 2015, TKM College of Engineering, Kollam, Kerala.
2. Processing and Characterization of Hypoeutectic Functionally Graded Aluminum – SiC Metal Matrix Composites,
   E. Jayakumar, Jibin C Jacob , T. P. D. Rajan , M. A. Joseph and B.C. Pai,
   International Conference on advanced Materials and Manufacturing Processes for Strategic Sectors (ICAMPS 2015), May 13-15,Trivandrum,Kerala.
3. Processing of Functionally Graded Aluminium Alloys and Composites for Engineering Applications,
   E. Jayakumar, K.M. Sree Manu, Akhil S. Karun, N. Anand, K.K. Ravikumar, T.P.D. Rajan and B.C. Pai, International Conference on Advanced Functional Materials (ICAFM 2014), February 19-21, 2014 Thiruvananthapuram, Kerala, India.
4. Processing of Functionally Graded Aluminium (A319)-SiC Metallic Composites by Centrifugal Casting Technique,
   E. Jayakumar, Jibin C Jacob, T. P. D. Rajan, K.K. Ravikumar, M. A. Joseph, B.C. Pai, National Aerospace Manufacturing Seminar (NAMS 2013), November 22 2013.
5. Tribological Behaviour of SiCp Reinforced Functionally Graded A319 Metal Matrix Composites,
   E. Jayakumar , A.P. Praveen, T. P. D. Rajan, B.C. Pai and V.R. Rajeev, International Symposium for Research Scholars on Metallurgy (ISRS-2012), Materials Science & Engineering, December 13 – 15, 2012, Indian Institute of Technology Madras, Chennai, India, (**Received Best paper award)**
6. Effect of Mg on Solidification Microstructures and Properties of Homogenous and Functionally Graded A390 Aluminium Alloys,
   E. Jayakumar, T.P.D. Rajan and B.C. Pai, Fifth International Conference on Solidification Science and Processing (ICSSP5), November 19-22, 2012, Indian Institute of Technology, Bhubaneswar, India
7. Developments in Processing and Applications of Functionally Graded Metal-Ceramic Composite Materials,
   E. Jayakumar, Jasim Akber Hyder, T.P.D. Rajan, B.C. Pai,National Aerospace Manufacturing Seminar (NAMS 2011), November 18, 19 2011.
8. Fabrication of Ultrafine Grain and Nanostructured Aluminium Alloys and Composites,
   S. Senthil Murugan, **E. Jayakumar**, M. Brahmakumar, T.P.D. Rajan, B.C. Pai, K. Manonmani, R.K. Gupta and P. Ramkumar, National Aerospace Manufacturing Seminar (NAMS 2011), November 18,19 2011.

9. Developments in solidification processing of functionally graded Al alloys and composites by centrifugal casting technique,
T.P.D. Rajan, **E. Jayakumar**, and B.C. Pai, Fifth International Conference on Solidification Science and Processing (ICSSP5), November 19-22, 2012, Indian Institute of Technology, Bhubaneswar, India .
10. Processing and Characterization of SiCp Reinforced Functionally Graded A6061 Aluminium Metal Matrix Composites,
Ramakrishna Vikas S., Manjunath Maiya U., **E. Jayakumar**, T. P. D. Rajan, B. C. Pai and Nagaraja, International conference on Advances in mechanical and robotics engineering (MRE 2014), 08-09 March,2014, Kualalumpur, Malaysia.
11. Processing and Characterisation of Functionally Graded SiC Particle Reinforced Epoxy Composite by Centrifugal Casting,
M.Maneesh, **E.Jayakumar**, T.P.D Rajan , S.S. Suneesh , K.E George, National conference for polymer composite for young researchers (PCYR-2014), 18-october 2014, Thiruvananthapuram, Kerala, India.
